
PREGNANCY RISK STRATIFICATION USING DESI-MS PROFILING OF VAGINAL MUCOSA

Dr Holly Victoria Lewis

Institute of Reproductive and Developmental Biology
Department of Surgery and Cancer
Imperial College London

Thesis Submitted to the University of London for the degree of Doctor of Philosophy

DECLARATIONS

Declaration of Originality

I certify that all work presented in this thesis was performed by myself unless stated otherwise.

Copyright Declaration

The copyright of this thesis rests with the author. Unless otherwise indicated, its contents are licensed under a Creative Commons Attribution-Non Commercial 4.0 International Licence (CC BY-NC). Under this licence, you may copy and redistribute the material in any medium or format. You may also create and distribute modified versions of the work. This is on the condition that: you credit the author and do not use it, or any derivative works, for a commercial purpose. When reusing or sharing this work, ensure you make the licence terms clear to others by naming the licence and linking to the licence text. Where a work has been adapted, you should indicate that the work has been changed and describe those changes. Please seek permission from the copyright holder for uses of this work that are not included in this licence or permitted under UK Copyright Law.

ABSTRACT

Preterm birth is the leading cause of childhood mortality. Despite decades of research, the pathophysiology of spontaneous preterm birth (SPTB) remains poorly understood. Prevention strategies are limited by our inability to reliably predict women at risk and stratify depending on underlying aetiology.

There is an established association between ascending vaginal infection and SPTB. More recently, highly diverse vaginal bacterial communities deplete of *Lactobacillus* species have been associated with SPTB. However, not all pregnant women with such community structures deliver preterm, highlighting the importance of individual host response. Medical swabs are routinely used for microbiological screening with culture-based techniques. However, these are time-consuming, have a narrow focus for specific microbes and provide no information regarding host response. We hypothesised that metabolic profiling of cervico-vaginal mucosa (CVM) may offer the ability to assess interactions between the vaginal microbiota and the pregnant host that are useful for prediction and stratification of SPTB risk.

To address this hypothesis, we developed a technique using DESI-MS that enabled rapid acquisition of metabolic information directly from vaginal swabs. In Chapter 3, method optimisation is described and its capacity to detect variations in the CVM associated with physiological changes in the host (e.g. pregnancy) and disruptions in bacterial community compositions during pregnancy (e.g. bacterial vaginosis) are presented.

The DESI-MS swab profiling approach was then used to characterise and compare CVM metabolic profiles associated with SPTB risk (Chapter 4). These results showed that the CVM metabolome associated with subsequent SPTB was highly variable, reflecting the heterogeneity of SPTB aetiology. In support of this, DESI-MS more effectively discriminated samples with differing severity of SPTB (early vs late) and phenotypes (SPTL and PPROM).

In Chapter 5, DESI-MS profiling of CVM was shown to facilitate prediction of PPROM as well as enable its robust diagnosis. DESI-MS also had capacity to characterise microbial compositions following PPROM suggesting its potential to assist in directed treatment strategies based on underlying aetiology.

This thesis highlights the predictive and therapeutic potential of DESI-MS in pregnancy.

ACKNOWLEDGEMENTS

My first son was born unexpectedly at 26 weeks. Sebby is now a robust little 7 year old, however the experience of having a preterm baby made me quite determined to help to future families avoid what we went through.

Thank you, Phillip Bennett for providing me with the opportunity to carry out a PhD in preterm birth research. I so appreciate your support over the years and admire your ability to draw connections and inspiration from everywhere in your research. Thank you also for expanding my knowledge of preterm birth management.

David MacIntyre; thank you for the hours you sat with me, editing abstracts, papers and presentations. I came not knowing anything about the microbiome, metabolome, multivariate statistics.....or how to make a proper cup of tea, apparently. Thank you for your mentorship, scientific insight, guidance and great sense of humour.

Zoltan Takats, thank you for your technical expertise, guidance and encouragement throughout this project.

Pamela Pruski, thank you for sharing your knowledge of mass spectrometry, your patience and company in the lab.

Paolo Inglese, thank you for your help with pre-processing and multivariate statistics which has been invaluable in enabling the project to reach its potential. You are an excellent teacher and I am grateful for the time you took to explain modelling concepts to me.

Lynne Sykes, thank you for inspiring me to delve into the world of preterm birth research. I am so grateful for your friendship and encouragement over the years as well as your motivating chats.

Richard Brown and Lindsay Kindinger for the samples and metadata for this project. Thanks for the clinical and research comradery over the years for which I also thank Anita Mitra, Joanna Cook and Denise Chan.

Yun Soo Lee (Yooni), for your kindness and looking after me. And to the other lab members; Kim Sung Hye, Fabienne Hanton, Zahirrah Rasheed, Belen Molina and Shah Mowla; thank you for your encouragement and keeping the chocolate desk well stocked.

Thank you to the Prem clinic midwives; Rachel Akers, Malko Adan and Rachel Quinlan for organising the clinics and making the long days so enjoyable. You all truly care about our patients

and it was a privilege to work with you all. I am also grateful to all our patients who selflessly provided samples for our research.

Genesis Research Trust for supporting my project, in particular; Martin, Heidi and Stacey for the welcomed coffee breaks and encouraging me to run the London Marathon for the charity. I really appreciated your cheerleading efforts around the city!

To my parents, thank you for your encouragement to take on new challenges. The ability to turn any hard situation into a positive, is learnt from you both for which I am very grateful. Thank you to my in-laws; Judie and Anthony for your support, interest in my project and stepping in when I went abroad to present my research. Thank you also to Wiola, Alessia, Ashley, Peggy and Jocelyn for helping to look after my boys.

Finally and most importantly I would like to thank my husband Jim for his unwavering support at every moment of this journey. I dedicate my thesis to him and our two children; Sebby who despite his untimely arrival, has defied every statistic and Alexander who managed to come at term...with a little help! We are immensely proud of them both.

DECLARATION OF CONTRIBUTION

All work in this thesis is by the author unless stated otherwise.

Drs Lindsay Kindinger and Richard Brown contributed to metadata and swab collection for the work described in Chapters 4 and 5.

All optimisation experiments included in this thesis (Chapter 3) were performed by Pamela Pruski and Holly Lewis. Additional experiments for optimisation studies, as referenced were carried out by Pamela Pruski. Acquisition of spectral data for the pilot studies (Chapter 3) and preterm birth studies (Chapter 4 & 5) using DESI-MS carried out by Holly Lewis and Pamela Pruski. MSMS experiments were carried out by Pamela Pruski.

Pre-processing of raw spectral data was carried out by Paolo Inglese as well as multivariate statistics using random forest. Analysis of data using SIMCA P and Graphpad were performed by Holly Lewis.

Richard Brown extracted swab sample DNA and PCR amplification for Chapter 5. Holly Lewis and David MacIntyre performed analysis of the microbiota data.

LIST OF PUBLICATIONS

Articles

Holly Lewis, Paolo Inglese, Pamela Pruski, Richard Brown, Ann Smith, Yun Lee, Phillip Bennett, Zoltan Takats and David A MacIntyre. (2019). Rapid mucosal metabolome profiling by desorption electrospray ionization MS (DESI-MS) for prediction and diagnosis of preterm pre-labour rupture of membranes (submitted).

Richard G Brown, Maya Al-Memar, Julian R Marchesi, Yun S Lee, Ann Smith, Denise Chan; Holly Lewis, Lindsay Kindinger, Vasso Terzidou, Tom Bourne, Phillip R Bennett and David A MacIntyre (2018). Establishment of vaginal microbiota composition in early pregnancy and its association with subsequent preterm prelabour rupture of the fetal membranes. *Translational Research*, Vol:207, Pages: 30 – 43.

Pamela Pruski, Holly Lewis, Yun Sun Lee, Julian R Marchesi, Phillip R. Bennett, Zoltan Takats, David MacIntyre (2018). Assessment of microbiota: host interactions at the vaginal mucosa interface. *Methods*, Vol:149, Pages:74-84.

Pruski P, MacIntyre DA, Lewis HV, Inglese P, Correia GDS, Hansel TT, Bennett PR, Holmes E, Takats Z et al. (2017). Medical Swab Analysis Using Desorption Electrospray Ionization Mass Spectrometry: A Non-invasive Approach for Mucosal Diagnostics, *Analytical Chemistry*, Vol: 89, Pages: 1540-1550.

Published Conference Abstracts

Lewis H, Inglese P, Brown R, Pruski P, Kindinger L, Lee Y, Bennett P, Takats Z, MacIntyre D. (2018). Rapid mucosal metabolome profiling by desorption electrospray ionization mass spectrometry for prediction of preterm prelabour rupture of membranes. *BJOG: Int J Obstet Gy*, Vol. 125, Page: E33.

Lewis HV, Inglese P, Pruski P, Brown R, Kindinger L, Lee Y, Bennett P, MacIntyre D. (2018). Rapid Mucosal Metabolome Profiling by Desorption Electrospray Ionization MS (DESI-MS) for Prediction of Preterm Pre-Labour Rupture of Membranes (PPROM). *Reproductive Sciences*, Vol: 25. Page: 65A.

Lewis H, Pruski P, Kindinger L, et al. (2017), Desorption electrospray ionisation mass spectrometry permits identification of vaginal mucosal metabolome signatures associated with preterm birth risk, *BJOG: Int J Obstet Gy*, Page: 135.

Lewis H, Pruski P, Kindinger, L, Lee Y, Bennett P, Takats Z, MacIntyre D. (2017). Relationship between Yeast, Vaginal Microbiota Composition and Pregnancy Outcomes *Reproductive Sciences*, Vol: 24, Page: 65A.

ORAL PRESENTATIONS

Examination of preterm birth phenotypes using vaginal mucosal profiling by Desorption Electrospray Ionization Mass Spectrometry (DESI-MS), Royal Society of Medicine Herbert Reiss Prize Meeting, London (2019).

Rapid Mucosal Metabolome Profiling by Desorption Electrospray Ionization MS (DESI-MS) for Prediction of Preterm Pre-Labour Rupture of Membranes (PPROM), 65th Annual Scientific Meeting of the Society-for-Reproductive-Investigation (SRI), San Diego (2018).

Rapid Mucosal Metabolome Profiling by Desorption Electrospray Ionization MS (DESI-MS) for Prediction of Preterm Pre-Labour Rupture of Membranes (PPROM), RCOG World Congress, Singapore (2018).

Desorption electrospray ionisation mass spectrometry permits identification of vaginal mucosal metabolome signatures associated with preterm birth risk, Bell Blair Academic Conference, London (2017).

Implications of Yeast & Vaginal Microbiota Interaction on Pregnancy Outcomes, 64th Annual Scientific Meeting of the Society-for-Reproductive-Investigation (SRI), Florida (2016).

Characterisation of vaginal swabs using Desorption electrospray ionization (DESI) MS permits rapid identification of metabolic signatures associated with preterm birth
Mass Spectrometry: Applications to Clinical Lab Annual Conference, Salzburg (2017).

Characterisation of vaginal swabs using Desorption electrospray ionization (DESI) MS permits rapid identification of metabolic signatures associated with preterm birth
3rd Annual Preterm Birth Conference, Liverpool (2017).

Implications of Yeast & Vaginal Microbiota Interaction on Pregnancy Outcomes.
6th annual International Human Microbiome Consortium Congress. Texas, USA (2016).

Implications of Yeast & Vaginal Microbiota Interaction on Pregnancy Outcomes.
5th Wellcome Exploring Human & Host-Microbiome Interactions in Health and Disease, Cambridge (2016).

POSTER PRESENTATIONS

High risk patient outcomes from a London Preterm Birth Surveillance Clinic. M de Carlofelice, L Sykes, P Bennet, H Lewis. 3rd European Spontaneous Preterm Birth Conference, Edinburgh (2018).

Medical swab analysis using desorption electrospray ionization mass spectrometry (DESI-MS), a novel, non-invasive approach for mucosal diagnostics. P Pruski, H Lewis, D MacIntyre, P Bennett, Z Takats. International Mass Spectrometry Conference, Toronto (2016).

Relationship between Yeast Infection and Vaginal Microbiome Composition in Pregnancy. H Lewis, L Kindinger, R Brown, T Teoh, P Bennett, D MacIntyre. Society of Reproductive Investigation Conference, Montreal (2016).

Real-time rapid medical swab analysis using DESI-MS to reveal pathogenic and inflammatory metabolomics markers. P Pruski, H Lewis, D MacIntyre, P Bennett, Z Takats. Mass Spectrometry: Applications to Clinical Lab, Salzburg (2015).

PRIZES

Royal Society of Medicine Herbert Reiss Prize: 2nd Place. (May 2019)

Society of Reproductive Investigation Presidents Prize. (March 2018)

RCOG World Congress 1st Prize Video presentation: 1st Prize. (March 2018)

Blair Bell Conference Poster presentation: 1st Prize. (March 2017)

LIST OF FIGURES

Figure 1-1. Estimated preterm birth rates by country.

Figure 1-2. Overview of definitions for preterm birth and related pregnancy outcomes.

Figure 1-3. Process of cervical remodelling with advancing gestational age.

Figure 1-4. Schematic representation of human fetal membranes and the ECM.

Figure 1-5. Transvaginal vaginal cervical length measurements.

Figure 1-6. Taxonomic allocation at genera and species levels using 16S rRNA sequencing.

Figure 1-7. From genome to metabolome; the inverted pyramid.

Figure 1-8. A Step wise workflow and time scheme for vaginal mucosal sampling.

Figure 1-9. Basic sequence of events in a mass spectrometer.

Figure 1-10. Schematic representation of a typical DESI MS experiment.

Figure 1-11. Typical mass spectrum with instrument annotations.

Figure 2-1. Overview of study design.

Figure 2-2. DESI-MS setup for medical swab analysis.

Figure 2-3. Sample preparation workflow for quality control (QC) swabs.

Figure 2-4. Pre-processing workflow for raw DESI-MS data.

Figure 2-5. Generation of PCA score and loading plots.

Figure 2-6. Statistical workflow for pilot & preterm birth studies

Figure 3-1. Overview of a mass spectrometer.

Figure 3-2. Comparison of average MS spectra of matched vaginal samples.

Figure 3-3. Average spectra for vaginal samples using different electrospray solvents.

Figure 3-4. Averaged DESI MS spectra of background runs; solvent, swab and solvent.

Figure 3-5. A DESI-MS set up showing direction of swab rotation.

Figure 3-6. different scanning positions of a swab surface using DESI-MS.

Figure 3-7. DESI-MS analysis of three vaginal swab replicates.

Figure 3-8. Comparison of biofluids to vaginal mucosa tested for quality control swab.

Figure 3-9 Averaged DESI mass spectra from pregnant and non-pregnant sample.

Figure 3-10. DESI-MS analysis of vaginal samples : pregnant vs non-pregnant.

Figure 3-11. DESI-MS analysis of vaginal samples : bacterial vaginosis vs healthy controls.

Figure 3-12. DESI-MS analysis of vaginal samples : bacterial vaginosis vs healthy controls.

Figure 4-1. DESI-MS analysis from vaginal samples : SPTB vs Controls.

Figure 4-2. DESI-MS analysis from vaginal samples : SPTB vs Controls.

Figure 4-3. abundance of hydroxyphenyllactate in SPTB vs. Controls.

Figure 4-4. PLDSA modelled on class information: SPTB vs. Controls

Figure 4-5. Comparison of the PLS-DA score plots for SPTB phenotypes.

Figure 4-6. Characterisation of CVM metabolome early SPTB vs late SPTB.

Figure 4-7. Vaginal microbial communities related to subsequent birth outcome .

Figure 4-8. Characterisation of CVM metabolomes SPTL VS PPROM.

Figure 4-9. Vaginal microbial communities related to subsequent birth outcome.

Figure 4-10. Multivariate analysis for prediction of subsequent cervical shortening.

Figure 4-11. Averaged MS spectra of vaginal samples with progesterone pessaries.

Figure 4-12. DESI-MS analysis with and without a cervical stitch.

Figure 5-1. PPROM diagnosis using DESI-MS vaginal swab metabolic profiling.

Figure 5-2. Abundance of selected metabolites following PPROM and amniotic fluid.

Figure 5-3. DESI-MS discrimination between microbial compositions following PPROM.

Figure 5-4. Prediction of PPROM by CVM metabolic profiling using DESI-MS swab analysis.

Figure 5-5. Relationship between microbial composition & metabolome prior to PPROM

LIST OF TABLES

Table 1. Risk factors associated with spontaneous preterm birth (SPTB).

Table 2. Cervical vaginal fluid biochemical markers used to assist in SPTB prediction.

Table 3. Summary of CVF metabolomic studies in relation to SPTB.

Table 4 Optimised source parameters & instrumental settings for DESI-MS analysis.

Table 5. BV metabolites differentially expressed in metabolic profiling studies.

Table 6. Demographic characteristics of before and after SPTB vs Controls.

Table 7. Metabolites differentially expressed SPTB vs Controls.

Table 8. Metabolites differentially expressed in late SPTB vs early SPTB.

Table 9. Metabolites abundant in early pregnancy in SPTL vs PPROM.

Table 10. Demographic characteristics before and after PPROM vs Controls.

Table 11. Metabolites abundant in *Lactobacillus* spp. dominant & deplete before PPROM.

Table 12. Metabolites differentially expressed in BV vs Healthy Controls.

Table 13. Metabolites differentially expressed before PPROM vs Controls.

Table 14. Metabolites abundant in *Lactobacillus* dominant & deplete POST PPROM.

Table 15. Metabolites abundant in subsequent PPROM VS CONTROLS.

ABBREVIATIONS

AF	Amniotic fluid
BMI	body mass index
bp	base pair (bp)
BV	Bacterial vaginosis
BVAB	Bacterial vaginosis associated bacteria
CI	Confidence interval
CRH	Corticotrophin releasing hormone
CL	Cervical length
CST	Community state type
CV	Cross validation
CVF	Cervico-vaginal fluid
CVM	Cervico-vaginal mucosa
Da	Dalton
DAG	Diacylglycerol
DESI-MS	Desorption electrospray ionisation MS
ECM	Extracellular matrix
ER	Estrogen receptor
ESI(-)/(+)	Electrospray ionisation –or + mode
FDA	Food and Drug Administration
GBS	Group B Streptococcus
GC-MS	Gas chromatography mass spectrometry
GWAS	Genome wide association study
HCA	Hierarchical clustering analysis
HIC	High income countries
HILIC	Hydrophilic interaction liquid
HPLC	High performance liquid chromatography
HVS	High vaginal swab
IGFBP-1	Insulin like growth factor binding protein-1
IL	Interleukin
IQR	Inter-quartile range
KEGG	Kyoto encyclopaedia of genes and genomes
LC-MS	Liquid chromatography mass spectrometry
LIC	Low income countries
LLETZ	Large Loop Excision of the Transformation Zone
MMPs	Matrix metalloproteinases
MS	Mass spectrometry
MS/MS	Tandem mass spectrometry
<i>mz</i>	Mass-to-charge ratio
NF- κ B	Nuclear factor – kappa B

Pregnancy Risk Stratification using DESI-MS Profiling of Vaginal Mucosa

NGS	Next generation sequencing
NHS	National Health Service
NMR	Nuclear Magnetic Resonance
NPV	Negative predictive value
PAMG-1	Placental alpha macroglobulin-1
PA	Phosphatidic acid
PCA	Principal component analysis
PCR	Polymerase chain reaction
PE	Phosphatidylethanolamine
PI	Phosphatidylinositol
PLSDA	Partial least squares Discriminant Analysis
POC	Point of care
PPROM	Preterm pre-labour rupture of membranes
PPV	Positive predictive value
PV	<i>per vaginam</i>
Q-ToF	Quadrupole time of flight
RCT	Randomised controlled trial
RCOG	Royal College of Obstetricians and Gynaecologists
REIMS	Rapid evaporative ionisation MS
RF	Random Forest
RPM	Revolutions per minute
spp.	<i>Species pluralis</i> , Latin for multiple species
SPTB	Spontaneous preterm birth
SPTL	Spontaneous preterm labour
STAMP	Statistical Analysis of Metagenomic Profiles
TAG	Triacylglycerol
TG	Triglyceride
TIC	Total ion count
TVUS	Trans-vaginal ultrasound scan
WHO	World Health Organisation
µg	Micrograms

TABLE OF CONTENTS

1	INTRODUCTION	17
1.1	Preterm Birth	18
1.2	Physiology of Normal Parturition.....	21
1.3	Pathophysiology of Preterm Birth.....	27
1.4	Prediction and Stratification of Preterm Birth Aetiology.....	31
1.5	Prevention of Preterm birth.....	36
1.6	The Vaginal Microbiome.....	41
1.7	The Host Immune Response	44
1.8	Systems Biology Approaches to Parturition and Preterm Birth.....	46
1.9	Justification and Hypothesis for Project.....	55
1.10	Aims	56
2	MATERIAL AND METHODS	57
2.1	Materials.....	58
2.2	Prospective Vaginal Mucosal Metabolome & Microbiome Studies	59
2.3	Vaginal Mucosal Metabolic Profiling by DESI-MS.....	62
2.4	Assessment of Vaginal Microbiota.....	69
3	DEVELOPMENT OF DIRECT SWAB METABOLIC PROFILING BY DESI-MS	72
3.1	Introduction	73
3.2	Study Design.....	74
3.3	Results: Optimisation of DESI-MS for Direct Swab Analysis.....	75
3.4	Results: Pilot Study	85
3.5	Discussion.....	91
3.6	Conclusion.....	96
4	CHARACTERISATION OF CVM CHANGES ASSOCIATED WITH PRETERM BIRTH	97
4.1	Chapter Summary	98
4.2	Introduction	100
4.3	Study Design.....	102
4.4	Results.....	103
4.5	Discussion.....	118
4.6	Conclusion.....	122
5	DIRECT SWAB ANALYSIS BY DESI-MS FOR PREDICTION, DIAGNOSIS AND RISK STRATIFICATION OF PPRM	123
5.1	Chapter Summary	124
5.2	Introduction	126

5.3	Study Design.....	128
5.4	Statistical Analysis.....	128
5.5	Results.....	129
5.6	Discussion.....	140
5.7	Conclusion.....	145
6	DISCUSSION	146
6.1	Introduction.....	147
6.2	Summary of Study Findings and Translation into Clinical Practice.....	147
6.3	Limitations and Future Work.....	150
6.4	Conclusion.....	151
7	REFERENCES	152
8	APPENDICES	179

1 INTRODUCTION

1.1 Preterm Birth

1.1.1 Preterm birth; a global health issue

Preterm birth (PTB), defined as delivery prior to 37 weeks gestational age is a major global health issue, affecting 15 million births worldwide [1]. It is the largest single cause of childhood death under five years of age [2] and responsible for more than half of all neonatal deaths [3]. Survivors have higher rates of long term morbidities including developmental and neurological disabilities compared to children born at term [4].

Based on data from 184 countries, the worldwide average PTB rate in 2010 was estimated to be 11 %; ranging from 5% in northern Europe to 18% in sub-Saharan Africa [1]. Contributing factors to higher rates in low income countries (LIC) include increased birth rates and limited access to antenatal care in pregnancy. A lack of availability of neonatal expertise following delivery, also contributes to higher rates of neonatal morbidity in these countries [5].

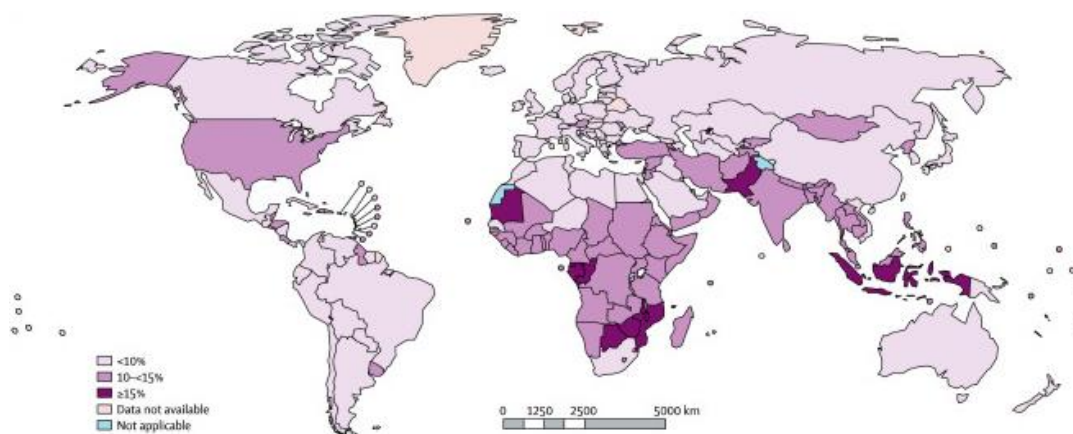


Figure 1-1. Estimated preterm birth rates by country for the year 2010. Reproduced from Blencowe et al. [2]

However, preterm birth is a truly global problem; in high income countries (HIC), the incidence of PTB over the last 2 decades has remained largely unchanged despite better healthcare resources. Some countries, including the USA, have even experienced increased rates of preterm birth over recent periods [1], which can be only partly attributed to increased rates of conception in older mothers, more frequent use of assisted reproduction techniques and higher rates of non-clinically indicated premature delivery [6]. In 2006 the preterm birth rate peaked in USA at 12.8%, although this rate declined to 9.6 % in 2015 more recently the rate has increased again to 9.9% in 2017 [7]. This is higher than other countries particularly in Europe. Sweden and Luxembourg have the lowest worldwide rate (5%) whilst UK ranks 50th out of 184 countries with an overall preterm birth rate of 7.4% in 2013 [8].

PTB rates differ by ethnicity and socioeconomic groups so within countries there can be regional differences depending on the local population. PTB rates in the UK are 7.0%, 8.0%, 10.0% and 7.5% for White, Black African, Black Caribbean and Asian mothers respectively [8]. Similarly in USA, PTB rates prior to 32 weeks were found to be twice as high in Afro-Americans compared to white women [7]. This is consistent with the global incidence of preterm birth which estimates that greater than 60% of all PTB cases occur in Africa and Asia in 2010 [1].

The WHO global action on preterm birth “Born Too Soon” report set a 50% reduction goal for preterm-specific mortality by 2025 [9]. To realistically hit this target, there is an urgent need for research into the underlying mechanisms of preterm birth and the development of diagnostic and prevention strategies to target PTB more effectively.

1.1.2 Defining preterm birth

PTB includes clinically indicated deliveries for maternal or fetal indications (30-35%) as well as spontaneous PTB (SPTB) (65-70%). In this thesis, only SPTB will be considered as a study focus.

SPTB can be categorised by two main presentations or phenotypes. Spontaneous preterm labour (SPTL), which is dilation of cervix with or without painful contractions and ultimate delivery, accounts for 40-45% all SPTB cases. Preterm premature rupture of membranes (PPROM) is initially not associated with uterine activity and is preceded by a latency period (time from rupture to delivery) of at least 24 hours before labour starts, and accounts for 25-30% of cases [10]. Despite being clearly different phenotypes, SPTL and PPRM are often combined into the same patient group, which may inadvertently prevent aetiology-specific differences in mechanism being identified [11, 12].

SPTB can also be sub-divided on the basis of gestational age at delivery; late preterm (32-36 weeks) very preterm (28-32 weeks) or extremely preterm (<28 weeks) [11]. These distinctions are of clinical importance as morbidity and mortality increases significantly as gestational age decreases and so the obstetric management often differs as a consequence of this (Figure 1-2). There is also a dramatic difference in survival of premature babies in LIC vs high income countries (HIC) at different gestational ages. For example, more than 90% of extremely preterm babies (less than 28 weeks) born in LIC die within days of life; yet less than 10% of extremely preterm babies die in HIC [1].

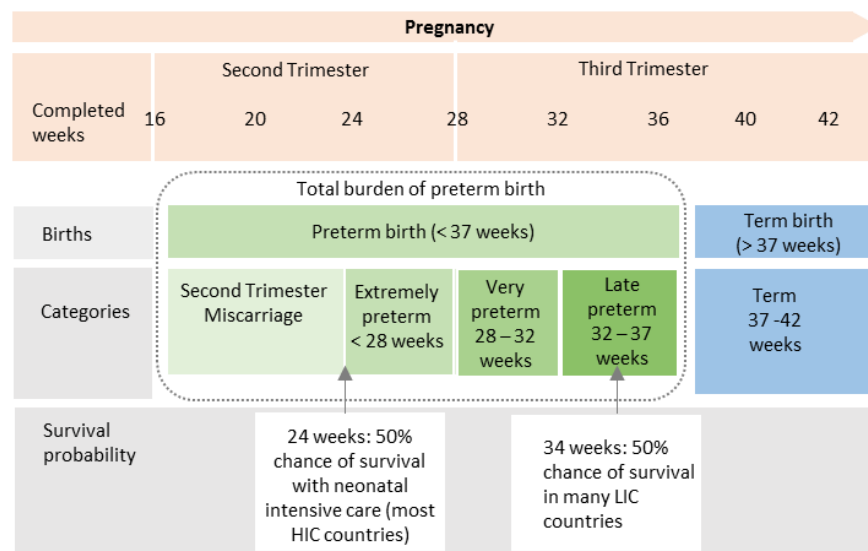


Figure 1-2. Overview of definitions for preterm birth and related pregnancy outcomes in HIC (high income countries) vs LIC (low income countries). Source: Adapted from Blencowe et al; 2011.) [1]

The lower cut off for SPTB is not specific and perceptions of viability (gestational age at which fetus is considered a baby) of extremely preterm babies changes depending upon the sophistication of neonatal intensive care that can be provided [3]. In most HIC, including the UK, 24 weeks is generally accepted as the limit of viability however neonates as young as 23 weeks are increasingly surviving with intensive neonatal support [9]. In some LIC, neonatal weight is used to determine viability and active resuscitation is only carried out if greater than 1 kg as prognosis without intensive neonatal care facilities is poor.

1.1.3 Neonatal morbidity and mortality

The severity of neonatal morbidity relates to the extremity of prematurity with earlier gestational age at birth correlating with poorer prognosis [13, 14]. Immediate complications include bronchopulmonary dysplasia, neonatal sepsis, intraventricular haemorrhage, retinopathy of prematurity and necrotising enterocolitis [15]. Longer-term conditions can be a direct consequence of immaturity at the time birth or arise from complications in early life e.g. sepsis. These include cerebral palsy, global developmental delay, chronic lung disease and visual impairment [16, 17]. Prematurity has adverse effects on IQ as shown in epidemiological studies following up cohorts of children born at less than 26 weeks [14]. The impact of prematurity can also be apparent in babies born at later gestational ages. A recent study reported a 36% increased risk of achievement below expected level as measured by standardized assessments in school age children when born at less than 34 weeks compared with term controls [18].

1.1.4 Financial and emotional toll of prematurity

The financial burden of preterm birth on the public sector has been estimated to be £3 billion per year with the largest contribution being related to neonatal inpatient costs after birth [19]. The personal economic impact upon families that experience premature deliveries are related to hospital stays of several months as well as reduced income due to extended maternity leave. Emotionally, prematurity is associated with increased rates of postnatal depression [20] and parental stress related to unknown prognosis of their child which may take months or years to fully manifest. Caring for a child with health problems such as cerebral palsy can entail greater medical costs, employment constraints, and childcare challenges. These demands may affect the health of the parents due to increased levels of stress, emotional problems and depression [21].

1.2 Physiology of Normal Parturition

The parturition pathway of labour involves a highly regulated interplay of anatomical, biochemical, immunological and endocrine events that occur in both the mother and fetus [22]. A clinical description of these events include; (1) cervical ripening (dilation and effacement); (2) decidua/fetal membrane activation and (3) myometrial activation and contractility as described below. These are mediated by inflammatory and endocrine pathways over a period of days to weeks which culminates in the birth of a neonate followed by placental separation and uterine involution [23-25].

1.2.1 Cervical Change

The function of the cervix is to retain and protect the growing fetus during pregnancy by creating an anatomical barrier with sufficient length and a mucus plug that can deter ascending microbes from the lower genital tract. Furthermore the cervix is thought to provide immunological protection through production of cytokines and antimicrobial properties [26, 27].

In early pregnancy the cervix is firm, composed of a highly cross-linked extracellular matrix (ECM) dominated by collagen fibres type I and type 2, that provide mechanical strength to maintain cervical closure [26, 28]. Towards term, this collagen-dense matrix is remodelled into a compliant structure that allows the fetus to pass through during the ultimate stage of labour. "Cervical remodelling" is the collective term for progressive cervical change and recovery during pregnancy and involves three pre-partum overlapping phases [29]. An overview is shown in figure 1.3 with the underlying proposed biochemical processes described.

Phase 1, is a long progressive softening phase that is associated with decreased collagen crosslinking [30], changes in the organisation of collagen fibrils, a reduction in proteoglycans which control packing of collagen fibrils [31, 32] and a transition in mature to immature collagen cross-links which increases tissue compliance [33]. In addition to these collagen changes, cervical softening is also likely to require alterations to other matrix proteins (e.g. thrombospondin2 and tenascin-C) that modulate collagen formation and interactions between cells and the ECM [34].

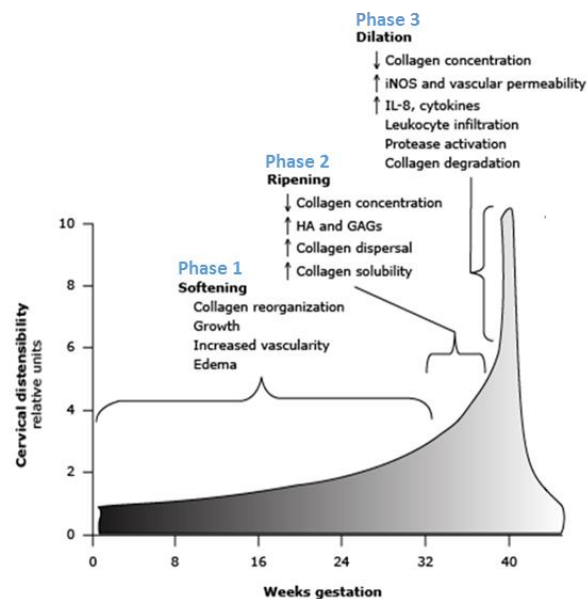


Figure 1-3. The process of cervical remodelling that occurs with a dvancing gestational age (Reproduced from Word et al 2007) [29]

Phase 2 is an accelerated phase of softening and increasing compliance near the end of pregnancy. It is defined as “ripening”, because in this stage, the cervix begins to shorten and thin out. Biochemical events include a decrease in collagen concentration secondary to a decline in both collagen synthesis and increased collagenase and matrix metalloproteinases (MMPs) activity that degrade the ECM [35-37]. Human in vivo studies using a collascope that estimates collagen concentration via fluorescence, have shown that collagen gradually decreases as pregnancy approaches the third trimester [38, 39]. A study of peri-partum cervical biopsies found a greater density of macrophages at end of pregnancy prior the onset of spontaneous term and preterm labour [40] supporting the hypothesis that ripening of the cervix at term reflects an inflammatory process that may be triggered prematurely in the case of SPTB. Cervical ripening has also been associated with an influx in cervical prostaglandin, pro inflammatory cytokines [41, 42], cell adhesion molecules, an increase in nitric oxide synthase production [43-45], and a decrease in prostaglandin breakdown [46].

In Phase 3 there is active dilation of the cervix prior to delivery. Due to the combination of biochemical changes, mechanical forces, and activation of inflammatory pathways, the already softened cervix dilates to efface with the uterus. To date, neither the way in which these elements interact or any of their underlying molecular mechanisms have been fully clarified.

1.2.2 Decidual/membrane activation

The chorio-amniotic membranes surround and protect the growing fetus from infections as well as mediate exchange of nutrients together with the placenta. Around the chorio-amniotic membranes is the decidua which is a thick layer of uterine endometrial cells. Amnio-chorionic membranes are comprised of 8 layers with 5 of these layers composing the amnion which is the fetal component of the membranes and 3 make up the chorion (Figure 1-4).

The first amnion layer is the epithelium, which rests on the basement membrane. Beneath the basement membrane lies the compact layer composed of types I, III, V and VI collagens secreted by the mesenchymal cells in the fibroblast layer. The spongy layer lies below the fibroblast layer, consisting of proteoglycans and glycoproteins and type III collagen. It separates the amnion from the chorion and allows the amnion to slide on the underlying chorion. The inner most layer of the chorion is the reticular layer, followed by the pseudo basement membrane and trophoblast layers. The ability of the fetal membranes to maintain integrity and withstand stretch imposed by the growing fetus and increasing liquor volume is largely maintained by the extracellular matrix (ECM), which is made up of both non-collagen components (hyaluronan, biglycan, decorin, elastin, and fibronectin) and collagens [47]. The latter is believed to provide the tensile strength of the membranes especially through type I and III interstitial collagens in the compact layers and type IV collagen in the basement and pseudo basement membranes [48].

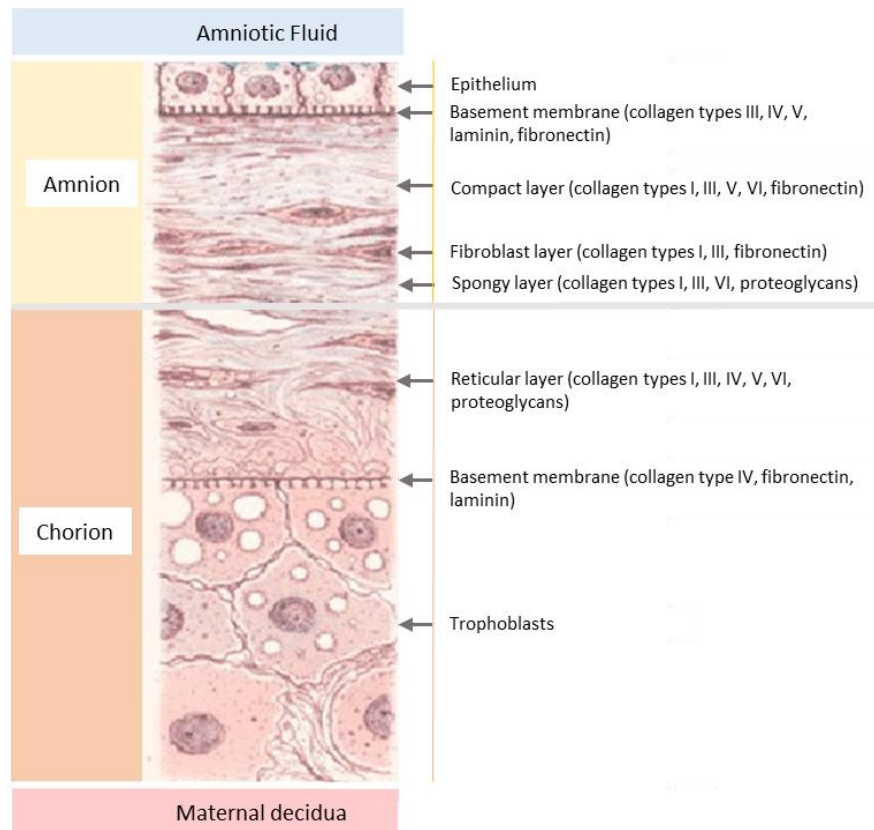


Figure 1-4. Schematic representation of human fetal membranes and the extracellular matrix composition.

Membrane activation consists of a complex sequence of biochemical and anatomical events which culminate in the separation of fetal chorioamniotic membranes from the maternally derived decidua with subsequent rupture of the membranes, delivery of the fetus and finally, the placenta. Collagens are degraded by a variety of collagenases, gelatinases, and stromelysins collectively belonging to the MMP (matrix metalloproteinases), a family of potent enzymes, which act on fibrillar collagen and the basement membrane [49]. Alterations in ECM content and composition of the fetal membrane are mediated in part by the balance of MMP and TIMP (tissue inhibitor of metalloproteinase). The fibrillar collagens (types I, II, III, V, XXIV, and XXVII) differ with respect to their susceptibility to cleavage by MMPs [47, 50]. MMP-1, MMP-2, MMP-3, MMP-8 and MMP-9 have been detected in amniochorion [51] and there is evidence that in particular MMP-9 is involved in remodelling of the amnion leading to weakness and susceptibility to membrane rupture [11].

It has been hypothesized that rupture of membranes at term is the consequence of the mechanical stresses of labour acting upon biochemically altered, pre-weakened fetal membranes [52, 53]. In normal parturition, activation of inflammatory innate pathways in the decidua and fetal membranes produce chemokines and cytokines. The pro-inflammatory

cytokines IL-1 β and IL-8 are up-regulated during labour in the amnion as are IL-6 and IL-8 in the chorio-decidea [42]. These trigger the release of matrix metalloproteinases (e.g. MMP-8, MMP-9) [54-56] and prostaglandins (e.g. PGE₂) [57], which degrade the extracellular matrix proteins of the chorio-amniotic membrane causing alterations in fetal membrane structure [58-60]. This is not demonstrated globally however, rather as a localised change or “altered morphology” in the para cervical region [61] where MMP mediated collagen remodelling and apoptosis drive subsequent structural weakening [48, 50, 52, 62]. These changes occur in the membranes at late gestation [45] and have been identified in samples taken at caesarean section without labour at term, implying they precede the onset of labour [50, 62].

1.2.3 Myometrial activation and contractility

The myometrium is the smooth muscle layer within the uterine wall which spontaneously contracts when stretched [63]. Uterine contractions result from the coupling of actin and myosin filaments within this layer. In pregnancy contractility is suppressed to permit uterine expansion to accommodate the growing fetus [64]. Uterine quiescence is largely mediated by the progesterone which appears to inhibit uterine excitability by the downregulation of proteins involved in the cross-linking of actin and myosin filaments [65]. It is hypothesised that at the end of gestation the uterus reaches capacity and the tensile force exerted exceeds inhibitory control, which in conjunction with functional progesterone withdrawal, initiates smooth muscle contractions [66]. Increased uterine tension induces an upregulation of labour associated proteins including ion channels, oxytocin receptors [67], ECM ligand proteins [68], focal adhesion kinases [69], prostaglandin receptors and myometrial gap junctions [70]. K⁺ channels ion channels regulate the excitability of myometrial cells [71]. Gap junction proteins such as connexins (connexin-43, connexin-40 and connexin-45) regulate contractility by controlling the interactions between myocytes for the propagation of action potentials through the myometrium [72].

As pregnancy advances toward term, circulating levels of the uterotonic hormone oxytocin rise. This hormone is released from the posterior pituitary gland and acts on the oxytocin receptor (OTR) leading to activation of Phospholipase C at the plasma membrane of the smooth muscle cells. This stimulates the production of diacylglycerol (DAG) and inositol triphosphate and which release Ca²⁺ from the intracellular stores which is required for actin-myosin coupling and contraction of myocytes [73, 74]. As pregnancy advances towards term, there is an increase expression of myometrial OTR concentration [75] which intensifies their action on the myometrial smooth muscle. Oxytocin also stimulates prostaglandin release which activates

inflammatory pathways via NF- κ B [76] which causes up regulation of pro-labour genes including cyclooxygenase type 2 (COX-2) and OTR [77, 78]. In addition to this there is also a shift in signalling between anti-inflammatory and pro-inflammatory pathways [22] with the influx of activated leukocytes to the myometrium and cervix, releasing cytokines that promote further prostaglandin synthesis [79, 80].

In combination, labour associated proteins prime the uterus for contractile stimuli provided by uterotonics including prostaglandins, corticotrophin-releasing hormone and oxytocin [81]. These convert low amplitude long lasting uterine tightenings that are experienced throughout pregnancy called “Braxton Hicks” [82] into the strong, rhythmic, synchronized contractions of labour.

1.2.4 Endocrine Function

Progesterone is a steroid hormone initially produced by the corpus luteum until 10 weeks gestation. The placenta then becomes the major source of progesterone during the rest of pregnancy, with serum levels increasing progressively until delivery [83]. Progesterone primarily acts to maintain myometrial and cervical quiescence through its capacity to promote anti-inflammatory and pro-relaxant pathways in the uterus. Progesterone also acts on the cervix by limiting prostaglandin induced collagenous remodelling of the cervical fibroblast [84-86].

A number of theories exist to explain how functional progesterone withdrawal occurs, including alterations in the ratio of nuclear progesterone receptor’s PR-A and PR-B expression at term [87], conversion of progesterone to an inactive form within the target cell before interacting with its receptor [88] or inflammation resulting in NF- κ B-mediated PR expression [89].

One of the hypotheses postulates that the differential expression of the progesterone receptor isoforms, PR-A and PR-B contributes to a functional withdrawal of progesterone and the onset of labour. These PR have opposing pro- and anti-inflammatory downstream effects. In pregnancy, endogenous progesterone is thought to have a largely anti-inflammatory downstream effects via PR-B dominant signalling [90, 91], which suppresses NF- κ B reducing prostaglandin and cytokine production [92, 93] and other pro-contractile genes, therefore inhibiting myometrial activation and promoting quiescence [94]. Throughout pregnancy, progesterone signalling is mediated by dominant expression of the full length receptor, PR-B. Toward the end of pregnancy, increased expression of the transcriptionally inactive, truncated PR-A isoform, results in an increase in the PR-A:PR-B ratio and removal of the anti-

inflammatory/anti-labour actions of progesterone and a shift towards a pro-inflammatory/pro-labour state [90].

Although there is a lack of compelling evidence to support any of these hypotheses on the mechanism of progesterone withdrawal, the theory of a 'functional withdrawal' remains valid since disruption of progesterone signalling through the administration of the PR antagonist, Mifepristone (RU486) at any stage of pregnancy induces the onset of labour. This has been shown in mice [95], rats [96] and women [97] while the treatment of pregnant rodents with progesterone delays myometrial contractions and parturition [98].

Rising levels of bioactive corticotrophin-releasing hormone (CRH) have also been proposed as the stimulus for uterine activation. CRH derived from the placenta is secreted into the maternal circulation in large amounts which increases across gestation peaking at the time of parturition [99]. CRH binding protein (CRHBP) is bound to CRH during pregnancy limiting its bioavailability and function. However during the third trimester, CRHBP levels decline and CRH is able to stimulate the production of prostaglandins via the up regulation of prostaglandin synthetic enzymes genes located in the amnion [100]. CRH also directly stimulates the production of MMPs in the amnion [101] and cervix [40]. CRH crosses the placenta to enter the fetal circulation and stimulates the fetal pituitary and adrenal glands resulting in the release of corticotrophin, cortisol and dehydroepiandrosterone (DHEA) [102]. Cortisol stimulates fetal lung maturation and the production of surfactant A and phospholipids, which are both pro-inflammatory and activate macrophages within the amniotic fluid [103]. DHEA is metabolised in the placenta to estrogen. This hormone is also produced and metabolised by the materno-fetal membranes and decidua during pregnancy [104]. Regulation of myometrial contractility is influenced by circulating estrogen which exerts pro-contractile effects through acting on the estrogen receptor (ER), ER α . Throughout pregnancy, progesterone inhibits expression of this receptor [105] however following functional progesterone withdrawal there is increased expression of ER α , which allows estrogen to promote myometrial contractility by increasing expression of gap junctions and synthesis of prostaglandins [90, 105].

1.3 Pathophysiology of Preterm Birth

The current hypothesis by which the length of human pregnancy is controlled proposes carefully regulated interactions between endocrine, mechanical and immune factors which collectively determine the timing of onset of labour. "Biological clocks" regulate these factors and thus

pregnancy length. Preterm birth is a consequence of one or more of the 'clocks' being chronologically advanced, or protective mechanisms breaking down [106, 107].

The Placental Clock

The Placental Clock Theory [108] proposes that the duration of human pregnancy is regulated through increasing placental CRH production as gestation advances. Prior to the onset of labour CRH concentrations exceed levels of CRHBP stimulating expression of labour associated genes and prostaglandin synthetic enzymes. In some pregnancies destined to deliver preterm, the rise in CRH is seen to occur earlier [107].

Abnormalities of placentation also increase the risk of preterm birth. Higher failure rate of physiologic transformation of the myometrial spiral arteries in women with preterm labour with intact membranes and those with PPROM has been observed compared to those that deliver at term [109, 110].

Vaginal bleeding during the first trimester is associated with a 2-fold increased risk of SPTB [111], this increases to 7-fold increase if the bleeding persists into the second trimester [112]. Following a term delivery, histological evidence of a decidual haemorrhage is 0.8% however historical haemorrhage is noted following PPROM and SPTL in 37.5% and 36% respectively [113]. Decidual necrosis and haemorrhage cause production of thrombin which converts fibrinogen to fibrin an essential component of clot formation. Thrombin also upregulates prostaglandin production in the amnion causing myometrial contractility and inducing an inflammatory response by activating neutrophils, and may enhance cervical ripening by activating matrix metalloproteinases [114].

Mechanical clock

A further factor thought to influence the length of human pregnancy is mechanical signal transduction [65]. At the end of gestation the uterus reaches capacity and the tensile force exerted exceeds inhibitory control, which in conjunction with functional progesterone withdrawal, initiates smooth muscle contractions [66]. In situations where the uterus expands more rapidly than normal, the balance between mechanical and endocrine signals will be affected with earlier stretch induced upregulation of labour associated proteins leading to preterm labour. Consistent with this preterm birth is more common in multiple pregnancies [7] polyhydramnios [66] and fetal macrosomia [115]. Fusion anomalies of the mullerian tract (unicornuate, bicornuate and didelphys uterus) are also associated with an 7-fold increase risk

of preterm birth [116] which is probably caused by limited ability of the uterus to expand to full term.

Immunological Clock

Immunological studies focusing upon the “immune clock of pregnancy” have demonstrated enhanced immunological function as gestation progresses [117, 118]. Complex yet highly coordinated, immune adaptations in healthy pregnancy have been identified with heightened TLR4 response in neutrophils and up regulation of T-cells peaking between 20-30 weeks of gestation. It is proposed that this results in a primed immunological state that may be more sensitive to pathogenic bacteria during this phase of pregnancy [119].

1.3.1 Inflammation and infection

Infection and associated inflammation is implicated in 40% of SPTB cases [120]. The evidence supporting the role of infection includes animal studies [121, 122] in which SPTB or miscarriage can be induced following the administration of bacteria or bacterial products. Local and systemic maternal infections such as pyelonephritis [123] and malaria [124] have also been associated with STPB. Intra-amniotic infection is also often associated with premature birth [125, 126]. It has been suggested that this may originate from the placenta which has a microbiome seeded from the oral microbiome [127]. However subsequent studies have concluded that placental bacterial load is very low and that bacterial DNA sequences amplified from normal placental tissue are likely to have been derived from laboratory contaminants rather than a genuine microbiome [128, 129]. The most common and plausible source for infection is pathogenic bacteria colonising the vagina, ascending the mucosal surfaces to the cervix and fetal membranes [130]. Supporting this concept; micro-organisms identified in the amniotic fluid of women in preterm labour are often observed in matched samples but there is an absence of bacteria in the sub-epithelial part of the amnion [130, 131]. Inflammatory cytokines strongly associated with SPTB have been found in cervico-vaginal fluid (CVF) and amniotic fluid, but not in plasma [132]. Furthermore when a preterm labour is complicated by chorioamnionitis, at the site of membrane rupture which is overlying the cervix there is histological evidence of chorion thinning and high bacteria load [133, 134].

The incidence of infection is higher in SPTB at earlier gestations. Studies based on histologic and microbiologic criteria have shown that in deliveries at less than 28 weeks 85% show evidence of intrauterine infection [135, 136] while at 34–36 weeks, only about 15-20% show this relationship [137, 138]. Depletion of Lactobacilli and increased bacterial diversity and load (e.g.

BV) is associated with increased risk of SPTB [139, 140]. SPTB has also been associated with specific species such as *Atopobium vaginae*, *Gardnerella vaginalis* [141], *Mycoplasma hominis* [142], *Prevotella* spp. [143] and *Ureaplasma urealyticum* [144].

Although the exact mechanism responsible for infection-mediated SPTB is not completely understood, a widely accepted paradigm is that perturbations to the vaginal microbiome allow colonisation by opportunistic pathogens which stimulates the host innate immune response [130]. This potential to be activated is also influenced by genetic predisposition [145, 146] and immunological state of pregnancy [117]. At 20-30 weeks of gestation age, it is hypothesised that this could be due to a potentially primed immunological state that may be more sensitive to pathogenic bacteria. Consistent with this a recent study showed that women destined for PPRM had a high prevalence of *Lactobacillus* spp. deplete communities at 24–30 weeks gestation. In contrast, women with subsequent term deliveries had predominately *Lactobacillus* spp. dominance at this stage of gestation [119]. These trends are consistent with a recent meta-analysis examining the vaginal microbiome during pregnancy, which reported that diversity increased throughout early pregnancy peaking between 20 and 29 weeks in women with subsequent SPTB, but fell progressively across gestation in women with term deliveries [147].

Following the stimulation of the host innate immune response by pathogens there is subsequent activation of pro-inflammatory transcription factors NF- κ B and AP-1. These initiate trafficking of immune cell and leucocyte infiltration, which drives cytokine and MMP production leading to collagen breakdown, prostaglandin release, cervical shortening, fetal membrane stretch and rupture. NF- κ B and AP-1 activation also drives labour associated gene expression in the myometrium resulting in myometrial contractions, and ultimately preterm labour and delivery [24].

1.3.2 Genetic factors

There is a clear role of genetics in the aetiology of SPTB [148] with racial and familial predisposition to PTB and identification of genetic polymorphisms via candidate gene studies and genome-wide association studies (GWAS).

Black women are twice as likely to deliver preterm compared to Caucasian women even following correction for socio-economic, educational and nutritional status [149]. Women who have had a previous SPTB are at increased risk of early delivery in a subsequent pregnancy. Furthermore, if they themselves were born preterm or if her mother or sisters had preterm deliveries their risk of SPTB is higher [150, 151]. There is also an association with maternal

Ehlers–Danlos syndrome and SPTB usually caused by PPRM. The risk is 12.5% if just the mother is affected, increasing to 40% if the fetus is affected [152]. Candidate gene studies have suggested a potential association between preterm birth and polymorphisms in genes involved in immunity and inflammation such as MMPS [153, 154], and cytokines/cytokine receptors [145, 155, 156] that are significantly associated with preterm birth however the results have generally failed to be replicated or generalized across populations [157, 158]. The disparate results could be related to the polymorphisms investigated, inconsistent phenotype definitions, small sample size and population differences [146]. A recently published large GWAS study that examined 44,000 white women, identified several maternal loci (EBF1, EEFSEC, and AGTR2) that may contribute to preterm birth [159].

1.3.3 Cervical insufficiency

Cervical insufficiency can be defined as the failure to maintain a pregnancy due to painless cervical dilatation in the absence of uterine contractions with no precipitating factors. It is generally attributed to a structural weakness of the cervix [160]. The incidence of cervical insufficiency is difficult to ascertain and is usually diagnosed retrospectively after a mid-trimester loss or early PTB. It is estimated that approximately 1% of all women are affected [161] with the recurrence risk of a subsequent SPTB in these women being 11 times higher compared to those with prior full-term delivery [162].

Although several theories of pathophysiology have been considered, the difficulty in obtaining biopsy samples from a human cervix before, during, and after deliveries, has hampered study of this aetiology. In some women it is thought there is an inherent biomechanical weakness of the cervix. This is supported by studies that have found lower cervical collagen concentration in women with a prior history of cervical insufficiency compared to those with prior term births [163, 164]. A weakened cervix may also be due to previous birth trauma [165], excisional treatment such as Large Loop Excision of the Transformation Zone (LLETZ) [166], damage during full dilation caesarean section [167] and over-dilation of the cervix during pregnancy termination [168]. Another hypothesis is that cervical insufficiency is associated with preterm ripening [39] caused by infection or an inappropriate inflammatory response [131, 169].

1.4 Prediction and Stratification of Preterm Birth Aetiology

Current treatment strategies for the prevention of preterm birth (Section 1.5) are limited in their effectiveness. One of the main reasons for this is because treatments are typically administered after patients have presented with symptoms (e.g. a short cervix, uterine contractions). The

ability to identify women at risk of preterm birth, and the underlying aetiology, early in pregnancy would facilitate appropriate antenatal management plans that may include risk modification (e.g. smoking cessation, microbial modulation) and targeting prophylactic interventions (e.g. cervical cerclage or progesterone). Risk prediction for symptomatic/asymptomatic women close to the time of delivery would still hold value in determining immediate management options such as corticosteroids administration for fetal lung maturation magnesium sulphate for fetal neuroprotection and transfer to hospital with the expertise to ensure optimal neonatal care. The current available prediction methods for SPTB are discussed below.

1.4.1 Presentation and risk Factors

Clinical risk factors for SPTB include demographic, behavioural and obstetric factors (Table 1). The strongest risk factor for PTB is a previous PTB before 34 weeks' gestation with a relative risk of 13 [170]. However, this is obviously only applicable to women with previous obstetric history and not useful for primigravid women. Although some demographic and baseline characteristics can provide insight into women that may benefit from closer surveillance, using risk factor assessment alone as a predictor of PTB is unreliable as over 50% of pregnancies that deliver preterm have none of these risk factors present [171].

Table 1. Demographic, obstetric and behavioural risk factors shown to be associated with spontaneous preterm birth

Demographic Characteristics	Obstetric History	Behavioural Factors
Low socioeconomic status	Previous PTB	Smoking
Poor antenatal care	Previous cone biopsy	Illicit drug use
Extremes of maternal age	Multiple pregnancy	Alcohol consumption
Malnutrition	Short cervix	Heavy physical work
	Uterine malformation	Stress

1.4.2 Cervical length estimation by ultrasound

Based on work in the 1990's by Iams et al., [172] and Heath et al., [173], pregnant women can be clinically stratified as to their risk of spontaneous preterm birth according to their mid trimester (16-24 weeks) cervical length (CL) measurement. This is typically obtained through transvaginal ultrasound scanning by plotting the distance between the internal and external cervical os as shown in figure 1.5 [174]. This technique is safe, reliable, and highly reproducible

when performed by trained providers [175]. A normal CL, considered to be over the 10th centile (>25mm) is reassuring and typically 90% will deliver at term [176]. CL < 25mm doubles the risk of PTB in women with previous PTB [174]. Despite this, routine mid-trimester screening for short cervical length in a “low risk population” is not currently recommended [174, 177]. The low incidence of short cervix in this group limits its utility as a screening test and furthermore, a recent study of low risk nulliparous women reported that only 23 % of SPTB cases were identified by transvaginal cervical length screening [175]. These findings are consistent other smaller studies that suggest only a small proportion of those without a history of a prior SPTB can be identified by transvaginal CL screening [178-180] However despite low sensitivity and predictive value, cervical length is currently the only predictor for which effective interventions are potentially available i.e. a cervical cerclage or progesterone.

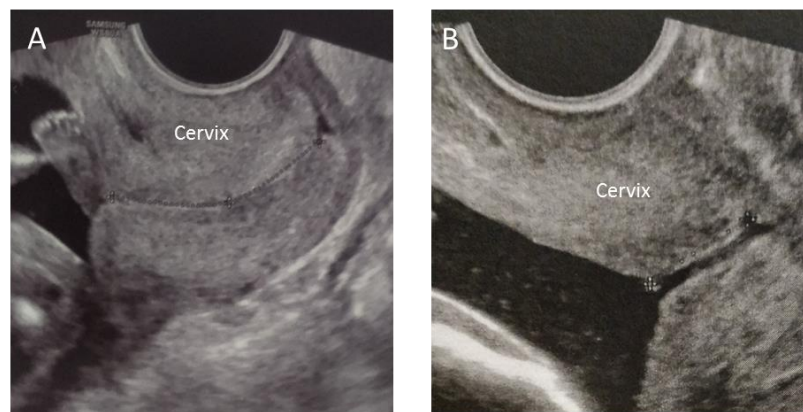


Figure 1-5. Transvaginal vaginal cervical length measurements (A): long, closed cervix, (B): shortened cervix. Source: Dr Holly Lewis, Imperial College NHS Trust prematurity clinic.

1.4.3 Biomarkers of Preterm Birth

There are several cervical vaginal fluid (CVF) biochemical markers that are used to assist in SPTB prediction. These include Fetal fibronectin (fFN), Phosphorylated insulin-like growth factor binding protein-1 (pIIGFBP1) and Placental alpha macroglobulin [181]. The physiological basis, as well as the limitations of each test are examined below.

- ***Fetal Fibronectin***

fFN is an extracellular matrix glycoprotein produced by fetal cells located between the chorion and decidua [182]. Following fusion of these tissues at the fetal-maternal interface, fFN concentrations decrease and may become undetectable from 18 weeks' gestation. After this time, release of fFN into the CVF is presumed to be due to an inflammatory, infectious or

mechanical event that disturb the ECM. Its presence at elevated concentrations has thus been associated with an increased likelihood of preterm delivery in high risk women [183, 184].

Traditionally a qualitative “positive (>50 ng/mL) or negative (<50 ng/mL)” test has been used in women with symptoms of SPTB at 22-34 weeks’ gestation. Draw backs of this test include low sensitivity, low positive predictive value [185, 186] and that it cannot be used in up to 50% of women due to recent vaginal digital examination, unprotected sexual intercourse, vaginal bleeding or amniotic fluid contamination from ruptured fetal membranes which may lead to false positive results [187]. Arguably, the greatest value in the test may lie in its high negative predictive value (NPV) of 82-99% which is used clinically to reassure patients and obstetricians that PTB within 2 weeks is unlikely and intervention unnecessary [185, 186]. An observational study in USA showed that introduction of fFN testing into clinical practice led to significant cost savings to the health service by reducing hospital admissions, length of stay and prescriptions of tocolytic agents [188]. It was suggested that this was due to knowledge of the fFN result which helped clinicians to reduce the use of unnecessary resources [189].

Table 2. Cervical vaginal fluid (CVF) biochemical markers that are used to assist in SPTB prediction

Biomarker	Test Name	Threshold (ng/ml)	Participants	Sen (%)	Spec (%)	PPV (%)	NPV (%)	References
Fetal Fibronectin (Qualitative)	Rapid fFN	50	541	77	83	10-35	82-99	Deshpande et al[185]. Honest et al[186].
Fetal Fibronectin (Qualitative)	Rapid fFN 10Q	10	455	32	32	14	98	Bruijn et al.[190]
		200	455	78	79	28	96	
		500	455	94	94	38	92	
phIGFBP-1	Actim Partus	10	2159	67	77	35	93	Conde-Agudelo et al.[191]
PAMG-1	Partosure	1	203	80	95	76	96	Nikolova et al[192]

In an attempt to improve SPTB prediction using fFN, a quantitative version of this test was developed which uses alternative thresholds of fFN detection (10, 50, 200, and 500 ng/ mL). Although one study has demonstrated enhanced clinical value compared with the traditional qualitative test [193] other studies concluded that quantitative fFN testing does not improve the prediction of SPTB within 7 days compared with qualitative fFN testing in combination with CL measurement [194] or just CL measurement on its own [195].

For asymptomatic women, the ability of quantitative fFN testing early in pregnancy has been used to predict subsequent SPTB. One study sampling women at high risk of SPTB (i.e. previous

history of preterm birth) was designed to predict delivery before 34 weeks measuring fFN at different time points in pregnancy. Initial sampling was at 18 - 21 weeks and then at 22-28 weeks of gestation using a threshold of > 200 ng/mL. Positive predictive values for the test at these time points were 39.2 (95% CI 25.8–53.9) and 43.2 (95% CI 28.3–59.0), respectively [196]. The use of cervical length measurements was been shown to improve the predictive accuracy amongst these women [183]. Quantitative fFN testing in asymptomatic low risk women (i.e. no previous SPTB) have not been shown to improve PTB prediction <37 weeks using quantitative fFN using a threshold of > 200 ng/mL. Positive predictive values for the following sampling time points 6-14 weeks; 8.6 (95% CI 6.0-11.1), 16-22 weeks; 8.3 (95% CI 3.8-12.8) and 22-30 weeks; 14.0 (95% CI 7.4-20.6) [175]. The use of fFN prior to 18 weeks for distant prediction of SPTB is limited by the fact that it is present in cervical secretions up until at least 18 weeks gestation. The performance of the test also appears to be influenced sampling site; a meta-analysis of fFN studies found that test performance was enhanced when sampling from the fornix rather than in the vagina or the cervix [197].

- ***Phosphorylated insulin-like growth factor binding protein-1***

PlGF1 is secreted by placental decidual cells and may leak into cervical secretions following disruption at the choriodecidual interface [198]. As a result, the detection of PlGF1 in CVF has been proposed for SPTB prediction and a commercially available product is now available (Actim® Partus). Like fFN its overall predictive ability for the identification of symptomatic and asymptomatic women at risk for preterm birth is limited and is largely marketed for its NPV [191], which is comparable to fFN [182, 194]. Advantageously, the test is cheaper than fFN and performance is not influenced by urine, intercourse, semen, vaginal medications, lubricants, bathing products or the presence of infection [199].

- ***Placental alpha macroglobulin 1***

Placental alpha microglobulin 1 (PAMG-1) is a glycoprotein synthesized by the decidua. It is present in the amniotic fluid in high concentrations and usually found in low concentrations in the CVF [200]. Lee et al., proposed the presence of high vaginal concentrations of PAMG-1 in cases of threatened preterm labour was due to transudation through chorioamniotic pores in fetal membranes during uterine contractions, or by the degradation of ECM in fetal membranes due to inflammatory process of labour or infection [201]. This has led to the development of a commercial product, PartoSure, which is offered as a bedside test in which the concentration of PAMG-1 is measured from a vaginal swab using a monoclonal immunoassay. A small number of articles have been published examining the ability of to predict SPTB within 7 days of testing in

symptomatic women with PPV of 76-78% [192, 202]. It has been suggested that PAMG-1 test is less affected by vaginal examination, thus possibly providing an advantage over other methods as can be used shortly after vaginal examination [203].

In summary, despite the availability of predictive tests offering negative predictive value and reassurance for asymptomatic and symptomatic women at risk of preterm birth, no test currently exists that can reliably predict future cervical change, preterm labour or PPROM [204]. This severely limits the capacity to identify women early in pregnancy who could be targeted for surveillance and targeted intervention strategies for the prevention of preterm birth.

1.5 Prevention of Preterm birth

Antenatal strategies for the prevention of SPTB are currently limited to progesterone and/or cervical cerclage. Additional intrapartum strategies can be offered to symptomatic women to improve neonatal outcome including timely administration of steroids, magnesium sulphate and transfer of the mother to ensure optimal neonatal care (RCOG, Greentop Guideline). Ensuring that preventative treatments target the correct women through predictive tests is fundamental to improve efficacy, reduce potentially harmful side effects and stress, and reduced unnecessary expense to health services.

1.5.1 Antenatal strategies

- ***Progesterone***

Progesterone treatment is primarily used in SPTB prevention as it is thought to maintain myometrial quiescence via downstream anti-inflammatory signalling that triggers the onset of parturition [90, 205]. Although not specifically licensed for this purpose, it has been widely adopted by clinicians around the world. Progesterone exists in two preparations, injectable intramuscular 17 α -hydroxyprogesterone caproate which was licensed in USA in 2011 by the FDA for the prevention of preterm birth. Natural progesterone in the form of vaginal pessaries is used in the UK. Despite the biological plausibility behind progesterone administration for PTB prevention, the evidence for its efficacy in clinical practice of both preparations remains contradictory [206, 207].

A systematic review of five RCT (n = 974) in 2018 found that vaginal progesterone was associated with a significant decrease in SPTB <28 and <36 weeks of gestation. They also found a significant reduction in the frequency of respiratory distress syndrome and composite neonatal morbidity

and mortality [208]. Another meta-analysis by same authors found that vaginal progesterone and cerclage were equally effective for preventing SPTB and improving perinatal outcomes in women with a previous spontaneous preterm birth, and a mid-trimester sonographic short cervix [209]. In contrast to this, the OPPTIMUM trial, the largest RCT to date (n = 1228) compared progesterone to placebo in high risk pregnancies (previous history SPTB, positive fFN or short cervix) and concluded no reduction in the risk of preterm birth <34 weeks or adverse neonatal outcome [210]. These findings were supported by another RCT which included women with a history of SPTB and found no difference in SPTB rates in progesterone and placebo groups [211]. The recently published PROGRESS trial also showed no differences in SPTB rate or respiratory distress syndrome between the progesterone and the placebo groups in women with previous SPTB [212].

Lack of consensus between studies may be due to heterogeneity of data with differences in subject inclusion criteria, gestational age at which progesterone treatment is initiated, dosing regimen as well as preparation type (intramuscular vs pessary; synthetic vs natural). This has made it difficult to draw definitive conclusions about the effectiveness of progesterone treatment for the prevention of SPTB but also likely suggests that progesterone may only be beneficial for a subpopulation of women, which are currently impossible to identify using available predictive tools.

- ***Cervical cerclage***

A cervical cerclage involves the insertion of a non-absorbable purse-string suture around the cervix under regional or general anaesthetic following detection of a short cervix (<25mm) on TVUS (trans-vaginal ultrasound). A history indicated stitch is typically inserted between 13-16 weeks and is indicated when there are historic risk factors i.e. a previous SPTB or mid trimester loss (MTL) that are suggestive of cervical weakness. It is subsequently removed at 36-37 weeks or earlier if there are signs of labour. A “rescue cerclage” can also be used in the context of painless cervical dilation with bulging membranes noted on speculum examination or TVUS. Although the mechanism of action is not fully understood, it is thought that the cerclage provides structural reinforcement to a weakened cervix, maintains cervical length and supports the endocervical mucus plug that acts as barrier to pathogens and ascending infection [213, 214].

Similarly, to progesterone, the evidence that cervical cerclage prevents preterm birth is conflicting. A meta-analysis by Bergella in 2011 of five RCT (n = 504) found that that cervical cerclage increased the gestational age at delivery and reduced SPTB in both women with a short

cervix and those with previous history of SPTB [215]. More recently, a meta-analysis of five RCTs (n = 419) by the same author studying only women with a short cervix and no prior history as a risk factor showed that cervical cerclage did not significantly reduce PTB rate or improve neonatal outcome in women only presenting with a short cervix [216]. However, in a planned subgroup analysis, a significant decrease in PTB <35 weeks in women with TVS cervical length (CL) = 10 mm was observed when tocolytics or antibiotics were used as additional therapy. A systematic review by Alfirevic et al., in 2017 including data from 3490 women with short cervix and/or prior history of SPTB found a reduction in PTB rate <34 weeks when comparing stitch vs no stitch but no significant impact on perinatal morbidity and mortality [217]. Considerable heterogeneity between studies again makes comparisons difficult [217]. However, the collective evidence suggests that cerclage reduces SPTB <34 weeks and may be more effective in specific patient groups and preterm birth aetiologies. Furthermore, the true effectiveness of cervical cerclage may be underestimated due to a significant confounding factor. Recent studies have shown the suture material used for the procedure can have an impact on outcome. A recent retrospective observational study showed that mersilene (braided suture) is associated with an increased pregnancy loss and PTB rate compared to cervical cerclage performed with nylon stitch (monofilament) [218, 219]. This difference is associated with a persistent shift toward vaginal microbial communities depleted in *Lactobacillus* species and enriched for pathogenic bacterial colonisation, increased production of inflammatory cytokines and early cervical remodelling compared with nylon [219]. A randomised controlled trial (C-STICH) designed to assess the impact of cervical cerclage material type on outcome is currently ongoing and will ultimately provide evidence on which suture material should be favoured.

- ***Antibiotics for prevention of preterm birth***

Bacterial vaginosis (BV), is characterised by a depletion of *Lactobacilli* spp. in the vagina and an overgrowth of anaerobic and facultative organisms including *Gardnerella vaginalis*, *Atopobium vaginae*, *Bacteroides* spp. and other fastidious BV-associated bacteria (BVAB) including *Megasphaera*, *Sneathia* and *Clostridiales* spp. [220, 221]. It is associated with adverse reproductive health outcomes including pelvic inflammatory disease [222], transmission of sexually transmitted infections and HIV [223-226], and when detected in early pregnancy is associated with a 5-7 fold increase in preterm birth and late miscarriage [139, 227-229]. Clindamycin and metronidazole are used for the eradication of BV [230], however the recurrence rate of BV following treatment is high [231, 232]. It remains unclear whether this is due to an inability of some women to re-establish a resilient *Lactobacillus*-dominant vaginal

microbiota [233], failure of current antibiotic regimens to eradicate BV associated bacteria (BVAB) due to biofilms or a combination of these factors [234].

BV (as assessed using culture and microscopy) [235] is a risk factor for SPTB [20, 236]. Despite this, controversy surrounds BV treatment in pregnancy [237, 238]. A meta-analysis suggested benefit of clindamycin administered to women with BV before 22 weeks gestation with reduction in late preterm birth (before 37 weeks), but not early preterm birth (before 33 weeks) [239]. However, other studies examining the use of antibiotics for treating BV in pregnancy found no reduction in preterm birth rates, including in the subgroup where treatment was started at less than 20 weeks gestation [140, 229, 237].

A challenge with BV treatment is the current suboptimal methods of diagnosis [240, 241]. Current clinical diagnostic tests (Amsel and Gram stain criteria) rely on a subjective microscopy assessment of the bacteria. Furthermore as no single causative infectious agent has been defined in BV, which can further challenge diagnosis [220]. Typically women report a fishy odour and vaginal discharge, however up to 50% of women may be asymptomatic despite the presence of BVAB [242].

1.5.2 Intrapartum Strategies

- ***Tocolytics***

Tocolytics are used in an attempt to suppress uterine contractions in women with threatened preterm labour. The most commonly used drugs are nifedipine (a calcium channel blocker) and atosiban (an oxytocin antagonist) [243]. The Apostel II trial showed no difference in prolongation of pregnancy using nifedipine as compared to placebo [244]. A meta-analysis using data from six studies showed similar results [245] with no difference between the nifedipine and control groups in delaying delivery and furthermore no difference in the incidence of perinatal death, intraventricular haemorrhage, necrotizing enterocolitis, and neonatal respiratory distress syndrome. The Apostel III trial comparing nifedipine and atosiban showed similar perinatal mortality rates; 5% and 2% respectively [246].

The inability of tocolytics to prevent preterm labour could be a result of the activation of multiple biochemical pathways meaning that once uterine contractility is established, they cannot be overcome by transient inhibition of the contractions.

- ***Antibiotics for PTB***

Despite a lack of evidence for antibiotics for the prevention of SPTB, the use of intrapartum antibiotics is widespread. Women and neonates may benefit from their use but they also have potential to do harm.

In women with confirmed PPROM, oral prophylactic erythromycin is widely used as a first-line treatment [247-249] this was following the results of the ORACLE 1 study which examined the effect of erythromycin and Co-amoxiclav in 4826 women following PPROM [250]. Erythromycin was shown to prolong pregnancy compared to placebo and was associated with reduced use of surfactant, neonatal oxygen dependence, and fewer major ultrasound cerebral abnormalities. Co-amoxiclav, the comparison antibiotic also prolonged pregnancy, but was associated with increased prevalence of neonatal necrotising enterocolitis. Based upon the short-term neonatal benefits reported in this trial it became the recommended practice in UK and most commonwealth countries [247-249]. However an assessment of longer-term outcomes have failed to show any identifiable childhood benefits compared to placebo [251, 252], and there are reports of increased risk of cerebral palsy and epilepsy following macrolide use during pregnancy [253, 254]. These adverse outcomes associated with erythromycin are supported by a recent longitudinal study of women with confirmed PPROM which showed that women with vaginal bacteria dominated with *Lactobacillus* spp. was associated with a shift towards dysbiosis during erythromycin treatment. In contrast, in women with *Lactobacillus* spp. depletion there was a reduction in both richness and diversity of the vaginal dysbiosis following erythromycin exposure [143]. Although further studies need to confirm these findings, the study suggests erythromycin should be a targeted therapy to maximize potential in some women and avoid detrimental effects in other.

Studies of antibiotic use in women with threatened preterm labour with intact membranes have also been conducted. ORACLE II was meta-analysis of 14 trials which showed although there was a reduction in maternal infection with antibiotic treatment (erythromycin and/or co-amoxiclav), it did not prolong pregnancy compared to placebo and was associated with increased rates of neonatal mortality [255]. At 7 years of age (ORACLE children study) an increased prevalence of functional impairment 38% to 42% and cerebral palsy 1.7% to 3.3% in children born to mothers treated with both erythromycin and co-amoxiclav compared to no antibiotics [253]. This highlights the potential dangers of indiscriminate use of antibiotics in pregnancy.

The ineffectiveness of antepartum or intrapartum antibiotic use to robustly improve pregnancy outcomes is likely due to the inability to identify those women most likely to benefit from treatment and a lack of consensus as to when to intervene. There is a need to improve our ability to predict and diagnose SPTB by increasing our understanding of pathophysiological mechanisms and underlying aetiologies involved. Better mechanistic understanding coupled with better tools for predication could help effective stratification of women into high/low risk groups and facilitate the development of targeted therapeutic agents and timing of clinical intervention.

1.6 The Vaginal Microbiome

The microbiome is the term used to describe all the microorganisms (bacteria, fungi and viruses), their genomes and in a surrounding biochemical environment [256]. The relationship between the vaginal microbiome and reproductive outcomes has long been recognised. BV has been associated with miscarriage [257, 258] PPRM [259] and SPTB [142, 227, 260]. More recently, studies have employed culture-independent approaches in an attempt to improve understanding of the role of the vaginal microbiome in pregnancy outcomes, particularly preterm birth risk [261-265]. Although bacteria are the most studied microbes in the vagina, it is recognised that fungi and viruses also are also key members of the reproductive tract microbiota and their interactions with the host and with one another are also important influences on health and disease states.

1.6.1 Microbiota

In a clinical setting, analysis of vaginal bacteria is most commonly performed using a combination of culture and microscopy based methods. Typically this involves the analysis of a vaginal swab sample using specific anaerobic and aerobic culture plates combined with assessment of microscopic features of the samples (e.g. presence of clue cells and bacterial morphotypes) [266-269]. However, these methods are limited as many microbes cannot be cultured *in vitro* [270] and furthermore it provides no information regarding the relative abundance of specific species within a community. Consequently, culture-independent, molecular-based approaches are increasingly applied to assess vaginal microbiota composition and structure [271].

Next-generation sequencing (NGS) enables analysis of microbial community within a sample and has revolutionised our ability to identify and characterise these communities across different body sites [272, 273]. Broadly, NGS encompasses two main approaches for assessment of

microbial community composition, metagenomics and metataxonomics. Metagenomics, is the untargeted ('shotgun') sequencing of all microbial genomes present in a sample [274]. Metataxonomics involves the sequencing of conserved genes within microbial communities that contain sufficient variability to distinguish taxonomy. In the case of bacteria, the most commonly sequencing gene is the 16S rRNA gene, which contains nine 'hyper-variable regions' (V1 – V9) that differ between bacteria [275], permitting bacterial taxonomic determination down to species levels allowing comprehensive characterisation of microbial profiles [272]. When the bacteria or pathogens of interest are known, metataxonomics provides a quicker, more inexpensive choice than metagenomics [276]. Compared to other body sites like the mouth and gut, bacterial diversity and richness is significantly lower in the vagina and is generally associated with dominance by *Lactobacillus* spp. [277]. This makes metataxonomic sequencing a more desirable approach for microbial analysis. Advances in this technology has permitted 16S sequencing to become more high-throughput and affordable, thus the complexity of the vaginal microbiome has become increasingly characterised. Cross-sectional studies of non-pregnant, reproductive age women have shown that vaginal microbiota profiles can be classified at genus level into *Lactobacillus* spp. dominant, deplete and intermediate groups (based upon the relative abundance of *Lactobacillus* spp. within a sample). Higher resolution of community composition can be achieved at species level where at least five main vaginal microbiota groups, termed Community State Types (CST), are often observed. The first study to characterise vaginal CSTs was performed by Ravel et al., who reported four CSTs characterised by almost complete dominance of either *Lactobacillus crispatus* (CST I), *L. gasseri* (CST II), *L. iners* (CST III) or *L. jensenii* (CST V) and an additional CST IV, characterised by low abundance of *Lactobacillus* species and increased diversity and richness of anaerobic bacteria often associated with BV (Figure 1-6)[278].

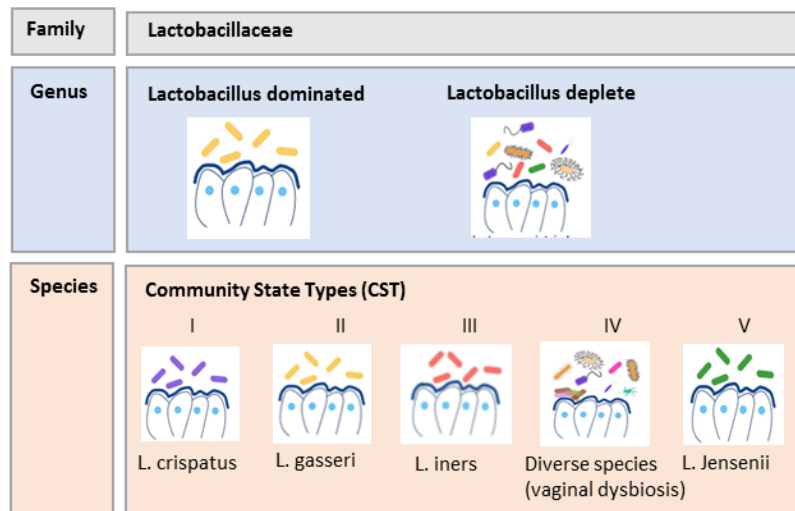


Figure 1-6. Taxonomic allocation at genera and species levels using 16S rRNA sequencing. 'Community state types' describes the common vaginal microbiome profiles among reproductive age women described by Ravel et al, 2011 [278].

Longitudinal studies of vaginal microbiota community composition have revealed the dynamic nature of these CSTs, which in some women change due to underlying hormonal influences related to the menstrual cycle, whilst in other women are highly stable [277]. In pregnancy, circulating concentration of oestrogen progressively rise [279] which mediates intracellular deposition of glycogen in the vaginal epithelium [280]. Glycogen is broken down by host α -amylase present in vaginal mucosa to products including maltose, maltotriose, and maltotetraose which are preferentially metabolised by *Lactobacillus* spp. [281] supporting their colonisation. Consistent with this proposed mechanism, a number of studies have shown that the estrogenic state of pregnancy is associated with a shift towards *Lactobacillus* spp. dominance and reduced bacterial diversity [282, 283], which is lost in the post-partum period following delivery where a fall in estrogen concentrations corresponds with a shift towards a high-diversity, *Lactobacillus* spp. deplete microbial composition [284].

Lactobacillus spp. domination is often considered a hallmark of vaginal health. *Lactobacilli* species protect against colonisation by pathogenic bacteria through production of various bacteriocidal and bacteriostatic compounds as well as production of lactic acid that lowers pH [285, 286]. A reduction in *Lactobacillus* spp. during pregnancy is frequently associated with a reciprocal increase in potential pathobionts. These include *E. coli*, Group-B Streptococcus (*S. agalactiae*), and BVAB including *Gardnerella vaginalis*, *Prevotella* and *Bacteroides* spp., and *Mycoplasma* spp. [287]. *Lactobacillus* spp. depletion is also associated with increased expression of inflammatory mediators detectable in the cervicovaginal fluid (CVF) [219, 288]. There is evidence that this pathogen-induced inflammatory vaginal environment, compromises

the integrity of the cervical epithelial barrier, and is thought to accelerate the downstream inflammatory-driven signalling cascade, culminating in preterm birth [120, 137, 289].

1.6.2 Limitations of microbiota profiling studies

In clinical practice, culture-based assessments of microbial communities are used in the decision-making process. However, a major draw-back of culture is that the majority of species cannot be cultured in vitro and results can take up to 72 hours. For this reason, proxy markers of infection/inflammation (e.g. serum C-reactive protein, white cell count) are often used in the short term and treatment with broad spectrum antibiotics when bacterial infection is suspected until culture results are available. As these markers can be elevated in the absence of a bacterial infection, it can lead to potential unnecessary exposure to an antibiotic regime. Although molecular-based, culture independent approaches such as 16S rRNA bacterial gene sequencing permits a fuller assessment of the community composition, this methodology can be biased by the choice of primers used and importantly, cannot differentiate between living or dead bacteria or cell-free DNA in samples [284]. Furthermore, the technique is costly and requires lengthy extraction and processing of the samples thus currently its application is limited to research settings. These approaches also fail to capture the functional interactions occurring between microbiota and the host, which ultimately dictate health and disease phenotypes in the reproductive tract [290]. For example, vaginal microbiota or community compositions associated with pathology or disease states can often still be observed in asymptomatic, healthy controls [291] providing evidence that bacterial presence or absence does not solely indicate host response. This highlights the likelihood of individual-level microbiota-host interactions, mediated by factors such as genetic background and individual host immunity, as being key determinants of either normal or pathological responses to vaginal microbiota [284].

1.7 The Host Immune Response

The vagina is protected by two inter-related mechanisms; the innate and adaptive immune response. Innate immunity is a non-specific reaction towards foreign antigens, whereas the adaptive response is an antigen-specific reaction [292]. The intricate interplay between these two arms of the immune system plus their interaction with the microbiota at the mucosal epithelial barrier collectively modulates health within the lower genital tract [293].

1.7.1 Innate immunity

The initial line of defence against pathogen colonisation within the lower reproductive tract is the cervico-vaginal mucosal barrier. Mucus secreted from glands within the cervix can trap pathogens [293] and provides a medium for antimicrobial molecules that can inhibit colonisation, attachment and adhesion to the vaginal epithelia [294]. The vaginal mucosal epithelium itself provides a physical barrier against microbes and is comprised of multiple layers of non-keratinized stratified squamous epithelium that rests on a lamina propria [295, 296]. There is a lack of tight junctions in the squamous epithelial layers which permits the movement of small molecules within epithelial spaces between cells such as water, soluble proteins, viruses, and is penetrable by vaginal microbiota and mediators of the immune system (e.g. CD4+ T cells, macrophages, cytokines) [296-298]. The epithelium provides additional immunological defence by tolerating colonisation by commensal vaginal microbiota such as *Lactobacillus* spp. which in turn prevents pathogen colonisation through competitive exclusion [299].

Recognition of commensal and pathogenic microbiota is achieved through the detection of microbe/pathogen-associated molecular patterns (MAMPs/PAMPs) by pattern recognition receptors (PRRs) including Toll-like receptors (TLRs) and nod-like receptors (NODs) which are expressed on epithelial and immune cells. These bind directly to ligands on the surface of microbes, or endotoxins and exotoxins, and respond by secreting of cytokines (e.g. IL-1 β , TNF- α), chemokines (e.g. IL-8), antimicrobial peptides (e.g. beta defensins, elafin) and secretory protease inhibitor [300-303]. Although a pro-inflammatory immune response elicited by pathogens is normally required to control infections [304], vaginal mucosal inflammation can promote transmission of infections such as HIV, by compromising epithelium integrity [305] and by recruiting and activating HIV target cells [306].

The vaginal epithelium is in intimate contact with microbiota and their metabolites which also interact and modulate mucosal immunity. *Lactobacillus* spp. help maintain this ecological equilibrium by preventing the colonization by other microorganisms such as anaerobes [307]. This is facilitated through the production of lactic acid which apart from acidifying the vagina, inhibits growth of other bacteria [286], and may prime anti-microbial epithelial immune responses [298, 308]. *Lactobacilli* spp. also excrete antimicrobial metabolites that inhibit other bacteria [309]. Consistent with this, *Lactobacillus* spp. dominance of microbial communities is associated with suppression of immune response, but this may be species specific. *L. crispatus* dominant communities appear to suppress pro inflammatory cytokines (e.g. IL-1 α , IL-1 beta and IL8) more effectively than communities dominated by *L. iners* [302, 310-312]. BVAB are linked

with excretion of short chain fatty acids (SCFAs) include acetate, propionate, butyrate, succinate, formate, valerate and caproate [313-320] which appear to potentiate a pro-inflammatory vaginal environment [321-324]. This may ultimately lead to reduced barrier integrity of the vaginal epithelium and increased risk of infection [325].

1.7.2 Adaptive Immunity

While innate immune responses are rapid, they lack specificity and memory. The adaptive immune response in the lower genital tract is an antigen-specific reaction consisting of T and B lymphocytes which can confer long-term immunity in the genital tract to certain pathogens. T and B cells are activated after microbial antigens have been recognised, processed and presented by presenting cells (APC). In the female genital tract APCs include macrophages, dendritic cells, Langerhans cells, and epithelial cells of the cervix [326]. B cells differentiate into plasma cells which secrete antigen-binding antibodies allowing phagocytosis or elimination of antigens through the complement system. T cells can be subdivided into T helper cells (CD4+) and cytotoxic T cells (CD8+). The cytokines produced by T helper cells play a central role in the protection against pathogens, but also play a role in allergy and autoimmune conditions. The cytotoxic T cells target virus-infected cells resulting in cell death [327]. In female reproductive tract, CD8+ T-cells predominate over CD4+ T cells [328].

1.8 Systems Biology Approaches to Parturition and Preterm Birth

With the aim of improving our understanding of determinates of health and disease, ‘systems biology’ is an emerging holistic approach attempting to decipher the complexity of a system. It is based on the concept that a biological system is made up of different parts, none of which individually possess the properties of whole system but combined together they create a phenotype. “Omic” methodologies provide the capacity to interrogate different levels of biological information within a given system. Each step, or approach yields distinctly different information in discovery research. These include genomics (study of genes and their functions), transcriptomics (study of the complete set of RNA transcripts produced by the genome with template for protein synthesis), proteomics (study of the complete set of proteins produced by a species) and metabolomics (study of small-molecule metabolite that are generated by cellular processes) [329] as shown in Figure 1.7.

Omic methodologies have been used in SPTB research; for example at the level of the genome, studies aimed at investigating genetic predisposition to SPTB (e.g. single nucleotide polymorphisms) [145, 155, 156]. At transcriptomics level, studies have been used to describe

mRNA expression in a particular tissue, for example a study of cervical tissue has shown mRNA profiles to differ in asymptomatic women at risk of PTB compared to healthy controls [330]. At the proteome level, studies of CVF found changes in proteins associated with SPTB including upregulation of acute-phase reaction proteins [331] and thrombospondin [332]. At the metabolome level which measures small metabolites (<1 kDa in molecular mass) that participate in metabolic reactions [329], recent studies have shown the application of this approach in SPTB research as described in more detail in section 1.8.3 [333-335].

Compared to other approaches, investigation of the metabolome provides an advantage as it represents the down-stream result of gene expression and protein synthesis and therefore serve as direct signatures of biochemical activity. It is thus deemed to be more closely associated with a phenotype [336, 337] which makes it a powerful methodology for biomarker discovery specific for aetiology or phenotype [338, 339].

Metabolic profiling of the vaginal mucosa offers an advantage over other bio-fluids e.g. serum and urine, as sampling is at the feto-maternal interface and thus able to characterise more relevant biochemical events related to labour and infection. Metabolic profiling studies of the vagina mucosa are discussed further below.

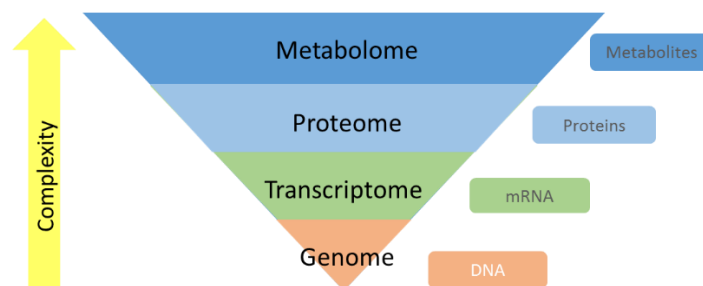


Figure 1-7. From genome to metabolome; the inverted pyramid represents different levels of “omic” applications which increase in functional complexity with have increasing numbers of interactions at each level.

1.8.1 The vaginal metabolome

The metabolome describes the collective presence and concentration of all metabolites and small molecule within a given sample [340] which include amino acids, peptides, lipids, carbohydrates and nucleotides.

In the vagina mucosa there is a continuum of biochemical processes and functional interactions between the host and microbiome that influence the metabolome. Pathogenic microbes present in the reproductive tract do not always activate the host immune response and

inflammation [341]. As demonstrated in BV studies whereby presence of BVAB can often still be observed in asymptomatic, healthy controls [291]. Furthermore BV-type bacterial profiles appears to be more prevalent in reproductive-aged women of Black and Hispanic ethnic background (40%) compared to White or Asian backgrounds (10-20%) [342, 343]. This highlights the likelihood of individual-level microbiota-host interactions, mediated by factors such as genetic background and host immunity, as being the key determinants of either normal or pathological responses to vaginal microbiota [284, 290]. Metabolic profiling of the vaginal mucosa allows for the assessment of these biochemical interactions and thus may provide insight into the interplay between host and vaginal microbiota which could ultimately dictate health and disease phenotypes in the reproductive tract. Metabolic profiling studies that have investigated the vaginal metabolome in the context of BV and SPTB are discussed below along with their key findings.

- ***Metabolic profiling of BV***

Metabolic profiling studies of cervico-vaginal samples using liquid chromatography mass spectroscopy (LC-MS) have identified a number of metabolites that correlate with increased bacterial diversity [344, 345]. For example, elevated levels of several bioamines; putrescine, cadaverine and tyramine are found in association with malodour in BV [346]. Increased production of short chain fatty acids (SCFAs) such as acetate, succinate and butyrate are linked to reduced antimicrobial activity and appear to potentiate a pro-inflammatory environment [293, 347]. Other metabolites isolated in BV have been shown to have potential diagnostic relevance e.g. γ -hydroxybutyrate [344]. *Gardnerella vaginalis*, a bacteria often implicated in BV, is a major producer of γ -hydroxybutyrate however the role of this metabolite in the pathology of BV remains to be determined. Furthermore, metabolic profiling approaches have identified 2 distinct metabolic profiles or “metabotypes” associated with BV [266]. BV-I is characterised by high levels of butyrolactone whereas BV-II is associated with increased hydroxylamine and glycolic acid, however the functional impact of these differences on host and/or microbial communities in BV remains unclear [348].

Shifts in the CVM metabolome have also been observed following antibiotic treatment for BV, which reflect the restoration of *Lactobacillus* spp. domination of bacterial communities and a corresponding decrease in metabolites associated with BVAB [345, 349]. Laghi et al. also identified differences in baseline metabolic profiles in women who subsequently experienced spontaneous remission of BV compared to those that had persistent infection indicating a group of patients in which antibiotic treatment may not be necessary or appropriate [349]. In addition,

vaginal douching, which is associated with increased risk of recurrent BV, leads to reduced vaginal mucosal levels of fatty acids (e.g., docosanoic acid, dodecanoic acid) [348].

- ***Metabolic profiling SPTB***

Given that the shifts in the microbial composition and corresponding symptoms correlate with specific changes in the metabolome, it has been proposed that profiling of biofluids collected during the antenatal period may offer the possibility of detecting metabolic deviations that are predictive of PTB. Early studies in this area examined the metabolic profile of amniotic fluid taken at amniocentesis and showed lactosylceramides to be associated with PTL associated with chorioamnionitis [350] and eicosanoids; PGE2 and PGD2 to be higher in subsequent term deliveries compared to preterm [351, 352]. However another study collecting samples in second trimester and assessing fatty acid concentration found no difference between subsequent term deliveries, PPROM and SPTL [353]. Using amniotic fluid via amniocentesis for the application of metabolic profiling is however clinically impractical given that the procedure carries increased risk of fetal/maternal infection and haemorrhage risks. Furthermore, these risks are particularly high when there is reduced amniotic fluid volume such as following PPROM.

Ascending infection from the vagina, through the cervix and into the gestational tissues is thought to be the primary route of infection associated with SPTB [136]. Therefore, metabolic biomarkers identified from cervico-vaginal samples, which are predictive of high risk vaginal microbial communities or subsequent infection, would provide a minimally invasive method for stratifying preterm risk. To date, a number of small studies in this area have been undertaken as shown in Table 3. Metabolic differences in cervico-vaginal fluid (CVF) samples were first reported by Auray-Blais studying profiles collected from 5 women although these differences were not predictive of preterm birth [354]. Using LC-MS and gas chromatography mass spectroscopy (GC-MS), Gharthey et. al compared PTB (n = 10) to term controls (n = 10) and identified down regulation of carbohydrate metabolites as well as increased levels of the anti-microbial agent methyl-4-hydroxybenzoate in women who subsequently delivered preterm [333]. These metabolite changes were independent of cervical length change however could not be validated in a larger cohort (n = 30) [334].

Using an NMR-based targeted metabolomics approach to examine concentrations of specified metabolites, Amabebe et al. found that succinate, formate, lactate, glucose, glutamate and alanine did not differ between term and preterm delivered women however symptomatic women who subsequently delivered preterm had higher levels of acetate. The authors proposed this metabolite to be predictive of SPTB and with a sensitivity 0.78% (95% CI 0.61–0.96) [335].

This metabolite was further validated using a spectrophotometric assay kit to measure acetate further combined with TVUS CL and fFN information, which improved prediction of PTB sensitivity to 83% and a specificity of 89% from 80 % and 84 % respectively [355]. The authors speculated that the source of acetate came from an overgrowth of pathogenic anaerobic bacteria [356], however a subsequent study by Stafford et al. (2017) in which 16S rRNA and 1H-NMR was used, showed no association between acetate and microbial communities or phenotype [357]. In the latter study, it was reported that women delivering prematurely had significantly higher abundance of *L. jensenii* and lower *L. crispatus* at 20–22 weeks as well as significantly lower levels of lactate. They also showed that at 26–28 weeks, women who ultimately delivered preterm had lower succinate levels compared to women that delivered at term. These findings, although encouraging, highlight the need for more metabolic profiling studies with larger cohorts. Furthermore, in terms of screening of CVF for potential biomarkers predictive of SPTB, there is a need for methodologies that can provide rapid, affordable and high throughput metabolic profiling data in a clinical setting. Current approaches and methodologies for metabolomics are discussed below.

Table 3 Summary of CVF metabolomic studies in relation to PTB.

Technique	Cohort	Gestational weeks	Main Metabolite changes	Year published	Reference
LCMS	Pre-PTB (n = 5) Controls (n = 30)	31-33	Variations in 17 unassigned metabolites	2011	[354]
LCMS/GCMS	Pre-PTB (n = 10) Controls (n = 10)	20-24, 24-28	↓ dipeptides, ↑ n-acetyl-neuraminate	2015	[333]
GCMS	Pre-PTB (n = 30) Controls (n = 30)	20	No relevant metabolite changes	2015	[334]
NMR	Pre-PTB (n = 15) Controls (n = 67)	24-36	↑ acetate	2016	[335]
NMR	Pre-PTB (n = 26) Controls (n = 107)	20-22, 26-28, 24-36	↓ succinate (26-28 wks)	2017	[357]

1.8.2 Metabolic profiling methods

Due to the wide dynamic concentration range of metabolites within human samples, no single-instrument or platform exists which can identify and analyse all metabolites present in a given sample [329]. Therefore, the characterisation of the “metabolome” of any given sample is often performed using targeted and/or untargeted metabolic profiling approaches, depending on the study design.

Targeted metabolomics

Targeted metabolomics refers to a method in which pre-specified metabolites are assayed. Its value is in hypothesis driven experiments, to validate a biological question or hypothesis that motivates the investigation of a particular pathway or to confirm data generated in an untargeted study [338].

Untargeted metabolomics

An untargeted metabolic profiling approach aims to simultaneously measure as many metabolites as possible from biological samples, without bias, as to permit the acquisition of dense metabolite information that can be used for hypothesis generation as well as biomarker discovery [358]. Depending on the solvent, pH, column chemistry and ionization technique used; untargeted metabolomics can provide a detailed assessment of the metabolites in a sample, revealing a wide range of metabolite classes [359]. These can be individually annotated or by another approach is called metabolic fingerprinting. This describes the examination of metabolite patterns in different experimental groups and subsequent classification of the patterns [329]. However, many of the small molecules and metabolites detected within samples are yet to be annotated in metabolite databases and structural libraries meaning that identification of target metabolites of interest remains a challenge [338].

The main analytical platforms used for characterising the metabolome by either targeted or untargeted approaches include nuclear magnetic resonance (NMR) and chromatography coupled mass spectrometry. A schematic workflow for metabolic profiling assays from vaginal swab extractions is presented in Figure 1-8.

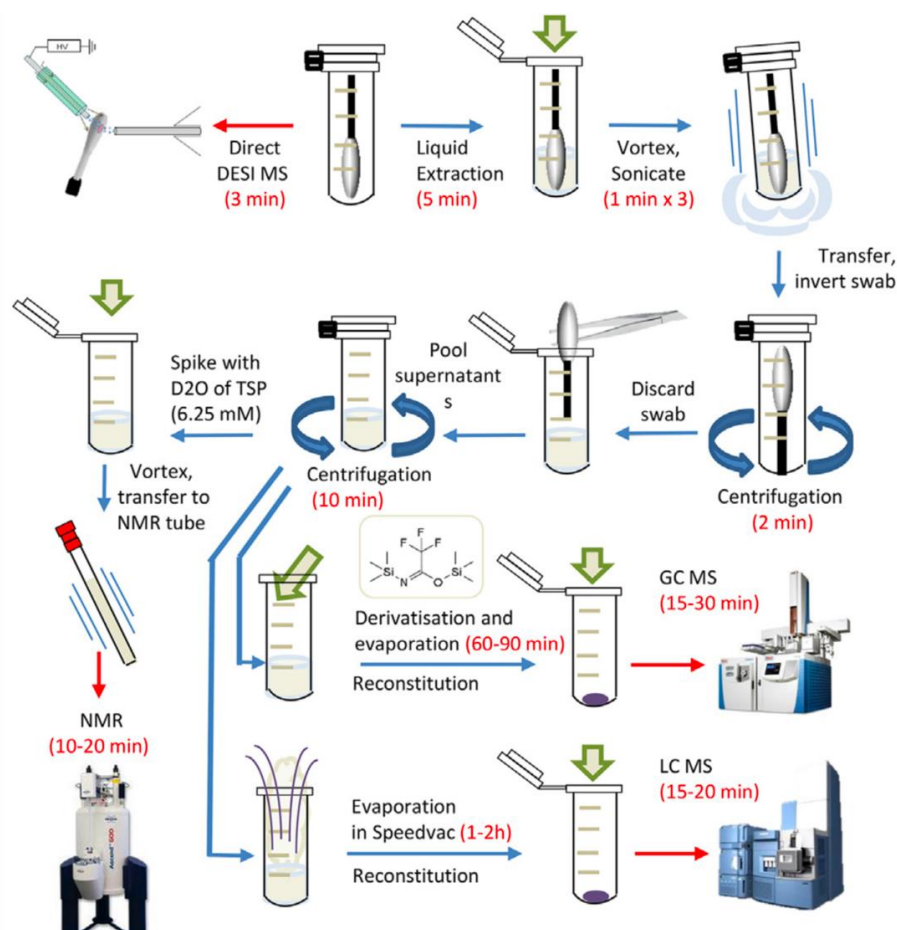


Figure 1-8. A Step wise workflow and time scheme for vaginal mucosal sampling, sample preparation and metabolite profiling assays using Nuclear magnetic resonance (NMR), gas chromatography-Mass Spectrometry (GC-MS), or liquid chromatography- Mass Spectrometry (LC-MS). Reproduced from Pruski et al [290]

- ***Nuclear magnetic resonance spectroscopy***

Nuclear magnetic resonance (NMR) spectroscopy permits high throughput metabolic profiling with high reproducibility. This method requires minimal sample preparation with no destruction of the sample and unlike mass spectrometry, it is inherently quantitative thus permitting absolute concentration of detected metabolites. However, only medium to high abundance (μM) metabolites can be detected with NMR and it lacks sensitivity compared to mass spectrometry [360].

- ***Mass spectrometry***

Mass spectrometry (MS) based metabolomics offers analyses with high sensitivity, selectivity and reproducibility for a wide range of compounds [359, 361]. Using MS-based metabolomics approaches it is possible to carry out targeted and untargeted profiling as well as metabolic

fingerprinting. The basic premise of this technique is a sample is ionized and the resulting ions are separated according to their mass and then detected (as shown in figure 1-9).

At a molecular level a sample contains atoms, molecules or fragments of molecules that carry one or more positive or negative electrical charges. An ion is created when the number of protons (i.e. positive charges) in the nucleus of a molecule is no longer balanced by the number of negatively charge electrons, this process is called ionization [360] and results in the creation of ions (Figure 1-9). These ions, which must be in a gaseous state are then manipulated by electrical or magnetic fields to allow their mass to be determined then separated by their mass to charge ratio (m/z). The ratio is obtained by dividing the mass of the ion (m) by the number of electrical charges (z) acquired during ionization process. In most cases there is only 1 charge on an ion thus the measured m/z value is equivalent to the mass of the ion ($z=1$). The mass spectrometer creates a digital output of the signals called a mass spectrum. This is a graphical representation of the distribution and intensity (abundance) of the ions introduced into the MS (Figure 1-11).

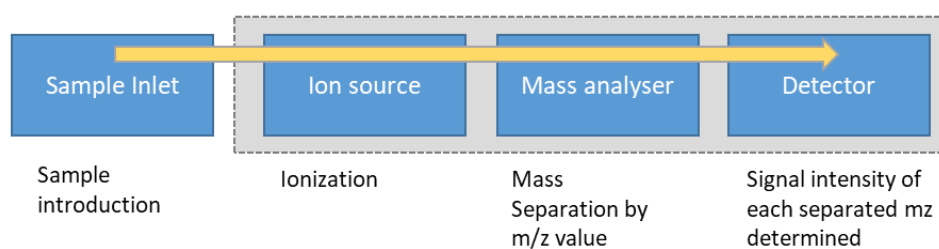


Figure 1-9. Basic sequence of events in a mass spectrometer. Vaporised sample enters the ion source where ionization takes place. Ions are accelerated to the mass analyser where they are separated by m/z ratio. In the ion detector signal intensities of each separated m/z value are determined. A vacuum system is shown as a grey box.

Prior to introduction of a sample to MS, metabolites are often first required to be extracted and then separated as to reduce complexity and enrich for molecular species of interest. GC-MS and LC-MS are two of the most common techniques that separate metabolites/compounds prior to ionisation. Although this minimizes signal suppression which allows for greater sensitivity [359], the process is complex and lengthy, making GC/LC-MS unsuitable for point of care diagnostics in a clinical setting. Another requirement of some MS techniques is that ionization is carried out in a vacuum system to prevent the loss of ions through collisions with neutral gas molecules. Ambient ionization techniques provide the ability to generate gas phase ions directly from the samples, without the need of chromatographic separation, sample preparation or a vacuum system [362]. This also permits the manipulation and movement of samples during data

acquisition [363, 364]. These techniques have resulted in straightforward handling and rapid analysis of intact biofluids and other biological and non-biological materials. This is appealing for clinical applications where rapid and robust acquisition of metabolic profiling data could assist in objective clinician decision making.

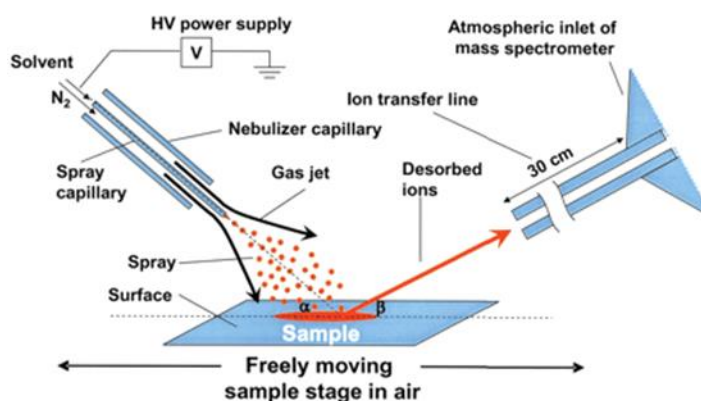


Figure 1-10. Schematic representation of a typical DESI MS experiment. The method works by directing a fine spray of charged solvent onto a sample. The impact of the charged particles on this sample produce gaseous ions that are carried via a capillary to a mass spectrometer. A spectral profile of the ions is instantly formulated, and subsequent quantitation and identification of the molecules present can be undertaken. Reproduced from Takats et al. [365]

The most widely used ambient ionisation technique is desorption electrospray ionization (DESI-MS), which was described first by Takats et al., in 2004 [366]. The method as shown in Figure 1-10, works by directing a pneumatically assisted electrospray comprising high-velocity, charged, aqueous droplets onto a sample. The solvent wets the surface and extracts analyte molecules to form a liquid film. The impact of incoming droplets results in the formation of secondary droplets departing from the surface [367]. Given that the surface is electrically non-conductive, the secondary droplets will still carry net electric charge or are ionized in the resulting plume. These ions are then transported toward the atmospheric pressure inlet of the mass spectrometer. A spectral profile is created which is shown in Figure 1-11.

The electrical voltage applied to the solvent spray determines the formation of positive ions or negative ions. In the positive ionisation mode, protonated and alkali adducts analyte molecules are generally observed in the mass spectra. In the negative ion mode operation peaks of deprotonated analyte molecules are observed.

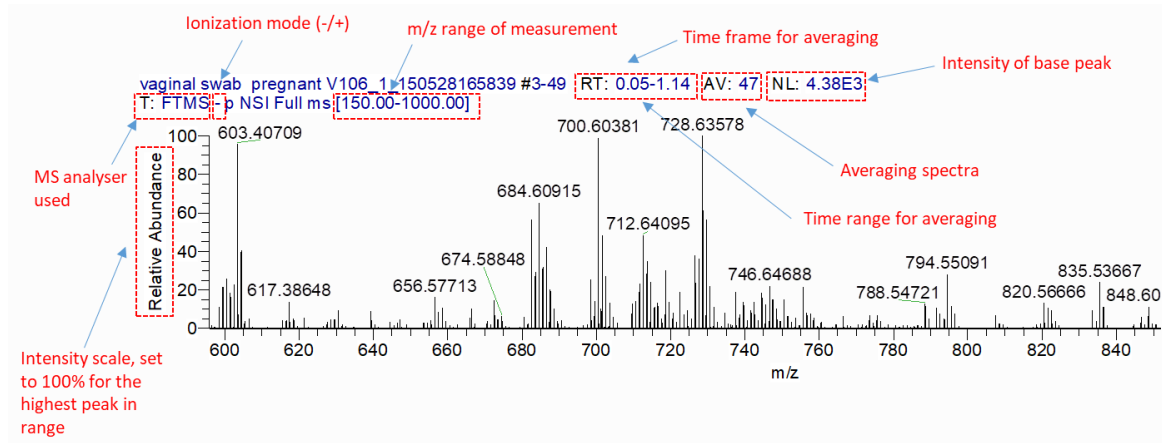


Figure 1-11. Typical mass spectrum with instrument annotations

1.9 Justification and Hypothesis for Project

Despite being recognised as a syndrome with multiple underlying aetiologies, SPTB is commonly managed by obstetricians as if it were a single disease. Similarly, research investigations and clinical trials of interventions do not taking into account the diversity of preterm birth aetiology [204]. There is a need to improve our ability to predict and diagnose PTB through improved mechanistic understanding coupled with better tools for prediction which could enable stratification of women according to risk. This would ultimately assist the timing of clinical intervention and the development of targeted therapeutic agents leading to improved maternal and neonatal outcomes.

Infection and inflammation are known to be causal in a large proportion of women who have a premature birth. Current strategies to assess vaginal microbes and infections (e.g. culturing, NGS) are not rapid techniques and fail to take into account the maternal host response to the presence of bacteria. The ability to assess these interactions between the vaginal microbiota and the pregnant host could enable screening, stratification and targeted intervention for at mothers at risk of infection-associated preterm birth.

Metabolic profiling of cervicovaginal mucosa (CVM) may offer the ability to assess interactions between the vaginal microbiota and the pregnant host that are reflected in the local biochemical environment [348, 368]. Current approaches are not rapid and thus limit their capacity to be used as point of contact tests. We hypothesised that DESI-MS vaginal swab profiling would provide objective biochemical information that will enhance our understanding of SPTB aetiology and provide a rapid way of identifying women at risk of PTB with or without infection.

Furthermore, we hypothesised that the presentations of SPTB (e.g. early vs late SPTB) have different underlying aetiologies that are reflected in the underlying CVM metabolome.

1.10 Aims

- 1) To develop a novel DESI-MS based approach for reproducible, rapid and direct metabolic profiling of vaginal swabs.
- 2) To identify vaginal mucosa metabolite biomarkers and signatures using DESI-MS that are associated with vaginal microbiome interactions and pregnancy outcome.
- 3) To identify vaginal mucosa metabolite biomarkers and signatures in early pregnancy using DESI-MS that can predict, diagnose and stratify subsequent spontaneous preterm birth from healthy term pregnant controls.
- 4) To identify vaginal mucosa metabolite biomarkers and signatures in pregnancy using DESI-MS associated with different phenotypes of SPTB (PPROM, STL, and subsequent cervical shortening in pregnancy).
- 5) To identify vaginal mucosa metabolite biomarkers and signatures in pregnancy using DESI-MS MS profiling permit stratification of patients that subsequently PPRM from healthy term pregnancy controls, confirm rupture of membranes and identify vaginal bacterial dysbiosis in women presenting with PPRM.

2 MATERIAL AND METHODS

2.1 Materials

DESI MS experiments	Description/Notes	Supplier
Equipment		
Rayon medical swab	Transwab MW170 with rayon bud	Medical Wire & Equipment
Freezer	-80 °C	Various
Gas cylinder	7 bar pressure	BOC
Gas regulator for cylinder	10 bar	BOC
Mass spectrometer	Xevo G2-XS	Waters Corporation
Mass spectrometer	LTQ-Orbitrap Discovery	Thermo Scientific
Home-built DESI ion source		Various
Home-built swab turner		Lego Power Function
Chemicals		
Acetonitrile	LC-MS grade	Sigma Aldrich
Formalin 10%	Buffered	Sigma Aldrich
Iso-propanol	LC-MS grade	Sigma Aldrich
LC-MS grade water		Sigma Aldrich
Methanol	LC-MS grade	Sigma Aldrich
MS standards		Sigma Aldrich
Bovine plasma		Sigma Aldrich
16S rRNA		
Equipment		
Illumina MiSeq platform		Illumina, Inc. San Diego, California
QIAamp DNA Mini Kit		Qiagen Catalogue No 51304
Liquid Amies swab		BBL™ CultureSwab™, Becton, Dickinson & Company
Glass beads		Sartorius Stedim Cat No BBI-8541400
Micro Dismembrator		Sartorius
QIAamp DNA Mini Kit		Qiagen
Enzymes		
Lysozyme B12.	10mg/ml in filter sterilised 10mM Tris.HCl pH 8.0	Sigma Aldrich
Mutanolysin .	25U/μl by dissolving 10,000units in 400 μl sterile water	Sigma Aldrich
Lysostaphin	4000U/ml by dissolving 23,915units in 20mM NaOAc	Sigma Aldrich
Buffers and solutions		
Filter sterilised phosphate-buffered saline		Sigma Aldrich
NaOAc (sodium acetate)		Sigma Aldrich
Tris.HCl	pH 8.0 10mM	Sigma Aldrich
TE50	10 mM Tris-HCl, 50 mM EDTA, pH 8.0	Sigma Aldrich
Ethanol (100%)		Sigma Aldrich
DNase / RNase free water		Sigma Aldrich
Polymerase chain reaction (PCR)		
NEB OneTaq® DNA Polymerase		BioLabs
dNTP 10mM B41		Sigma Aldrich
5 x Buffer		BioLabs
6 x loading dye		B43PROMEGA G190A 1006034
Agarose gels	Electrophoresis grade 1-1.5%	Invitrogen
SYBR Safe DNA Stain		Invitrogen Cat
Molecular weight marker	Bioline Hyperladder 100bp	Biolabs
TBE buffer	Tris/Borate/EDTA	Sigma Aldrich
Universal primers		
Forward Primer 10picomol/μl	27F-5'-AGAGTTTGATCCTGGCTCAG-3'	
Reverse Primer 10picomol/μl	338R-5'-GCTGCCTCCCGTAGGAGT-3'	
Microbiology		
	Description	Notes Supplier
Blood agar		Thermo Scientific Oxoid
Sabaouroud agar		Thermo Scientific Oxoid
Aztreonam agar		Thermo Scientific Oxoid
Transwab® MW170 with rayon bud type		Medical Wire & Equipment
Glass slides		Western Laboratory service
Plastic disposable loops		Western Laboratory service

2.2 Prospective Vaginal Mucosal Metabolome & Microbiome Studies

2.2.1 Study design

The studies described in this thesis focus on the assessment of vaginal mucosal metabolic profiles using DESI-MS direct swab analysis. Initial experiments were carried out to adapt and optimise the DESI-MS technique. Subsequently, a series of pilot studies were performed to exam the potential capacity of this innovative platform to assess the relationship of the CVM metabolome with pregnancy outcomes. In the first results chapter (Chapter 3), DESI-MS swab method development is described. Chapter 4, describes the ability of DESI-MS to characterise metabolic changes in the CVM in a longitudinal cohort of patients who subsequently experience preterm birth (multiple aetiologies) or term birth. Chapter 5 explores the capacity of DESI-MS to characterise important clinical time points across the pregnancy journey of women experience PPRM (e.g. prediction of PPRM, diagnosis of membrane rupture and underlying at microbial composition).

2.2.2 Ethical approvals

The following studies were approved by the National Health Service (NHS) National Research Ethics Service Committee London–Stanmore in order carry out the research in this thesis.

1. DESI-MS Pilot Study: (RESPI-SAM 15/LO/0444)
2. DESI-MS PPRM Study: (REC 14/LO/0328)
3. DESI-MS SPTB study: (REC 12/LO/2003)

All participants provided written informed consent.

2.2.3 Patient recruitment

Women were prospectively recruited for all studies. Exclusion criteria included; sexual activity within 72 hrs of sampling, vaginal bleeding in preceding week, HIV or hepatitis positive serology, < 18 years of age, multiple pregnancy and uterine anomalies.

DESI-MS Pilot study cohort

Non-pregnant women of reproductive age were recruited from the general gynaecology clinic and pregnant women from the antenatal clinic between 8-40 weeks gestation at Queen Charlotte's Hospital from September 2015 and January 2016.

DESI-MS Preterm birth study cohort

Pregnant women were recruited between 8-12 weeks from three maternity hospital sites across Imperial College Healthcare NHS Trust: St Mary's Hospital (SMH) and Queen Charlotte's and Chelsea Hospital (QCCH) and Chelsea and Westminster Hospital from January 2013 to January 2015. Women with no underlying risk factors or previous history of preterm birth were considered "low risk" and were recruited from routine midwifery led antenatal booking appointments. Women with previous spontaneous mid-trimester miscarriage or preterm birth between 16⁺⁰ and 36⁺⁶ weeks gestation in a singleton pregnancy prior to the index pregnancy, or excisional cervical treatment of depth >1cm for CIN grade II or III, prior to the index pregnancy were considered "high-risk" for preterm birth and were recruited from the preterm birth surveillance clinic. A second group of women were recruited upon presentation with ruptured membranes between October 2013 and June 2015. As per participating hospitals guidelines, PPRM was defined as rupture of the fetal membranes, diagnosed by pooling of amniotic fluid on speculum examination, prior to 37 weeks gestation more than 24 hours prior to spontaneous preterm delivery or clinical indicated delivery or induction of labour. Vaginal samples were taken within 12 hours of erythromycin treatment (250mg four times a day for 10 days) which is the standard treatment recommended by the UK RCOG guidelines [248].

Following delivery, outcome data for study participants were categorised into the following cohorts

- a) Uncomplicated term delivery > 37 weeks gestation (Control)
- b) Subsequent spontaneous preterm delivery < 37 weeks gestation (SPTB)
- c) Confirmed PPRM < 37 weeks. Sample taken within 12 hours of rupture before antibiotics (Post PPRM)

2.2.4 Metadata

Metadata was collected for all participants included maternal age, BMI, ethnicity, smoking habits, gestational age at research visit and subsequent interventions for preterm birth. Following delivery, details regarding mode of delivery, gestation age at delivery and presentation if preterm (i.e. SPTL or PPRM) was documented and stored electronically.

2.2.5 Transvaginal cervical length

In the pregnant cohort, cervical length (CL) scanning was carried out using transvaginal ultrasound (TVUS) by trained clinicians at each sampling visit using a consistent technique of measuring the length

(mm) a straight line between the internal os and external os. Three measurements were taken with the shortest length being recorded in the database.

2.2.6 Preventative interventions for preterm birth

As per clinic guidelines, a cervical stitch was offered to women when CL was ≤ 25 mm before 24 weeks gestation. Women with a short cervix (CL ≤ 25 mm) and > 24 weeks gestation were allocated to receive progesterone vaginal pessaries (400 mg every night). All women receiving these interventions continued with longitudinal follow up according to specified research time-points.

Cervical cerclages were removed between 36⁺⁰ and 36⁺⁶ weeks and progesterone pessaries were administered until 34 weeks unless spontaneous labour occurred prior to this.

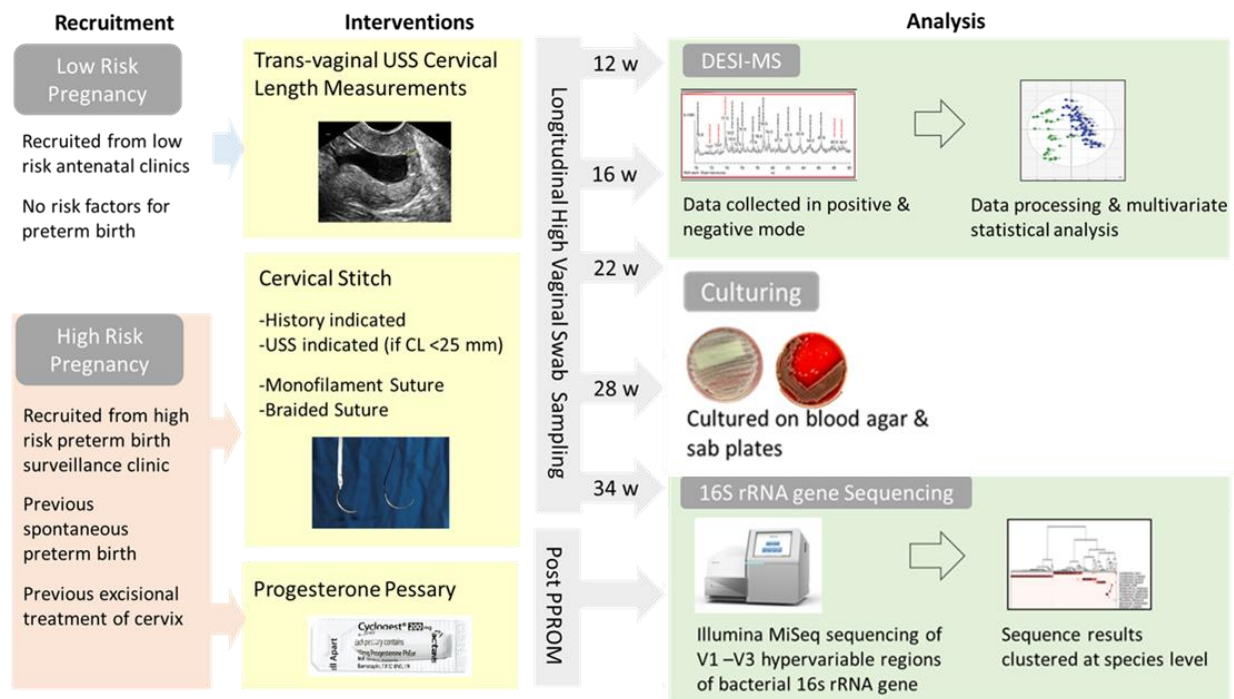


Figure 2-1. Overview of study design. Recruitment of low and high risk pregnant women who were then longitudinally sampled throughout pregnancy. Post PPRM group were recruited within 12 hours of membrane rupture prior to erythromycin treatment. All women had 3 samples taken for metabolic profiling, 16S rRNA sequencing and microbiology culturing.

2.2.7 Sampling

All vaginal samples were taken under direct visualization using a speculum, the cervico-vaginal mucosa (CVM) was sampled from the posterior fornix.

DESI-MS Pilot Study

High risk and low risk for preterm pregnancies were longitudinally sampled at specified time points in pregnancy (weeks + days). 12+0 weeks, 16+0 weeks, 22+0 weeks, 28+0 weeks, 34+0 weeks. In the Post-PPROM cohort the following swabs were taken within 12 hours of rupturing membranes

1. Metabolomics swabs for DESI-MS analysis: Transwab® MW170 (Medical Wire & Equipment) with rayon bud type
2. Microbiology swab (vaginal): Transwab® MW170 with rayon bud

DESI-MS Pre term birth studies

1. Metabolomics swabs for DESI-MS analysis : (vaginal) Transwab® MW170 with rayon bud
2. 16S rRNA gene sequencing : BBL™ CultureSwab™ MaxV Liquid Amies swab

2.2.8 Storage and clinical microbial swab analyses

Vaginal swabs for 16S rRNA amplicon sequencing were collected into Amies transport media and placed immediately on ice before being store within 10 minutes of collection time at before being immediately stored at -80°C. Swabs taken for metabolomics had their wet weight recorded to permit subsequent normalisation of metabolite concentrations and facilitate sample to sample comparison of data. Swabs were then put directly into a sterile 1.5ml microfuge tube and then on ice before being immediately stored at -80°C. Microbiology swabs were sent to the on-site NHS microbiology laboratory for immediate culture and microscopy based analyses.

2.3 Vaginal Mucosal Metabolic Profiling by DESI-MS**2.3.1 DESI-MS analysis of mucosal swab samples**

DESI-MS for direct swab analysis was performed using an in-house DESI source mounted on an Orbitrap Discovery hybrid mass spectrometry (Figure 2.2). A medical swab was secured within a swab holder and positioned horizontally in front of the MS inlet capillary with a swab-capillary distance of less than 2 mm (Figure 2-2B). The DESI sprayer was directed at the centre of the medical swab with a tip-sample distance of approximately 2mm and an altitude difference between the tip and the inlet capillary of 2 mm. The medical swabs tip was analysed by DESI through clockwise rotations of the swab toward the MS capillary turning at 100 rpm.

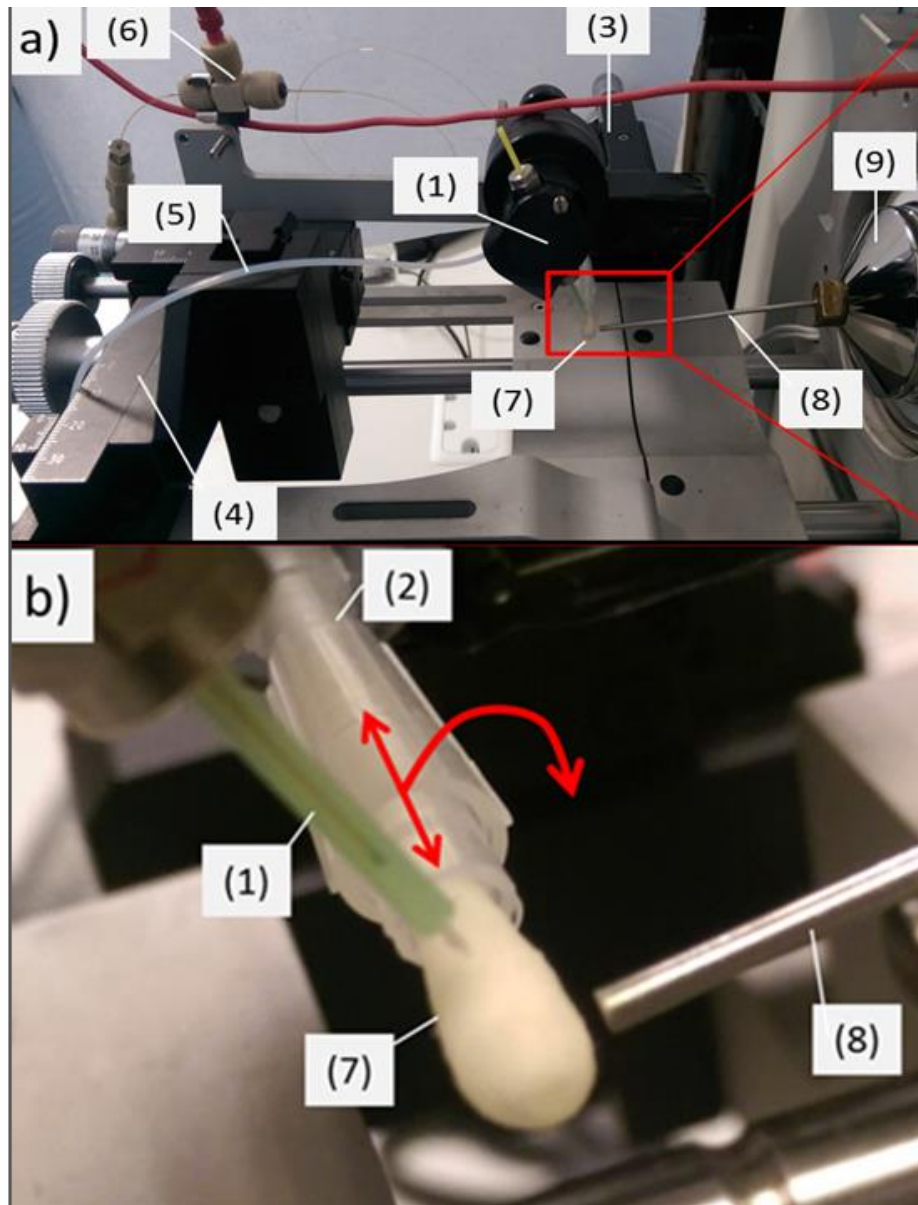


Figure 2-2. DESI-MS setup for medical swab analysis. A) Home-built DESI source mounted on an Orbitrap Discovery hybrid instrument. DESI sprayer (1) and medical swab holder (2) are secured onto a separate 3D moving stages (3,4) allowing manual adjustment in the x-, y-, and z-axis. The DESI sprayer is connected with a nitrogen gas supply (5) and power supply (6). The charged solvent passing through the sprayer is methanol:water. B) The medical swab (7) is inserted into the automatic swab holder (2) and positioned horizontal to the inlet capillary (8). During DESI-MS analysis the medical swab is rotated toward the atmospheric inlet capillary of the mass spectrometer (9).

The DESI source operating parameters and instrumental settings are listed in Table 4. Full scan mass spectra (m/z 50-1000) were recorded in the negative and positive ionization mode for 30 seconds each. Stored mucosal swabs were randomized prior to analysis by DESI-MS to avoid bias in the statistical analysis due to analytical batch effects.

Table 4 Optimized source parameters and instrumental settings for DESI-MS analysis of medical swabs.

Source parameters and DESI-MS instrumental settings			
Nebulizing gas pressure	7 bar	Microscans	1
Spray voltage	4.3 kV	Mass range	150-1000
Capillary temperature	250 °C	Mass resolution	30.000
Capillary voltage	50 V	Tip-to-surface height	< 2 mm
Solvent flow rate	10 $\mu\text{l min}^{-1}$	Distance inlet-sample	2 mm
Tube lens voltage	120 V	Angle tip-sample	50°
Spray solvent	methanol/water (95:5)	Angle inlet	10°
Max. injection time	500 ms	Distance tip-inlet	4.5 mm

2.3.2 Quality control swabs

Quality control (QC) swabs were developed as to permit assessment of experimental variability and technique reproducibility. This workflow was designed by fellow PhD student P. Pruski. Bovine plasma was precipitated using a 4 to 1 ratio of ice-cold acetonitrile and incubation for 1 hour at -80 degrees C. The precipitate was recovered following removal of the supernatant after centrifugation (1000 x g for 10 seconds) and dried for approximately 1 hour at room temperature until reaching a gel-like consistency. The gel was then distributed uniformly on the swab surface by rotating the swab on aluminum foil so that each swab contained approximately 50 mg of plasma precipitate [369] (Figure 2.3).

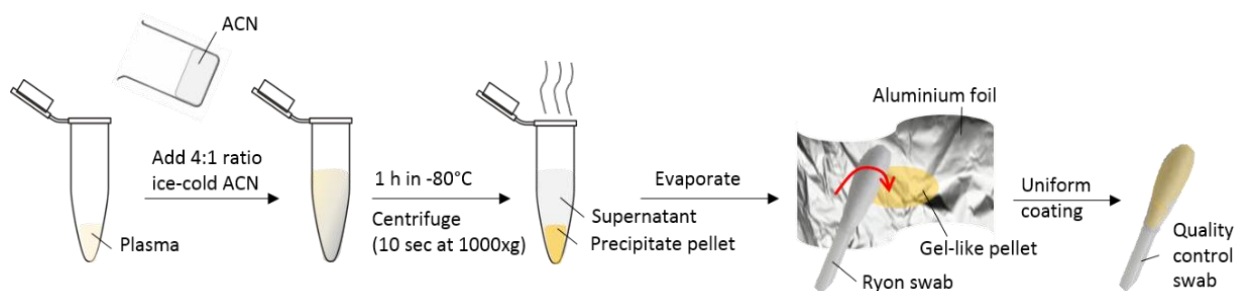


Figure 2-3. Sample preparation workflow for quality control (QC) swabs [369]

2.3.3 Data processing and analysis for DESI-MS data

- **Mass spectral data pre-processing**

Raw spectral data in both negative and positive mode were converted to *imzML* format [370] via the ProteoWizard *msConverterGUI* (Vanderbilt University, Nashville, TN, USA) [371] and then imported into R with a resolution of 0.01 Δm_z . Figure 2-4 shows an overview of the pre-processing workflow carried out on this data. The first step was normalisation which was performed by Total Ion Current

(TIC). This is the sum of all spectral intensities for each feature in a sample, divided by the number of scans [372]. The peaks detected in each sample were allocated to bins with an interval of $\Delta m_z=0.001$. Detected peaks were those with a signal to noise ratio greater than 5. Following this all spectra were peak picked within 20 ppm followed by smoothed histogram peak alignment to correct small mass shifts within the data set [373]. A log₂ transformation of intensity values was applied to correct data skewness. This was done using the formula $10\log(C_1*x+C_2)$. Background swab and solvent peaks were filtered, using the spectra acquired from the only swabs and solvent, the ions with an intensity different from 0 in all the samples are retrieved. Those ions are matched with the ions detected in the DESI samples (+/- 1.5 ppm). All the ions with a Spearman's correlation larger or equal to 0.5 with at least one of the matched ions are considered biologically uninformative and removed.

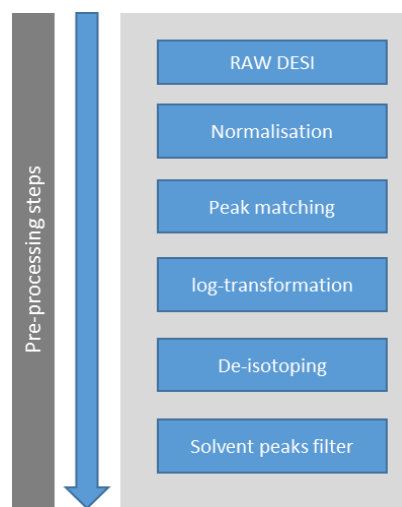


Figure 2-4. Pre-processing workflow for raw DESI-MS data collected in positive and negative ionisation mode

- ***Multivariate statistical analysis***

DESI-MS pre-processed data was analysed using both unsupervised and supervised multivariate statistical approaches for data reduction, classification of samples and identifying spectral variables important for class separation.

Unsupervised data modelling

Principal components analysis (PCA) is an unsupervised multivariate statistical technique that models data in an exploratory fashion without any a priori knowledge of classes (e.g. SPTB, control). PCA provides information on the model as a whole and permits visualisation of clusters and trends within the data and to identify potential outliers [374]. As shown in

Figure 2-5, an X data matrix holds all the data captured from an experiment. The rows represent the observations (individual patient/samples) and the columns are the variables which are the

measurements made to capture the properties of the observations e.g. m/z features. A PCA transforms X data matrix into 2 interpretable plots; a score plot relates to the observations and a loadings plot relates to the variables.

X data matrix

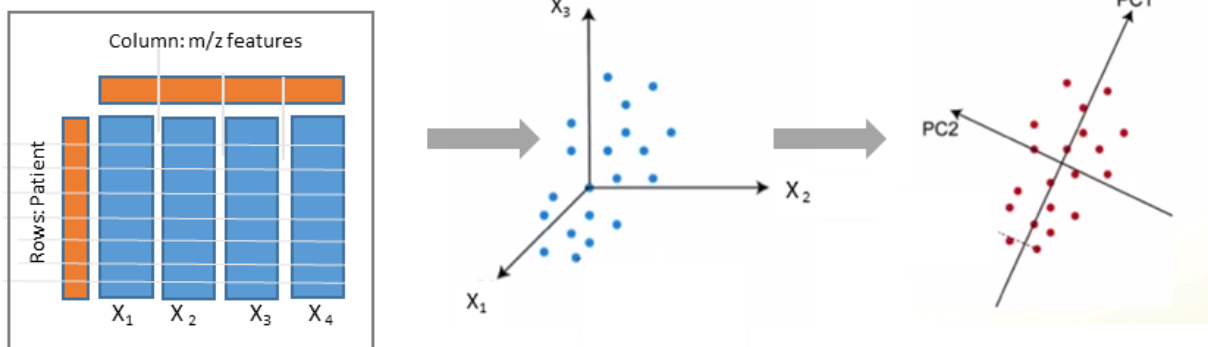


Figure 2-5. Generation of PCA plot from X data matrix. Observations (rows) are plotted on the X₁, X₂, X₃ etc axis in 3D space as shown by blue dots. PCA 1 is a line that is drawn through the area of maximum variation in this plot. PC2 is orthogonal to this line. The plot is then projected into 2D space (red dots). This image forms the PCA score plot. The cosines of the angles made by the PC with the original coordinate axes (X₁, X₂) are termed the “loadings” which are used to generate a loadings plot.

The variable columns (m/z features) each become a variable axis; X₁, X₂, X₃ etc. The rows (observations) are plotted onto these variable axis as represented in Figure 2.5, by the blue spots. These become points in multi-dimensional space. PCA identifies the direction of the maximum variation in the data that is the most common pattern among the samples. A line is drawn through this trend and this is termed the first principal component (PC1). PC2 can be drawn, this is always orthogonal to PC1. PCA is a projection method, this can be thought of as “switching on a light” on to reveal the shadows of the blue dots which were in the multidimensional space. The shadows are the red dots in two-dimensional space and projected to the new “PC axis,” this image forms the score plot. The cosines of the angles made by the PC with the original coordinate axes are termed the “loadings”. Importantly, the directions in the score plot correspond to directions in the loading plot, and vice versa, assisting interpretation of any potential cluster separation and underlying structure. Additional principal components can be added orthogonal to the previous ones which increases how much of the variation can be explained by the model. Strong outliers can be removed from the plot if that are deemed to adversely affect the model.

Validation of the model can be performed by using leave one sample out (1 in 7) cross validation (CV) with these results being expressed as the Q²X value. This procedure involved leaving out one sample from the sample set and calculation of a new model using the remaining data set. The withheld data are then projected into the new model and classified into one of the classes.

Supervised data modelling

Supervised modelling methods use a priori known structure to set rules with which enable the prediction of new data. PLS-DA (Partial Least Squares Regression-Discriminant Analysis) models on such methods that examines specifically the relationship between the spectra and provided class information using multivariate regression methods [375]. PLS-DA offers the ability to not only identify important variables with respect to a particular attribute but also provides a better understanding of the internal X data matrix structure. PLS-DA modelling involves an internal correlation of data matrix X with data matrix Y which has the class information (i.e. term or preterm birth). It can define the most importance variables that explain X and correlate to Y, termed variable importance for the projection (VIP).

Another supervised technique includes using a Random forest (RF) classifier [376] and can be used for both classification and regression analysis. This technique uses multiple decision trees which are built (into a forest) and merged together using a machine learning algorithm in order to obtain features of importance. It is possible to just select the top-N features that contribute to model prediction which can reduce the potential of overfitting the model as less features including noise are included [377].

To assess feature importance and the predictive power of the supervised models, a leave one sample out cross-validation strategy can be employed to predict the label of the validation sample.

- ***Statistical workflow***

Initial modelling of data for both preterm birth and pilot studies were carried out using SIMCA P+ (v14.0, Umetrics, Umea, Sweden). As shown figure 2.6 this involved an unsupervised PCA analysis with removal of outliers. PCA was then re-run and PLS-DA plots generated. Leave one out cross validation was performed and variable ranking (VIP) to assess features that were importance to class separation.

A second workflow also performed on the preterm birth studies using a random forest classifier. This has been shown to have a more robust classification performance than other supervised methods including PLS-DA [377]. All variables were initially passed to the RF classifier but only the top-N variables were used by the classifier for training and prediction. A varying number of variables and trees were tested to determine the optimal configuration in terms of predictive accuracy. The final combination (number of variables/number of trees) corresponded to the maximum value of the accuracy. If more combinations corresponded to the maximum accuracy, only the one with the lowest number of variables was considered. Variables included all features in negative and positive mode. In the PPRM study, clinical data including BMI and ethnicity were included as additional variables. The discriminating models were validated through leave one out cross validation with accuracies

presented as confusion matrices [378]. A further validation of feature discriminative power was performed applying a hierarchical clustering (Euclidean distance, Ward linkage) to the selected variables values in the full dataset. An exact Fisher's test was employed to test the difference between the clinical-related class labels and the cluster labels.

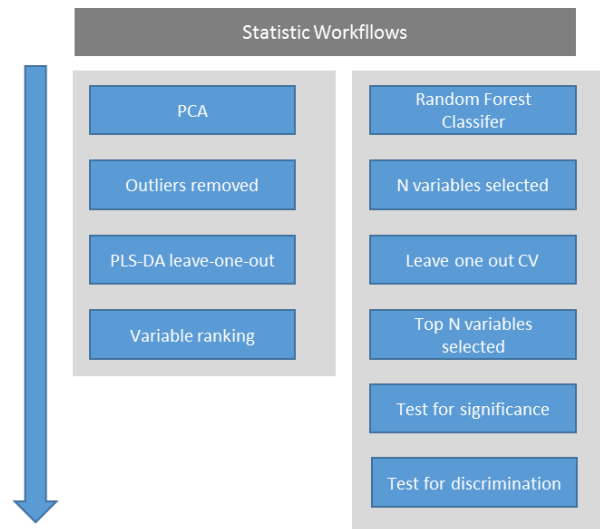


Figure 2-6. Statistical workflow for pilot and preterm birth studies under multi and uni-variant analysis.

- ***Univariate data analysis approaches***

Intensity values and median fold change of binned *mz* values were analysed using the univariate Kruskal-Wallis tests to identify discriminatory *mz* values (P-values reported). This test was used to determine if there was statistically significant differences between the groups. Mass spectral data are not normal distributed by definition therefore this test was used as it does not require the data to be parametric.

False discovery rate correction (< 0.01) was performed using the Benjamini-Hochberg-Yekutieli method (q-values).

Mean abundance and standard error were calculated for selected metabolites represented in scatterplots which were constructed in Graph Prism (Graphpad software, La Jolla, CA).

2.3.4 Metabolite identification

METLIN

Features of interest were initially putatively identified by their isotopic pattern and the accurate *mz* value using the METLIN database and Lipid maps [379, 380]. Metabolite hits were searched for using a tolerance ± 5 ppm with adducts [M-H]⁻, [M+Cl]⁻, and [M-H₂O-H]⁻ in the negative mode and [M+H]⁺,

[M+K] and [M+Na] in positive mode. Results generated after database searches were compared with metabolites identified in previously published studies reporting metabolites of vaginal [333, 368, 381, 382] and amniotic fluid origin [353, 383].

MS/MS

Where possible, masses of interest that contributed strongly to class separation in the multivariate models were selected for tandem mass spectrometry (MS/MS). This was performed using a Xevo G2-XS Q-ToF instrument in collision gas mode with a collision energy set at 31 Volts and MS/MS mode selected.

2.4 Assessment of Vaginal Microbiota

Vaginal microbiota was assessed using a combination of both clinical microbiology approaches (culture and microscopy) and culture-independent 16S rRNA amplicon sequencing as described below.

2.4.1 Clinical microbiology

To assess yeast presence, the vaginal swab was streaked on a Sabouraud agar plate followed by 40-48 hours of culture. Colony formation in the third or fourth quadrant of agar plate was defined as moderate to heavy growth. Normal flora (*Lactobacillus* spp.) was assessed by streaking on a blood agar plate and cultured for 18-14 hours. Colony formation in the third or fourth quadrant of agar plate was defined as moderate to heavy growth. The presence of Group B *Streptococcus* was determined using growth on an aztreonam agar plate. Gram staining was also performed for identification of bacterial vaginosis (BV). The swabs were dabbed onto glass slides and then heat fixed. Slides were then assessed under a microscope and graded according to the Hay/Ison Criteria [384].

2.4.2 16S rRNA amplicon sequencing

This work was performed by Dr Richard Brown and has been described previously [282].

- **DNA extraction**

Vaginal swabs were thawed on ice and re-suspended in Amies Liquid transport medium by vortexing. The swab solution was then transferred to a sterile DNase/RNase free 2ml tube and centrifuged at 3000 x g for 5 minutes. The supernatant was aspirated and the pellet re-suspending in 230µl Enzyme cocktail for 1h at 37°C. Following enzymatic lysis, samples underwent mechanical disruption through oscillation at 2000 rpm for 1 minute using a Mikro-Dismembrator with 0.1 mm acid washed glass beads. The resulting lysate was collected transferred to the QIAamp DNA Mini Kit. A total of 20µl of

Proteinase K and 200µl Buffer AL was added per 200µl of lysate, and incubated at 56°C for 30 minutes. 200µl Ethanol was added per sample, the lysate was then transferred to the QIAamp Spin Column. The columns were centrifuged at 6000 x g for 1 minute. The supernatant was discarded and the column washed with 500µl AW1 buffer at 6000 x g and then 500µl AW2 buffer at 20000 x g for 3 minutes. Finally, the DNA within the column was eluted in 100µl AE buffer at 8000 rpm for 1 minute.

- ***Polymerase chain reaction (PCR) amplification***

Extracted bacterial DNA was amplified by PCR using universal primers, forward 27F-5'-AGAGTTTGATCCTGGCTCAG-3' and reverse 338R-5'-GCTGCCTCCCGTAGGAGT-3'. DNA integrity was confirmed using agarose gel electrophoresis. Agarose gel (1.5%) was prepared by microwaving 1.5g agarose powder in 100 ml 1x TBE buffer until dissolved. 1µl Sybr Safe DNA gel stain was then added and the gel was allowed to set. DNA loading dye was added to each DNA extract, alongside with a molecular weight marker. In addition to each DNA extracts being analysed, each gel also had two negative controls (one blank swab, and one pure water to be processed in parallel. Samples were separated by electrophoresis at 140 V for 10 to 20 minutes. The gel was trans-illuminated and fluorescent bands visualised with the UV light.

- ***DNA sequencing***

The V1-V2 hypervariable regions of 16S rRNA genes variable regions were amplified for sequencing using forward and reverse fusion primers. This hypervariable regions was targeted for amplification as it considered that together, these regions provide a comprehensive differentiation of all bacterial species to the genus level [275].

The forward primer consisted of an Illumina i5 adapter (5'-AATGATACGGCGACCACCGAGATCTACAC-3'), an 8-base pair (bp) bar code, a primer pad (forward, 5'-TATGGTAATT-3'), and the 28F primer (5'-GAGTTTGATCCTGGCTCAG-3') [385]. The reverse fusion primer was constructed with an Illumina i7 adapter (5'-CAAGCAGAAGACGGCATAACGAGAT-3'), an 8-bp bar code, a primer pad (reverse, 5'-AGTCAGTCAG-3'), and the 388R primer (5'-TGCTGCCTCCCGTAGGAGT-3'). Sequencing was performed at RTL Genomics (Lubbock, TX, USA) using an Illumina MiSeq platform (Illumina Inc.).

- ***Data processing and statistical analyses for microbial data***

Resulting sequence data were analysed using the MiSeq SOP Pipeline of the Mothur package [386] Sequence alignment was performed using the Silva bacterial database (www.arb-silva.de/) and sequence classification by the RDP (Ribosomal Database Project) database reference sequence files and the Wang method [387]. The RDP MultiClassifier script was used to determine the operational

taxonomic unit taxonomies (phylum to genus) and species-level taxonomies by USEARCH with 16S rRNA gene sequences from cultured representatives [388]. Data were resampled and normalized to the lowest read count in Mothur. Measures of diversity; Inverse Simpson and richness; total species observed (SOB) were calculated with Mothur and R using the Vegan package.

Examination of statistical differences between vaginal microbiota was performed at genera level in the Statistical Analysis of Metagenomic Profiles software package (STAMP) [389]. Samples were classified into according to Ward's linkage hierarchical clustering analysis (HCA) of bacterial species using a clustering density threshold of 0.75 with the 50 most abundant species displayed. Clusters were sub-grouped on the basis of *Lactobacillus* abundance into *Lactobacillus* dominant (>79%) and deplete / dysbiotic (<64%). Samples were also classified at species level according to ward clustering into five CSTs; I (*L. crispatus*), II (*L. gasseri*), III (*L. iners*), V (mixed bacterial species), and VI (*L. jensenii*) as described by Ravel et al. [291]. Significance of differences between richness and diversity measures between patient groups was assessed using Mann-Whitney t-test.). Alpha and beta indices were calculated from the dataset with Mothur and R using the Vegan package to create the following measures of diversity; Inverse Simpson and richness; total species observed (SOB).

3 DEVELOPMENT OF DIRECT SWAB METABOLIC PROFILING BY DESI-MS

The work described in this chapter was published as Pamela Pruski, David A. MacIntyre, Holly V. Lewis et al., Medical Swab Analysis Using Desorption Electrospray Ionization Mass Spectrometry: A Non-invasive Approach for Mucosal Diagnostics Analytical Chemistry (2017) [369]. I worked closely alongside fellow PhD candidate Pamela Pruski optimising the DESI-MS experimental platform for direct swab analysis including the creation of the automated swab turning device. I also performed initial experiments; trouble shooting and assisting with DESI-MS data acquisition. Once the protocol was further optimised, I performed data acquisition, data analysis following pre-processing of the data and data interpretation.

3.1 Introduction

A shift in the composition of the vaginal microbiome from *Lactobacillus* spp dominance towards a high diversity state is associated with increased risk of PTB [125, 126, 287, 390]. However, current clinical methods for assessing vaginal microbial composition are limited to culture and microscopy-based approaches. These methods fail to capture important information regarding relative abundance of bacteria and to identify fastidious microbes [290]. This has led to a rapid increase in the application of culture-independent techniques such as 16S rRNA gene amplicon and whole shotgun sequencing approaches that enable identification and estimation of relative abundance of almost all species within a given sample. However, these approaches are still comparatively costly and time consuming, which has limited their use in clinical settings [290]. Next generation sequencing methods also fail to assess the host response to microbiota [391] i.e. the mere presence of bacteria does not confer activation of immune recognition and induction of inflammatory responses [341].

The vaginal mucosa is the site of innate and acquired immune responses against host infection in the reproductive tract [298, 326, 392, 393]. The intricate interplay between these two components of the immune system, plus their interaction with the microbiome and host epithelial cells, is ultimately responsible for lower genital tract health [293]. Recent studies have shown that integration of LC-MS based metabolomic and microbiota compositional data from vagina mucosa samples enables the identification of metabolic profiles that are strongly associated with bacterial vaginosis [368, 381, 394], a common vaginal pathology characterised by the reduction in commensal *Lactobacillus* species and increase in anaerobic bacteria often accompanied by activation of inflammation [368]. These studies have shown that both bacterial and host-derived metabolites are implicated in symptomology [368, 381] as well as immune modulation that enhance inflammation and infection risk [305, 347]. These metabolites have potential use as prognostic and diagnostics markers of vaginal health and disease [290, 394]. However, despite the quality of the information provided by LC-MS and 16S rRNA sequence data, their application for clinical point of care (POC) diagnostics is limited due to extensive, time-consuming sample preparation and metabolite extraction.

Ambient ionization mass spectrometry was developed as a sample preparation-free alternative to these traditional MS-based workflows [395]. DESI-MS is an ambient technique which permits acquisition of metabolic data from a wide range of samples including unaltered biological specimens [396, 397] thus offering a possible analytical platform for POC applications [398, 399]. In DESI-MS, a stream of charged solvent droplets is directed towards a surface of interest which forms a thin film which gently dissolves molecules from the sample. Secondary charged droplets, which contain

constituents of the sample, are formed and eventually produce molecular ions of the analytes upon evaporation in the atmospheric pressure interface of the mass spectrometer [395, 396]. Subsequently, these ions are then separated and analysed to create an almost instant spectral profile, which can be used to quantify and identify the molecules present in the sample.

DESI-MS preferentially ionizes lipids (fatty acids, phospholipids, and diglycerides and triglycerides) [400] but can ionize a variety of other compounds such as peptides, proteins and drug molecules [401]. DESI-MS imaging has been shown to provide high specificity, selectivity, and sensitivity in direct tissue analysis in the discrimination of disease states and tissue types [402-404]. It also has the ability to discriminate purified bacterial samples at species level direct from glass slide smears or directly from agar plates [404-406].

In this study, we aimed to develop an analytical protocol for the direct analysis by DESI-MS of medical swabs, which are used in standard practice for mucosal sampling. Ideally the method would not need modification or alteration to the swab and only standard clinical sample collection protocols for microbial analysis would be necessary.

Experiments were first designed in order to maximise the metabolic information obtained from the swab and assess the repeatability and reproducibility of the method.

We next aimed to assess if DESI-MS swab analyses could identify changes in the local biochemical milieu of the vaginal mucosa induced by pregnancy.

To provide further evidence of potential diagnostic application of DESI-MS, swab samples collected from pregnant women with clinically diagnosed BV were also analysed by DESI-MS and compared to healthy controls.

3.2 Study Design

Two sets of studies were carried out:

- i) DESI-MS technique optimisation studies
- ii) DESI-MS vaginal mucosal metabolic profiling pilot studies

For these studies, women were recruited from Queen Charlotte's Hospital from September 2015 to January 2016. Non-pregnant women of reproductive age (n = 25) were recruited from the general gynaecology clinic and pregnant women (n = 43) were recruited from the antenatal clinic between 8-40 weeks gestation.

Following informed written consent vaginal mucosal samples for metabolic profiling were taken using standard medical swabs from the posterior vaginal fornix under direct visualization. In the pregnant cohort, matched vaginal swabs were also sent for clinical microbial assessment. Diagnosis of BV was performed via the assessment of gram staining using the Hay/Ison criteria [267]. Detailed maternal and neonatal metadata were collected for all participants from the hospital case notes and the electronic patient databases Cerner Millennium.

3.3 Results: Optimisation of DESI-MS for Direct Swab Analysis

For the optimisation studies, different components of the DESI-MS spectrometer are all considered in the optimisation of this technique for direct swab analysis. As shown in Figure 3-1, we considered the impact of different aspects of DESI-MS profiles in data acquisition. We first investigated different mass analysers, then the ion source i.e. DESI and finally the physical and geometrical effect of electrospray parameters. Once parameters were optimised, technique precision was assessed by testing repeatability and reproducibility. An overview of a mass spectrometer with the study design is shown in figure 3.1.

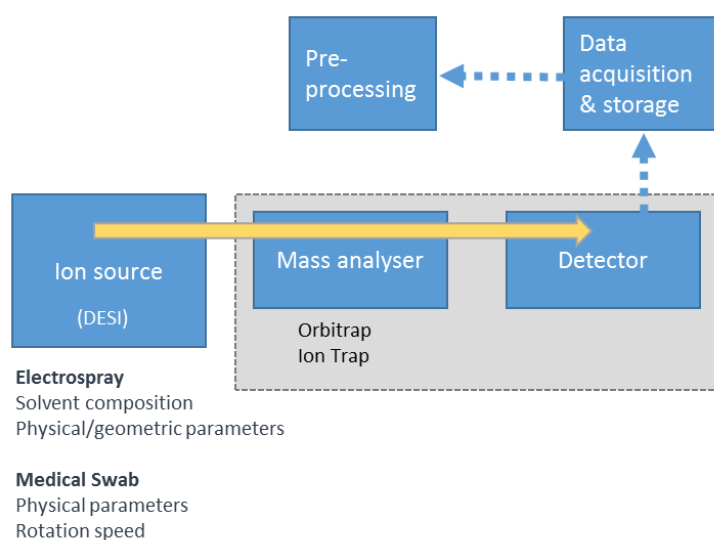


Figure 3-1. Overview of a mass spectrometer. In DESI-MS, ions (represented by yellow arrow) are generated at the ion source i.e. via the electrospray directed at a sample. The vapourised ions are directed into the mass analyser where the ions are separated according to their m/z ratios. In the ion detector the signal intensities of each separated ion are determined. The mass analyser and detector are under vacuum (represented by grey box) to prevent loss of ions through collisions with the walls of the analyser and neutral gas molecules. Data acquisition, storage then subsequent pre-processing are operations all controlled via a computer. Experiments that we carried out to assess impact on DESI-MS profiles included those that investigated electrospray, swab parameters and the mass analyser.

3.3.1 Examination of the impact of mass analysers on DESI-MS profiles

Mass analysers separate ions according to their m/z ratio so that ions and their intensities can be recorded by a detector. Two commonly used analysers are Ion trap and Orbitrap. Ion trap mass analysers use a combination of electric or magnetic fields to capture or “trap” ions inside the mass analyser [407]. The trapping field is continuously varied which alters that trajectories of these trapped ions that become unstable, and simultaneously leave the trapping field in order of m/z ratio. Upon ejection from the Ion trap, ions strike a detector and provide an output signal. In contrast an Orbitrap mass analyser, stores all ions in a stable flight path (orbit around an inner spindle-like electrode). This is achieved by balancing their electrostatic attraction by their inertia. The frequency of the axial motion around the inner electrode is related to the m/z of the ion [363].

The impact of different mass analysers on the detection of vaginal mucosal metabolites by DESI-MS was tested by comparing average spectra obtained from Orbitrap MS (LTQ-Orbitrap Discovery, Thermo Scientific) and ion trap which uses the same mass analyser but interfaced to a linear ion trap (LTQ-Orbitrap Discovery, Thermo Scientific). Data acquisition from matched vaginal samples in both polarities were collected. Figure 3.2 shows the average spectrum of matched vaginal samples with putatively identified lipids. Overall Orbitrap MS provided the most informative mass spectra with the highest spectral richness (130 lipids putatively identified), mass accuracy (<5 ppm) and higher signal to noise ratio. The mass spectral data acquired with ion-trap provided comparatively lower mass accuracy (>50 ppm), lower baseline signal/noise ratio and a smaller number of detected spectral features (13 lipids putatively identified). In consideration of these findings, subsequent pilot experiments for DESI-MS were performed using an LTQ-Orbitrap Discovery mass spectrometer (Thermo Scientific, Bremen, Germany).

signal intensities and number of spectral features obtained in the GPL region were found when using MeOH:H₂O and CH₂Cl₂:MeOH. In the positive ionisation mode, background solvent and swab peaks were found in the region *mz* 300-400 for all of the solvents. In addition, a PEG polymer arising from desorption of rayon swab material was noted when using isopropanol as a solvent, which extended from *mz* 400-900. Overall MeOH:H₂O (95:5) provided the most intense signals and more spectral features in our regions of interest with the least amount of background signal (swab and solvent peaks) and thus was used for all future DESI-MS experiments.

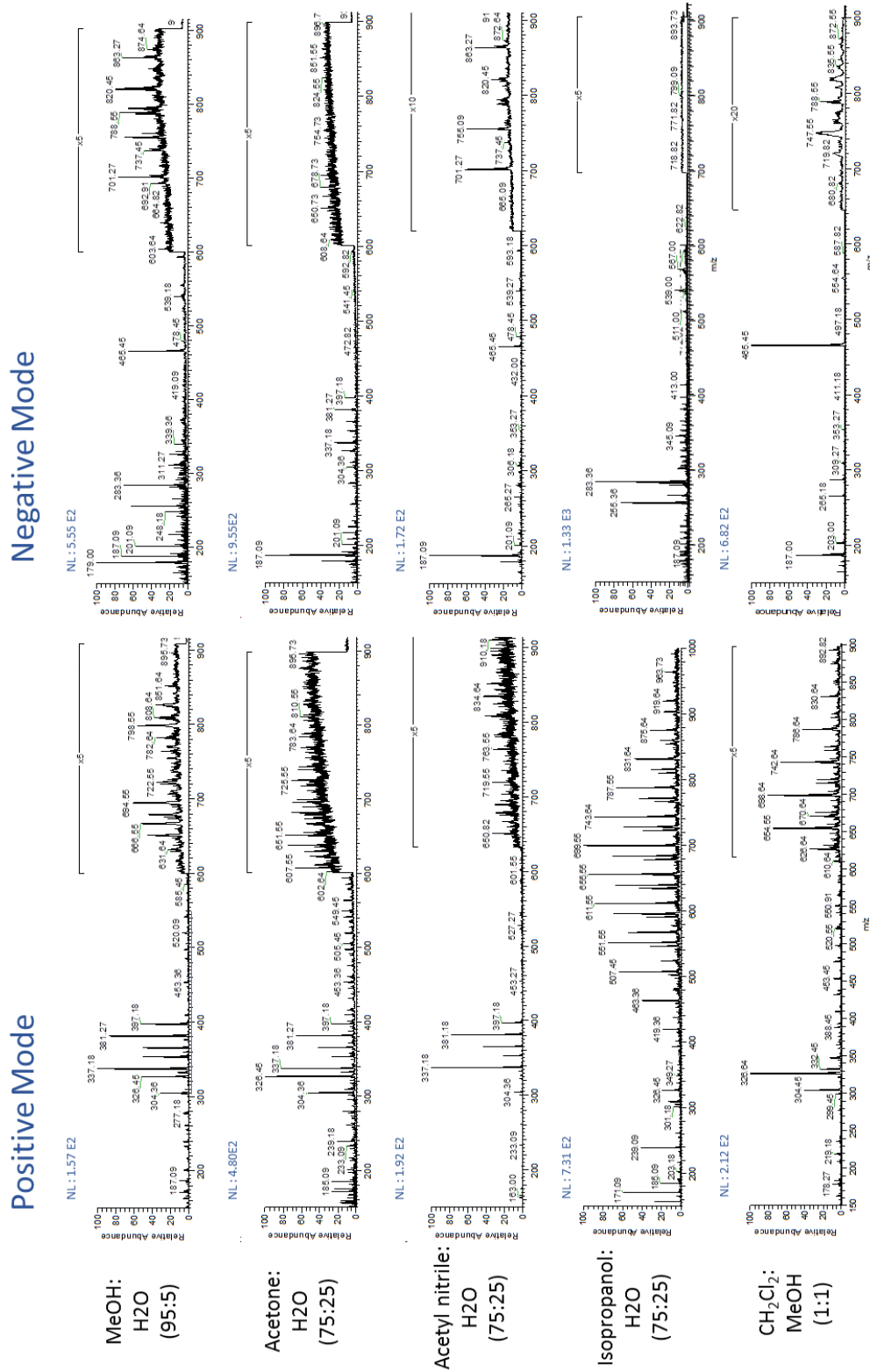


Figure 3-3. Average spectra for vaginal swab samples using different electrospray solvents in positive and negative ionisation mode. Solvents mixed with water included; methanol, acetone, acetyl nitrile and isopropanol. Dichloromethane mixed with methanol was also tested

Results: Development of Direct Swab Metabolic Profiling by DESI-MS

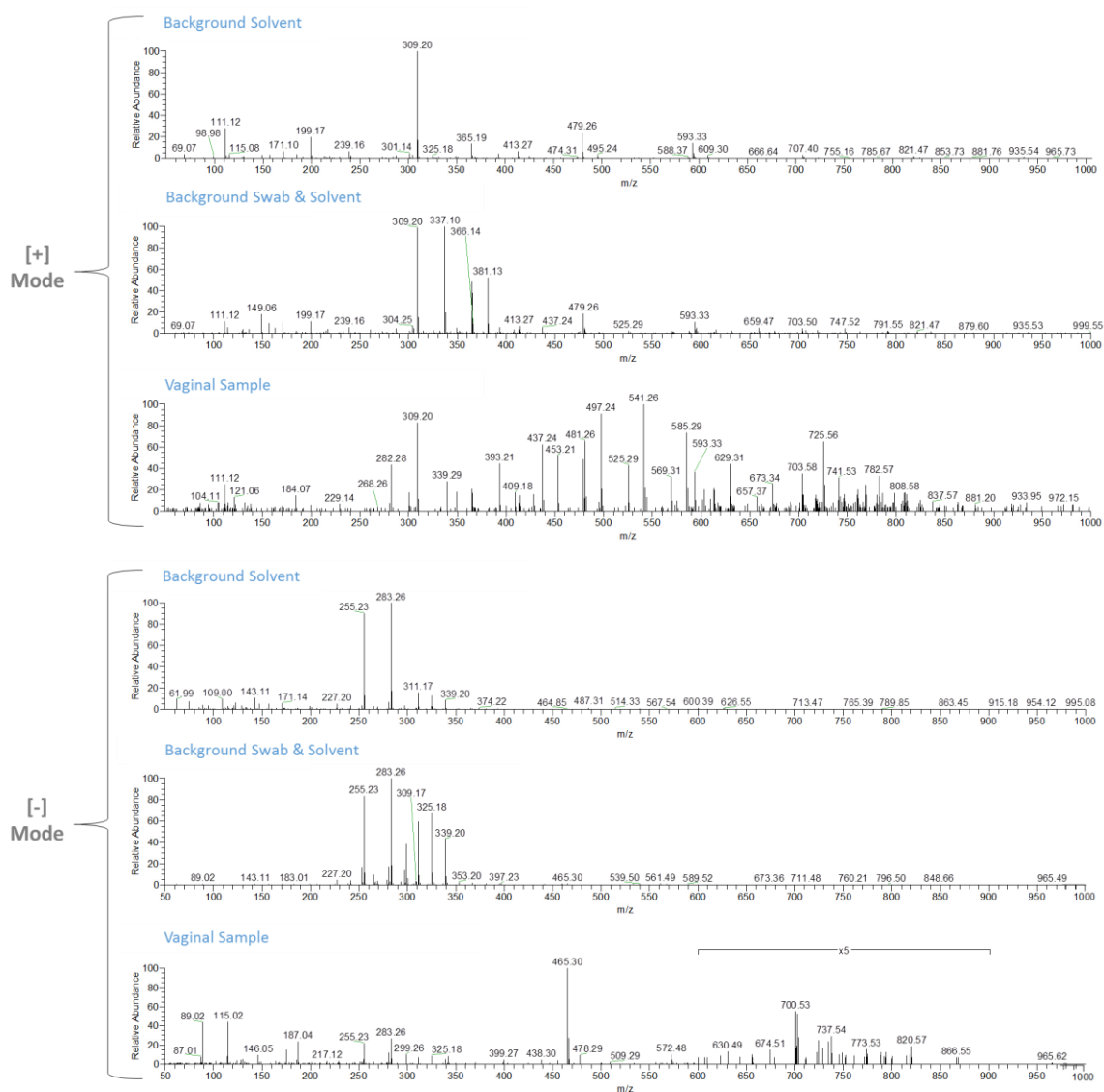


Figure 3-4. Averaged DESI MS spectra of background runs; solvent, swab and solvent. A control vaginal sample is also shown in each ionisation mode

In order to assess which peaks were arising from the sample and which were noise (i.e. from solvent or swab material) a series of experiments were carried out. Figure 3.4 shows an average spectrum in both positive and negative ionisation modes with just the selected solvent (MeOH:H₂O), the rayon swab with the solvent and finally of a vaginal mucosal sample (solvent, swab and sample). Features that are related to the background can be visualised in positive mode; solvent peak (m/z : 309.20), swab peak (m/z : 337.10) and in negative mode; solvent peak (m/z : 283.26) and swab peak (m/z : 339.20). The swabs with samples clearly reveal signals related to the sample; positive mode (m/z : 725.56 [SM (34:1) + H⁺]) and negative mode (m/z : 465.30 [cholesterol sulphate-H⁻]). Signals arising from the solvent and from desorption of rayon swab material were removed as part of the pre-processing step. Runs ($n = 20$) were recorded in both polarities and consistent features in each of these runs were then subsequently removed during pre-processing of the raw data.

Additional optimisation experiments for the DESI-MS set up were carried out by Pamela Pruski as part of her PhD project. Modifiable electrospray solvent parameters that were systematically tested included solvent flow rate, nebulizing gas flow rate, and electric potential applied to generate the electrospray. In addition, her work showed that a data acquisition time period of 30 seconds provided the most stable and constant signal ion intensities when analysing the same position of the swab. Data acquisition beyond this time period was associated with a linear decrease in signal intensity [369].

The geometric parameters of the DESI set-up included the height of sprayer tip relative to the swab surface, distance of swab to the MS inlet capillary and the angle of the sprayer tip to the sample surface (Figure 3-5). These parameters were all adjusted in a systematic fashion.

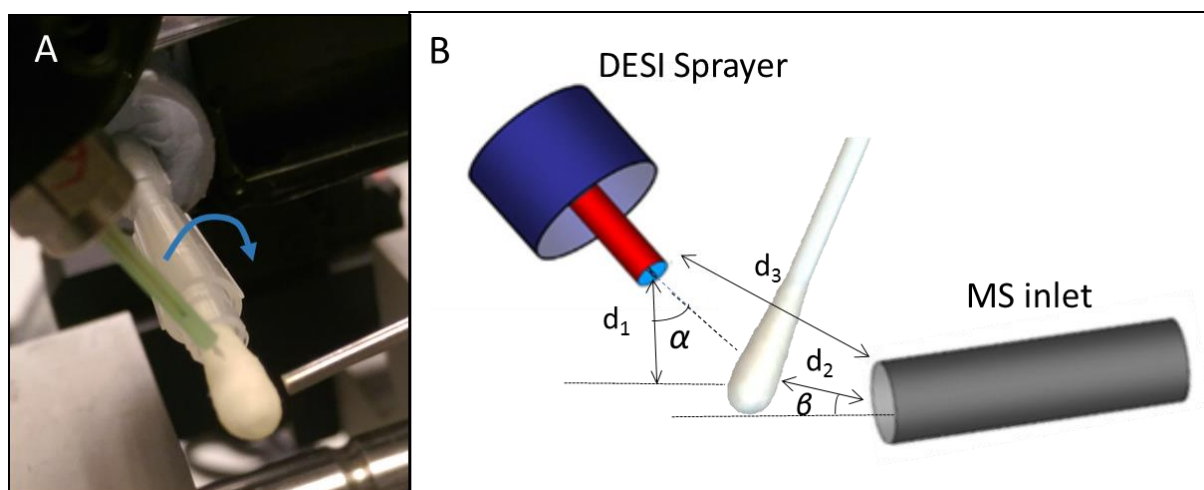


Figure 3-5. A DESI-MS set up showing direction of swab rotation. B: Illustration of the DESI-MS sprayer and mass spectrometer inlet with respect to geometrical parameters. The various parameters are: α , angle of sprayer tip to sample surface; β , angle of MS inlet capillary relative to sample surface; d_1 , height of sprayer tip to sample surface; d_2 , distance of MS inlet capillary to sample surface; d_3 , distance of sprayer tip to MS inlet capillary (adapted from Takats et al. [365]).

The DESI-MS sprayer was used in conjunction with a 3D-XYZ integrated linear stage, which provided a movable platform for the home-built swab turner which held the sample and positioned the sprayer relative to the MS capillary inlet and sample. The optimal physical and geometric parameters for the DESI electro sprayer are shown in Table 4. With regard to geometric parameters: α and d_1 have direct effects on the ionization process, while β and d_2 have important effects on the collection efficiency [365].

3.3.3 The impact of medical swab parameters on DESI-MS profiles

We next examined the impact of swab rotation speed and scanning position on resultant profiles. To achieve this, a home built automated swab turning device (powerfunction medium motor) was used to hold and rotate the swab in a fixed position. This device has a permanent 9V supply and was able to achieve a maximum rotation speed of 405 rotations per minute (rpm). Using an inbuilt speed dimmer to adjust the rotation speed, mass spectra were acquired at 0, 101, 202 and 405 rpm. Further, data acquisition was performed at different areas of the swab (tip, centre, bottom) as to define the optimal scanning position for data acquisition (Figure 3.6). Stationary DESI-MS data acquisition (0 rpm) resulted in poor signal intensity regardless of the scanning position. The maximal rotation speed (405 rpm) resulted in high signal intensities however these were inconsistent largely due to the instability of the swab caused by high revolutions. A medium rotation speed (202 rpm) provided the highest, most stable ion signal intensities (1-2 orders of magnitude higher than 101 rpm). Analysis of data obtained from differing swab positions showed that the highest *mz* intensity was acquired at the swab bottom, followed by tip and centre. The bottom of the swab was therefore used as the primary site of data acquisition for subsequent experiments.

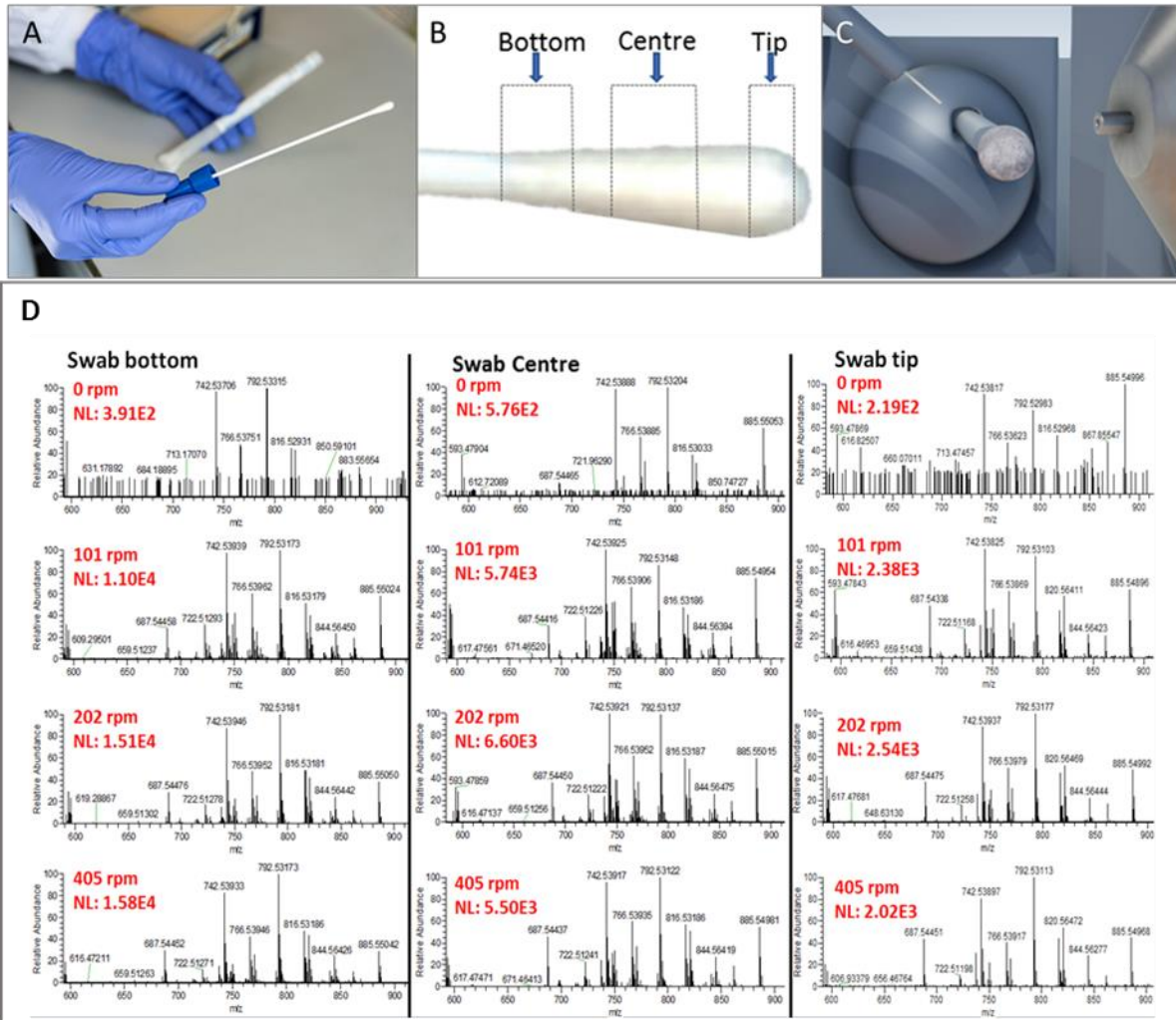


Figure 3-6. A: Images of standard medical swab. B: Indicates different potential scanning positions (bottom, centre, tip) of a swab surface using DESI-MS C: Schematic of DESI-MS set up; position of swab holder with mounted swab in relation to electro spray and capillary inlet. D: Average spectra at different swab positions (bottom, centre and tip) using different swab rotation speeds (0, 101, 202, 405 rpm). NL: Normalised Level and reflects the intensity of the base peak [369].

- **Measurement of precision**

The precision of an instrument is defined the closeness of agreement between independent test results obtained under stipulated conditions [409]. Repeatability specifically describes the precision obtained with the same method on identical test items in the same laboratory by the same operator using the same equipment within short intervals of time. Reproducibility is the precision obtained under changing conditions with the same method on identical test items.

Technique Repeatability

To investigate repeatability of DESI-MS direct swab analysis, three vaginal mucosal samples were taken from the same patient on the same day with each replicate sample analysed by DESI-MS using the same optimised protocol, equipment and the same operator. Examination of negative mode data obtained in the mass range of 50-1000 *mz* revealed highly consistent metabolic profiles with minimal variation in ion intensity observed and approximately 90% identical spectral features detected across replicates. Similar results were obtained for positive mode data acquisition.

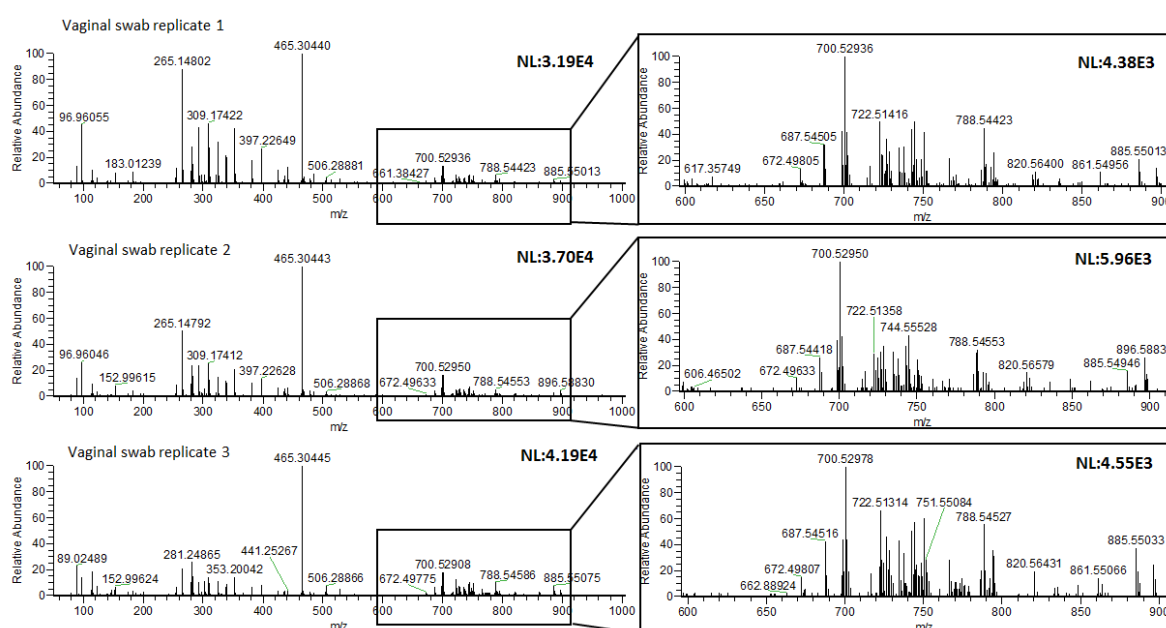


Figure 3-7. DESI-MS analysis of three vaginal swab replicates, sampled from the same patient taken at same time point. Averaged mass spectra are shown from each replicate swabs analysed in the negative ion mode in the mass range of *mz* 50–1000 (magnified lipid mass range is shown between *mz* 600 and 900). Both mass ranges indicate similar spectral features within all analysed replicates [369]

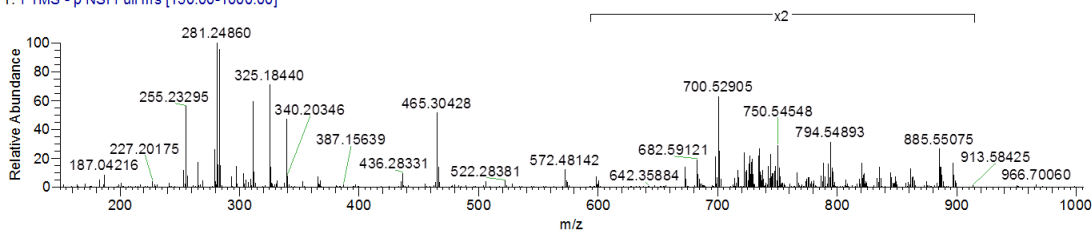
Technique Reproducibility

The reproducibility of direct swab analysis by DESI-MS was tested by assessing inter-swab variability of specific lipid peaks over a period of 9 days using quality control (QC) swabs. Two biomaterials were tested with the aim of creating a QC swab that reflected the lipid rich metabolic profile of vaginal mucosa; precipitated bovine plasma and amniotic fluid (see figure 3.8). Precipitated plasma provided a gel-like consistency that could be uniformly spread onto the surface of standard swab. In comparison, amniotic fluid, although relatively viscous, tended to saturate and absorb into the centre of the swab

material. Spectral profiles of precipitated plasma had higher relative abundance of lipids and more signals in the GPL region compared to amniotic fluid. Thus for ongoing experiments, precipitated plasma was used as the QC swab. DESI-MS profiling of the QC swabs was performed over a 9 day period and the ion intensity of four selected lipids examined as to assess inter swab reproducibility. These experiments were carried out by Pamela Pruski. The mean coefficient of variation for the selected lipids was $21 \pm 3 \%$, which is comparable to previous analyses of DESI-MS reproducibility for imaging of tissue sections [404] and within the range of co-efficient of variance (CV) for reproducibility for analytical techniques stipulated by the U.S. Food and Drug Agency (FDA) [410].

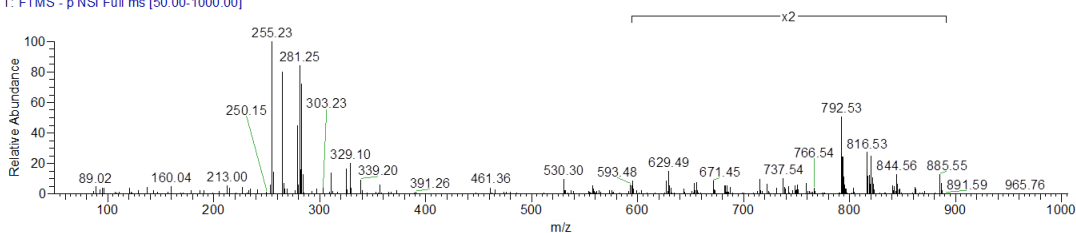
Vaginal mucosa

vp v2 122 3_FTMS neg 021215_Recal #16-49 RT: 0.39-0.59 AV: 3 NL: 3.72E4
T: FTMS - p NSI Full ms [150.00-1000.00]



Precipitated plasma

QC 30_FTMS NEG_Recal #31-40 RT: 0.49-0.64 AV: 4 NL: 3.66E4
T: FTMS - p NSI Full ms [50.00-1000.00]



Amniotic fluid

af-1_12-01-15 #8-25 RT: 0.17-0.59 AV: 18 NL: 4.31E4
T: FTMS - p NSI Full ms [150.00-1000.00]

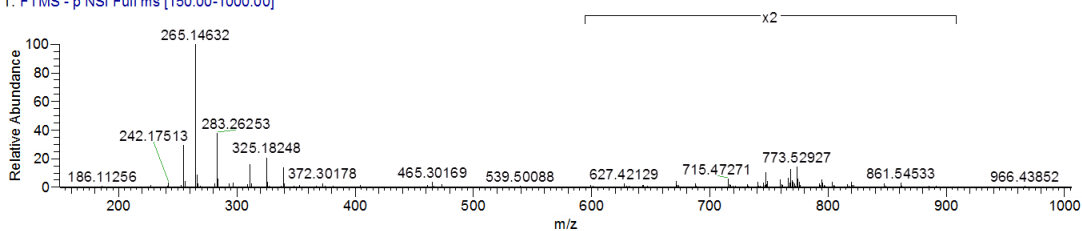


Figure 3-8. Comparison of biofluids (amniotic fluid and precipitated plasma) were tested as potential quality control swabs. Biofluids were assessed to see if spectral profiles were similar to vaginal mucosa swab profiles.

3.4 Results: Pilot Study

Having determined optimised parameters for DESI-MS medical swab analysis, the ability of the technique to characterise physiologically important changes in vaginal mucosal biochemistry was tested. This was achieved by examining changes in the vaginal mucosal metabolome induced by pregnancy and bacterial vaginosis (BV).

3.4.1 Detection of biochemical alterations induced by pregnancy

Vaginal mucosa samples taken from subjects during pregnancy (n=43) were compared with samples obtained from non-pregnant subjects (n=23). Averaged DESI-MS spectrum for non-pregnant and pregnant vaginal mucosa samples showed clear spectral differences, particularly in the lipid mass range m/z 700-900 (Figure 3-9).

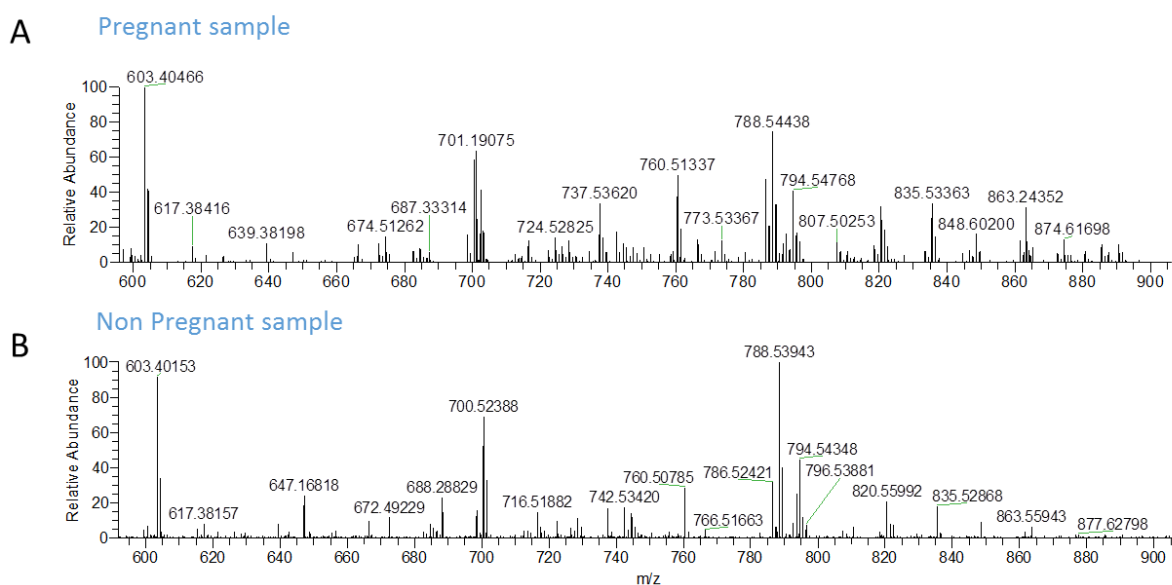


Figure 3-9: Averaged DESI mass spectra from pregnant (A) and non-pregnant (B) sample, acquired in the negative ion mode in the mass range m/z 150-1000.

Unsupervised multivariate analysis of the resulting spectral profiles by PCA showed separation of non-pregnant and pregnant swabs (Figure 3-10A). Differences in the DESI-MS profiles could be largely attributed to significant differences in abundance of specific lipid species identified using a random forest classifier (Figure 3.10B; $P < 0.05$, Kruskal-Wallis test). Differences were identified in both ionisation modes and showed that non-pregnant women had significantly high levels of ceramides whereas pregnant women had higher concentrations of sphingomyelins, glyceroceramides and acylcarnitines.

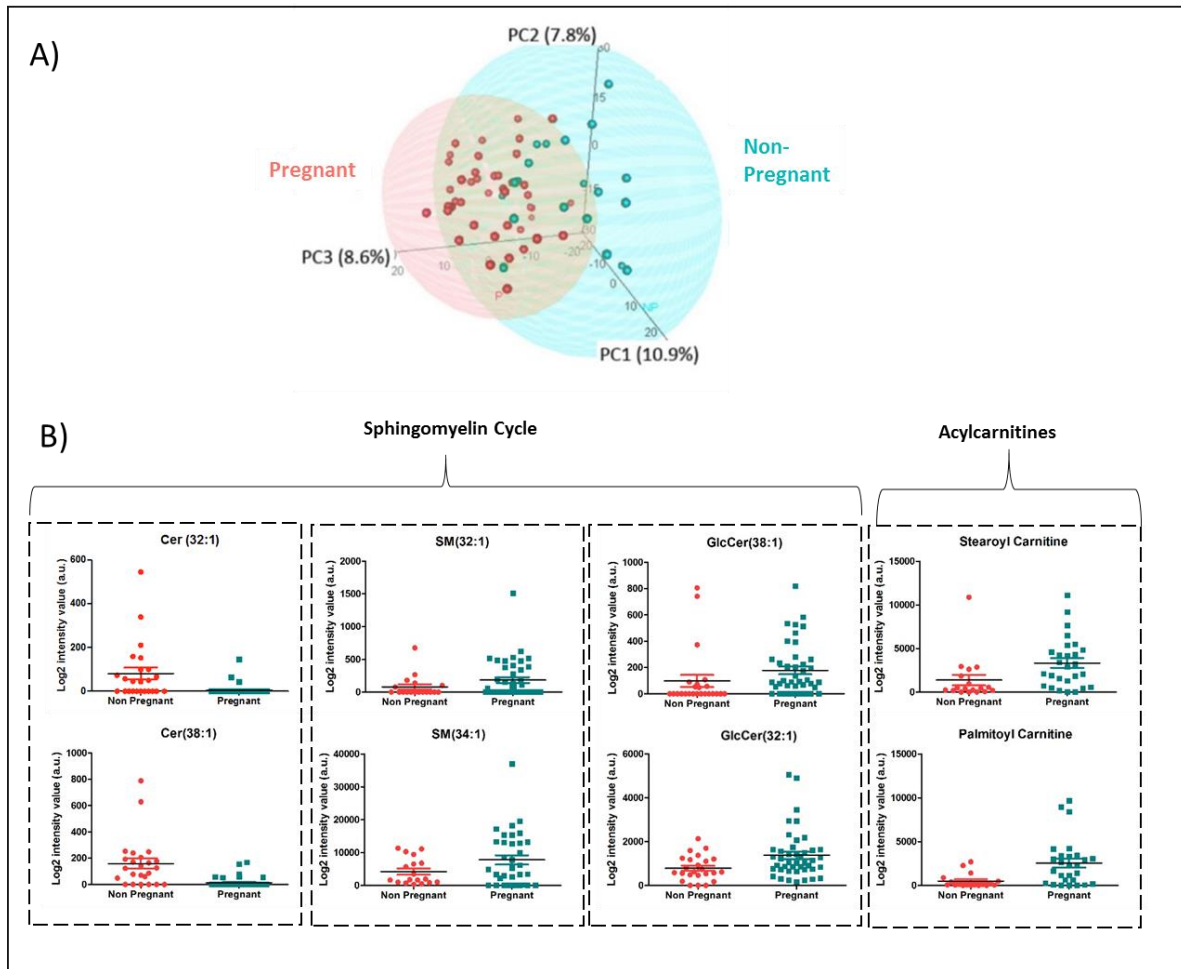


Figure 3-10. DESI-MS analysis of vaginal swab samples collected in pregnancy and non-pregnant women. A: PCA analysis of DESI-MS data collected in negative mode separates both groups based on different mass spectral fingerprints. B: Selected differential metabolites indicate significant differences in the abundance of selected lipid peaks between pregnant and non-pregnant women (obtained with a random forest classifier) ($p < 0.05$ using Kruskal–Wallis test)

3.4.2 Identification of mucosal metabolic profiles associated with bacterial vaginosis

Vaginal swab samples collected in pregnancy from women with bacterial vaginosis ($n=21$) were then compared with healthy pregnant control swabs ($n=43$) with *Lactobacillus* spp. dominated cultures as to determine if differences in microbial community composition in pregnancy could be rapidly assessed with DESI-MS (Figure 3-11). Unsupervised PCA analysis of DESI-MS data collected in both ion modes revealed major underlying differences in the vaginal mucosal metabolome of BV patients compared to healthy controls. Swabs from BV patients contained consistently higher levels of amino acid catabolites including cadaverine, putrescine and tyramine as well as higher concentrations of short chain fatty acids (SCFA) such as succinate, valerate and caproate. BV swabs also consistently had decreased levels of tyrosine and lactic acid in BV patients compared to healthy controls. A full table of discriminatory metabolites are presented in Appendix Table 12. PLS-DA modelling of negative mode

data revealed good explained variance ($R^2Y:0.984$) and strong prediction ($Q^2:0.6$) with comparable results achieved in positive mode PLSDA ($R^2Y: 0.964$, $Q^2: 0.613$) (Figure 3-11 B). Random forest classification, further verified by using leave one out cross validation resulted in an overall prediction accuracy of 78%. Comparable prediction accuracy was also observed in the positive ion mode between the three classes with overall prediction accuracy 77%.

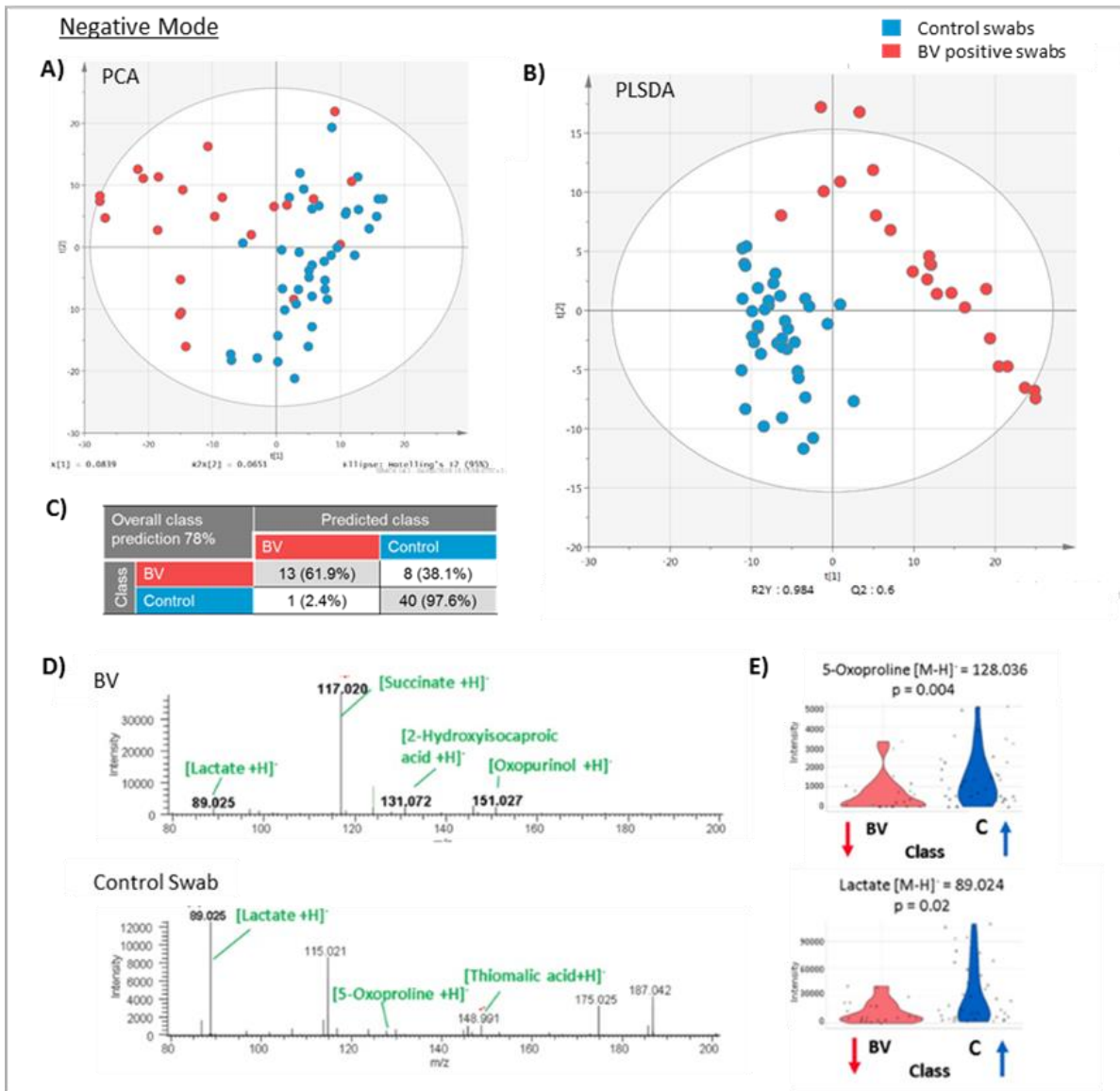


Figure 3-11. DESI-MS analysis of vaginal swab samples collected in pregnancy from women with bacterial vaginosis (BV, n = 21) and healthy controls (n = 41) collected in negative ionisation mode. Unsupervised PCA (A) of DESI-MS revealed underlying differences in the vaginal mucosal metabolic profiles. PLSDA modelling (B) using 4 components revealed good explained variance (R2Y:0.984) and prediction (Q2:0.6). C: Random forest classification, further verified by using leave one out cross validation resulted in an overall prediction accuracy of 78%. (D) Averaged DESI-MS spectra in negative ion mode performed on BV and healthy control swabs with annotation of selected significant metabolites. (E) Violin plots showing selected metabolites decreased in BV swabs; 5-oxoproline and lactate. P < 0.05 using Kruskal-Wallis test.

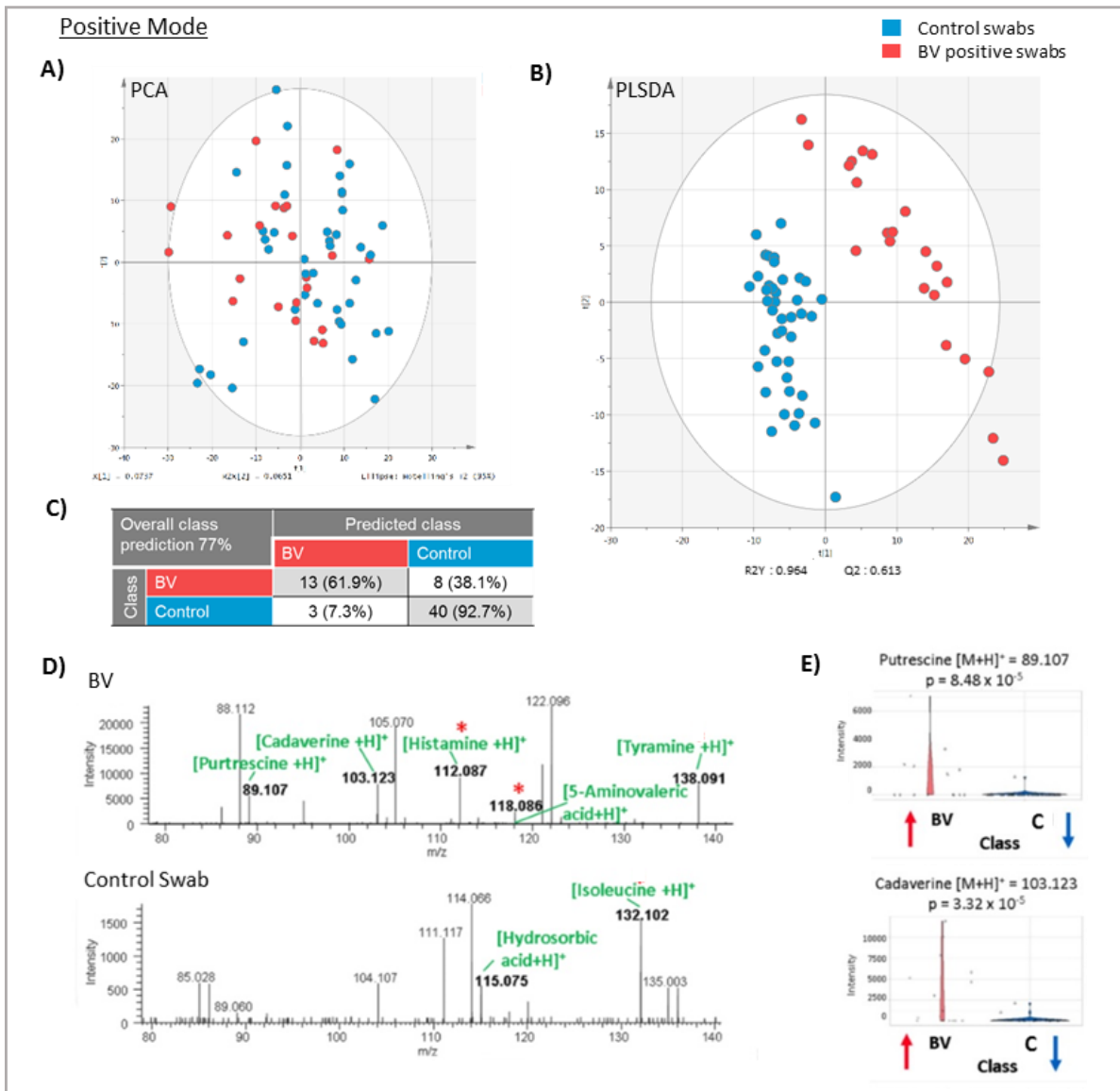


Figure 3-12. DESI-MS analysis of vaginal swab samples collected in pregnancy from women with bacterial vaginosis (BV, n = 21) and healthy controls (n = 41) collected in positive ionisation mode. Unsupervised PCA (A) of DESI-MS revealed underlying differences in the vaginal mucosal metabolic profiles. PLSDA modelling (B) using 3 components revealed good explained variance (R2Y:0.984) and prediction (Q2:0.613). (C) Random forest classification, further verified by using leave one out cross validation resulted in an overall prediction accuracy of 77%. (D) Averaged DESI-MS spectra in positive ion mode performed on BV and healthy control swabs and annotation of selected significant metabolites. (E) Violin plots of selected differential metabolites included increased levels of cadaverine and putrescine in BV swabs compared to healthy controls. *p < 0.05 using Kruskal-Wallis test.

3.5 Discussion

In this proof-of-concept study we report the development of a rapid direct mass spectrometric profiling approach of the vaginal mucosal metabolome. The method permits rapid detection (approximately 30 seconds per swab) of variations in this biochemical environment associated with physiological changes in the host (e.g. pregnancy) and disruptions in the bacterial communities (e.g. bacterial vaginosis). The technique can be applied directly to swabs without sample preparation, metabolite extraction or enclosed chambers for desorption/ionization therefore making it applicable as a potential bedside technique for point of care testing.

DESI-MS is suited to the detection of lipids in biological tissue and fluids [400, 411] this is due to their high abundance, limited solubility in aqueous solvent systems and ability to ionise [404]. In our study, the ionisation of lipids was sought in two regions of interest; mz 300-500 and mz 600-900; where fatty acids and phospholipids are found respectively. Vaginal mucosal epithelia comprises of layers of keratinized stratified squamous epithelium [296] which are rich in phospholipids and fatty acids [412, 413]. The presence of certain bacteria/inflammation are known to physically disrupt and alter this mucosal barrier [293, 414]. Microbial metabolism can result in the direct production of short chain fatty acids such as lactate, acetate, propionate, butyrate, and succinate which are known to modulate immune function in the vagina [347]. Pathogens also can modify the fatty acid composition of host cell lipids from both extracellular and intracellular locations [415] exploiting host lipids for conversion into carbon sources and energy [416]. Phospholipids are also a component of microbial membranes. These lipids can be associated with certain bacterial groups e.g. phosphatidylethanolamines (PE) are found at higher concentrations in gram negative bacteria compared to gram positive [417]. In contrast phosphatidylcholine (PC) is only found in 15% of bacteria so when highly abundant, they are more likely to be a host derived lipids [418].

As part of the optimisation of the method, different mass analysers were compared in this study. Ion trap has the advantage of comparatively reduced cost compared to the Orbitrap and has the ability to consistently detect common, abundant spectral features including lipid molecules [290]. However, we found that the Orbitrap mass analyser to provide a higher mass resolution (the ability of a mass spectrometer to generate distinct signals for two ions with a small mz difference), higher mass accuracy (precision of the measured mz) and higher signal to noise ratio compared to the Ion trap analyser. A more informative mass spectra with greater spectral richness, is advantageous for our study as it provides opportunity to capture more metabolic information from our samples to allow us

to discriminate between classes. Further-more a superior mass resolution and mass accuracy is desirable as to facilitate calculation of empirical formulas for compound identification.

Previous studies have shown that chemical and physical properties of solvent composition significantly affect desorption and ionization of analytes during DESI-MS experiments, and thus the resulting molecular information captured [400, 419, 420]. The solvent can enhance or promote the ionization of different species depending on which analytes are dissolved and desorbed from the sample surface. In DESI-MS imaging studies mixtures of water with methanol, acetonitrile or isopropanol were able to analysis tissue with high lipid content [421, 422]. Another binary solvent system includes methanol and dichloroform which has also been found to significantly enhance the desorption of membrane lipids [423]. In our study we found that methanol (Me:OH) and water provided the highest, most stable ion signal intensities. Me:OH is able to adequately dissolve lipids from animal tissues however it quickly evaporates at high concentrations [367]. The addition of water to solvents increases evaporation time and also reduces the solubility of lipid analytes [424].

Comparison of DESI-MS data acquisition at different swab positions showed that the bottom section of the swab provided the best signal to noise ratio and most reproducible profile data. In comparison, deformation of the swab tip could be observed in a 10% of cases. This may have been caused during the sampling procedure itself or during frozen storage. The unequal swab surface subsequently led to resulting spectra being less consistent with lower signal intensities observed compared to the bottom of the swab where deformation was rarely observed. Lower signal to noise ratio was also observed when ionisation was performed at the central portion of the swab. It is feasible that this section of the swab has the deepest absorbent material and thus both the sample and solvent may have been drawn away through capillary action from the surface in turn reducing the opportunity for desorption and ionisation of molecules at the surface of the swab.

Swab material types (polyester, cotton and rayon) were not tested in our pilot study as samples for the preterm birth studies had been previously collected already using rayon swabs, the standard swab tip material used in NHS hospitals. A previous study however, using touch spray ESI showed that rayon was superior swab tip material in comparison to polyester and cotton. It provided the highest signals in the GPL region of interest and least background noise from the swab material. Of note this study also tested different solvents and methanol provided the highest lipid signals [399].

The distance from the sprayer tip to the sample surface was adjusted from 1 to 5mm with 1mm increments. The optimum setting was found to be 2mm with respect to the number of spectral features and total ion current for the *mz* range 600-900. Examination of the effect of swab rotation

on resulting spectral profiles showed that a swab rotation speed of 202 rpm provided best signal to noise ratio and most stable ion signal intensities. This speed provided a good compromise between formation of a liquid area of primary charged solvents for secondary ion droplet generation and time required for travel of ions into the inlet capillary. It is likely that at a higher RPM, the tip and centre of swab no longer span evenly along an axis and thus subsequent take up of secondary droplets diminished. Stable and constant signal ion intensities were observed when analysing the same position of the rotating swab for 30 seconds. After this time, a linear decrease in signal intensity was observed. This was circumvented through slight adjustment of swab position (approximately shift of 0.5-1mm toward centre of swab) between switching polarity of data acquisition mode as to avoid loss of information during spectral acquisition from previously ablated areas.

Repeatability of the DESI-MS technique for direct vaginal swab analysis was shown using swab replicates. The averaged mass spectra for each indicated >90% similar spectral features within all analysed replicates with similar intensity. For reproducibility, inter swab variability was assessed using QC swabs over 9 days. Mean coefficient of variation for selected masses of lipids was $21 \pm 3 \%$, which is comparable to previous analyses of DESI-MS reproducibility for imaging of human oesophageal cancer tissue sections [404]. It is also within the range stipulated by the U.S. Food and Drug Agency (FDA) for analytical techniques [410]. Although beyond the scope of this thesis, future DESI-MS experiments should include identical test items analysed in different laboratories with different operators using different equipment.

Application of DESI-MS swab profiling to vaginal mucosa samples identified deprotonated cholesterol sulphate (m/z 465.3) as the most dominant signal generated in the negative acquisition mode. It is likely that this metabolite appears to originate from host epithelial cells and consistent with this, other MS platforms have reported its detection in non-keratinized stratified squamous epithelial samples including oesophagus, cornea and soft tissue within the oral cavity [399, 425-427]. It is thought to act as a stabilising and regulatory component of cell membranes with an associated biological role in cell signalling, epidermal differentiation and apoptosis [428, 429].

Our study also showed that direct swab profiling by DESI-MS permits the detection of vaginal mucosa changes associated with physiological adaptations to pregnancy including major alterations in phospholipid metabolism, amino acid derivatives and fatty acid oxidation. Specifically, pregnancy was associated with modified sphingolipid metabolism characterised by decreased ceramide levels and increased sphingomyelins and galactosylceramides. The mechanisms underlying these changes are not clear nor are the physiological significance of such alternations. However, evidence implicates

sphingolipid metabolism as an important regulator of innate immunity in pregnancy. The sphingolipid pathway influences the receptive state of the endometrium [430], is a key regulator of decidualisation at the time of implantation and has been shown to be a critical modulator of innate immune responses at the fetomaternal interface during pregnancy [431]. Furthermore, the glycosphingolipid α -galactosylceramide (α -GalCer) was recently identified as a potent inducer of protective immunity in the murine female genital tract [432].

The influence of the vaginal microbiota on the corresponding mucosal metabolome as assessed using common metabolic profiling platforms is well documented [368, 381, 433]. A study by McMillian et al. compared non-pregnant and pregnant population in women with BV using LCMS and were unable to find biochemical differences [433]. This implies that the diverse microbial composition related to BV in these women have a stronger influence on the metabolome than the biochemical alterations related to pregnancy.

In pregnancy hormonal changes are known to impact on the vaginal microbiota composition resulting in a dominance of *Lactobacillus* species [127, 282]. This is thought to be mediated through an oestrogen driven mechanism by which increasing circulating concentrations of oestrogen [279] promote maturation of the vaginal epithelia and deposition of glycogen [280]. Glycogen is then broken down by host α -amylase present in vaginal mucosa to carbon products which are preferentially metabolised by *Lactobacillus* spp. [281] supporting their colonisation. Recent evidence suggests that certain species of *Lactobacillus* may even be able to directly metabolise glycogen. Consistent with this proposed mechanism, numerous studies have shown that healthy pregnancy vaginal bacterial diversity reduces with advancing gestation and is characterised by a shift towards *Lactobacillus* spp. dominance [282, 283]. We therefore hypothesised that women with BV in pregnancy, characterised by *Lactobacillus* spp. depletion and high diversity, would have an altered vaginal mucosal metabolome that could be readily detected using direct swab analysis by DESI-MS. This is of important clinical relevance as BV is associated with increased risk of preterm birth and other adverse pregnancy outcomes [235, 434] whereas *Lactobacillus* spp. dominance is associated with protection against preterm birth [435]. Our pilot study showed that DESI-MS could identify a robust metabolic signature associated with BV that was particularly sensitive for accurate detection of healthy controls (98% negative predictive value). This may be because *Lactobacillus* spp. dominance has a more homogenous influence on the vaginal mucosal metabolome than BV, which encompasses the overgrowth of multiple anaerobic species that are likely to contribute a variable distribution of metabolite features.

Consistent with previous studies using GC and LC-MS based metabolic profiling platforms to explore metabolic profiles of vaginal mucosa associated with BV [368, 381, 433], our study identified numerous discriminate metabolite markers that permitted robust prediction of BV from women with *Lactobacillus* species dominance in pregnancy (Table 5). Although GC and LC-MS based platforms are more sensitive, DESI-MS has the obvious advantage of not requiring any sample preparation and the capacity to acquire detailed metabolic profiles directly from a swab in only a fraction of the time. Data acquisition time by DESI-MS was approximately 70% less compared to standard UPLC- or GC/MS acquisitions (5–15 min) without accounting for detailed sample extraction procedures required for other metabolic profiling platforms [369].

DESI-MS analysis of vaginal mucosal samples detected high abundance of amino acid catabolites including cadaverine, putrescine and tyramine in swabs from BV patients. These compounds are largely responsible for the fishy odour associated with BV but also have been reported to have antimicrobial and immune modulatory activities [368, 436]. Other vaginal metabolic profiling studies have also noted BV samples to contain numerous amino acid catabolites, whereas *Lactobacillus* spp. are associated with intact amino acids and dipeptides suggesting increased metabolism of amino acids in BV [368]. The amino acid arginine can act as a precursor for polyamines putrescine, spermidine and spermine and consistent with this, BV is associated with reduced arginine and increased putrescine [368]. Other amino acids we found to be depleted in BV samples in our DESI-MS study included isoleucine, tyrosine and tryptophan. Higher levels of the SCFA succinate was also observed in our BV samples. Succinate is produced by *Gardnerella vaginalis* and *Bacteroides* [314, 437] and despite being historically associated with BV, recent studies have shown succinate levels elevated in microbial communities dominated by *Lactobacillus crispatus* [344, 438]. Lower levels of lactate were also identified in BV patients which is likely to reflect *Lactobacillus* spp. depletion. Glycogen is used as primary carbon sources by *Lactobacillus* species during anaerobic glycolysis, which results in the production of lactic acid [439, 440] and contributes to their capacity to dominate the niche. *Lactobacillus* species also have the capacity to metabolise glucose, consistent with this we found glucose to be lower in our healthy control samples.

Alterations in lipid metabolism specific to the carnitine synthesis pathways were also observed in our BV study. Carnitine is a product of lysine or methionine degradation, involved in transport of long-chain fatty acids and was found to be lower in vaginal mucosal samples isolated from BV patients. One proposed mechanism for lower carnitine levels in BV is through the its conversion to trimethylamine by BVAB, this metabolite is responsible for the classic fishy odour characteristic of BV [368].

Table 5. Metabolites and their classes found increased/decreased abundance in DESI-MS and other metabolic profiling studies

Compound	Chemical Formula	Class	Abundance: DESI-MS metabolic profiling	Abundance: BV metabolic studies (LCMS/GCMS)	References
5-Oxoproline	C5H7NO3	Amino acid	↓ BV	↓ BV	[381]
Cadaverine	C5H14N2	Amino Acid	↑ BV	↓/↑ BV	[368, 381, 441] [433]
Glutamate	C5H9NO4	Amino Acid	↑ BV	↓ BV	[368, 441] [433] [368, 381]
Isoleucine	C6H13NO2	Amino Acid	↓ BV	↓ BV	[368, 381]
Phenylalanine	C9H11NO2	Amino Acid		↓ BV	[441] [433]
5-Aminovaleric acid	C5H11NO2	Amino Acid	↑ BV	↑ BV	[368] [433]
Tryptophan	C11H12N2O2	Amino Acid		↓ BV	[368, 441]
Tyramine	C8H11NO	Amino Acid	↑ BV	↑ BV	[368, 441] [433]
Tyrosine	C9H11NO3	Amino Acid	↓ BV	↓ BV	[368, 441] [433]
Putrescine	C4H12N2	Amine	↑ BV	↑ BV	[368, 381] [436] [433]
Histamine	C5H9N3	Amine	↑ BV	↑ BV	[368] [433]
Glucose	C6H12O6	Carbohydrate	↑ BV	↓/↑ BV	[368, 441] [433]
Pyruvate	C3H4O3	Carbohydrate		↑ BV	[441] [368]
Lactate	C3H6O3	Carboxylic acids	↓ BV	↓ BV	[368]
Succinate	C4H6O4	Carboxylic acid	↑ BV	↓/↑ BV	[368, 441] [433]
Carnitine	C7H15NO3	Lipid	↑ BV	↓ BV	[368]
Stearic acid	C18H36O2	Lipid	↑ BV	↑ BV	[381]

3.6 Conclusion

We have shown that DESI-MS medical swab analysis have desirable features as a sampling method for ambient MS analysis. It is simple to use, low cost, readily available and familiar in the clinical environment. Using our adapted DESI-MS technique with real samples, we provide evidence for its direct applicability for mucosal metabolome profiling permitting rapid assessment of variations in the CVM associated with physiological changes in the host (e.g. pregnancy) and disruptions in the bacterial communities (e.g. bacterial vaginosis). We show that is a simple rapid approach cost-effective approach making it applicable as a potential bedside technique for point of care testing.

4 CHARACTERISATION OF CVM CHANGES ASSOCIATED WITH PRETERM BIRTH

4.1 Chapter Summary

Hypothesis

Interactions between the vaginal microbiota and the pregnant host are reflected in the local biochemical environment (i.e. in the CVM) and can be assessed rapidly characterized using direct vaginal swab analysis by DESI-MS.

Vaginal microbial and pregnant host interactions are related to birth outcome and preterm birth phenotypes which can be rapidly assessed using DESI-MS.

Metabolic signatures from vaginal swabs DESI-MS profiling can be used to predict, diagnose and stratify spontaneous preterm birth risk.

Aims

Test the ability of direct swab analysis by DESI-MS to detect CVM metabolite changes in early pregnancy that precede the phenotypic changes associated with SPTB, such as cervical remodelling and membrane rupture, that are predictive of SPTB at > 37 weeks.

To test if DESI-MS could identify metabolic alterations that could predict early or late PTB as well as phenotype (PTL or PPROM).

Methods

High vaginal swabs were collected prospectively from women at 15 weeks gestation prior to intervention (e.g. cervical cerclage, progesterone treatment) and were analysed directly using DESI-MS. Resulting spectral data were processed and analysed using multivariate modelling approaches to examine relationships between spectral features, metabolite levels and patient outcome as well as clinical phenotype.

Results

DESI-MS swab profiling enabled detection of approximately 1500 spectral features within 1 minute. Analysis of metabolite features using a random forest classifier resulted in overall prediction of 68% for SPTB prediction. A sub-analysis of SPTB swabs identified vaginal mucosal metabolites that were significantly associated with subsequent early PTB (<34/40) vs late PTB (>34/40) or SPTL from PPROM.

Conclusion

Our results highlight the capacity of DESI-MS to rapidly characterise the vaginal metabolome in early pregnancy. We hypothesise that relatively poor prediction of SPTB by DESI-MS swab profiles may be due to the heterogeneity of PTB aetiology (e.g. infection vs non-infection), which is supported by the ability of the technique to discriminate samples with different severity of PTB (early vs late) and phenotype (SPTL v PPROM).

4.2 Introduction

Preventing prematurity remains limited by our inability to reliably predict women at risk of preterm birth. This is complicated by the fact that SPTB is a syndrome with multiple underlying aetiologies and women often display different clinical presentations [11, 12]. Spontaneous preterm labour (SPTL) with intact membranes accounts for 70% of births with preterm premature rupture of membranes (PPROM) accounting for the remaining 30% of births [10]. Although the aetiology of SPTB is multifactorial; infection and inflammation are thought to be associated with 40% of spontaneous preterm deliveries [125, 126, 287] and evidence suggests that these tend to be the earlier preterm deliveries rather than those closer to term [135, 137, 442].

Early identification of at-risk women would allow targeted interventions to be initiated with the aim of preventing SPTB. Current methods for risk stratification include assessment of obstetric history, which is estimated to be unreliable in 50% of cases [171], and routine cervical length measurement by ultrasonography [174, 177]. Premature cervical shortening can be detected by transvaginal ultrasound (TVUS) several weeks prior to the onset of the clinical symptoms of preterm birth [443]. Pregnant women with a short cervix; <25 mm before 24 weeks of gestation are considered at highest risk of preterm birth [172, 173]. However, increasing evidence suggests that the composition of the vaginal microbiome may be a risk factor for SPTB and predict outcome following intervention. For example, a recent study has shown that women who present with painless second trimester cervical dilatation and undergo a 'rescue' cervical cerclage have different outcomes depending on the microbial composition prior to cerclage [444]. Women experiencing pregnancy loss following rescue cerclage were more likely to be colonised with *G. vaginalis* whereas *Lactobacillus* spp. dominance of the vaginal microbiome was associated with successful outcomes and term delivery. This suggests at least two mechanisms of preterm cervical dilatation; one 'host-microbe/inflammation' associated, which cannot be resolved by cervical cerclage, the other due to genuine mechanical incompetence, which does respond to cerclage. Early diagnosis of cervical shortening with or without infection would allow timely and targeted intervention with cervical cerclage or antibiotics to potentially prolong pregnancy.

There are several CVF biochemical markers that are currently used to assist in SPTB prediction including fetal fibronectin [185, 186, 445], phosphorylated insulin-like growth factor binding protein-1 (phIGFBP-1) [191] and placental alpha microglobulin 1 (PAMG-1) [181, 446]. These tests are however aimed at symptomatic women (i.e. those presenting with uterine contractions) and thus direct the treatment of SPTB rather than prevention. They have not been shown to be effective at SPTB

prediction in asymptomatic women in early pregnancy [175]. There is thus a need for improved mechanistic understanding of SPTB coupled with better tools that could permit prediction of SPTB and stratification of women into risk groups enabling targeted therapeutic strategies and improved timing of clinical intervention [204].

CVM provides an important diagnostic site to monitor maternal and fetal health in pregnant women. It is a site of complex microbial-host interactions where it provides both a physical and immunological barrier to ascending infection in pregnancy [290]. It can be readily sampled using a swab and its chemical composition is strongly influenced by microbial composition and host responses. For example, depletion of *Lactobacillus* species and increased colonisation of anaerobes as observed in bacterial vaginosis induces a marked shift in the CVM metabolome that is readily detected using metabolic profiling approaches [368, 381, 382, 447].

Studies investigating vaginal metabolic profiles in relation to preterm risk in asymptomatic women are conflicting. While two studies have reported changes in the vaginal metabolome of asymptomatic women associated with subsequent SPTB [333, 354], a third study failed to detect any CVM metabolite changes predictive of SPTB [334]. These studies all applied traditional metabolic profiling platforms for the assessment of CVM. The utility of such approaches to a clinical setting are severely limited by cost, lengthy sample preparation and extraction protocols with long data acquisition times [360]. The recently developed direct swab analysis by DESI-MS [365, 366] circumvents many of these issues by permitting rapid acquisition of detailed chemical profiles of CVM directly from vaginal swab samples without the requirement of sample preparation [369]. The procedure is performed in ambient conditions with a total data acquisition time of 1 minute, highlighting the potential of direct swab analysis by DESI-MS for diagnostic point of care applications [290, 369].

This chapter aimed to test the ability of direct swab analysis by DESI-MS to detect CVM metabolite changes in early pregnancy that precede the phenotypic changes associated with SPTB, such as cervical remodelling and membrane rupture, that are predictive of SPTB at less than 37 weeks. We also aimed to test if DESI-MS could identify metabolic alterations associated with specific of PTB phenotypes.

4.3 Study Design

4.3.1 Sample collection

To characterise the CVM metabolome and microbiome of women prior to SPTB and to obtain gestation age matched samples from women with healthy term outcomes (controls) a cross-sectional cohort of pregnant women with and without risk factors for preterm birth were prospectively recruited from the preterm surveillance and antenatal clinics of Queen Charlotte's & Chelsea Hospital. High vaginal swabs were taken within the gestational time frame of 8-16 weeks. Cervical length (CL) measurements were taken by transvaginal ultrasound scan. Women with $CL \leq 25\text{mm}$ were considered at increased risk of PTB and were treated with cervical cerclage and/or progesterone vaginal pessaries. All vaginal swab samples were taken prior to any intervention. Women that had a cerclage in pregnancy and then a subsequent term delivery were excluded from our study. Detailed maternal and neonatal metadata was collected for all participants from the hospital case notes and the electronic patient databases Cerner Millennium.

Bacterial DNA was extracted from the vaginal swabs and 16S RNA gene sequencing of V1-V2 hypervariable regions performed as described in Chapter 2.

Metabolic profiling of CVM was performed directly on swabs using an LTQ Orbitrap Discovery mass spectrometer connected to a DESI source as previously described (Chapter 3) [369].

Spectral data in both negative and positive mode were pre-processed using customised scripts in R (chapter 2). The resulting final peak list consisted of 108 peaks in negative mode and 117 peaks in positive mode.

4.3.2 Statistical analysis

Unsupervised and supervised multivariate analyses were initially carried out in SIMCA P. + v 14.0 software (Umetrics, Umea, Sweden).

To reduce complexity of the models, subsequent analysis used a Random Forest (RF) classifier. This was trained on the training samples and used to predict the label of the validation sample. Accuracies were calculated on the entire vector of predicted labels. The top-N variables were used and sorted by their RF importance, calculated on the training set, and only the first N variables were passed to the classifier. A leave-one-out cross-validation strategy was employed to assess the predictive power of these supervised models. PLSDA models were tested with a varying number of variables and

components to determine the optimal configuration in terms of predictive accuracy. The final combination (number of variables/number of components) corresponded to the maximum value of the accuracy. The obtained classification accuracy was visualized with confusion matrices.

Data were summarised using frequency distributions for categorical data, and median, interquartile range and range for continuous data. Categorical outcomes were compared using Chi-square and Fisher's exact tests, and continuous outcomes compared using Mann-Whitney tests. P-values <0.05 were considered statistically significant.

To assess the impact of the vaginal microbiome on the metabolome, characterisation of vaginal microbiota from matched samples was performed at species level according to ward clustering into five CSTs: I (*L. crispatus*), II (*L. gasseri*), III (*L. iners*), V (mixed bacterial species), and VI (*L. jensenii*) as described by Ravel et al.[291].

4.4 Results

4.4.1 Clinical characteristics of study cohort

The clinical characteristics of patients are presented in table 6. A total of 56 pregnant women were included in the study controls (n=32) who delivered at > 37 weeks of gestation and SPTB (n=24) delivered at < 36+6 weeks of gestation. Vaginal swabs were taken at 10+0-18+6 weeks (median 15+3 weeks). There was no difference in gestational age at sampling between the controls and subsequent SPTB (P=0.07, Mann-Whitney). All swabs were taken prior to interventions (i.e. cervical cerclage or progesterone treatment). There were no significant differences in age (P=0.93, Mann-Whitney), BMI (P=0.08, Mann-Whitney) or smoking habits (P=0.64, Fisher's exact) between controls and the SPTB group. There were more black women in the SPTB cohort compared to controls (28.1% vs 13.5%, P=0.05 Fisher's Exact). In the SPTB group, more women had a previous pregnancy complicated by a premature birth/mid trimester loss (70.8% vs 3.1%, P= <0.01 Fisher's Exact). The median cervical length measured with TVUS was also significantly shorter in the SPTB group compared to control (35.5mm vs 40.0mm, P=0.04 Mann-Whitney). In this group 41.6% of these women also went on to have cervical shortening which was defined as a cervical length <25mm by 24 weeks. All women in the control group had CL>25 mm. A cervical cerclage (history or USS indicated) was carried out in 11/24 (45.8%) of the SPTB group. The remaining 13/24 (54%) had no interventions in pregnancy as they either presented unexpectedly in premature labour or did not have risk factors (e.g. CL <25 mm or previous PTB/MTL) to warrant a cervical cerclage. No women in the low risk control group received any intervention.

Results: Characterisation of CVM Changes Associated with Preterm Birth

SPTB was further sub-categorised depending on gestation at delivery; early SPTB (24+0 - 33+6 weeks); 9/24 (37.5%) and late SPTB (34+0-36+6); 15/24 (62.5%). SPTB was also sub-categorised depending on clinical presentation; 13/24 (54.2%) had SPTL and 11/24 (45%) had PPROM.

Table 6. Demographic characteristics of pregnant women sampled in pregnancy. Patients were assigned to groups once birth outcome known. Controls delivered at term (>37 weeks), preterm birth included all deliveries <36+6 weeks.

	Controls >37 wks	PTB <37 wks	P Value
n/N (%)	32/56 (57%)	24/56 (43%)	
Age			
Median (IQ range)	33 (31-34)	33 (32-34)	0.930
BMI			
Median (IQ range)	23.0 (20.7-24.0)	25.5 (21.5-28)	0.080
Ethnicity			
Caucasian	24 (75%)	14 (43.8%)	0.152
Asian	3 (9.4%)	1 (3.1%)	0.624
Black	4 (12.5%)	9 (28.1%)	0.054
Smoker	2 (6.3%)	3 (12.5%)	0.642
Previous PTB/MTL	1 (3.1%)	17 (70.8%)	<0.01
Gestation at Sample (wks + days)			
Median (IQ range)	16+1 (13+6-17+1)	14+6 (12+6-14+5)	0.069
Cervical Length (mm)			
Median (IQ range)	40.0 (34.7-48.2)	35.5 (31.0-41.5)	0.042
Cervical Shortening <25mm	0	10 (41.6%)	
Subsequent intervention			
No Intervention	0	13 (54.2%)	
Cerclage	0	11 (45.8%)	
Gestation at delivery (wks + days)			
Early PTB < 33+6	0	9 (37.5%)	
Late PTB 34+0 to 36+6	0	15 (62.5%)	
Term > 37+0	32 (100%)	0	
Preterm birth			
SPTL	0	13 (54.2%)	
PPROM	0	11 (45.8%)	

BMI: body mass index; SPTB: spontaneous preterm birth, SPTL: spontaneous preterm labour, PPROM: preterm prelabour rupture of the fetal membranes. Data presented as median (interquartile range) or number (%). P values: t-test/Mann-Whitney U (depending upon distribution), Fisher's exact for proportional data.

4.4.2 SPTB prediction overall

DESI-MS spectral data was collected and pre-processed using customised scripts (chapter 2). The resulting final peak list consisted of 108 peaks in negative mode and 117 peaks in positive mode. These lists were used for multivariate analysis.

Results: Characterisation of CVM Changes Associated with Preterm Birth

We first set out to examine the capacity of DESI-MS to distinguish women who experienced subsequent SPTB <37 weeks (24+0-36+6 weeks) from those that delivered at term (controls). Unsupervised analysis of all metabolite data (both ionisation modes) was first performed using PCA (Figure 1A). Examination of resulting score plot showed high variability amongst the samples with the majority of the variance explained in the first two components of the model that were not associated with term birth or SPTB. To examine variation in the data associated specifically with SPTB, supervised modelling by PLSA-DA was then performed. Poor discrimination was observed with the resulting 2 component model (R^2Y : 0.494, Q^2Y : -0.319) indicating no robust metabolome differences between the two groups.

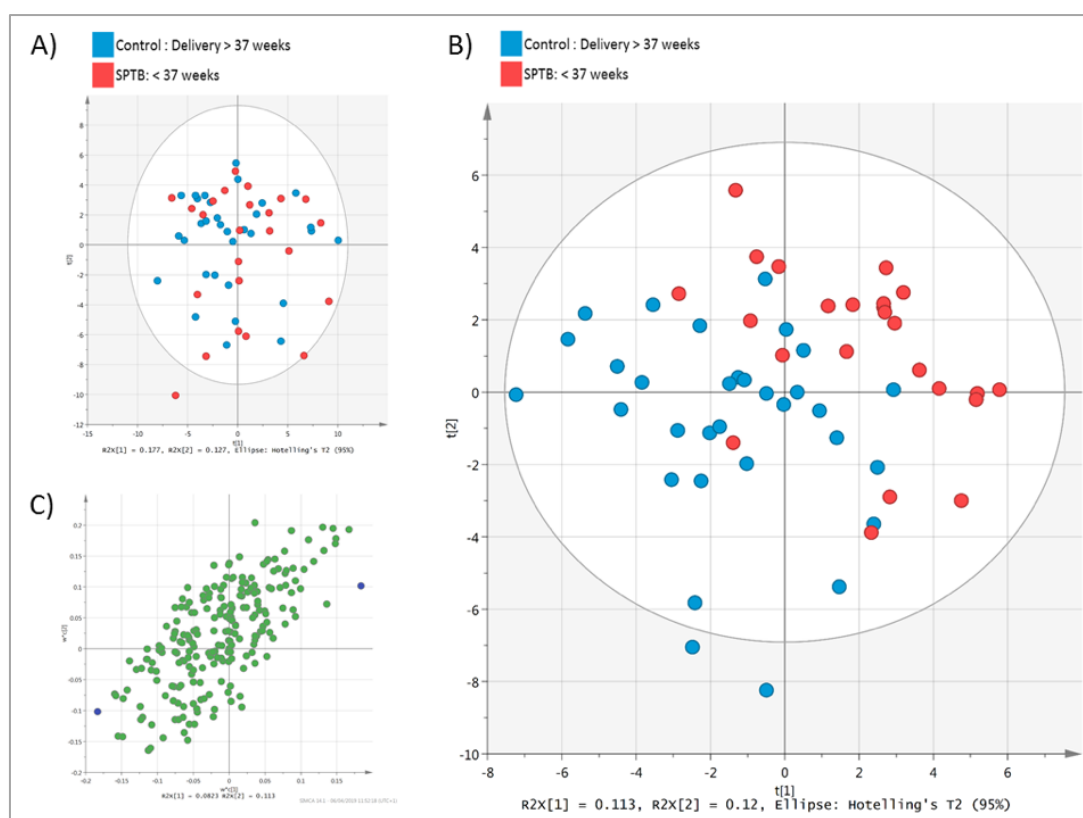


Figure 4-1. Multivariate modelling of DESI-MS data from vaginal swabs collected at 15 weeks from women who subsequently experienced SPTB or term deliveries. A: PCA score plot using both positive and negative ion mode data coloured by class (SPTB = red, Controls = blue). PLS-DA score plot (B) and loadings plot (C) of DESI-MS swab profiles collected from women who subsequently delivered at term ($n=32$) or preterm ($n=24$) (R^2Y : 0.494 and Q^2Y : -0.319)

In an attempt to reduce data complexity and remove non-class associated variability, the top 50 discriminatory mz features between SPTB and controls were identified using a random forest (RF) classifier. This data was then modelled for representation using PCA (Figure 4-2A). Although poor discrimination between classes was still observed, higher variability in the metabolic profiles of

Results: Characterisation of CVM Changes Associated with Preterm Birth

women subsequently experiencing SPTB compared to controls was evidenced by the wider spread of metabolic profiles across the first two components. This was reflected in the random forest confusion matrices which showed a model accuracy for class prediction using leave-one out cross validation of 67% for SPTB prediction and 75% for controls (Figure 4-2B).

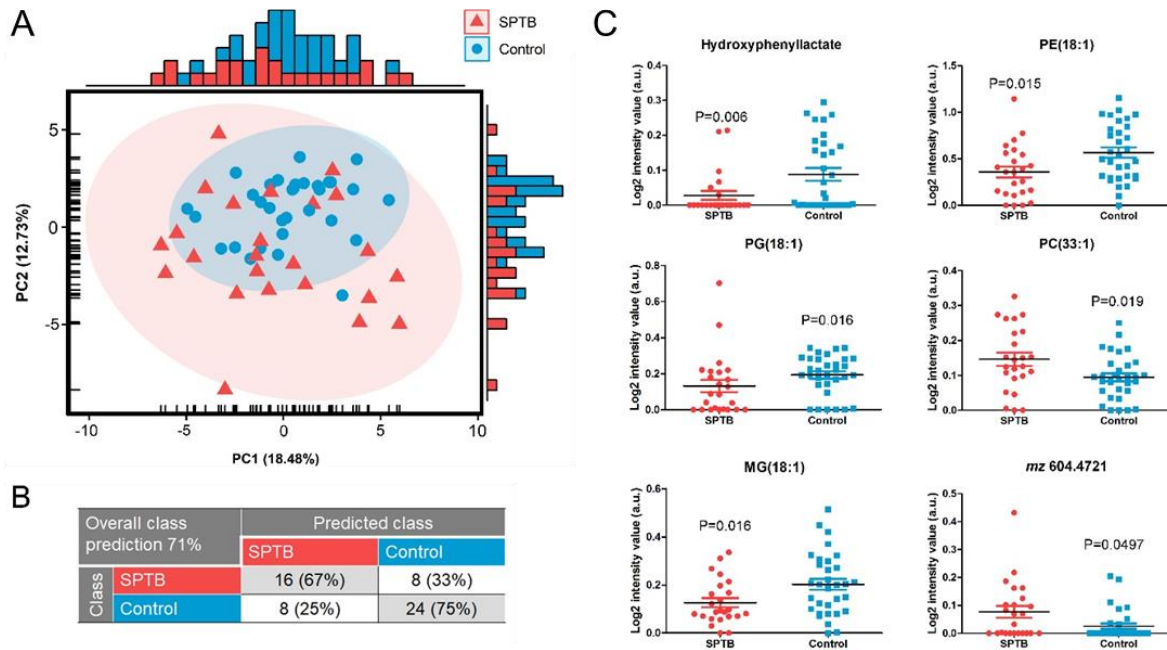


Figure 4-2. Examining the capacity of DESI-MS to distinguish between subsequent SPTB and term deliveries using vaginal samples collected at 15 weeks. SPTB <37 Weeks ($n = 24$) vs control ($n = 32$). A: PCA score plot using all variables and colour coded with subsequent birth outcome; red: SPTB and blue: Control/term deliveries. B: Random forest normalised confusion matrices showing the overall accuracy for class prediction of 71% for SPTB prediction. C: Scatter plots indicate significant differences in the abundance of selected metabolites (assigned by MSMS) upregulated in each group $p < 0.05$

Despite multivariate modelling not identifying any robust CVM metabolic profiles associated with SPTB, univariate statistics identified a number metabolites significantly differing in relative concentration between control and SPTB patients (Table 7 and Figure 4.2C). Metabolites significantly higher in samples from women subsequently experiencing SPTB included phosphatidylcholine; PC(33:1) and a metabolite of unknown identity with a mz ratio of 604.4721. Control samples contained significantly higher concentrations of hydroxyphenyllactate, PE(18:1), PG(18:1) and MG(18:1).

Results: Characterisation of CVM Changes Associated with Preterm Birth

Table 7. Metabolites significantly more or less abundant in early pregnancy in women that subsequently experience SPTB compared to those that experience term birth (control).

m/z observed	m/z theoretical	PPM	Mode	Adduct	Formula	SPTB vs Control	Fold-change	P-value	Compound	Assignment
181.0508	182.0579	0.19	(-)	[M-H]-	C9H10O4	↓ in SPTB	3.2134	0.0062	Hydroxyphenyllactic acid	MSMS
478.2939	478.2939	-0.01	(-)	[M-H]-	C23H46NO7P	↓ in SPTB	1.6739	0.0146	PE(18:1)	MSMS
509.2891	509.2885	1.18	(-)	[M-H]-	C24H47O9P	↓ in SPTB	1.4113	0.0155	PG(18:1)	Putative
379.2816	379.2819	-0.63	(+)	[M+Na]+	C21H40O4	↓ in SPTB	1.6570	0.0164	MG(18:1)	Putative
489.3149	489.3141	1.72	(-)	[M+Cl]-	C30H46O3	↓ in SPTB	2.5684	0.0198	3beta-3-Hydroxy-11-oxolanosta-8,24-dien-26-al	Putative
326.3785	326.3781	1.29	(+)	[M+H]+	C22H47N	↓ in SPTB	1.4907	0.0224	Docosanamine	MSMS
399.2689	399.2687	0.47	(-)	[M-H]-	C21H40N2O3S	↓ in SPTB	1.7874	0.0247	N-(5-Oxo-2-sulfanyl-1,3-oxazolidin-2-yl)octadecanamide	MSMS
342.2473	342.2472	0.10	(-)	[M-H]-	C19H37NO2S	↓ in SPTB	1.7330	0.0264	NA	MSMS
365.2807	365.2810	-0.61	(-)	[M-H]-	C21H38N2O3	↓ in SPTB	2.1599	0.0424	N-Benzyl-N,N-dimethyldodecan-1-aminium nitrate	Putative
271.2278	271.2279	-0.39	(-)	[M-H]-	C16H32O3	↓ in SPTB	1.8720	0.0479	hydroxy palmitic acid	MSMS
744.5576	744.5549	3.62	(-)	[M-H]-	C41H80NO8P	↑ in SPTB	0.6296	0.0187	PC(33:1)	Putative
604.4721	0.04	(-)				↑ in SPTB	0.3256	0.0497		

As hydroxyphenyllactate is a well know metabolite produced by *Lactobacillus* and *Bifidobacteria* [448], we next examined the potential relationship between the relative levels of this metabolite and bacterial composition of the vaginal samples (Figure 4.3). High abundance of hydroxyphenyllactate was typically associated with CST I (*L. crispatus*) dominated vaginal microbiota communities. We examined the relationship between CST groups other molecules that were significant in this analysis and there appeared to be no other associations.

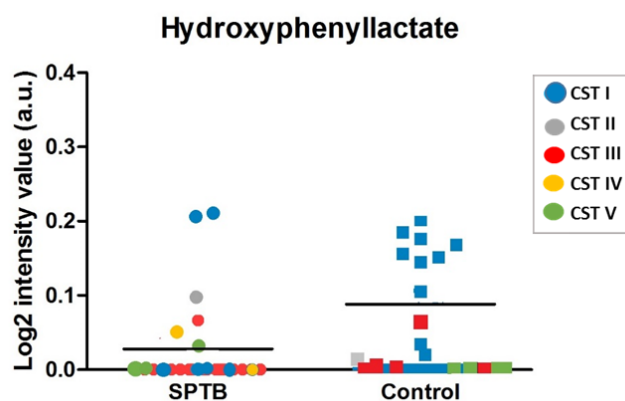


Figure 4-3. Scatter plots indicate significant difference in the abundance of hydroxyphenyllactate in SPTB vs. Control. Plot has been recoloured depending on the associated with CST group; *L. crispatus* (CST I), *L. gasseri* (CST II), *L. iners* (CST III), High diversity (CST V) *L. jensenii* (CST IV) [278].

4.4.3 SPTB Phenotypes

It was hypothesised that the observed high levels of patient-to-patient variability in the vaginal mucosal metabolome identified by DESI-MS may reflect variable influence of a wide range of factors including microbial composition, sample properties (e.g. pH), ethnicity and/or clinical aetiologies (e.g. SPTB with or without PPROM; early or late SPTB; SPTB with or without cervical shortening). To examine

this further, PLS-DA score plots modelling SPTB class associated variation were recoloured to highlight to the potential relationship between these factors and the vaginal mucosal metabolomes (Figure 4.4).

In the PLS-DA plot there appeared to be clustering within the classes (SPTB vs term birth) that could be explained by the underlying microbial composition. Women with CST I dominance were more frequently observed in the control group (47%; 15/32) compared to SPTB (25%; 6/24). In contrast, the SPTB group had a higher prevalence of CST III dominance (31%; 10/32) compared to the control group (25%; 8/32). Two women in the SPTB group that had CST IV which is characterised by reduced *Lactobacillus* spp. and an overgrowth of anaerobes. These samples were also classified as BV on culture. A further sample in the SPTB group was defined as BV on culture, and had co existing *L. iners* dominance (CST III). Yeast was found on culture in 21% (5/24) SPTB samples and 17% (5/32) controls. Group B Streptococcus (GBS) was found in 8% (2/24) in the SPTB group and 17% (5/32) of term deliveries.

Vaginal pH varies in relation to health with a pH of 3.0-4.5 considered a signature of a normal vaginal environment and variations upwards a sign of an imbalanced vaginal environment, e.g. the onset of BV [449]. In our cohort sample pH showed no obvious clustering with pH <5.0. There were four samples that had pH >5.3 and these clustered in the lower portion of the plot. Three of these samples were in the control group and one sample in the SPTB group. There didn't appear to be any correlation with microbial composition and pH in these samples.

There were more black women in the SPTB group, and although there does appear to be a small cluster of black women in the SPTB group there are also black women spread elsewhere in this group and throughout the control group.

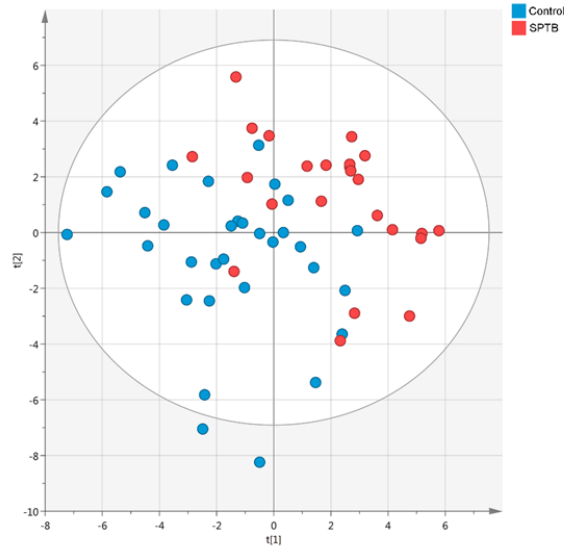
Clusters were noted within the SPTB group in relation to different phenotypes/presentation of preterm birth as shown in figure 4-5. In order to visualise these more clearly, the control group was hidden from the plot and CVM metabolic clusters were ringed with dashed line to improve visualisation. Initially we looked at timing of SPTB i.e. early SPTB (<34 weeks) vs late SPTB (34-36+6 weeks). CVM metabolic profiles showed that early SPTB separated along the first component of the PLS-DA model. PPRM and SPTL CVM metabolic profiles tended to separate in the second component with all PPRM samples falling in the upper two quadrants of the score plot. Recolouring of the PLS-DA score plot on the basis of CL shortening (defined as women who had shortening of < 25 mm by 24 weeks of pregnancy) showed that all these women fell in the upper two quadrants of the PLS-DA score plot. These results might be indicative of congruence or an overlap between clinically measured parameters of risk (cervical shortening) and preterm birth phenotype (PPROM/SPTL, early/late SPTB)

Results: Characterisation of CVM Changes Associated with Preterm Birth

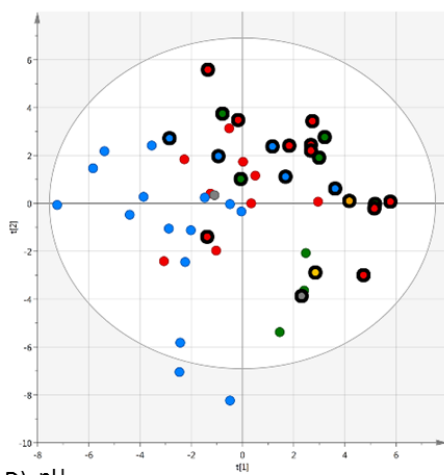
that is reflected in the vaginal mucosal metabolome. We therefore considered these analysis in more detail. Modelling was subsequently carried out using a RF classifier to identify the top features that were responsible for class discrimination which were then displayed in PCA plot.

Results: Characterisation of CVM Changes Associated with Preterm Birth

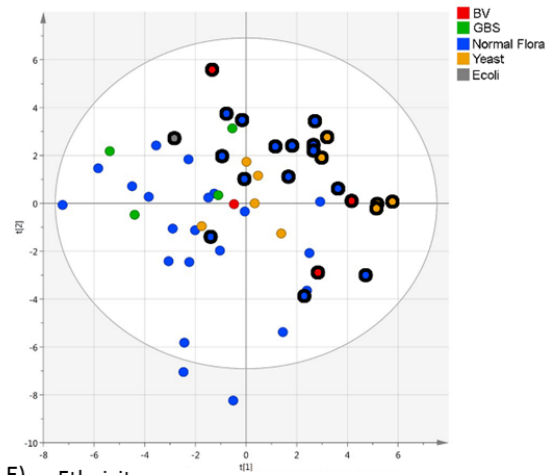
A) Overall: SPTB vs term deliveries



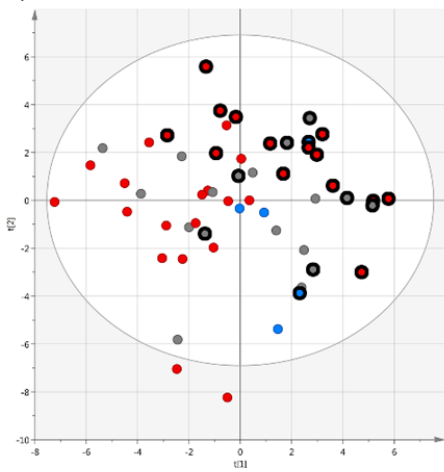
B) 16S rRNA CST



C) Microbial culture



D) pH



E) Ethnicity

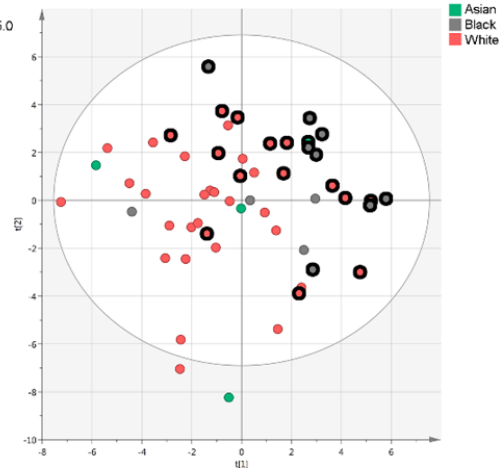


Figure 4-4. A: PLSDA modelled on class information: SPTB < 37 weeks (Red) vs. Controls (blue); $R^2Y: 0.494$, $Q^2: 0.319$. Plots recoloured using underlying microbial composition (B,C), pH (D) and ethnicity (E) to assess for metabolic clusters in classes; SPTB (bold outline) vs Controls (no outline).

Results: Characterisation of CVM Changes Associated with Preterm Birth

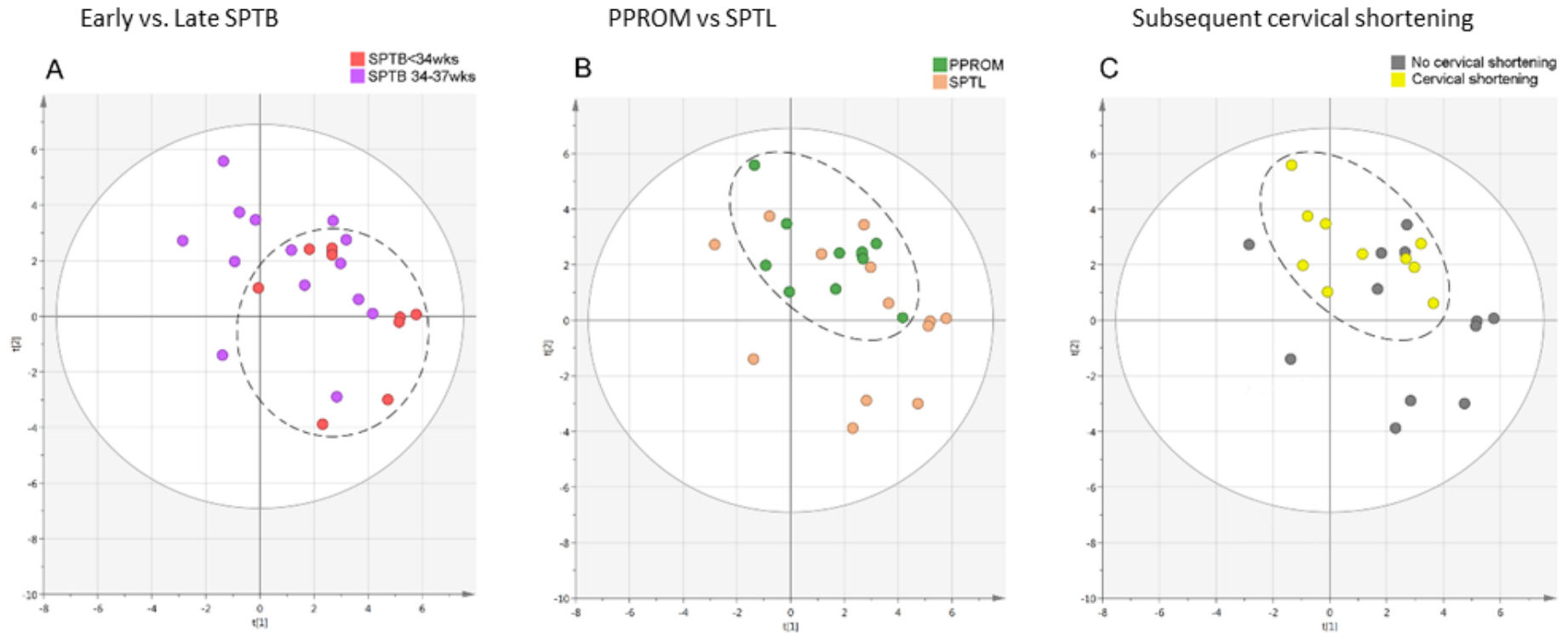


Figure 4-5. Comparison of the PLS-DA score plots for SPTB phenotypes. Controls have been hidden from plot and clinical phenotype clusters are ringed with dashed line to improve visualisation. A: early SPTB; <34 weeks (red) vs late SPTB; 34-36+6 weeks (purple), CVM metabolic profiles showed that early SPTB separate along the first component of the PLS-DA model. B: PPROM (green) and SPTL (brown) CVM metabolic profiles tended to separate in the second component of the PLS-DA model with all PPROM samples falling in the upper two quadrants of the score plot. Similarly, recolouring of the PLS-DA score plot on the basis of CL shortening (C): showed that all patients with CL shortening (yellow) also fell in the upper two quadrants of the PLS-DA score plot compared to non-shortening (grey).

4.4.4 SPTB: Early vs Late

In this analysis we characterised the CVM metabolome by DESI-MS in women who subsequently experienced early (24^{+0} - 33^{+6} weeks) or late SPTB (34^{+0} - 36^{+6} weeks). The microbial composition of the CVM is known to influence the metabolome [344, 368] therefore a matched swab was also characterised using 16S rRNA sequencing to determine underlying CST group.

For CVM metabolome analysis a random forest classifier was used which identified 65 features for modelling; providing an overall prediction accuracy of 68%. The model was more superior at predicting late SPTB (80%) compared to early SPTB (56%). Figure 4.6B shows a PCA score plot providing visualisation of the data using the top variables. It shows separation of classes (early vs late SPTB) based on the selected features is primarily in the first component. The RF selected features used for modelling were exclusively more abundant in the late SPTB group compared to early SPTB. The top 9 of these discriminatory metabolites are shown in table 8 with a selection represented as scatter plots in figure 4.6C which include phosphatidylglycerols, phosphatidic acid and triglyceride.

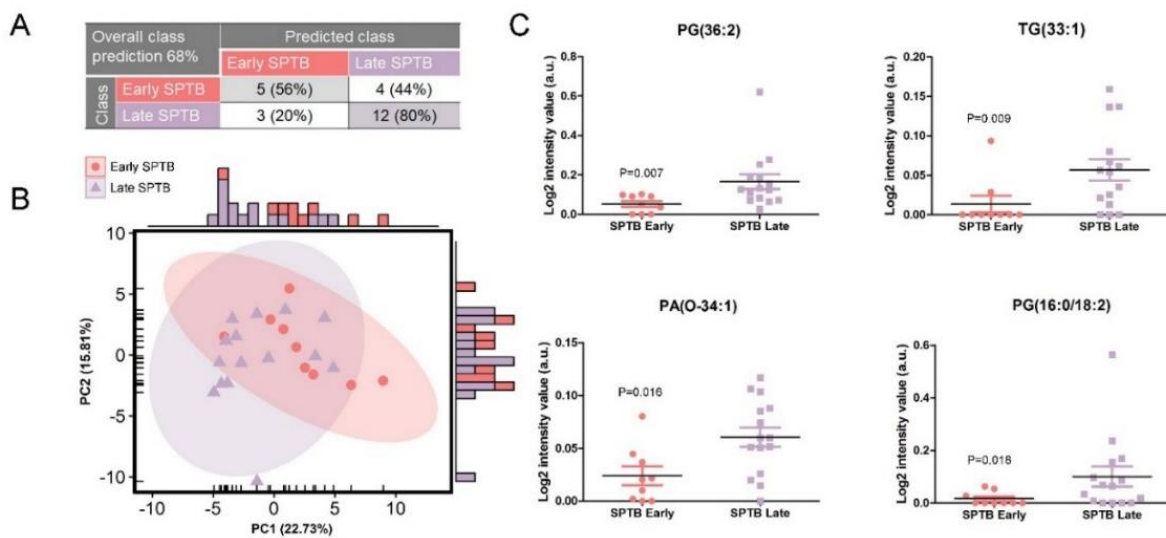


Figure 4-6. Characterisation of CVM metabolome by DESI-MS in women who subsequently experience early SPTB; <34 weeks (n=9) from late SPTB; >34 weeks (n=15). A: Supervised random forest normalised confusion matrices showing the accuracy for class prediction 80% for late SPTB (purple) and 56% for early SPTB (pink). B: PCA score plot using top 65 RF selected features for a analysis. C: Scatter plots indicate significant differences in the abundance of selected metabolites in each group $p < 0.05$

Results: Characterisation of CVM Changes Associated with Preterm Birth

Table 8. Metabolites significantly more or less abundant in early pregnancy in women that subsequently experience late SPTB compared to those that experience early SPTB

m/z observed	m/z theoretical	PPM	ModeAdduct	Formula	Late vs Early PTB	Fold-change	P-value	Compound	Assignment
773.5353	773.5338	1.92	(-) [M-H]-	C42H79O10P	↑ in Late SPTB	0.2927	0.0066	PG(36:2)	Putative
869.7020	869.6995	2.88	(+) [M+K]+	C53H98O6	↑ in Late SPTB	0.2375	0.0092	TG(33:1)	Putative
661.5160	661.5167	-1.01	(+) [M+H]+	C37H73O7P	↑ in Late SPTB	0.3923	0.0156	PA(O-34:1)	Putative
745.5032	745.5025	0.92	(-) [M-H]-	C40H75O10P	↑ in Late SPTB	0.1460	0.0184	PG(34:2)	Putative
760.5143	760.5134	1.17	(-) [M-H]-	C40H76NO10P	↑ in Late SPTB	0.2948	0.0201	PS(34:1)	Putative
724.5288	724.5287	0.16	(-) [M-H]-	C41H76NO7P	↑ in Late SPTB	0.6483	0.0343	PE(O-16:0/20:4)	Putative
79.9577	79.9574	4.42	(-) [M-H]-	HO3S	↑ in Late SPTB	0.3598	0.0443	Sulfatite	Putative
504.3427	504.3424	0.41	(+) [M+Na]+	C24H52NO6P	↑ in Late SPTB	0.3459	0.0450	PC(O-15:0/O-1:0)	Putative
455.3314	455.3297	3.68	(-) [M+Cl]-	C27H48O3	↑ in Late SPTB	0.3366	0.0498	5-b-Cholestane-3a,7a,12a-triol	Putative

Examination of vaginal bacterial composition at 15 weeks of gestation showed that the early SPTB (<34 weeks) group was more frequently dominated by *L. iners* (CST III); 67% (6/9) compared to late SPTB; 27% (4/15), although not statistically significant (Fishers exact: 0.09). The controls had a similar proportion of samples to late SPTB with CST III (31%). Similarity *L. crispatus* dominance (CST I) was found in proportionally more swabs in both the late SPTB and controls, 40% (6/15) and 52% (15/29) respectively. In contrast early SPTB had no samples with CST I (0%; 0/9) at this time-point. Finally high diversity, vaginal microbial compositions that were deplete of *Lactobacillus* spp. (CST IV) were only observed in a small proportion of late SPTB (13%; 2/15). No association between the discriminatory CVM metabolites and the underlying the underlying microbial composition was found.

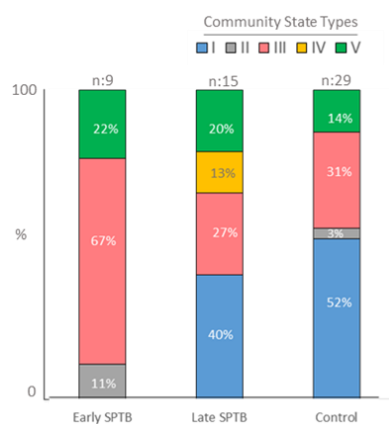


Figure 4-7. Vaginal microbial communities defined by CST at 15 weeks related to subsequent birth outcome; early (<34 weeks), late (>34 weeks) vs term birth (>37 weeks). *L. crispatus* (CST I), *L. gasseri* (CST II), *L. iners* (CST III), High diversity (CST V) *L. jensenii* (CST IV) [278].

4.4.5 SPTB: PTL vs PPROM

We next examined if it was possible to characterise DESI-MS metabolic profiles of CVM swab samples on the basis of clinical presentations of SPTB; i.e. SPTL and PPROM. Based on the top 5 RF selected variables, the overall accuracy for class prediction of the model was 77% for SPTL and 73% for PPROM (Figure 4.8A). The PCA scores plot using these selected variables showed good discrimination between the classes (SPTL vs PPROM) (Figure 4.8B). Significant discriminatory metabolites for PPROM included phosphocholine. In contrast oleamide, ceramide(38.2) and lactic acid were shown to be of a higher abundance in the SPTL group. These discriminatory metabolites are shown in (Figure 4.8C) and table 9.

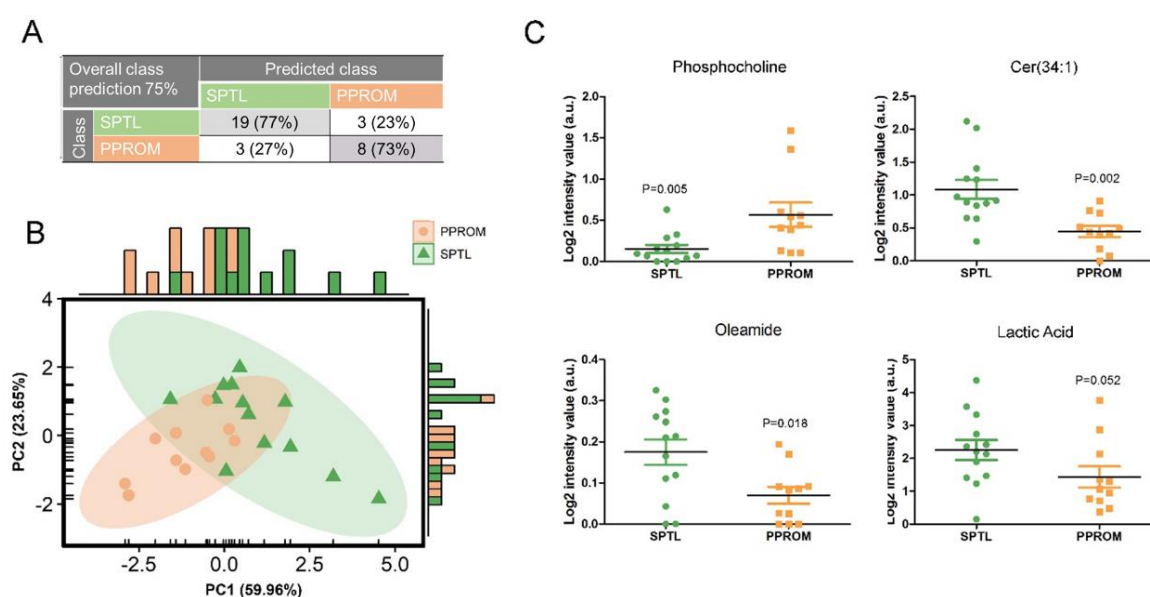


Figure 4-8. Metabolic profiles as characterised by DESI-MS of the clinical presentations of SPTB; i.e. SPTL (n = 13) and PPROM (n = 11). A: Supervised random forest normalised confusion matrices showing the overall accuracy for class prediction of 75% for prediction of SPTB presentation. B: PCA of top 5 variables. C: Scatter plots indicate significant differences in the abundance of selected metabolites upregulated in each group p < 0.05

Table 9. Metabolites significantly more or less abundant in early pregnancy in women that subsequently experience SPTL compared to those that experience PPROM

<i>m/z</i> observed	<i>m/z</i> theoretical	PPM	Mode	Adduct	Formula	SPTL vs PPROM	fold-change	p-value	Compound	Assignment
572.4810	572.4815	0.8647	(-)	[M+Cl]-	C ₃₄ H ₆₇ NO ₃	↑ SPTL	0.3063	0.0016	Cer(34:1)	Putative
184.0734	184.0733	0.5433	(+)	[M+H]+	C ₅ H ₁₄ NO ₄ P	↑ PPROM	4.7205	0.0049	Phosphocholine	Putative
304.2608	304.2611	0.9268	(+)	[M+Na]+	C ₁₈ H ₃₅ NO	↑ SPTL	0.3841	0.0184	Oleamide	Putative
626.5375	626.5285	0.0862	(-)	[M+Cl]-	C ₃₈ H ₇₃ NO ₃	↑ SPTL	0.2964	0.0154	Cer(38:2)	Putative
89.0248	89.0244	4.2797	(-)	[M-H]-	C ₃ H ₆ O ₃	↑ SPTL	0.5074	0.0523	lactic acid	Putative

The microbial composition of PPROM and SPTL based on CST characterisation are shown in figure 4.9A and found to be statistically similar. This was unexpected as lactic acid was found to be a discriminatory metabolite with a higher abundance in the SPTL compared with PPROM. Lactic acid is produced by *Lactobacillus* spp. [285, 286], therefore it was expected that PPROM would have a microbial composition depleted of *Lactobacillus* spp. and dominated by anaerobes (CST IV). However this CST IV was found equally in both groups: 8% (1/13) in SPTL and 9% (1/11) in PPROM (Fisher's exact $P=1.00$). We therefore explored this further and went on to examine the relationship between the relative levels of this metabolite and bacterial composition of the vaginal samples (figure 4.9B). We show that overall lactic acid abundance was less in the PPROM group and CST III appeared to be the microbial composition most associated with this reduced metabolite. In both the SPTL and PPROM group there is each one sample with reduced lactic acid that belonged to CST IV. There were 4 samples with CST I (*L. crispatus*) with lower abundance of lactic acid. Two of these women had subsequent conversion to CST III at 17 weeks. In the other two women, one had CST I at all other time points in pregnancy. The other women had no longitudinal data available.

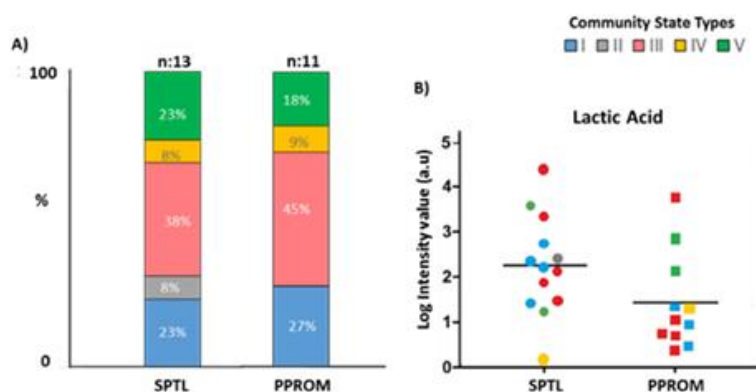


Figure 4-9. Vaginal microbial communities defined by CST at 15 weeks related to subsequent birth outcome; SPTL (n=13) and PPROM (n=11). B: Scatter plots indicate significant difference in the abundance of lactic acid in SPTL vs PPROM. Plot has been recoloured depending on the associated with CST group.

4.4.6 Prediction of subsequent cervical length shortening

Our final analysis was to assess if it was possible to detect metabolic differences in the CVM predictive of subsequent cervical length shortening in samples taken at 15 weeks of pregnancy. Using the top 5 RF selected variables we found poor predictive ability with only 20% of women being correctly

identified in this group. The ability to identify women with no shortening was 96% however this should be interpreted with caution as the overall prevalence of shortening is low.

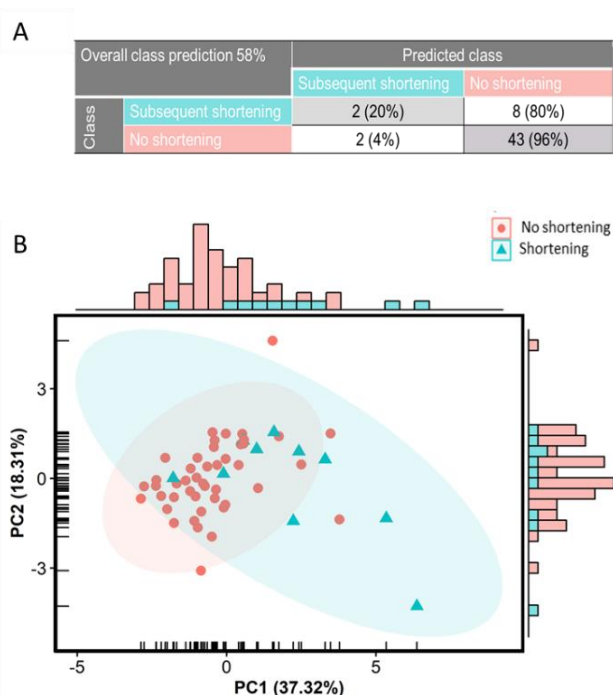


Figure 4-10. A: Supervised random forest normalised confusion matrices showing the overall accuracy for class prediction of 20% for prediction of subsequent cervical shortening. B: PCA score plot showing separation between classes; no subsequent shortening (pink) vs shortening using top 5 RF selected variables.

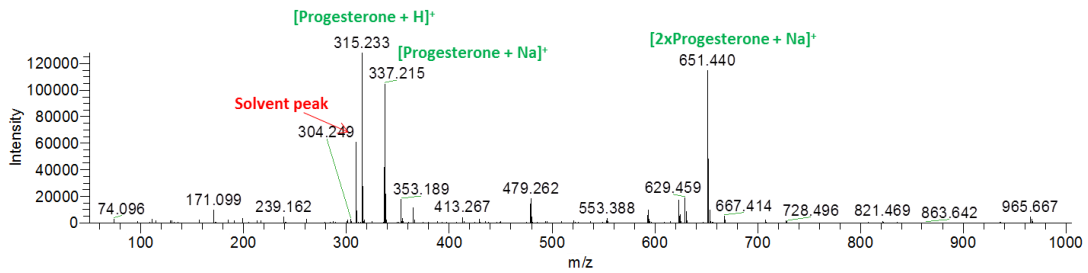
4.4.7 SPTB Interventions to prevent SPTB

We restricted our study to samples collected at 15 weeks which was prior to any interventions. A predictive test at this point in pregnancy would facilitate early stratification of women found to be high risk for SPTB. However this time point may have been too early for metabolic changes to become apparent in the CVM. However using samples taken later in pregnancy would potentially have metabolic profiles confounded by the presence of a progesterone pessary or cervical stitch. To test this we used samples taken at 25-30 weeks of gestation to assess the impact of interventions i.e. cervical cerclage and progesterone on the CVM metabolome.

Figure 4-11 shows DESI-MS spectra obtained with and without progesterone pessary. The progesterone signals are clearly seen and found to suppress signals in the region of interest (range: mz : 600-900) which is where glycerophospholipids are typically found.

Results: Characterisation of CVM Changes Associated with Preterm Birth

A Vaginal mucosal profile : Progesterone pessary



B Vaginal mucosal profile : No progesterone Pessary

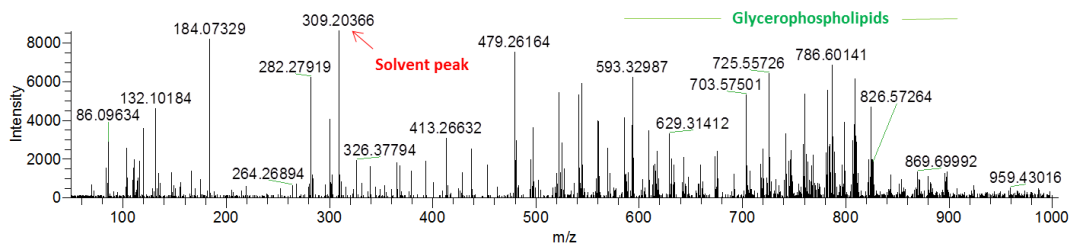


Figure 4-11. Averaged MS spectra of vaginal samples in positive ionisation mode taken from patient using vaginal progesterone pessaries (A) and from a patient not on treatment.

We next compared the metabolic profiles of women with a vaginal stitch in situ to controls with no stitch. Two types of cervical stitch exist and their use is primarily based on the operating surgeons' preference. Mersilene is a thicker multifilament stitch whereas nylon is thin and monofilament. Figure 4.12 shows PCA plots of the metabolic profiles of samples collected in pregnancy from women with no cervical stitch ($n=34$) and compared to those with mersilene ($n=30$) or nylon ($n=17$) stitch to determine the impact on underlying CVM. The indication for stitches were either history or USS indicated. Unsupervised PCA analysis of DESI-MS data collected in both ion modes revealed little difference between the metabolic profiles of CVM from women with a nylon stitch compared to controls. In contrast, the metabolic profile of 7 CVM samples from women with a mersilene stitch were outside the Hotelling's T2 ellipse indicating major differences compared to the rest of the samples in the dataset.

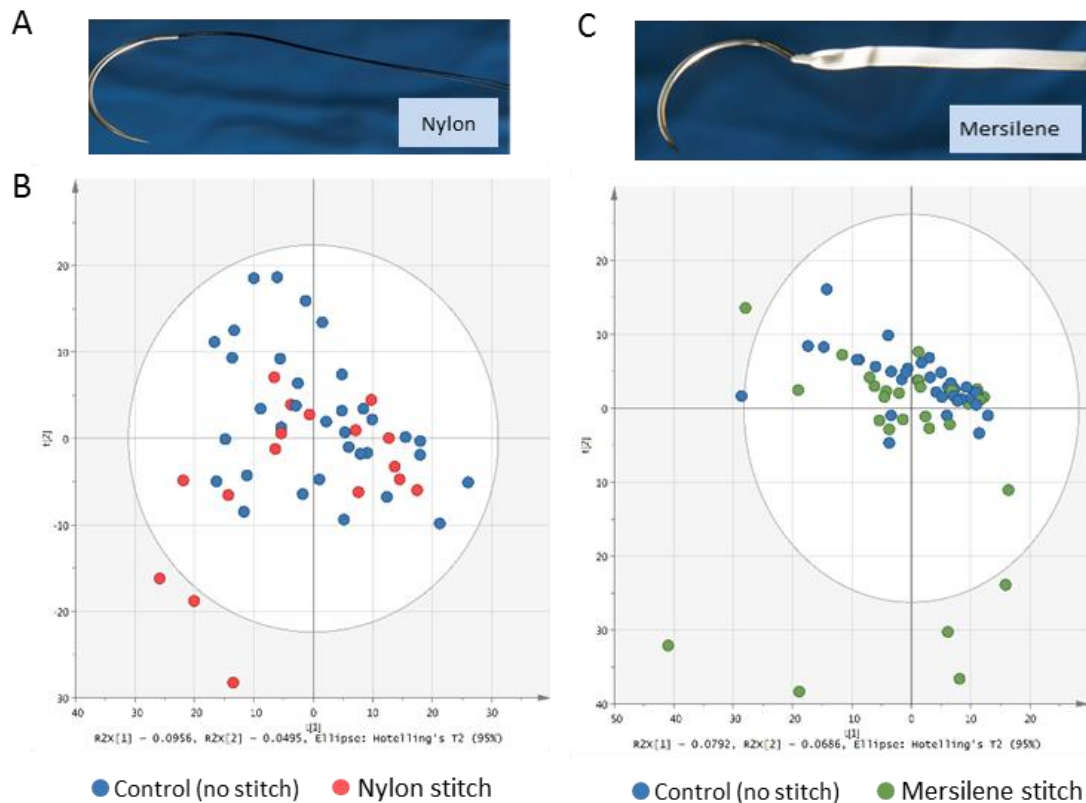


Figure 4-12. DESI-MS analysis of vaginal swab samples collected in pregnancy with no stitch, nylon (A) and mersilene (B) stitch. PCA analysis of DESI-MS data collected in negative mode shows over view of metabolic data with differences in the vaginal mucosal metabolic profiles in the presence of nylon stitch (B) and a more similar metabolic profiles in the presence of mersilene (D). Hotelling's T² ellipse defines the 95% confidence interval of the model variation with samples observed outside the confidence ellipse considered outliers.

4.5 Discussion

The ability to reduce rates of preterm birth is hampered by a lack of a tool or test that can reliably predict SPTB early in pregnancy where interventions are likely to be most effective [204]. The development of such test has been difficult partly since the underlying aetiologies of SPTB are highly heterogeneous. Commercial predictive tests that are available mainly offer negative predictive value and reassurance for symptomatic women at risk of preterm birth [175, 181, 446] and do not identify causal factors. This severely limits our ability to identify women in early pregnancy who could be targeted for surveillance and intervention strategies for the prevention of SPTB.

In this chapter I set out to examine if CVM metabolic signatures or biomarkers detectable by DESI-MS swab analysis are present in early pregnancy and could permit prediction of SPTB. Consistent with

other metabolic profiling CVM studies a robust, predictive signature was not detected [333, 334, 354], with the CVM metabolome associated with SPTB risk being highly variable, and a likely consequence of multiple underlying aetiologies of SPTB. However, despite being unable to find a specific signature predictive of all SPTB cases, DESI-MS swab profiling identified a number of metabolites that were significantly different between SPTB and controls. Compared to controls, women subsequently experiencing SPTB typically had higher levels of phosphatidylcholine (33:1) and an unknown metabolite with an *mz* of 604.47 as well as reduced levels of hydroxyphenyllactate. These metabolites were not upregulated or downregulated in all SPTB samples highlighting the metabolic variability of CVM existing within the patient group. Phosphatidylcholines are thought to be of host origin as they are predominately found in animal cells and are mostly absent from bacteria [450]. Their synthesis in eukaryotes occurs via the Kennedy pathway through the transfer of Cytidine 5'-diphosphocholine to diacylglycerol [451]. Although identification of the unknown metabolite (*mz* 604.47) was not possible, it was found within the region typical of phospholipids (*mz* 600-900) [234] so likely to be of this lipid class.

Higher levels of hydroxyphenyllactate in the control patients is consistent with it being a potential marker of microbiota composition in these patients. *In vitro* studies have shown that this metabolite is produced in high concentrations by *Lactobacillus spp.* [448, 452] and appears to play a role as a natural antioxidant participating in the regulation of the ROS production in both the circulation and tissues in sepsis. We found that this metabolite was positively associated with *L. crispatus*, consistent with a recent study integrating of LC-MS based metabolomics and microbiota compositional data from vagina mucosa sample in a non-pregnant cohort [368]. These findings collectively indicate vaginal microbiota composition has an important influence on the CVM metabolome. This was further highlighted by examining the relationship between vaginal microbiota composition, as determined using 16S rRNA amplicon sequencing, and supervised metabolic profiling of the DESI-MS swab profiles by PLS-DA. This analysis showed a strong relationship between CVM metabolic profiles and CST I (*L. crispatus*) dominated vaginal bacterial communities. This analysis also revealed that yeast colonisation (as assessed using culture) impacts the CVM metabolome whereas sample pH contributes minimally to CVM metabolic variability. Similarly, ethnicity was not a major source of CVM metabolic variations associated with SPTB prediction as indicated by even distribution of ethnic groups (Black, Asian and Caucasian) This was important to assess given that SPTB is known to affect Black women more frequently than Caucasian women [453, 454], which was reflected in our recruited cohort.

Given the high variability observed in CVM metabolic profiles, we hypothesised that the predictive performance of DESI-MS swab profiling could be improved by stratifying on the basis of clinical phenotypes (i.e. early vs late SPTB; SPTL vs PPRM; cervical shortening etc.) as they are likely to reflect different aetiologies and thus have different CVM metabolic profiles. Consistent with this DESI-MS could characterise CVM profiles related to early and late SPTB which may be the result of differences in the underlying microbial compositions in these classes. A higher proportion of *L. crispatus* dominance (CST I) was seen in the late SPTB group and *L. iners* dominance (CST III) in the early. In support of this, other studies have shown that microbial composition can contribute to the metabolome [344, 368]. *L. iners* colonisation is considered an intermediary between *Lactobacillus* spp. dominance and depletion and has been associated with BV [338] and SPTB [263, 265]. Of the 65 discriminatory features used by the RF classifier, none were shown to be significantly increased in the early SPTB patients which had a higher portion of *L. iners* colonisation. The co-existence of anaerobic species with *L. iners* may contribute a variable distribution of metabolite features in the mucosal metabolome, in contrast *Lactobacillus* spp. dominance (i.e. with *L. crispatus*) that has a more homogenous influence and thus in this modelling technique provides the discriminatory features just in the late group.

Clinical presentations of SPTB were also identified through differences in the CVM metabolome as characterised by DESI-MS swab analysis. PPRM was associated with higher levels of phosphocholine whereas SPTL without rupture was associated with increased ceramides, and oleamide. While the functional significance of these changes in the context of SPTB are yet to be determined, these compounds have important biological roles that may reflect underlying physiological alterations associated with specific SPTB presentations that are reflected in the CVM metabolome. Ceramides are known to contribute to the structural integrity and fluidity characteristics of cell membranes, and to regulate multiple cellular processes including induction of apoptosis and necrosis [11]. The fatty acid amide, oleamide has been linked to inflammation with capacity to inhibit LPS-induced production of NO, prostaglandin and NF- κ B activation [455].

Lactic acid was also found to be of a lower abundance in women went on to experience PPRM. Longitudinal studies of vaginal microbial communities during pregnancy have shown that a shift in the second trimester from *Lactobacillus* species dominance toward high diversity compositions void of *Lactobacillus* occur in approximately 25% of PPRM cases predominately occurring during the second trimester [143, 456]. Although examination of microbiota compositions in our cohorts did not identify

any significant differences in the distribution of *Lactobacillus* species dominant and deplete samples in SPTB with and without PPRM, lactic acid was found to be significantly higher in SPTL compared to PPRM.

Lactic acid exists as two isomers; L- and D-lactic acid. Vaginal epithelial cells almost exclusively produce L-lactic acid, whereas major *Lactobacillus* spp. encode genes for the production of both L- and D-isomers [457, 458]. Other bacteria often associated with CST IV also have the capacity to produce lactic acid (e.g. *Atopobium*, *Streptococcus*, *Staphylococcus*) although this tends to be at a lower concentration [241]. *L. crispatus* is known to have the highest high lactic acid production [308]. Consistent with this, in our study we found CVM levels of lactic acid in CST IV samples had lower mean average abundance of lactic acid compared to CST I.

L. iners dominance (CST III) was also associated with reduced abundance of lactic acid production. In some cases, CST III can transition from *Lactobacillus* spp. dominance to dysbiosis/BV [338]. In the women with CST III and low lactic acid, these could represent an intermediary CST III which has *L. iners* dominance however the overall counts are low with co-existing growth of anaerobes which is more likely to transition to CST IV/dysbiosis.

The final part of our study was to assess if there is a correlation between metabolites and subsequent sonographic shortening of the cervix. This was not found, however this may be due to lack of power or alternatively at 15 weeks gestation, biochemical changes in the CVM are not yet present and may only become apparent at the time of actual cervical shortening.

Our data demonstrates promise for rapid DESI-MS metabolic characterisation of the CVM in early pregnancy, in asymptomatic women destined to have a SPTB. Additionally our study highlights metabolic differences within the SPTB group indicating that in future studies with larger cohorts, the predictive capacity of DESI-MS swab analysis could be further improved.

Our study also considered the impact of interventions on the CVM metabolome and found that it was possible to detect the presence of progesterone pessaries. DESI-MS may have useful application to assess patient compliance of treatment through examining the presence of progesterone signals in the CVM. We also found that the CVM metabolome was influenced by the presence of a cervical mersilene stitch with less impact seen with a nylon stitch. This may be due to the presence of stitch material in the cervix which is more readily exposed than the nylon stitch. Alternatively, it may be the consequence of a disruption in the underlying microbiome. A retrospective observational study has

shown that mersilene stitch compared to nylon is associated with a persistent shift toward a microbiome depleted in *Lactobacillus* species and enriched for pathogenic microbial colonisation, with an increased production of inflammatory cytokines [219]. The ability of DESI-MS to distinguish between BV and healthy controls has been shown in Chapter 3. Mersilene has been associated with an increased pregnancy loss and SPTB rate compared to cervical cerclage performed with nylon stitch [218, 219]. A potential future application for DESI-MS could be to rapidly compare treatments and interventions through CVM metabolome characterisation.

4.6 Conclusion

SPTB is a multi-factorial condition that is reflected in the CVM metabolome in pregnancy. We have identified a number of potential sources of this variation which appear to be related to a number of aetiologies. Our results highlight the capacity of DESI-MS to rapidly characterise metabolic differences in the CVM metabolome associated with SPTB risk. We hypothesise that predictive potential of DESI-MS direct swab analysis may be limited by the heterogeneity of PTB aetiology, which is supported by the ability of the technique to discriminate samples with different severity of PTB (early vs late) and phenotype (SPTL vs PPRM). This work has important potential implications for future stratification of PTB risk studies as success is highly reliant upon accurate identification of the underlying aetiology.

5 DIRECT SWAB ANALYSIS BY DESI-MS FOR PREDICTION, DIAGNOSIS AND RISK STRATIFICATION OF PPROM

5.1 Chapter Summary

Hypothesis

Biochemical changes associated with premature fetal membrane and cervical remodelling preceding PPROM as well as interactions between the vaginal microbiota and the pregnant host are reflected in the local biochemical environment (i.e. the vaginal mucosa) and can be characterised rapidly using direct vaginal swab analysis by DESI-MS. These interactions are related to birth outcome and can be used for diagnosis preterm pre-labour rupture of membranes (PPROM) and stratify patient groups on the basis of underlying aetiology.

Aims

To use direct swab analysis by DESI-MS to identify metabolic signatures within CVM at the time of presentation for PPROM that facilitate its diagnosis.

To identify CVM metabolites in swabs predictive of underlying aetiology at the time of presentation (e.g. presence or absence of vaginal pathogenic bacterial compositions).

To identify CVM metabolite biomarkers of vaginal microbiota-host interactions in pregnant women predictive of PPROM.

Methods

Matched high vaginal swabs were taken prospectively from pregnant women prior to PPROM and at the time of presentation. Samples were also taken from a cohort of control patients matched for gestational age who experienced uncomplicated term delivery. Bacterial composition profiling was performed using MiSeq-based sequencing of the bacterial 16S rRNA gene amplicons. Direct swab profiling by DESI-MS was used to assess the CVM metabolic profiles of matched swabs.

Results

DESI-MS profiling of CVM swabs enabled acquisition of approximately 1500 spectral features within 1 minute, which were used for subsequent multivariate modelling. Analyses of metabolic profiles allowed robust discrimination of PPROM compared to matched controls with intact membranes. Rupture of membranes was associated with *Lactobacillus* spp. depletion in bacterial communities in 45% (13/45) of cases. These samples could be rapidly discriminated using DESI-MS profiling. Samples collected earlier in pregnancy prior to PPROM permitted identification of MS features predictive of outcome, which were putatively identified by exact mass and MS/MS experiments.

Conclusion

Our results highlight the capacity of DESI-MS to rapidly detect differences in the CVM metabolome associated with subsequent PPROM and underlying microbial structure. Our data also suggests that DESI-MS has the potential to assist in directed treatment strategies based on aetiology.

5.2 Introduction

Approximately 30% of all preterm birth cases are preceded by preterm pre-labour rupture of membranes premature (PPROM) [459]. At presentation PPROM is not accompanied by uterine activity and is typically followed by a latency period of at least 24 hours before labour starts. Subsequently, 80% of women with PPROM deliver within 9 days of presentation [460]. The development of chorioamnionitis following PPROM is a common and serious complication linked to microbial exposure of the gestational tissues following amniotic sac rupture, which is associated with adverse outcomes for both neonate and mother [461-467]. Ascending vaginal infection is considered to be a key aetiological factor of PPROM [468, 469] which involves premature activation of the innate immune system [459] and subsequent inflammatory cascade [470-473] leading to remodelling and disruption of membrane architecture and premature rupture of membranes [58-60, 474, 475]. Consistent with this, recent analyses of vaginal microbial communities throughout pregnancy show a shift in the early second trimester from *Lactobacillus* species dominance towards a high diversity composition enriched with potential pathogenic bacteria is a risk factor for PPROM [143, 456].

Oral prophylactic erythromycin is widely used in many countries as a first-line treatment for women presenting with PPROM [247-249]. However, this practice is increasingly controversial with doubts over efficacy being reported [476] as well as an association between increased risk of cerebral palsy, epilepsy, asthma and obesity in children of women exposed to erythromycin during pregnancy [251, 254, 462]. We recently showed that erythromycin treatment following PPROM is associated with *Lactobacillus* spp. depletion in the vagina and increased bacterial diversity, a vaginal microbial composition that correlates with increased risk of chorioamnionitis with funisitis and subsequent early onset neonatal sepsis [143]. However, erythromycin treatment in women with high diversity vaginal microbial communities initially deplete in *Lactobacillus* spp. was associated with a reduction in both richness and diversity. This implies that stratification of patients on the basis of vaginal microbial composition following PPROM and targeted antibiotic therapy could enhance outcomes in some women.

Diagnosis of PPROM is currently performed via clinical examination with a speculum and confirmation of amniotic fluid pooling in the vagina [248]. However, it is estimated that diagnosis is ambiguous in up to 20% of cases, particularly when amniotic fluid is intermittent or low [15]. Commercial tests that detect proteins highly expressed in amniotic fluid can be used to improve PPROM diagnosis [477, 478]. AmniSure ROM is monoclonal immunoassay-based detection of the protein PAMG-1, which is abundant in amniotic fluid (2000-25000 ng/ml) and almost undetectable in cervicovaginal secretions

(5-25 ng/ml). Alere Actim[®] PROM detects the presence of Insulin-like Growth Factor Binding Protein-1 (IGFBP-1) which is similarly found in high concentrations in amniotic fluid but at extremely low background concentrations in the vagina. The ROM Plus[®] test also detects the presence of IGFBP-1 as well as Alpha-fetoprotein. Overall the diagnostic performance characteristics are similar between AmniSure ROM and ROM Plus (sensitivity 89.3 vs 96.4%, specificity 100 vs 98.8%, PPV 100 vs 96.4% and NPV 96.5 vs 98.8% respectively) [478]. And a meta-analysis showed the accuracy of Actim[®] PROM and AmniSure[®] for the detection of PPROM to also be comparable [477]

Despite the ability to diagnose PPROM accurately, these tests are limited by the fact that they do not provide information regarding underlying aetiology, such as the presence or absence of infection that could direct provision of appropriate antibiotics or conservative management. Current diagnosis of chorioamnionitis relies upon culture results, blood tests (CRP, WBC) or suggestive maternal signs (tachycardia, pyrexia) infection [479]. These are late makers of infection and signal that delivery should be expedited rather than the use of antibiotics [248]. These late markers also confer a poorer prognosis to the neonate. Attempts to diagnose this subclinical infection earlier with amniocentesis being used in some countries to assess pro-inflammatory cytokines e.g. IL-6 [480]. This procedure is invasive and furthermore unfortunately not been shown to be effective in decreasing perinatal mortality in PPROM [481].

As the clinical course following PPROM is unpredictable and the rupture event itself irreversible, the ability to predict PPROM and offer preventative intervention is highly desirable. Currently no predictive test for PPROM exists [481] however there are emerging studies attempting to identify women at risk [482-485]. This would assist in stratification of those women most likely to benefit from antibiotics due to an infectious aetiology and/or timely administration of antenatal steroids if delivery was considered imminent. Alternatively the value of reassurance for women that are low risk should not be underestimated. This has beneficial effects on the mother and health care cost savings with reduced admissions and treatments [189].

As described previously in this thesis, CVM is a site of complex microbial-host interactions and acts as both a physical and immunomodulatory barrier against pathogenic colonisation. Accordingly, the chemical composition of CVM is strongly influenced by both host and microbial derived factors, which can be readily detected using metabolic profiling approaches [368, 381, 382, 447]. However, the application of traditional metabolic profiling platforms for assessment of CVM in a clinical setting are limited due to lengthy extraction and processing protocols or in the case of NMR, a lack of sensitivity [360]. This chapter details efforts to assess the ability of rapid direct swab analysis by DESI-MS to

detect CVM metabolite changes diagnostic of PPRM and indicative of underlying aetiology (e.g. presence or absence of lower reproductive pathogens). We also aimed to test if this method could identify metabolic alterations in CVM that precede phenotypic changes associated with PPRM, such as cervical remodelling and membrane rupture.

5.3 Study Design

To characterise the CVM metabolome and microbiome of women prior PPRM and to obtain gestation age matched samples from women with healthy term outcomes (controls) a cross-sectional cohort of pregnant women with and without risk factors for preterm birth were prospectively recruited from the preterm surveillance and antenatal clinics of Queen Charlotte's & Chelsea Hospital. High vaginal swabs were taken within the gestational time frames of 8-12, 19-25, 27-30 and 32-36 weeks of gestation. A proportion of these women went on to experience PPRM formed the before-PPROM group. To examine the metabolome and composition of the vaginal microbiome following membrane rupture a second cohort were recruited upon presentation with preterm membrane rupture. PPRM was defined as; rupture of the fetal membranes, diagnosed by pooling of amniotic fluid on speculum examination, prior to 37 weeks of gestation and more than 24 hours prior to spontaneous preterm delivery, clinical indicated delivery or induction of labour. When speculum examination was ambiguous, evidence of oligohydramnios or anhydramnios on ultrasonography and patient history was accepted as a diagnosis of PPRM. Vaginal swabs were taken at presentation, within 12 hours of rupture and prior to administration of oral erythromycin (250mg, 4 times per day) as per national guidelines [248].

Bacterial DNA was extracted from the vaginal swabs and 16S RNA gene sequencing of V1-V2 hypervariable regions performed as described in Chapter 2.

Metabolic profiling of CVM was performed directly on swabs using an LTQ Orbitrap Discovery mass spectrometer connected to a DESI source as previously described (Chapter 3) [369].

5.4 Statistical Analysis

To examine differences between the metabolic data derived from different classes (before PPRM vs control) and (PPROM vs control) a leave-one-out cross-validation strategy was employed to assess the predictive power of the supervised models. A Random Forest (RF) classifier was trained on the training samples and used to predict the label of the validation sample. The variables were first sorted by their RF importance, calculated on the training set, and only the first N variables were passed to the

classifier. A varying number of variables were tested to determine the optimal configuration in terms of predictive accuracy. In both methods, a varying number of RF trees were tested. The final combination (number of variables/number of trees) corresponded to the maximum value of the accuracy. Variables included all features in negative and positive mode following removal of isotopes in the pre-processing step. Clinical data including BMI and ethnicity were included as additional variables. The top-N variables were subsequently extracted from the entire dataset for univariate statistical analysis. A comparison of the scatter plot of the first two principal components using all the variables and the top-N variables was used to evaluate the discriminative power of the selected variables. A further validation of their discriminative power was performed applying a hierarchical clustering (Euclidean distance, Ward linkage) to the selected variables values in the full dataset. An exact Fisher's test was employed to test the difference between the clinical-related class labels and the cluster labels.

To assess the impact of the vaginal microbiome on the metabolome; characterisation of vaginal microbiota from matched samples was performed at bacterial genera level using the Statistical Analysis of Metagenomic Profiles software package (STAMP). Using this additional class information (*Lactobacillus* spp. dominant and *Lactobacillus* spp. deplete) multivariate analysis were carried out to assess if the vaginal metabolome could predict these microbial community structures in the before PPRM and after PPRM groups.

5.5 Results

5.5.1 Clinical characteristics of the study cohort

A graphical representation of the patient cohorts sampled and analysed in this study is presented in figure 5.1A. A total of 136 women were included, who collectively provided 168 swab samples for analysis. Of the women that subsequently experienced PPRM; 11 were sampled at 16 weeks gestation (range 12⁺⁵ - 17⁺³ weeks), corresponding to a median of 17⁺³ weeks (13 - 21⁺⁵ weeks) prior to PPRM. Separate cohorts of women (n = 9) were sampled 7 weeks (5⁺¹ – 9⁺² weeks) prior to PPRM and 2 weeks (1⁺⁰ – 2⁺⁴ weeks) prior PPRM. An additional 29 women were sampled at presentation, within 12 hours of PPRM and prior to receiving erythromycin treatment. All PPRM cohorts were compared with independent control samples matched for gestational age at an approximate 2:1 ratio. Control samples were derived from a low risk population that subsequently delivered at term following uncomplicated pregnancy.

Results: Direct Swab Analysis By DESI-MS for Prediction, Diagnosis & Risk Stratification of PPRM

Analysis of patient demographics showed no significant difference in maternal age, smoking habits or previous excisional cervical treatment when comparing the PPRM cohorts vs the low risk, gestational age matched controls (Table 10). There was a significant difference in BMI in the before PPRM group compared with controls (27.0 vs 23.5; P=0.04 Mann–Whitney). The after PPRM group contained a significantly higher proportion of black women compared to controls (34 % vs 8 % P=0.0008 Fisher’s Exact). Similarly, patients sampled before PPRM were more likely to be of black ethnicity compared to controls (52% vs 8%, P=0.001 Fisher’s Exact).

Medial cervical length (mm) was significantly longer in the controls group compared to before PPRM cohort (32mm vs 27 mm. P=0.04 Mann–Whitney). As expected, the gestational age at delivery was significantly different between the PPRM groups and controls and a small difference in gestation age at delivery was also observed in the before and after PPRM groups (median gestational age 34 v 32 weeks respectively, P=0.05 Fisher’s Exact).

Table 10. Demographic characteristics pregnant women sampled after PPRM (within 12 hours of ruptured membranes). Before PPRM were samples taken longitudinally throughout pregnancy prior to rupture. All controls had intact membranes at time of sampling and experienced healthy term birth outcomes.

	Controls	After PPRM	p value (Controls vs. after PPRM)	Before PPRM	p value (Controls vs. before PPRM)	p value (Before PPRM vs. after PPRM)
n	112	29		27		
BMI						
Median (IQ range)	23.5 (21-24)	24.5 (22-28)	0.08	27 (24-28)	0.04*	0.83
Age (years)						
Median (IQ range)	33 (27-38)	34.5 (26-37.8)	0.77	34 (26-38)	0.46	0.99
Ethnicity						
Caucasian	92 (82%)	12 (41%)	<0.0001*	11 (41%)	<0.0001*	1.00
Black	9 (8%)	10 (34%)	<0.0001*	14 (52%)	<0.0001*	0.28
Asian	11 (10%)	7 (24%)	0.06	2 (7%)	1	0.02*
Cervical Length (mm)						
Median (IQ range)	32 (28.5-37)	N/A	N/A	27 (23-33.5)	0.04*	N/A
Smoker						
	5 (4%)	1 (3%)	1	1 (7%)	0.62	1
Previous LLETZ						
	12 (11%)	4 (14%)	0.74	4 (15%)	1	0.67
GA at delivery (weeks + days)						
Median (IQ range)	39+4 (39+0-40+3)	32 (27+2-34+5)	<0.0001*	34 (30+0-35+1)	<0.0001*	0.05

Data presented as number (%) or median (interquartile range). BMI: body mass index, LLETZ: Loop Lazer Excisional of Transformation Zone, GA: gestational age, PPRM: Preterm prelabour rupture of the fetal membranes. P values: t test/ Mann-Whitney U (depending upon distribution), Fisher’s exact for proportional data.

5.5.2 PPRM diagnosis using DESI-MS metabolic profiling

Metabolic profiles of vaginal mucosa were obtained within 1 minute. Raw mass spectrometric data was converted to *imzML* format and imported for pre-processing (chapter 2) resulting in a final peak list consisting of 115 peaks in negative mode and 137 peaks in positive mode. These lists were combined and used for multivariate analysis with the top metabolites in each model defined by RF were used for modelling.

We first set out to examine the capacity of DESI-MS to distinguish patients with PPRM and those with intact membranes that delivered at term (controls). A random forest classifier was used which identified 45 features for modelling; providing an overall prediction accuracy of 97.5%. Figure 5.1C shows a PCA score plot providing visualisation of the data using the top variables. It shows very strong separation of these groups primarily along the first component. Hierarchical clustering of *mz* intensity values showed a significant correlation between the classes (control vs PPRM) and metabolite clusters (Fisher's exact $P < 0.0001$). In general, PPRM samples exhibited decreased levels of the top 45 discriminatory variables (Table 13). These were primarily derived from positive ionisation mode with 31% of ions belonging to the lipid class phosphatidylcholine. Selected significant ions ($p < 0.05$) are shown in the scatter plots and include Lyso-phosphatidylcholine (18:1), sphingosine, sphinganine and 5-oxoproline (figure 5.1E).

Results: Direct Swab Analysis By DESI-MS for Prediction, Diagnosis & Risk Stratification of PPRM

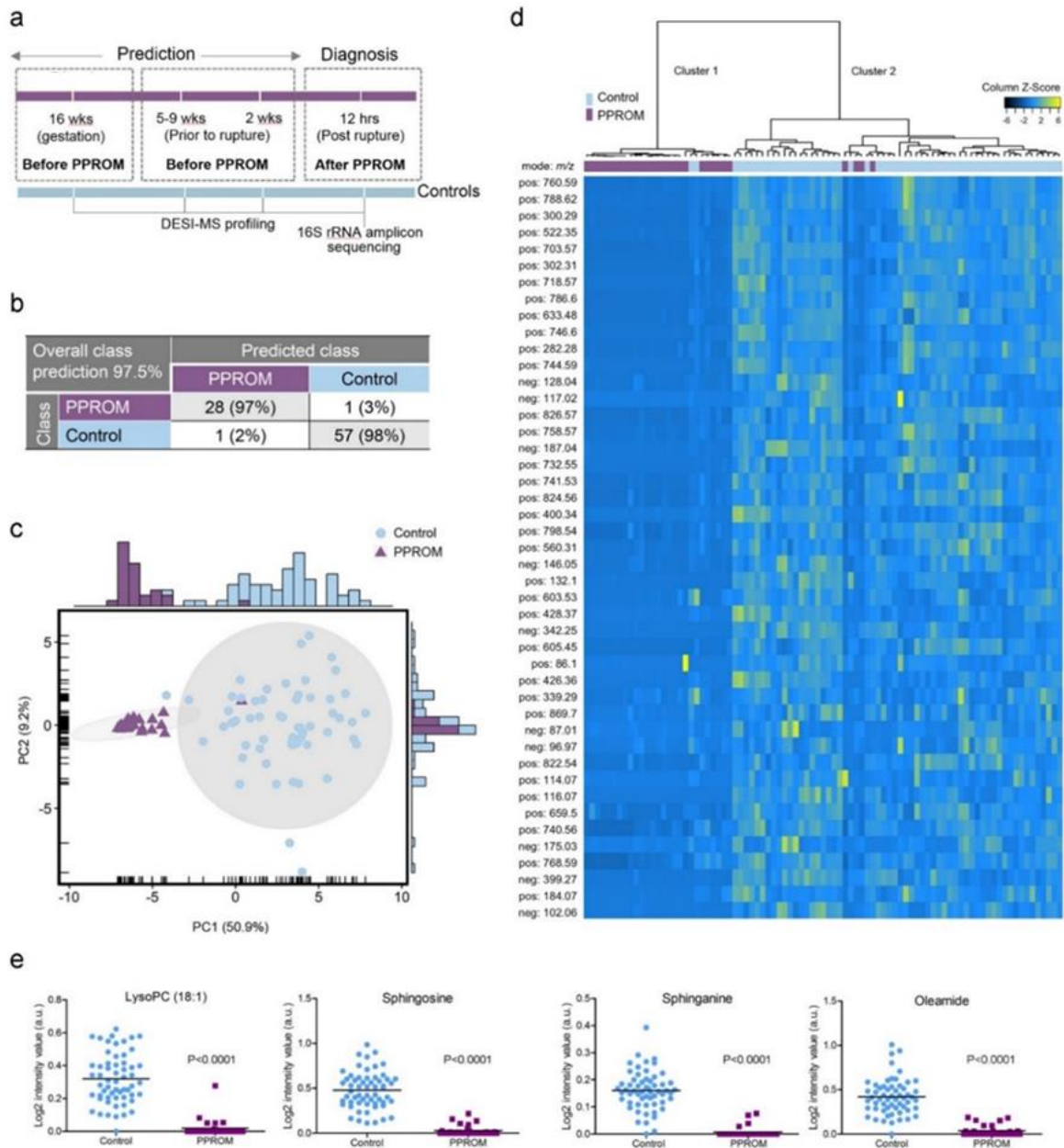


Figure 5-1. PPRM diagnosis using DESI-MS vaginal swab metabolic profiling. (A) Schematic representing vaginal swab sampling time-points in relation to PPRM. Samples for the prediction analysis were taken before PPRM at 16 weeks of gestation (distal). Samples nearer to rupture event were retrospectively assigned; 5-9 weeks prior to rupture (mid) and 2 weeks prior to rupture (proximal). After PPRM samples were taken within 12 hours of membrane rupture before antibiotics. Using the top 45 variables identified with random forest classifier; (B): Supervised random forest normalised confusion matrices showing the overall accuracy for class prediction of 97.5% (C) PCA scores plot using the top 45 RF features shows clear separation in PPRM and control group. (D) Heat map of all metabolites present in each group with log fold changes relative to mean profile across all samples. The row displays metabolite and the column represents the samples. Metabolites significantly decreased were displayed in blue, while metabolites significantly increased were displayed in yellow. The brightness of each colour corresponded to the magnitude of the difference when compared with

Results: Direct Swab Analysis By DESI-MS for Prediction, Diagnosis & Risk Stratification of PPRM

average value. (D) Scatter plots indicate significant differences in the abundance of selected metabolites (assigned by MSMS) upregulated in control group $p < 0.05$.

Although a small number of phospholipid species eg PC (38:7) and PI (36:2) were found to significantly more abundant in the PPRM samples. The majority of top discriminatory m/z features detected were in the presence of intact membranes. This indicates that amniotic fluid may “swamp” or suppress signals normally detected in CVM by DESI-MS. To investigate this further, DESI-MS was performed on a swab briefly dipped into amniotic fluid recovered during caesarean section. Figure 5.2B shows an averaged DESI-MS spectra of this sample which despite saturation of the swab there appears to be a low intensity signal in the m/z 600-900 (GPL region) with high signals in the m/z 250-350 range which relate to the solvent. Signals found in the amniotic fluid could also be identified in the PPRM samples; e.g. PI(36:2), indicating the presence of amniotic fluid in these samples.

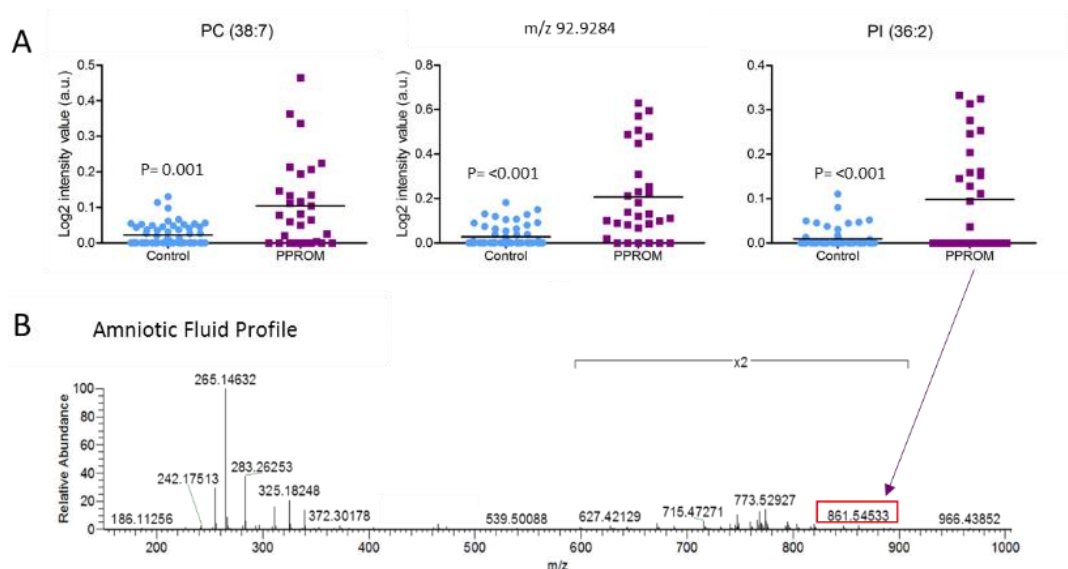


Figure 5-2. (A) Scatter plots indicate significant differences in the abundance of selected metabolites following PPRM ($p < 0.05$). (B) Averaged DESI-MS spectra in positive ion mode of amniotic fluid collected during caesarean section with annotation of selected significant metabolite found also in PPRM sample.

5.5.3 Assessment of CVM microbial composition using DESI-MS following PPRM

To examine if DESI-MS could identify metabolite signatures predictive of CVM microbial composition at the time of PPRM presentation, 16S rRNA amplicon sequencing was used to characterise microbiota in matched swabs (Figure 5-3A). Hierarchical clustering of relative abundance bacterial data permitted samples to be classified into 2 major groups characterised by *Lactobacillus* spp. dominance (>79% relative abundance; $n = 16$) or depletion (<64% relative abundance; $n = 13$) (Figure 5.3A). Richness and diversity were significantly increased in the *Lactobacillus* spp. deplete samples

compared to *Lactobacillus* spp. dominant (Figure 5.3B). PPROM was associated with a significantly higher proportion of *Lactobacillus* spp. depletion compared to gestational aged matched controls without membrane rupture 55% (16/29) vs. 4% (2/57); (Fisher's exact : $P < 0.0001$).

Feature selection by RF identified 50 features (Table 14) identified by DESI MS that could be used to discriminate between *Lactobacillus* spp. dominant and *Lactobacillus* spp. deplete samples with an overall accuracy of 70% (Figure 5.3C). Analysis of these features by PCA showed good separation of these classes although some overlap was observed (Figure 5-3D). High diversity, *Lactobacillus* spp. deplete samples were enriched for phosphatidylecholines whereas *Lactobacillus* spp. dominant samples typically contained higher levels of diglycerides, phosphatidylethanolamines and cholesterol sulphate.

Results: Direct Swab Analysis By DESI-MS for Prediction, Diagnosis & Risk Stratification of PPRM

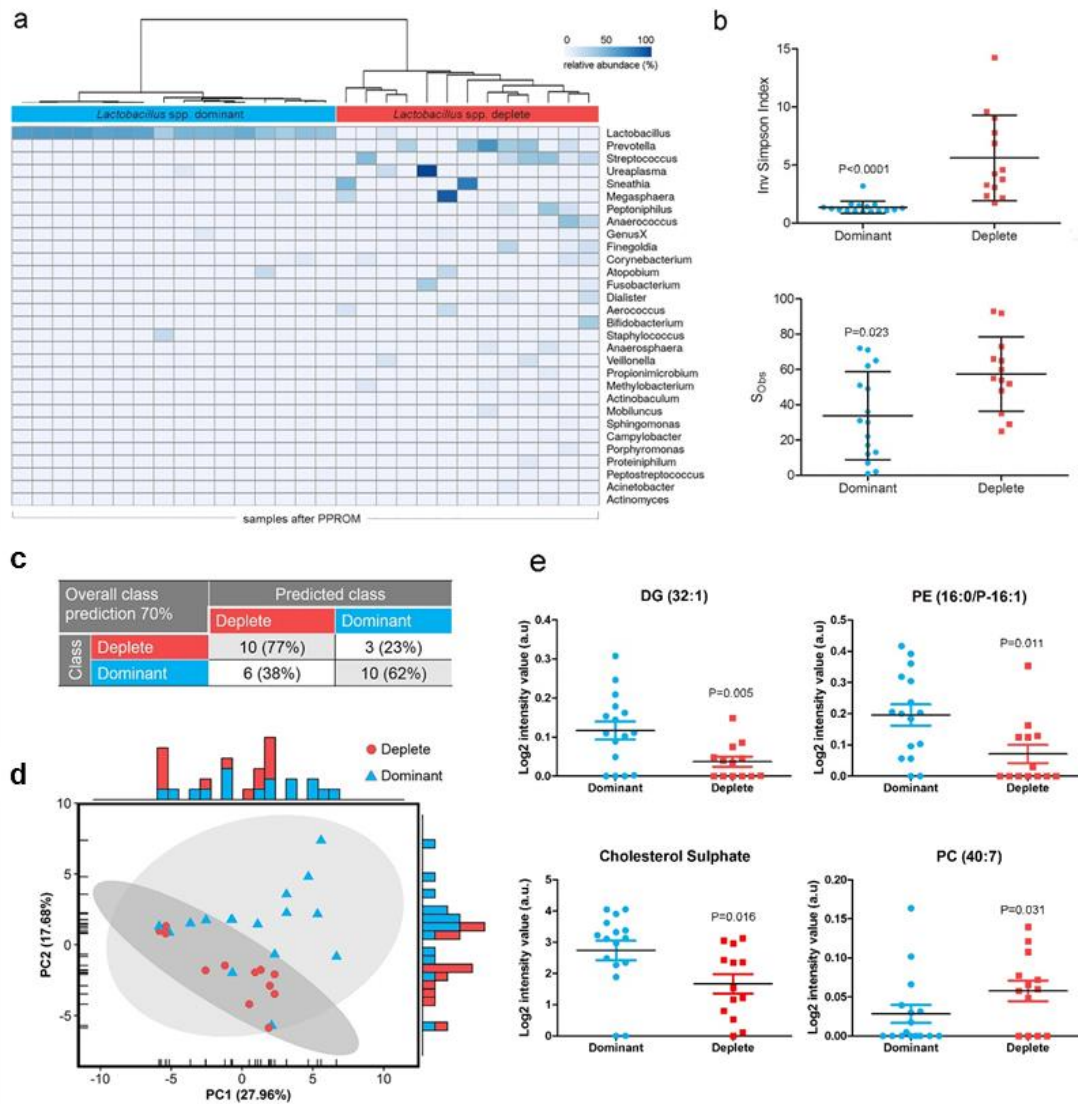


Figure 5-3. DESI-MS can discriminate between microbial compositions within 12 hours following rupture of membranes prior to antibiotics. (A) Ward's linkage HCA of vaginal bacterial species data from cervical vaginal fluid samples collected from women following PPRM within 12 hours and prior to antibiotics (n = 29). Vaginal bacterial communities were classified at genera level; Dominant >79% (n = 16), deplete <64% (n = 13). (B) Scatter plots showing increased richness and diversity in the *Lactobacillus* spp. deplete samples. Investigation of the vaginal metabolome following PPRM using DESI MS using top 50 random forest selected variables. (C) Supervised random forest normalised confusion matrices showing the overall accuracy for class prediction of 70% for *Lactobacillus* spp. vs deplete samples. (D) PCA score plot using top 50 random forest selected variables showing discrimination between *Lactobacillus* spp. dominant samples (n = 16, blue triangle) and *Lactobacillus* spp. deplete samples (n = 13 red circle). (E) Scatter plots indicate significant differences in the abundance of representative metabolites (assigned by MSMS) upregulated in control group p < 0.05.

5.5.4 Prediction of PPROM using DESI-MS of CVM swabs

We next sought to investigate the potential of DESI-MS swab profiling during pregnancy for the prediction of PPROM. Firstly, CVM metabolic profiles of samples collected 2 weeks prior to rupture were examined. A RF classifier identified 20 features that provided strong prediction of subsequent PPROM with an overall accuracy for class prediction of 93 %.

The top-20 variables, identified by RF from the full dataset, included 19 metabolites and black ethnicity as a clinical parameter. PCA of these variables revealed strong differentiation between controls and women who subsequently experienced PPROM (Figure 5-4A). Significant metabolites upregulated in the women that subsequently PPROM included adenine and pyruvate (Figure 5-4C), which were 13- and 6-times higher respectively compared to controls. These metabolites were also significantly upregulated 5-9 weeks prior to PPROM (Figure 5-4F). At this time point, positive prediction of the model for PPROM was poor (44%), however the model provided strong prediction of term control deliveries (88%). Similarly at 2 weeks prior to PPROM the model provided a higher prediction accuracy in the controls (91%) compared with subsequent PPROM (64%). Metabolites highly abundant 2 weeks prior to rupture in the control group include hydrophenyllactate, phenyllactate and hydroxypalmitic acid (Figure 5-4I) with the latter metabolite being also higher at 5-9 weeks prior to rupture. At 2 weeks prior to rupture, increased BMI was also a significant feature that influenced class discrimination.

Results: Direct Swab Analysis By DESI-MS for Prediction, Diagnosis & Risk Stratification of PPRM

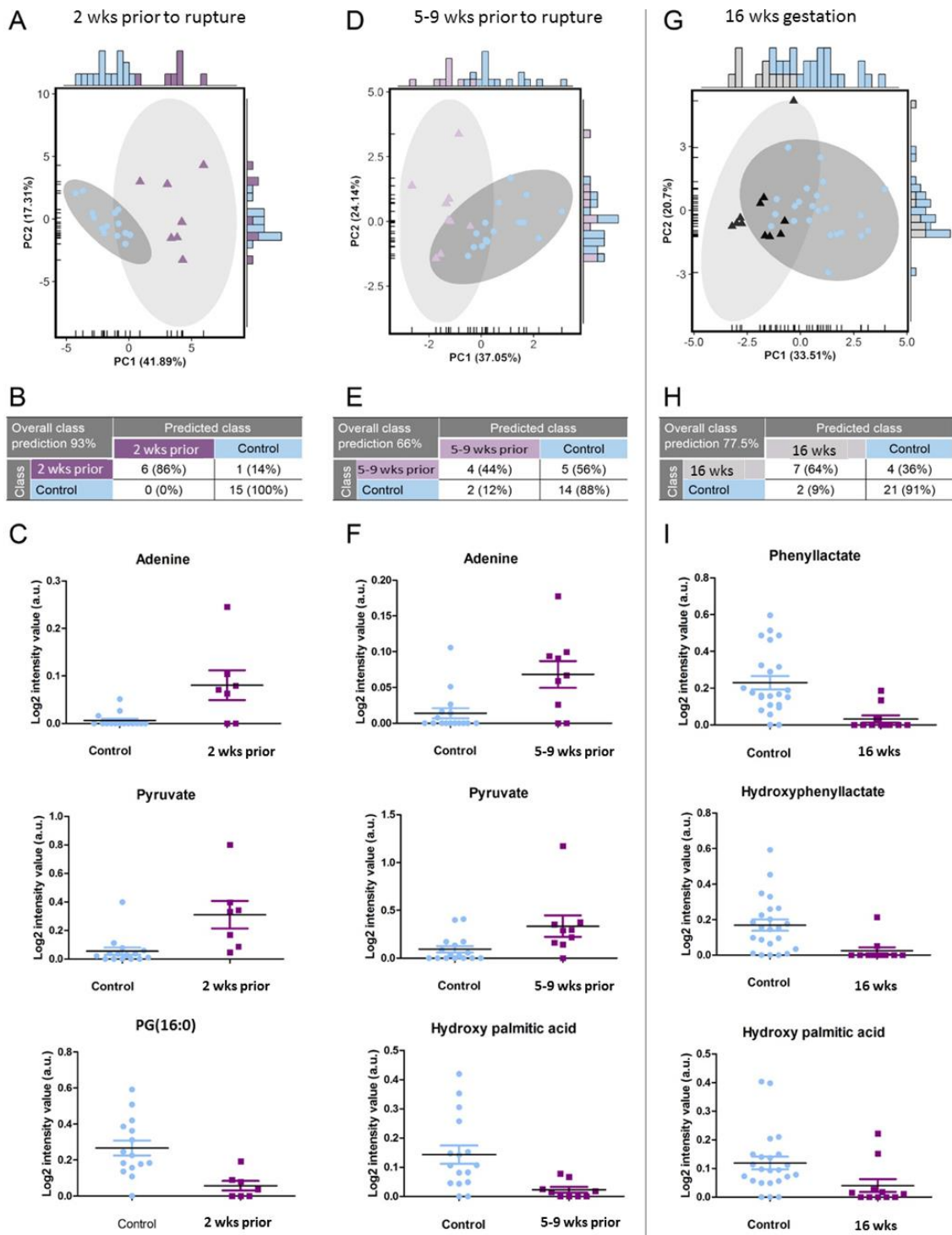


Figure 5-4. Prediction of PPRM by CVM metabolic profiling using DESI-MS swab analysis. DESI-MS analysis of vaginal swab samples collected 2 weeks prior to rupture, 5-9 weeks prior to rupture and at 16 weeks gestation. All samples compared with gestation matched controls. (A, D, G) PCA score plots of DESI-MS data reveal underlying differences in the vaginal mucosal metabolic profiles of women who subsequently go to PPRM compared with controls. (B, E, H) Confusion matrices showing overall class prediction in proximal, mid and distal to be 93%, 66% and 78% respectively. (C,F,I) Scatter plots of

representative metabolites significantly different between gestation aged match control and women that subsequently PPRM. ($P < 0.05$).

We next considered the underlying microbial structure of the vaginal swabs to examine if underlying differences in bacterial composition may associate with CVM metabolome. As shown in Figure 5.5A, control swabs at the distal sampling time-point (16 weeks gestation) were characterised by *Lactobacillus* spp. dominance; (100%; 20/20) whereas 91% (6/7) of women who subsequently experienced PPRM had *Lactobacillus* spp. dominance. However at the time points nearer to the rupture; 5-9 weeks prior and 2 weeks prior, there was a shift towards *Lactobacillus* spp. depletion, in women that subsequently experienced PPRM compared to controls; (43% vs 19% Fisher's Exact $P=0.2049$) and (54% vs 7% Fisher's Exact $P=0.0139$) respectively.

To examine the capacity of DESI-MS to distinguish between *Lactobacillus* spp. deplete and dominant samples prior to rupture, time-points 5-9 weeks and 2 weeks were combined and analysed together. Based on the top 20 RF selected variables, the overall accuracy for class prediction of the model for *Lactobacillus* spp. dominance was 94% and *Lactobacillus* spp. deplete was 33%. The PCA scores plot using these selected variables showed discrimination between the classes (*Lactobacillus* spp. dominance vs *Lactobacillus* spp. deplete) (Figure 5.5C). Significant discriminatory metabolites for *Lactobacillus* spp. deplete samples included lactose and propionate. In contrast in PG(16:0) and PE(O-34:1) were shown to be highly abundant in in the *Lactobacillus* spp. dominant group. These discriminatory metabolites are shown in (Figure 5.5E) and table 11.

Results: Direct Swab Analysis By DESI-MS for Prediction, Diagnosis & Risk Stratification of PPROM

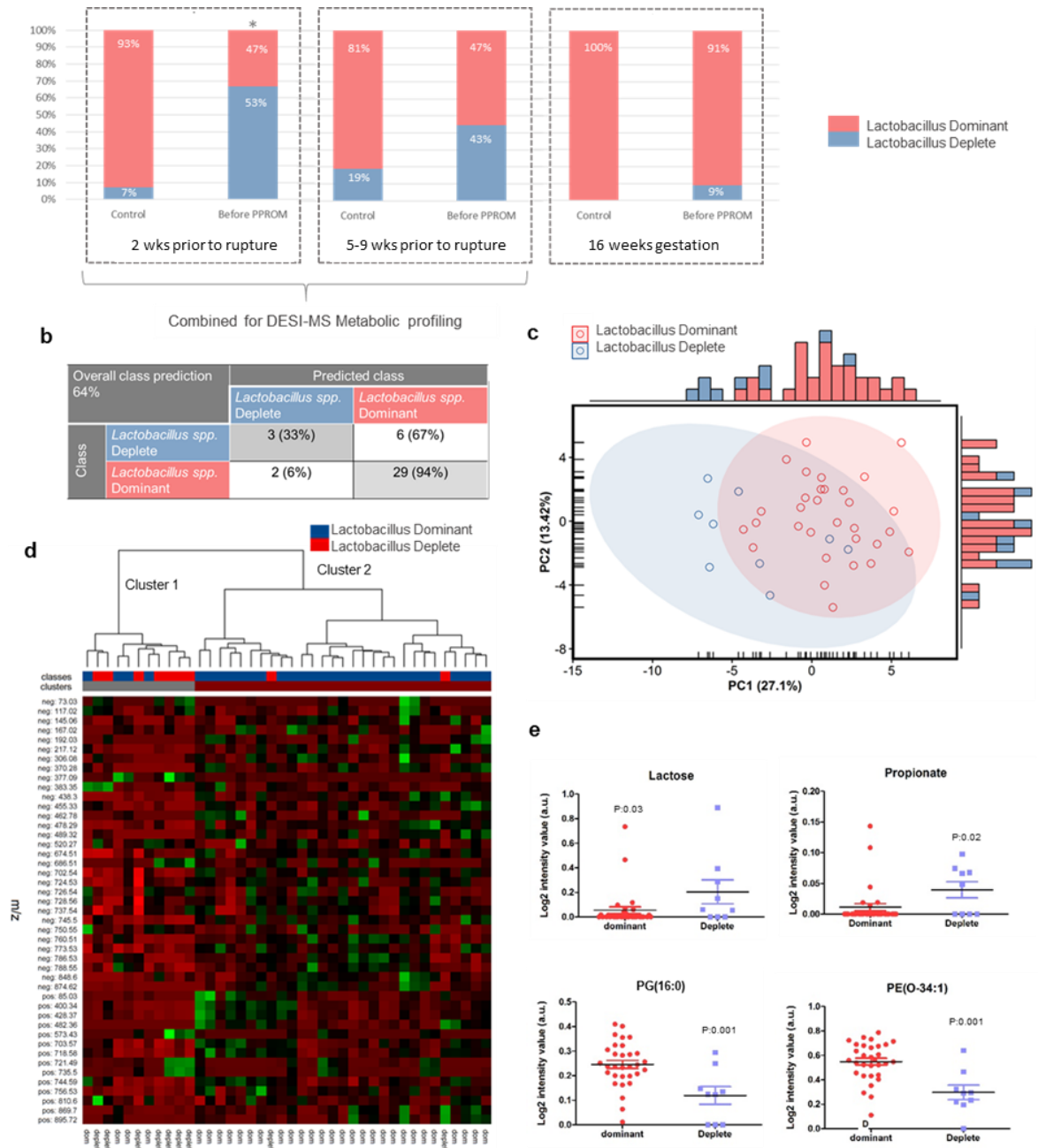


Figure 5-5. Relationship between microbial composition and metabolome in CVM during pregnancy prior to PPROM or uncomplicated term delivery. (A) Proportion of *Lactobacillus* spp. dominant and deplete samples at defined time-points in women subsequently experiencing PPROM or uncomplicated term delivery. (B) PCA scores plot using top 50 random forest selected variables coloured on the basis of microbial composition (*Lactobacillus* spp. deplete samples, $n = 9$, purple circles; *Lactobacillus* spp. dominant samples, $n = 31$, red circles). (C) Heat map discriminatory metabolites present in each group with log fold changes relative to mean profile across all samples. Metabolites significantly decreased are displayed in red, while metabolites significantly increased are displayed in green. The brightness of each colour corresponded to the magnitude of the difference when compared with average value. (D) Scatter plots of representative discriminatory metabolites identified by MSMS.

Results: Direct Swab Analysis By DESI-MS for Prediction, Diagnosis & Risk Stratification of PPRM

Table 11. Top significant metabolites used in random forest analysis that are differentially expressed in *Lactobacillus* spp. dominant and deplete samples taken from the mid and proximal time points in women that subsequently experience PPRM and gestation matched controls. Abundance of metabolite related to other DESI-MS studies noted

m/z observed	m/z theoretical	PPM	Mode	Adduct	Formula	Dominant vs Deplete	Fold-change	P value	Compound	Assignment
428.3738	428.3734	-0.69	(+)	[M+H] ⁺	C25H49NO4	↑ in dominant	2.4623	0.0224	Stearoylcarnitine	MSMS
605.4546	605.4541	0.00	(+)	[M+H] ⁺	C33H65O7P	↑ in dominant	2.1310	0.0083	PA(O-30:1)	Putative
426.3577	426.3578	0.09	(+)	[M+H] ⁺	C25H47NO4	↑ in dominant	2.5521	0.0438	Vaccenyl carnitine	MSMS
702.5445	702.5443	-2.28	(-)	[M-H] ⁻	C39H78NO7P	↑ in dominant	1.9899	0.0014	PE(O-34:1)	MSMS
674.5132	674.5130	0.50	(-)	[M-H] ⁻	C37H74NO7P	↑ in dominant	2.1113	0.0046	PE(14:0/P-18:0)	Putative
760.5147	760.5134	-0.12	(-)	[M-H] ⁻	C40H76NO10P	↑ in dominant	3.3711	0.0061	PS(34:1)	Putative
773.5345	773.5338	0.88	(-)	[M-H] ⁻	C42H79O10P	↑ in dominant	1.6950	0.0206	PG(36:2)	Putative
489.3153	489.3141	-2.66	(-)	[M-H] ⁻	C30H46O3	↑ in dominant	4.7357	0.0050	3beta-3-Hydroxy-11-oxolanosta-8,24-dien-26-al	Putative
483.2730	483.2728	-1.16	(-)	[M-H] ⁻	C22H45O9P	↑ in dominant	7.7555	0.0020	PG(16:0)	MSMS
399.2688	399.2687	-0.61	(-)	[M-H] ⁻	C21H40N2O3S	↑ in dominant	3.3523	0.0032	N-(5-Oxo-2-sulfanyl-1,3-oxazolidin-2-yl)octadecanamide	Putative
400.3424	400.3421	-0.36	(+)	[M+H] ⁺	C23H45NO4	↑ in dominant	2.3644	0.0286	Palmitoyl-L-carnitine	MSMS
73.0298	73.0295	3.79	(-)	[M-H] ⁻	C3H6O2	↑ in deplete	0.2862	0.0223	Propionate	Putative
377.0852	377.0856	-0.83	(-)	[M+Cl] ⁻	C12H22O11	↑ in deplete	0.2526	0.0323	Lactose	MSMS

5.6 Discussion

CVM is a site of complex microbial-host interactions which can be readily detected using metabolic profiling approaches [368, 381, 382, 447]. Ascending vaginal infection is considered to be a key aetiological factor of PPRM [468, 469]. Consistent with this, a longitudinal study of vaginal microbial communities shows a shift in the early second trimester from *Lactobacillus* species dominance towards a high diversity microbiome [143, 456]. Following PPRM, chorioamnionitis commonly occurs, this is linked to microbial exposure to the gestational tissues following amniotic sac rupture, which is associated with adverse outcomes for both neonate and mother [461-467]. Currently erythromycin is given to all women following PPRM in an attempt to reduce the risk of infection however this may not be beneficial in all cases [143].

In this chapter we assessed the ability of rapid direct swab analysis by DESI-MS to detect CVM metabolite changes diagnostic of PPRM and indicative of underlying aetiology (e.g. presence or absence of infection). We tested the predictive capacity of DESI-MS swab analysis to identify metabolic alterations in CVM that precede phenotypic changes associated with PPRM, i.e. cervical remodelling and membrane rupture.

Examination of the cohort studied in this chapter revealed that a higher proportion of women of black ethnicity experienced PPRM. This is consistent with previous reports indicated that PPRM affects black women more frequently than Caucasian women [453, 454]. Ethnicity has also been shown to influence vaginal microbiota compositions. *Lactobacillus* spp. deplete communities are more frequently observed in asymptomatic, black ethnic groups compared to White and Asian populations [486] and often to not associate with pathology [232]. Overall we show that there was no difference in maternal age, smoking habits or previous excisional cervical treatment in our cohort. BMI was

significantly higher in the before PPRM group compared with controls. High BMI has been linked to PPRM in a large population based study [487]. Median cervical length (mm) was also significantly shorter in those that subsequently experienced PPRM compared to the control groups. The shorter cervical lengths (<25mm) were all however at a gestational age greater than 28 weeks therefore were not offered cervical cerclage. Short cervix has been linked to PPRM in one study with speculation that a shortened length predisposes the membranes to ascending infection, inflammation and subsequent rupture [200]. However in this study more than half their cohort had a cervical cerclage in situ which has also been associated with subsequent PPRM [199, 219].

We show that DESI-MS vaginal swab profiling can permit stratification of patients experiencing PPRM from healthy controls with a prediction accuracy of 98% which is comparable to the accuracy of current bedside tests [477]. The robust diagnostic capacity of this model was largely driven by decreased detection of metabolites in PPRM samples that were otherwise present in relatively high concentration in controls with intact membranes. Of the 45 discriminatory features used by the RF classifier, none were shown to be significantly increased in PPRM patients. This indicated the possibility of an ion suppression effect of amniotic fluid upon CVM metabolites, which resulted in global decreased detection of metabolites readily detectable in the absence of amniotic fluid. Consistent with this, DESI-MS analysis of amniotic fluid alone led to the detection of a relatively small number of *mz* features with poor signal to noise ratio compared to CVM swabs (figure 5.2). Amniotic fluid contains peptides and intact proteins [488] which have large molecular weights and thus are harder to ionise than low molecule weight molecules e.g. lipids [365]. This can cause ion suppression as it alters the efficiency of droplet formation and evaporation, which in turn affects the amount of charged ion in the gas phase that ultimately reaches the detector [489]. To improve the ionisation of peptides and proteins a small distance from the electrospray tip to swab/sample is preferred as well as decreasing solvent flow rates and increasing the nebulizing gas flow rate [365].

The optimisation of parameters for our DESI-MS vaginal swab analysis was for CVM with intact membranes. For future studies investigating PPRM i.e. in the presence of amniotic fluid, parameters may need to be adjusted to improve the ionisation of proteins and thus reduce potential ion suppression. Another reason why the metabolic profiles in PPRM have reduced signal is that the comparatively low viscosity of amniotic fluid and high volume (as in the case of pooling at presentation) leads to rapid absorption of the sample into the centre of the swab due to capillary action. In turn this may result in reduced biomass presentation on the outside surface of the swab and decreased detection of metabolites. Adaption of the swab material to make it less absorbent may also improve results and would need to be investigated in future studies in order to optimise results.

Despite this it was possible to find significant metabolites that were more abundant in the PPRM samples. These were lipid species including PC(36:2) being likely to originate from amniotic fluid as it was also found in the pure amniotic sample. Metabolites increased in the control group (i.e. with intact membranes) included intermediates of the sphingolipid metabolic pathway (sphinganine and sphingosine). These are thought to be influenced by sex hormones as levels are higher in pregnant compared to postmenopausal women [490]. 5-oxoproline was also shown to be higher in controls and has been noted to be present in the vagina in other studies with a positive association with *Lactobacillus* presence and negative association with BVAB [368, 381]. Furthermore in one study assessing the CVF among pregnant women found 5-oxoproline to be upregulated in term birth compared to preterm term birth this metabolite was nearly two times higher [333].

Following rupture of membranes, standard practice in the UK and other commonwealth countries is to give a broad spectrum antibiotic, erythromycin for 10 days for all women with PPRM in an attempt to reduce the risk of chorioamnionitis [248]. Its use was recommended following the Oracle I trial which showed that it had comparatively less side effects when compared with Augmentin or placebo [491]. However subsequent studies have linked its use to cerebral palsy and epilepsy [253, 254] and shown that it is strongly associated with depletion of *Lactobacillus* spp. in the vagina [143, 492-494]. This is likely due to the fact that concentrations of Erythromycin that reach the vaginal lumen following oral administration are strongly effective against *Lactobacillus* spp. in vitro but ineffective against most gram negative bacteria [492], *Mycoplasma* spp. and *Ureaplasma* spp. [476]. However, erythromycin treatment may be of some benefit to women who present with highly diverse, *Lactobacillus* spp. deplete vaginal microbiota at the time of PPRM presentation [143]. These findings suggest that there are at least two groups of patients who present with PPRM; one group which may benefit from erythromycin and another in which its use is likely detrimental. Analysis of swab samples collected at the time of PPRM presentation, prior to administration of erythromycin, showed that DESI MS can predict *Lactobacillus* spp. depletion with an accuracy of 77%. These women represent a potentially stratifiable cohort of patients who may benefit from antibiotics whereas women with *Lactobacillus* spp. dominance may not have an infectious aetiological cause of PPRM and thus may benefit from a conservative approach. This could involve monitoring of systemic inflammatory markers (e.g. CRP, WBC) combined with monitoring of local microbial composition and host response using a method such as DESI-MS.

DESI MS swab analysis of CVM samples taken within 12 hours following PPRM revealed metabolic changes associated with the underlying microbial composition. Nonyl 2,3-bis(dodecyloxy)propanoate was significantly associated with *Lactobacillus* spp. depletion. This metabolite was also found to be

highly abundant in our BV DESI-MS pilot study [369]. In *Lactobacillus* spp. dominant group; prediction was only accurate in 62% of cases, this would result 38% of patients who were receiving antibiotics unnecessarily.

Currently no predictive test for PPROM exists [481] and advancement in this field is inhibited as most prediction studies currently combine this phenotype with spontaneous preterm labour despite them having different aetiologies [495]. Here we show that 2 weeks prior to rupture, DESI-MS can discriminate between women that subsequently PPROM and those that ultimately deliver at term. Both adenine and pyruvate were significantly higher in CVM from women subsequently experiencing PPROM. These metabolites are also found to be significantly higher 5-9 weeks prior to rupture suggesting that they are potential metabolic markers associated with biochemical changes preceding PPROM (e.g. disruption of fetal membrane integrity, cervical remodelling). Adenine is a purine base that has been shown to increase in response to inflammatory pathways activation both in vitro and in vivo. It decreased level in murine models with overwhelming inflammation following lung viral infection [496] Adenine administration was shown to inhibit the induction of inflammatory cytokines (TNF- α , IL-8) in intestinal epithelial cells as well as inflammatory colitis in a mouse model [497], suggesting that adenine plays a role in maintaining anti-inflammatory homeostasis. In our study adenine is up-regulated in PPROM which could be a potential response to premature activation of premature cervical remodelling pathways. The negative affect of adenine could be ultimately overwhelmed by the inflammatory cascade pathways that lead to uterine contractions, membrane rupture and untimely birth. Pyruvate has been identified in other studies to be positively associated with bacterial vaginosis [368, 447]. The absence of *Lactobacillus* spp. and polymicrobial colonization of the vagina has long been recognised as a risk factor for PPROM [469] and preterm birth [139, 219, 261, 498]. It is thought that the compounds released by these bacteria are recognised by the maternal host immune response system. This activates an inflammatory cascade from the decidua and fetal membranes to produce chemokines and cytokines. These trigger release of matrix metalloproteinases (e.g. MMP-8, MMP-9) [54-56] and prostaglandins (e.g. PGE₂) [57] which degrade the extracellular matrix proteins of the cervix and chorioamniotic membrane causing cervical remodelling and rupture of fetal membranes leading to PPROM [58-60].

Phenolic acids; phenyllactate and hydroxyphenyllactate are metabolites found to be up-regulated in the healthy controls at the distal time point. Studies suggest that the origin of these metabolites are likely to be microbial and in particular being associated with *Lactobacillus* spp. [448, 452]. Studies have shown that these phenolic acids inhibit growth of bacterial pathogens [499] and decrease reactive oxygen species production in the mitochondria, thus exhibiting an antioxidant/anti-inflammatory

effect [448, 500]. In our previous study using a different sample set, hydroxyphenyllactate was also found to be upregulated in the control term group when compared with women that subsequently experience SPTB furthermore it appeared to be strongly associated with *L. crispatus*.

At 16 weeks gestation and 5-9 weeks prior to rupture hydroxy-palmitic acid is up-regulated in the control group. Hydroxy-stearic acid was found to be more abundant in women that subsequently PPRM. Fatty acids such as oleic, stearic and palmitic acid are likely to be of host origin [501] and found to be abundant in the vagina with minor differences in fatty acid pattern were found between women in first trimester and at term [502]. Their conversion to hydroxylated fatty acids can be via the action of microbial hydroxylation enzymes released by *Lactobacillus* spp. [503-505] and *E.coli* [506]. Properties of these hydroxylated fatty acids include anti-tumour effects, antibacterial, antifungal, and anticancer [506-508].

Lactic acid was shown to be increased in the control group at 16 weeks, although it can be host derived, it is made in higher abundance by Lactobacilli species [446, 457]. Its production results in a low vaginal pH which protects against colonisation by pathogenic bacteria [509]. Interestingly it is also of higher abundance, 2 weeks prior to PPRM. However we show that in 47% of women at this time-point there is *Lactobacillus* spp. domination implying that in a significant proportion of women there may not be an underlying infectious cause to their PPRM.

When assessing the impact of the microbial communities on the vaginal metabolome using all samples from the mid and proximal time-point regardless of birth outcome; it is possible to discriminate between *Lactobacillus* spp. dominance and depletion based on the underlying metabolic profiles. Metabolites that were found to be proportionally higher in the *Lactobacillus* spp. deplete group were propionate and lactose. The former was also found to be higher in our earlier pilot DESI-MS study in association with BV. This is supported by other BV metabolic profiling studies using LCMS platforms [368, 381, 447] Propionate is a bacteria-derived short chain fatty acids which is thought to induce a pro-inflammatory response by increasing neutrophil migration [510]. Lactose was also found to be higher in the *Lactobacillus* spp. deplete samples, this was also found to be associated with BV in our earlier pilot DESI-MS study. *Lactobacillus* species (with the exception of *L. iners*) have the genetic potential to ferment lactose [511] which could explain why this carbon source is lower in the *Lactobacillus* dominate group compared to deplete.

Other metabolites found to be more highly abundant in the control group were also found to be higher in our previous studies in the control group when tested against confirmed PPRM (Stearoyl carnitine, Vaccenyl carnitine). We saw metabolites that were up regulated in the *Lactobacillus* spp. dominant

group following rupture to also be upregulated in the *Lactobacillus* spp. dominant group pre rupture; these included various phospholipids Phosphatidylethanolamine (PE), Phosphatidylserine (PS) and Phosphatidylglycerol (PG).

5.7 Conclusion

Our results highlight the capacity of DESI-MS to robustly and rapidly detect differences in the vaginal metabolome associated with PPRM prediction, diagnosis and has the potential to assist therapeutic decision-making by identifying cases of PPRM which may preferentially benefit from targeted treatment strategies (e.g. antibiotics) which may improve maternal and neonatal outcomes.

This study highlights the predictive and therapeutic potential of DESI-MS in not only facilitating the early identification of those patients at greatest risk of PPRM but also in enhancing our understanding of these disease processes to determine therapeutic interventions. Our evidence along with other studies suggest the role of ascending vaginal infection in the pathophysiology of PPRM in a proportion of cases [143]. We can predict which women are less likely to PPRM and this may be due to *Lactobacillus* spp. dominance which is known to be associated with healthy birth outcomes. These women could be reassured that more likely to have a term delivery. Proximal to rupture regardless of trigger (i.e. with or without infection) DESI MS can predict rupture likely due to biochemical pathways leading to PPRM that that ultimately lead to PPRM could be the same regardless of the triggering event. Changes in the biochemical environment related to bacterial presence and host inflammatory response can be detected by DESI MS [512]. This would allow can be identified and targeted for surveillance and therapy in order to improve neonatal outcome through timely administration of steroids, magnesium sulphate and transfer mother to ensure optimal neonatal care.

DESI MS has the ability to effectively assess rupture or not and can assess microbial communities has dominance and so could just offer conservative management and who would require antibiotics specific to anaerobes.

Despite strengths of our study results these findings need to be evaluated in the context of the study limitations. Our study size is limited by the practicalities and costs associated with prospectively recruiting large numbers of women subsequently experiencing PPRM however it represents a unique assessment of the vaginal metabolome prior to rupture of fetal membranes using a novel platform DESI MS. Further functional studies of identified metabolites and their related pathways may help to elucidate the molecular and physiological underpinnings of PPRM.

6 DISCUSSION

6.1 Introduction

Preterm birth is the leading cause of childhood mortality [2] is responsible for more than half of all neonatal deaths [3] and is a major cause of neonatal morbidity and lifelong handicap, resulting in significant financial and emotional impact on families [20] and the public sector [19]. Despite decades of research, the pathophysiology of SPTB is not fully understood and the incidence continues to rise on a global scale [3]. The development of strategies to prevent SPTB remains limited by our inability to reliably predict women at risk. [204]. This severely limits our capacity to identify women who could be targeted for surveillance and intervention strategies for the prevention of preterm birth.

There is an established association between dysbiotic vaginal microbial composition and subsequent premature delivery [513]. However, not all pregnant women with dysbiosis deliver preterm, which highlights the importance of individual host responses to vaginal microbiota. The vaginal metabolome reflects vaginal mucosal metabolites associated with specific microbiota, host metabolism and the interaction between them [368]. Furthermore, metabolic endpoints of biochemical pathways involved early phenotypic changes prior to preterm birth (e.g. cervical shortening, fetal membrane remodelling) are also likely to be reflected in the CVM metabolome. These concepts informed the rationale for the investigations outlined in this thesis and the development of the DESI-MS direct methodology, which would provide a potential point of care (POC) platform for rapid CVM metabolic profiling.

6.2 Summary of Study Findings and Translation into Clinical Practice

The first series of studies described in this thesis were designed to assess the capacity of DESI-MS vaginal swab profiling to rapidly interrogate the vaginal mucosal metabolome. This was then extended to assess the potential for vaginal mucosa metabolites detected by DESI-MS to act as biomarkers of SPTB risk. Finally, I assessed the capacity of DESI-MS metabolic profiling to characterise SPTB clinical phenotypes, the diagnosis of PPRM and assessment of underlying microbiota composition, which may facilitate targeted treatment strategies.

As detailed in Chapter 3, optimised direct swab analysis by DESI-MS provided rapid, reproducible and robust assessment of the CVM metabolome. Our proof of concept studies showed the ability of DESI-MS to discriminate between pregnant and non-pregnant women. DESI-MS was also successfully used to identify discriminatory metabolites that could robustly predict BV in pregnancy. These metabolites were also observed in CVM metabolic BV profiling studies using more established techniques e.g. LCMS/GCMS [368, 369, 381], however the DESI-MS method provides an obvious major advantage in

that acquisition of data can be achieved without the need for sample processing and extraction [290]. These attributes provide desirable qualities for point of care testing whereby metabolic profiles identified by DESI-MS could be obtained within minutes and rapidly translated into clinically relevant information. Further-more the test could be potentially carried out in clinical setting e.g. in an antenatal clinic or on labour ward.

In Chapter 4, the capacity of DESI-MS to identify metabolites or metabolic profiles predictive of subsequent SPTB was tested. Metabolic profiling was performed using swabs collected at 15 weeks gestation, which coincides with the routine appointment visit by women in early pregnancy and thus using a time-point that is easy to integrate into current maternity timetable visits. The ability to predict subsequent SPTB early in pregnancy would permit timely stratification and potential treatment as discussed later in this chapter. Currently there is no test that can robustly determine SPTB risk however detection of vaginal fFN is widely used for prediction. This test's merit relies primarily on its negative predictive value however its performance is not reliable in asymptomatic women and ineffective at gestations less than 22 weeks [175]. The underlying aetiology of SPTB is complex therefore it is perhaps not surprising that the use of single biomarker has not permitted robust prediction. We show that composite biochemical fingerprints using DESI-MS provide comprehensive molecular information which improved prediction of SPTB in early pregnancy. There was however still high variation in these data which reflective of the complex pathophysiology underlying this heterogeneous condition. Using DESI-MS swab profiling we showed that the predictive performance was improved by stratifying on the basis of clinical phenotypes (i.e. early vs late SPTB; SPTL vs PPRM). These are likely to be due to different aetiologies which are reflected in the CVM metabolic profiles. The capacity to predict phenotypes could potentially allow more directed treatment options. For example earlier preterm delivery has been more closely associated with infection than preterm delivery closer to term [135, 137, 442] and therefore might be prevented by clearance of pathogens (i.e. antibiotics) and/or modulation (i.e. probiotics).

In chapter 5 we extended our study of SPTB phenotypes to show the capacity of DESI-MS swab profiling to identify molecular fingerprints predictive of subsequent PPRM unique to early pregnancy and nearer to the rupture event (2 weeks prior). This provides the potential to attempt prevention or delay in rupture of membranes and the opportunity to ensure appropriate transfer to hospital with the expertise to ensure optimal neonatal care. DESI-MS swab profiling was also able to robustly confirm rupture of membranes with results being comparable to commercially available bedside tests. Our method however offers an advantage with its ability to identify vaginal microbial dysbiosis in women presenting with PPRM. Current practice in many countries including UK is to give the broad

spectrum antibiotic erythromycin to all women presenting with PPROM. In women whose PPROM is not linked to the vaginal dysbiosis this practice may not be necessary and may have a detrimental effect on the microbial composition in the vagina [143]. DESI-MS profiling following PPROM allows stratification of patients based on metabolomic prediction of the vaginal microbiota which would allow more appropriate targeted provision of antibiotics. This stratification by DESI-MS can also assist in the timing of steroid injections which are used to promote fetal lung maturity. The optimum window of benefit is within 48 hours of delivery [514]. In women with dysbiosis, which suggests of an underlying microbial aetiology, delivery is expedited and thus immediate provision of steroids is warranted. However when *Lactobacillus* spp. dominance, reflective of a non-infective aetiology, this results in a longer latency period. In these women, steroids could be withheld and given depending on the serial metabolic profiles captured using DESI-MS. This would ensure maximum benefit of steroids was provided to the neonate.

Using DESI-MS profiling, discriminatory metabolites related to the underlying microbial composition were also identified in early pregnancy providing the capacity to identify women that could benefit from modulation of the microbial community i.e. removal of pathogens and promoting *Lactobacillus* spp. dominance. Attempts to treat vaginal dysbiosis have so far been disappointing producing conflicting results, with failure to reduce the rate of SPTB in most cases [140, 229, 237]. BV studies have shown high rates of clearance with antibiotic regimes [515] however the recurrence rate of BV following treatment is high [231, 232]. This could be in part due to a woman's inability to re-establish a resilient *Lactobacillus*-dominant vaginal microbiome [233]. The presence of a probiotic may be sufficient to disrupt the pathogens and create an environment conducive to return of the individuals own *Lactobacillus* or colonisation with the species in the probiotic. Consistent with this improved BV clearance has been achieved with using probiotic therapy together with antibiotics [516-518] however this has been limited to *L. delbrueckii*, *L. rhamnosus* and *L. reuteri* species rarely found in the vagina. *L. crispatus* is associated with term delivery [263, 357, 435] and has been shown to produce multiple bacteriocins [519], have immunomodulatory properties [520] and to offer protection against various pathogens [521, 522] and viruses [343]. A specific strain of *L. crispatus* (CTV-05) has been commercialised for promoting reproductive health and has been shown to successfully adhere to epithelial cells [523], colonise the vagina and reduce rates of BV recurrence [524]. Vaginal microbiota modulation in women identified to be at risk of SPTB could include targeted antibiotic treatment followed by vaginal *L. crispatus* probiotics to re-colonise the vagina. We have shown that that hydrophenyllactate appears to be associated with *L. crispatus* dominance. Longitudinal metabolic profiling of swabs could be used to assess for the presence of this metabolic biomarker and thus successful colonisation using DESI-MS.

In the future another potential application of DESI-MS could be not only as a bedside diagnostic test but also to provide real-time vaginal mucosal measurements to personalise the dose of a treatment or to modulate or intensify therapy offered to an individual. Furthermore investigation of underlying molecular pathways implicated in SPTB could reveal potential targets for future interventions i.e. to block or alter production of certain compounds in order to influence the bacterial composition of the vagina [340].

6.3 Limitations and Future Work

Direct swab analysis of the vaginal mucosa using DESI-MS as presented here is a novel proof-of-concept study. Future research is necessary to advance the methodology before implementation of the technique as a direct sampling methods in a clinical environment. Small changes in swab orientation and distance from MS inlet can affect signal quality and primary signal intensity thus affecting reproducibility of the technique [399]. We used a swab turner to reduce variability of parameters between each swab analysis, however in a hospital ward setting this set up may not be suitable as it is too fragile. The design of a robust static enclosed structure or cartridge to reduce variability between measurements could be one possible approach to address this in a clinical setting.

The solvent used in our study (MeOH:H₂O) enabled data acquisition to provide the highest signal intensities and number of spectral features in two main regions of interest; the GPL and FA region. Whilst this worked well for vaginal mucosal sampling it did not provide intense metabolic signals in the presence of amniotic fluid which is likely due to ion suppression from the presence of protein and peptides. An alternative solvent as well as alterations to the spray parameters (distance to swab, solvent and gas flow) could have the capacity to better ionise this biofluid so it is less prone to ion suppression effects.

Currently the swab shape in our study was designed for sampling rather than for the purpose of DESI-MS analysis. Shape and dimension could be adapted which might improve spray formation with more sample being directed in the capillary inlet. Material selection and porosity could also be modified to improve analyte recovery and reduce chemical noise from the material. A potential limitation with our study was that our samples were in extended frozen storage. However studies have shown that the metabolic content of tissues are stable at -80 degrees [525].

To have widespread applicability any diagnostic tests should have high reproducibility. We found that it was possible to reproduce the data in our laboratory however in the future we would test different instruments in different laboratories to examine this aspect further. A clear protocol would be required to ensure that there is standardisation using this direct sampling method; this is to ensure

that all experimental conditions are the same to ensure reduced variation in ionisation efficiencies and sensitivities. Another aspect of developing the technique for future implantation as a bedside test would be the miniaturization of the mass spectroscopy instrument. There are emerging miniature MS systems that are capable of analysing biofluids and tissue samples by coupling with direct sampling methods however these tend to be for targeted MS approaches [526]. There would also be a need to implement a robust bioinformatics pipeline and information translation, ideally within the machine itself.

Future studies are required to validate DESI-MS as a diagnostic tool. Our studies are currently limited by small sample sizes. As these were novel study designs, pre-determined power calculations were not possible. For on-going validation SPTB studies using DESI-MS it will be vital that SPTB is distinguished by its different phenotypes prior to analyses. For larger clinical cohorts sample analysis time could be further reduced by barcoded sampling for faster acquisition times [290].

In the future metabolic biomarkers identified by DESI-MS could potentially be used for clinical decision making e.g. as part of a chip based assay. This could remove the necessity to have access to DESI-MS which might not be possible in antenatal clinics run outside of a hospital setting.

In the work described in this thesis we focused upon bacteria. However it is recognised that fungi [527] and viruses [528, 529] are also key members of the reproductive tract microbiota and their interactions with the host and with one another are an important influence on health and disease. This could be why we do not observe clear cut results between bacterial composition and metabolic profiling data and that future studies designed to examine the mycome and virome may offer improved insight into the biochemical events occurring in the vaginal mucosa.

6.4 Conclusion

DESI-MS direct swab analysis of the vaginal mucosa holds potential as a diagnostic tool to rapidly generate features that are unique to an individual. This information could empower clinicians to enable care that is personalised, depending on underlying aetiology and host response, with the aim of prolonging pregnancy in those at risk of SPTB. [38].

This work described in this thesis highlights the predictive and therapeutic potential of DESI-MS in pregnancy, in not only facilitating the early identification of those patients at greatest risk but also in enhancing our understanding of these disease processes to determine therapeutic interventions. This work has important potential implications for future stratification of PTB risk, identification of the underlying aetiology and development of new therapeutic strategies.

7 REFERENCES

1. Blencowe, H., et al., *National, regional, and worldwide estimates of preterm birth rates in the year 2010 with time trends since 1990 for selected countries: a systematic analysis and implications*. The Lancet, 2012. **379**(9832): p. 2162-2172.
2. WHO, W.H.O. *Causes of child mortality*. 2015 [cited 2015 01.11.2015]; Available from: http://www.who.int/gho/child_health/mortality/causes/en/.
3. Liu, L., et al., *Global, regional, and national causes of child mortality in 2000-13, with projections to inform post-2015 priorities: an updated systematic analysis*. Lancet, 2015. **385**.
4. Costeloe, K.L., et al., *Short term outcomes after extreme preterm birth in England: comparison of two birth cohorts in 1995 and 2006 (the EPICure studies)*. BMJ, 2012. **345**: p. e7976.
5. Beck, S., et al., *The worldwide incidence of preterm birth: a systematic review of maternal mortality and morbidity*. Bull World Health Organ, 2010. **88**(1): p. 31-8.
6. Chang, H.H., et al., *Preventing preterm births: trends and potential reductions with current interventions in 39 very high human development index countries*. Lancet, 2013. **381**(9862): p. 223-234.
7. Martin JA, H.B., Osterman MJ, Curtin SC, Matthews TJ. , *Births: final data for 2015*. National vital statistics reports, 64. Hyattsville, MD: National Center for Health Statistics; 2017.
8. ONS (2015) *Pregnancy and ethnic factors influencing births and infant mortality: 2013, England*, <https://www.ons.gov.uk/peoplepopulationandcommunity/healthandsocialcare/>
9. H Blencowe, Z.B.A., C. Howson, *Born too soon: a global action report for 15 million preterm births*. International Journal of Gynecology & Obstetrics 119:S171-S172, October 2012.
10. Goldenberg RL, C.J., Iams JD, et al. , *Epidemiology and causes of preterm birth*. . The Lancet 2008. **371**(9606): p. 75-84.
11. Ramkumar, M. and J.F. Stephen, *The Role of Matrix Degrading Enzymes and Apoptosis in Rupture of Membranes*. Journal of the Society for Gynecologic Investigation, 2004. **11**(7): p. 427-437.
12. Bernard, J.C., et al., *The Chorion Layer of Fetal Membranes Is Prematurely Destroyed in Women With Preterm Premature Rupture of the Membranes*. Reproductive Sciences, 2013. **20**(10): p. 1246-1254.
13. Petrou, S., *The economic consequences of preterm birth during the first 10 years of life*. BJOG, 2005. **112 Suppl 1**: p. 10-5.
14. Marlow, N., et al., *Neurologic and developmental disability at six years of age after extremely preterm birth*. N Engl J Med, 2005. **352**(1): p. 9-19.
15. Mercer, B.M., *Preterm premature rupture of the membranes*. Obstet Gynecol, 2003. **101**(1): p. 178-93.
16. Mwaniki, M.K., et al., *Long-term neurodevelopmental outcomes after intrauterine and neonatal insults: a systematic review*. Lancet, 2012. **379**(9814): p. 445-52.
17. Costeloe, K. and E.S. Group, *EPICure: facts and figures: why preterm labour should be treated*. BJOG, 2006. **113 Suppl 3**: p. 10-2.
18. Woythaler, M., *Neurodevelopmental outcomes of the late preterm infant*. Semin Fetal Neonatal Med, 2019. **24**(1): p. 54-59.
19. Mangham, L.J., et al., *The Cost of Preterm Birth Throughout Childhood in England and Wales*. Pediatrics, 2009. **123**(2): p. e312.
20. Callahan, B.J., et al., *Replication and refinement of a vaginal microbial signature of preterm birth in two racially distinct cohorts of US women*. Proceedings of the National Academy of Sciences, 2017.
21. Brehaut, J.C., et al., *Health Among Caregivers of Children With Health Problems: Findings From a Canadian Population-Based Study*. American Journal of Public Health, 2009. **99**(7): p. 1254-1262.
22. Romero, R., et al., *The preterm parturition syndrome*. BJOG, 2006. **113 Suppl 3**: p. 17-42.

23. Rinaldi, S.F., et al., *Anti-inflammatory mediators as physiological and pharmacological regulators of parturition*. Expert Review of Clinical Immunology, 2011. **7**(5): p. 675-696.
24. Lindstrom, T.M. and P.R. Bennett, *The role of nuclear factor kappa B in human labour*. Reproduction, 2005. **130**(5): p. 569-81.
25. Migale, R., et al., *Modeling hormonal and inflammatory contributions to preterm and term labor using uterine temporal transcriptomics*. BMC Med, 2016. **14**(1): p. 86.
26. Word, R.A., et al., *Dynamics of cervical remodeling during pregnancy and parturition: mechanisms and current concepts*. Semin Reprod Med, 2007. **25**(1): p. 69-79.
27. Becher, N., et al., *The cervical mucus plug: Structured review of the literature*. Acta Obstetrica et Gynecologica Scandinavica, 2010. **88**(5): p. 502-513.
28. Sohan, K., R. Wiggins, and P. Soothill, *Cervical physiology in pregnancy and labour*. Fetal and Maternal Medicine Review, 2000. **11**(3): p. 135-141.
29. Word, R.A., et al., *Dynamics of cervical remodeling during pregnancy and parturition: mechanisms and current concepts*. Semin Reprod Med, 2007. **25**.
30. Read, C.P., et al., *Cervical remodeling during pregnancy and parturition: molecular characterization of the softening phase in mice*. Reproduction, 2007. **134**(2): p. 327-340.
31. Akgul, Y., et al., *Dynamic Changes in Cervical Glycosaminoglycan Composition during Normal Pregnancy and Preterm Birth*. Endocrinology, 2012. **153**(7): p. 3493-3503.
32. Anderson, J., et al., *Utilization of Different Aquaporin Water Channels in the Mouse Cervix during Pregnancy and Parturition and in Models of Preterm and Delayed Cervical Ripening*. Endocrinology, 2006. **147**(1): p. 130-140.
33. Yoshida, K., et al., *Quantitative Evaluation of Collagen Crosslinks and Corresponding Tensile Mechanical Properties in Mouse Cervical Tissue during Normal Pregnancy*. PLoS ONE, 2014. **9**(11): p. e112391.
34. Akins, M.L., et al., *Cervical Softening During Pregnancy: Regulated Changes in Collagen Cross-Linking and Composition of Matricellular Proteins in the Mouse*. Biology of Reproduction, 2011. **84**(5): p. 1053-1062.
35. Westergren-Thorsson G, N.M., Bjornsson S et al. , *Differential expressions of mRNA for proteoglycans, collagens and transforming growth factor-beta in the human cervix during pregnancy and involution*. Biochim Biophys Acta 1998; . **1406**: p. 203-213.
36. Osmers, R., et al. , *Collagenase activity in the cervix of non-pregnant and pregnant women. .* Arch Gynecol Obstet, , 1990. . **248**(2): p. 75-80.
37. Iwahashi M et al, *Decreased type I collagen expression in human uterine cervix during pregnancy*. J Clin Endocrinol Metab, 2003. . **88**(5): p. 2231-5.
38. Maul H, S.G., Garfield RE. , *Prediction of term and preterm parturition and treatment monitoring by measurement of cervical cross-linked collagen using light-induced fluorescence. .* Acta Obstet Gynecol Scand. , 2005. **84**: p. 534-6.
39. Schlembach, D., et al., *Cervical ripening and insufficiency: From biochemical and molecular studies to in vivo clinical examination*. European Journal of Obstetrics & Gynecology and Reproductive Biology, 2009. **144**: p. S70-S76.
40. Dubicke, A., et al., *Density of Stromal Cells and Macrophages Associated With Collagen Remodeling in the Human Cervix in Preterm and Term Birth*. Reproductive Sciences, 2015. **23**(5): p. 595-603.
41. Bokstrom, H.e.a., *Leukocyte subpopulations in the human uterine cervical stroma at early and term pregnancy. .* Hum Reprod, , 1997. **12**(3): p. 586-90.
42. Osman, I., et al., *Leukocyte density and pro-inflammatory cytokine expression in human fetal membranes, decidua, cervix and myometrium before and during labour at term*. Mol Hum Reprod, 2003. **9**(1): p. 41-5.
43. Ellwood DA, M.M., Anderson AB et al. , *The in vitro production of prostanoids by the human cervix during pregnancy: preliminary observations. .* Br J Obstet Gynaecol 1980; . **87**: p. 210-214.

44. Ledingham M, T.A., Macara L et al. , *Changes in the expression of nitric oxide synthase in the human uterine cervix during pregnancy and parturition.* . Mol Hum Reprod 2000. **6**: p. 1041-1048.
45. Tornblom SA, K.A., Bystrom B et al. , *Non-infected preterm parturition is related to increased concentrations of IL-6, IL-8 and MCP-1 in human cervix.* . Reprod Biol Endocrinol 2005. **3**(39).
46. Tornblom SA, P.F., Bystrom B et al. , *15-hydroxyprostaglandin dehydrogenase and cyclooxygenase 2 messenger ribonucleic acid expression and immunohistochemical localization in human cervical tissue during term and preterm labor.* J Clin Endocrinol Metab 2004. **89**: p. 2909-2915.
47. Gordon, M.K. and R.A. Hahn, *Collagens.* Cell and tissue research, 2010. **339**(1): p. 247-257.
48. Malak, T.M., et al., *Confocal immunofluorescence localization of collagen types I, III, IV, V and VI and their ultrastructural organization in term human fetal membranes.* Placenta, 1993. **14**(4): p. 385-406.
49. Woessner, J.F., *Matrix metalloproteinases and their inhibitors in connective tissue remodeling.* The FASEB Journal, 1991. **5**(8): p. 2145-2154.
50. Strauss, J.F., *Extracellular Matrix Dynamics and Fetal Membrane Rupture.* Reproductive Sciences, 2013. **20**(2): p. 140-153.
51. Moore, R.M., et al. , *The physiology of fetal membrane rupture: insight gained from the determination of physical properties.* . Placenta, , 2006. . **27**(11-12): p. 1037-51.
52. Kumar, D., et al., *The physiology of fetal membrane weakening and rupture: Insights gained from the determination of physical properties revisited.* Placenta, 2016. **42**: p. 59-73.
53. Joyce, E.M., et al., *In-vivo Stretch of Term Human Fetal Membranes.* Placenta, 2016. **38**: p. 57-66.
54. Athayde N, E.S., Romero R, Gomez R, Maymon E, Pacora P, *A role for matrix metalloproteinase-9 in spontaneous rupture of the fetal membranes.* Am J Obstet Gynecol., 1998. **179**: p. 1248-53.
55. Maymon E, R.R., Pacora P, Gomez R, Athayde N, Edwin S,, *Human neutrophil collagenase (matrix metalloproteinase 8) in parturition, premature rupture of the membranes, and intrauterine infection.* . Am J Obstet Gynecol. , 2000. **183**: p. 94-9.
56. Vadillo-Ortega F, E.-G.G., *Role of matrix metalloproteinases in preterm labour* BJOG., 2005. **112**: p. 19-22.
57. Romero R, M.K., Mitchell MD, Wu YK, Oyarzun E, Hobbins JC *Infection and labor. IV. Cachectin-tumor necrosis factor in the amniotic fluid of women with intraamniotic infection and preterm labor.* . Am J Obstet Gynecol. , 1989;(161): p. 336-41.
58. Nold C, A.L., Brown A, et al, *Inflammation promotes a cytokine response and disrupts the cervical epithelial barrier: a possible mechanism of premature cervical remodeling and preterm birth.* Am J Obstet Gynecol 2012. **206**(3): p. 208.
59. Tanaka Y, N.H., Takai N, Yoshimatsu J, Anai T, Miyakawa I. , *Interleukin-1 β and interleukin-8 in cervicovaginal fluid during pregnancy.* Am J Obstet Gynecol, 1998. **79**: p. 644-649.
60. Challis JR1, S.D., Alfaidy N, Lye SJ, Gibb W, Patel FA, Whittle WL, Newnham JP, *Prostaglandins and mechanisms of preterm birth.* Reproduction 2002. **124**(1): p. 1-17.
61. Malak TM, B.S., *Structural characteristics of term human fetal membranes: a novel zone of extreme morphological alteration within the rupture site.* . Br J Obstet Gynaecol 1994. **101**: p. 375-86.
62. McParland, P.C., D.J. Taylor, and S.C. Bell, *Mapping of zones of altered morphology and chorionic connective tissue cellular phenotype in human fetal membranes (amniochorion and decidua) overlying the lower uterine pole and cervix before labor at term.* American Journal of Obstetrics & Gynecology. **189**(5): p. 1481-1488.
63. Hua, R., et al., *Stretch and inflammatory cytokines drive myometrial chemokine expression via NF- κ B activation.* Endocrinology, 2012. **153**(1): p. 481-91.

64. Riemer, R.K. and M.A. Heymann, *Regulation of uterine smooth muscle function during gestation*. *Pediatric research*, 1998. **44**(5): p. 615-627.
65. Soloff, M.S., et al., *Effects of progesterone treatment on expression of genes involved in uterine quiescence*. *Reprod Sci*, 2011. **18**(8): p. 781-97.
66. Sooranna, S.R., et al., *Mechanical stretch activates type 2 cyclooxygenase via activator protein-1 transcription factor in human myometrial cells*. *Mol Hum Reprod*, 2004. **10**(2): p. 109-13.
67. Terzidou, V., et al., *Mechanical stretch up-regulates the human oxytocin receptor in primary human uterine myocytes*. *J Clin Endocrinol Metab*, 2005. **90**(1): p. 237-46.
68. Shynlova, O., et al., *Uterine stretch regulates temporal and spatial expression of fibronectin protein and its alpha 5 integrin receptor in myometrium of unilaterally pregnant rats*. *Biol Reprod*, 2007. **77**(5): p. 880-8.
69. Wu, X., et al., *Myometrial mechanoadaptation during pregnancy: implications for smooth muscle plasticity and remodelling*. *J Cell Mol Med*, 2008. **12**(4): p. 1360-73.
70. Oldenhof, A.D., et al., *Mitogen-activated protein kinases mediate stretch-induced c-fos mRNA expression in myometrial smooth muscle cells*. *Am J Physiol Cell Physiol*, 2002. **283**(5): p. C1530-9.
71. Khan, R.N., et al., *Potassium channels in the human myometrium*. *Exp Physiol*, 2001. **86**(2): p. 255-64.
72. Sparey, C., et al., *The Differential Expression of Myometrial Connexin-43, Cyclooxygenase-1 and -2, and Gsa Proteins in the Upper and Lower Segments of the Human Uterus during Pregnancy and Labor*. *The Journal of Clinical Endocrinology & Metabolism*, 1999. **84**(5): p. 1705-1710.
73. Wray, S., *Uterine contraction and physiological mechanisms of modulation*. *Am J Physiol*, 1993. **264**(1 Pt 1): p. C1-18.
74. Lye, S.J., et al., *The molecular basis of labour and tocolysis*. *Fetal and Maternal Medicine Review*, 1998. **10**(3): p. 121-136.
75. Fuchs, A.-R., et al., *Oxytocin receptors in the human uterus during pregnancy and parturition*. *American Journal of Obstetrics and Gynecology*, 1984. **150**(6): p. 734-741.
76. Kim, S.H., et al., *Oxytocin activates NF-kappaB-mediated inflammatory pathways in human gestational tissues*. *Mol Cell Endocrinol*, 2015. **403**: p. 64-77.
77. Terzidou, V., et al., *Labor and inflammation increase the expression of oxytocin receptor in human amnion*. *Biology of reproduction*, 2011. **84**(3): p. 546-552.
78. Khanjani, S., et al., *NF Kappa B and AP-1 Drive Human Myometrial IL8 Expression*. *Mediators of Inflammation*, 2012. **2012**: p. 8.
79. Aguilar, H.N. and B.F. Mitchell, *Physiological pathways and molecular mechanisms regulating uterine contractility*. *Hum Reprod Update*, 2010. **16**(6): p. 725-44.
80. Slater, D., V. Allport, and P. Bennett, *Changes in the expression of the type-2 but not the type-1 cyclo-oxygenase enzyme in chorion-decidua with the onset of labour*. *Br J Obstet Gynaecol*, 1998. **105**(7): p. 745-8.
81. Hertelendy, F. and T. Zakar, *Prostaglandins and the myometrium and cervix*. *Prostaglandins Leukot Essent Fatty Acids*, 2004. **70**(2): p. 207-22.
82. Hertelendy, F. and T. Zakar, *Regulation of myometrial smooth muscle functions*. *Curr Pharm Des*, 2004. **10**(20): p. 2499-517.
83. Stjernholm, Y., et al., *Potential roles for gonadal steroids and insulin-like growth factor I during final cervical ripening*. *Obstet Gynecol*, 1997. **90**(3): p. 375-80.
84. Carbonne, B., et al., *Effects of progesterone on prostaglandin E(2)-induced changes in glycosaminoglycan synthesis by human cervical fibroblasts in culture*. *Mol Hum Reprod*, 2000. **6**(7): p. 661-4.
85. Nold, C., et al., *Prevention of preterm birth by progestational agents: what are the molecular mechanisms?* *Am J Obstet Gynecol*, 2013. **208**(3): p. 223 e1-7.

86. Yellon, S.M., et al., *Loss of progesterone receptor-mediated actions induce preterm cellular and structural remodeling of the cervix and premature birth*. PLoS One, 2013. **8**(12): p. e81340.
87. Merlino, A.A., et al., *Nuclear progesterone receptors in the human pregnancy myometrium: evidence that parturition involves functional progesterone withdrawal mediated by increased expression of progesterone receptor-A*. J Clin Endocrinol Metab, 2007. **92**(5): p. 1927-33.
88. Mitchell, B.F. and S. Wong, *Changes in 17 β ,20 α -hydroxysteroid dehydrogenase activity supporting an increase in the estrogen/progesterone ratio of human fetal membranes at parturition*. American Journal of Obstetrics and Gynecology, 1993. **168**(5): p. 1377-1385.
89. Allport, V.C., et al., *Human labour is associated with nuclear factor-kappaB activity which mediates cyclo-oxygenase-2 expression and is involved with the 'functional progesterone withdrawal'*. Mol Hum Reprod, 2001. **7**(6): p. 581-6.
90. Tan, H., et al., *Progesterone receptor-A and -B have opposite effects on proinflammatory gene expression in human myometrial cells: implications for progesterone actions in human pregnancy and parturition*. J Clin Endocrinol Metab, 2012. **97**(5): p. E719-30.
91. Mesiano, S., Y. Wang, and E.R. Norwitz, *Progesterone receptors in the human pregnancy uterus: do they hold the key to birth timing?* Reprod Sci, 2011. **18**(1): p. 6-19.
92. Hardy, D.B., et al., *Progesterone receptor plays a major antiinflammatory role in human myometrial cells by antagonism of nuclear factor-kappaB activation of cyclooxygenase 2 expression*. Mol Endocrinol, 2006. **20**(11): p. 2724-33.
93. Loudon, J.A., et al., *Progesterone represses interleukin-8 and cyclo-oxygenase-2 in human lower segment fibroblast cells and amnion epithelial cells*. Biol Reprod, 2003. **69**(1): p. 331-7.
94. Anderson, L., et al., *The effect of progesterone on myometrial contractility, potassium channels, and tocolytic efficacy*. Reprod Sci, 2009. **16**(11): p. 1052-61.
95. Dudley, D.J., et al., *Induction of preterm birth in mice by RU486*. Biol Reprod, 1996. **55**(5): p. 992-5.
96. Garfield, R.E., J.M. Gasc, and E.E. Baulieu, *Effects of the antiprogesterone RU 486 on preterm birth in the rat*. American Journal of Obstetrics and Gynecology, 1987. **157**(5): p. 1281-1285.
97. Maria, B., et al., *Termination of early pregnancy by a single dose of mifepristone (RU 486), a progesterone antagonist*. Eur J Obstet Gynecol Reprod Biol, 1988. **28**(3): p. 249-55.
98. Kokubu, K., et al., *Differentiation and elimination of uterine natural killer cells in delayed implantation and parturition mice*. J Reprod Dev, 2005. **51**(6): p. 773-6.
99. Grammatopoulos, D.K. and E.W. Hillhouse, *Role of corticotropin-releasing hormone in onset of labour*. Lancet, 1999. **354**(9189): p. 1546-9.
100. Jones, S.A., A.N. Brooks, and J.R. Challis, *Steroids modulate corticotropin-releasing hormone production in human fetal membranes and placenta*. J Clin Endocrinol Metab, 1989. **68**(4): p. 825-30.
101. Li, W. and J.R. Challis, *Corticotropin-releasing hormone and urocortin induce secretion of matrix metalloproteinase-9 (MMP-9) without change in tissue inhibitors of MMP-1 by cultured cells from human placenta and fetal membranes*. J Clin Endocrinol Metab, 2005. **90**(12): p. 6569-74.
102. Romero, R., et al., *Evidence for a local change in the progesterone/estrogen ratio in human parturition at term*. Am J Obstet Gynecol, 1988. **159**(3): p. 657-60.
103. Emanuel, R.L., et al., *Direct effects of corticotropin-releasing hormone and thyrotropin-releasing hormone on fetal lung explants*. Peptides, 2000. **21**(12): p. 1819-29.
104. Mitchell, B.F., et al, *Formation of unconjugated estrogens from estrone sulfate by dispersed cells from human fetal membranes and decidua*. J Clin Endocrinol Metab, 1984. **58**(5): p. 845-9.
105. Mesiano, S., *Myometrial progesterone responsiveness and the control of human parturition*. J Soc Gynecol Investig, 2004. **11**(4): p. 193-202.

106. Menon, R., et al., *Novel concepts on pregnancy clocks and alarms: redundancy and synergy in human parturition*. Hum Reprod Update, 2016. **22**(5): p. 535-60.
107. Smith, R., *Parturition*. N Engl J Med, 2007. **356**(3): p. 271-83.
108. McLean, M., et al., *A placental clock controlling the length of human pregnancy*. Nat Med, 1995. **1**(5): p. 460-3.
109. Kim, Y.M., et al., *Failure of physiologic transformation of the spiral arteries in patients with preterm labor and intact membranes*. Am J Obstet Gynecol, 2003. **189**(4): p. 1063-9.
110. Kim, Y.M., et al., *Failure of physiologic transformation of the spiral arteries in the placental bed in preterm premature rupture of membranes*. Am J Obstet Gynecol, 2002. **187**(5): p. 1137-42.
111. Williams, M.A., et al., *Adverse infant outcomes associated with first-trimester vaginal bleeding*. Obstet Gynecol, 1991. **78**(1): p. 14-8.
112. Harger, J.H., et al., *Risk factors for preterm premature rupture of fetal membranes: a multicenter case-control study*. Am J Obstet Gynecol, 1990. **163**(1 Pt 1): p. 130-7.
113. Salafia, C.M., et al., *Histologic evidence of old intrauterine bleeding is more frequent in prematurity*. Am J Obstet Gynecol, 1995. **173**(4): p. 1065-70.
114. Elovitz, M.A., et al., *Effects of thrombin on myometrial contractions in vitro and in vivo*. Am J Obstet Gynecol, 2000. **183**(4): p. 799-804.
115. van Zijl, M.D., et al., *252: What is the influence of macrosomia on spontaneous preterm delivery?* American Journal of Obstetrics & Gynecology, 2016. **214**(1): p. S148.
116. Hua, M., et al., *Congenital uterine anomalies and adverse pregnancy outcomes*. American Journal of Obstetrics and Gynecology, 2011. **205**(6): p. 558.e1-558.e5.
117. Aghaeepour, N., et al., *An immune clock of human pregnancy*. Sci Immunol, 2017. **2**(15).
118. Chen, S.J., Y.L. Liu, and H.K. Sytwu, *Immunologic regulation in pregnancy: from mechanism to therapeutic strategy for immunomodulation*. Clin Dev Immunol, 2012. **2012**: p. 258.
119. Brown, R.G., et al., *Establishment of vaginal microbiota composition in early pregnancy and its association with subsequent preterm prelabor rupture of the fetal membranes*. Transl Res, 2019. **207**: p. 30-43.
120. Romero, R., S.K. Dey, and S.J. Fisher, *Preterm labor: one syndrome, many causes*. Science, 2014. **345**.
121. Gravett, M.G., et al., *An experimental model for intraamniotic infection and preterm labor in rhesus monkeys*. Am J Obstet Gynecol, 1994. **171**(6): p. 1660-7.
122. Dombroski, R.A., et al., *A rabbit model for bacteria-induced preterm pregnancy loss*. Am J Obstet Gynecol, 1990. **163**(6 Pt 1): p. 1938-43.
123. Cunningham, F.G., G.B. Morris, and A. Mickal, *Acute pyelonephritis of pregnancy: A clinical review*. Obstet Gynecol, 1973. **42**(1): p. 112-7.
124. McDonald, C.R., A.M. Weckman, and A.L. Conroy, *Systemic inflammation is associated with malaria and preterm birth in women living with HIV on antiretrovirals and co-trimoxazole*. 2019. **9**(1): p. 6758.
125. Goldenberg, R.L., et al., *Epidemiology and causes of preterm birth*. The Lancet, 2008. **371**(9606): p. 75-84.
126. Ekman-Ordeberg, G. and A. Dubicke, *Preterm Cervical Ripening in humans*. Facts Views Vis Obgyn, 2012. **4**(4): p. 245-53.
127. Aagaard, K., et al., *A metagenomic approach to characterization of the vaginal microbiome signature in pregnancy*. PLoS One, 2012. **7**(6): p. e36466.
128. Lager, S., et al., *Detecting eukaryotic microbiota with single-cell sensitivity in human tissue*. Microbiome, 2018. **6**(1): p. 151.
129. Perez-Munoz, M.E., et al., *A critical assessment of the "sterile womb" and "in utero colonization" hypotheses: implications for research on the pioneer infant microbiome*. Microbiome, 2017. **5**(1): p. 48.

130. Romero, R., S.K. Dey, and S.J. Fisher, *Preterm labor: one syndrome, many causes*. Science, 2014. **345**(6198): p. 760-5.
131. Romero, R., et al., *Infection and labor. VIII. Microbial invasion of the amniotic cavity in patients with suspected cervical incompetence: prevalence and clinical significance*. Am J Obstet Gynecol, 1992. **167**(4 Pt 1): p. 1086-91.
132. Wei, S.Q., W. Fraser, and Z.C. Luo, *Inflammatory cytokines and spontaneous preterm birth in asymptomatic women: a systematic review*. Obstet Gynecol, 2010. **116**(2 Pt 1): p. 393-401.
133. Hillier, S.L., et al., *A case-control study of chorioamnionic infection and histologic chorioamnionitis in prematurity*. N Engl J Med, 1988. **319**(15): p. 972-8.
134. Fortner, K.B., et al., *Bacteria Localization and Chorion Thinning among Preterm Premature Rupture of Membranes*. PLOS ONE, 2014. **9**(1): p. e83338.
135. Onderdonk AB, H.J., McElrath TF, Delaney ML, Allred EN, Leviton A. , *Colonization of second-trimester placenta parenchyma*. . Am J Obstet Gynecol, 2008. **199**(1): p. 1-52.
136. Goldenberg, R.L., W.W. Andrews, and J.C. Hauth, *Choriodecidual infection and preterm birth*. Nutr Rev, 2002. **60**(5 Pt 2): p. S19-25.
137. Goldenberg, R.L., Hauth, J. C., & Andrews, W. W, *Intrauterine infection and preterm delivery*. New England Journal of Medicine 2000. **342**: p. 1500-1507.
138. G Cassell, J.H., W Andrews, G Cutter, *Chorioamnion colonization: correlation with gestational age in women delivered following spontaneous labor versus indicated delivery*. American Journal of Obstetrics Gynecology, 1993: p. 168-424.
139. Hillier, S.L., et al., *Association between bacterial vaginosis and preterm delivery of a low-birth-weight infant. The Vaginal Infections and Prematurity Study Group*. N Engl J Med, 1995. **333**(26): p. 1737-42.
140. Donders, G.G., et al., *Predictive value for preterm birth of abnormal vaginal flora, bacterial vaginosis and aerobic vaginitis during the first trimester of pregnancy*. BJOG, 2009. **116**(10): p. 1315-24.
141. Menard, J.P., et al., *High vaginal concentrations of Atopobium vaginae and Gardnerella vaginalis in women undergoing preterm labor*. Obstetrics and gynecology, 2010. **115**(1): p. 134-140.
142. Holst, E., Goffeng, A.R. and Andersch, B. , *Bacterial vaginosis and vaginal microorganisms in idiopathic premature labor and association with pregnancy outcome*. . J. Clin. Microbiol. , 1994. **32**: p. 176-186
143. Brown, R.G., et al., *Vaginal dysbiosis increases risk of preterm fetal membrane rupture, neonatal sepsis and is exacerbated by erythromycin*. BMC Medicine, 2018. **16**(1): p. 9.
144. Paras, M.V., C.L. Skevaki, and D.A. Kafetzis, *Preterm birth due to maternal infection: Causative pathogens and modes of prevention*. Eur J Clin Microbiol Infect Dis, 2006. **25**(9): p. 562-9.
145. Genc, M.R., et al., *Polymorphism in the interleukin-1 gene complex and spontaneous preterm delivery*. Am J Obstet Gynecol, 2002. **187**(1): p. 157-63.
146. Strauss, J.F., et al., *Spontaneous preterm birth: advances toward the discovery of genetic predisposition*. American Journal of Obstetrics and Gynecology, 2018. **218**(3): p. 294-314.e2.
147. Haque, M.M., et al., *First-trimester vaginal microbiome diversity: A potential indicator of preterm delivery risk*. Scientific Reports, 2017. **7**(1): p. 16145.
148. Muglia, L.J. and M. Katz, *The enigma of spontaneous preterm birth*. N Engl J Med, 2010. **362**(6): p. 529-35.
149. Kistka, Z.A., et al., *Racial disparity in the frequency of recurrence of preterm birth*. Am J Obstet Gynecol, 2007. **196**(2): p. 131.e1-6.
150. Winkvist, A., I. Mogren, and U. Hogberg, *Familial patterns in birth characteristics: impact on individual and population risks*. Int J Epidemiol, 1998. **27**(2): p. 248-54.
151. Porter, T.F., et al., *The risk of preterm birth across generations*. Obstet Gynecol, 1997. **90**(1): p. 63-7.

152. Lind, J. and H.C. Wallenburg, *Pregnancy and the Ehlers-Danlos syndrome: a retrospective study in a Dutch population*. Acta Obstet Gynecol Scand, 2002. **81**(4): p. 293-300.
153. Frey, H.A., et al., *Genetic variation associated with preterm birth in African-American women*. Am J Obstet Gynecol, 2016. **215**(2): p. 235.e1-8.
154. Romero, R., et al., *Identification of fetal and maternal single nucleotide polymorphisms in candidate genes that predispose to spontaneous preterm labor with intact membranes*. Am J Obstet Gynecol, 2010. **202**(5): p. 431.e1-34.
155. Moore, S., et al., *An investigation into the association among preterm birth, cytokine gene polymorphisms and periodontal disease*. Bjog, 2004. **111**(2): p. 125-32.
156. Macones, G.A., et al., *A polymorphism in the promoter region of TNF and bacterial vaginosis: preliminary evidence of gene-environment interaction in the etiology of spontaneous preterm birth*. Am J Obstet Gynecol, 2004. **190**(6): p. 1504-8.
157. McPherson, J.A. and T.A. Manuck, *Genomics of Preterm Birth--Evidence of Association and Evolving Investigations*. Am J Perinatol, 2016. **33**(3): p. 222-8.
158. Sheikh, I.A., et al., *Spontaneous preterm birth and single nucleotide gene polymorphisms: a recent update*. BMC genomics, 2016. **17**(Suppl 9): p. 759-759.
159. Zhang, G., et al., *Genetic Associations with Gestational Duration and Spontaneous Preterm Birth*. New England Journal of Medicine, 2017. **377**(12): p. 1156-1167.
160. J. Ludmir, H.M.S., *Anatomy and physiology of the uterine cervix*. Clin Obstet Gynecol, 2000. **43**: p. 433-439.
161. Shennan, A. and B. Jones, *The cervix and prematurity: aetiology, prediction and prevention*. Seminars in Fetal and Neonatal Medicine, 2004. **9**(6): p. 471-479.
162. Edlow, A.G., S.K. Srinivas, and M.A. Elovitz, *Second-trimester loss and subsequent pregnancy outcomes: What is the real risk?* American Journal of Obstetrics and Gynecology, 2007. **197**(6): p. 581.e1-581.e6.
163. Petersen, L.K. and N. Ulbjerg, *Cervical collagen in non-pregnant women with previous cervical incompetence*. European Journal of Obstetrics & Gynecology and Reproductive Biology, 1996. **67**(1): p. 41-45.
164. Sundtoft, I., et al., *Cervical collagen is reduced in non-pregnant women with a history of cervical insufficiency and a short cervix*. Acta Obstetrica et Gynecologica Scandinavica, 2017. **96**(8): p. 984-990.
165. Vyas, N.A., et al., *Risk factors for cervical insufficiency after term delivery*. American Journal of Obstetrics and Gynecology, 2006. **195**(3): p. 787-791.
166. Jakobsson, M., et al., *Loop Electrosurgical Excision Procedure and the Risk for Preterm Birth*. Obstetrics & Gynecology, 2009. **114**(3): p. 504-510.
167. Watson, H.A., et al., *Full dilation cesarean section: a risk factor for recurrent second-trimester loss and preterm birth*. Acta Obstetrica et Gynecologica Scandinavica, 2017. **96**(9): p. 1100-1105.
168. Schulz, K., D. Grimes, and W. Cates, *Measures to prevent cervical injury during suction curettage abortion* The Lancet, 1983. **321**(8335): p. 1182-1185.
169. Lee, S.E., et al., *The frequency and significance of intraamniotic inflammation in patients with cervical insufficiency*. American Journal of Obstetrics and Gynecology, 2008. **198**(6): p. 633.e1-633.e8.
170. Esplin M. S., O.B.E., Fraser A *Estimating recurrence of spontaneous preterm delivery*. Obstetrics and Gynecology, 2008. **112**(3): p. 516-523.
171. Dekker G. A., L.S.Y., North R. A., McCowan L. M., Simpson N. A. B., Roberts C. T. , *Risk factors for preterm birth in an international prospective cohort of nulliparous women*. PLoS ONE, 2012. **7**(7).
172. Iams, J.D., et al., *The length of the cervix and the risk of spontaneous premature delivery*. National Institute of Child Health and Human Development Maternal Fetal Medicine Unit Network. N Engl J Med, 1996. **334**(9): p. 567-72.

173. Heath, V.C., et al., *Cervical length at 23 weeks of gestation: prediction of spontaneous preterm delivery*. *Ultrasound Obstet Gynecol*, 1998. **12**(5): p. 312-7.
174. K.M. Orzechowski, R.C.B., J.K. Baxter, V. Berghella, *A universal transvaginal cervical length screening program for preterm birth prevention*. *Obstet Gynecol*, 2014. **124** p. 520-525.
175. Esplin, M., et al., *Predictive accuracy of serial transvaginal cervical lengths and quantitative vaginal fetal fibronectin levels for spontaneous preterm birth among nulliparous women*. *JAMA*, 2017. **317**(10): p. 1047-1056.
176. Crane, J.M. and D. Hutchens, *Transvaginal sonographic measurement of cervical length to predict preterm birth in asymptomatic women at increased risk: a systematic review*. *Ultrasound Obstet Gynecol*, 2008. **31**(5): p. 579-87.
177. Bloom, S.L.a.K.J.L., *Unproven technologies in maternal-fetal medicine and the high cost of us health care*. *JAMA*, 2017. **317**(10): p. 1025-1026.
178. Boelig, R.C., K.M. Orzechowski, and V. Berghella, *Cervical length, risk factors, and delivery outcomes among women with spontaneous preterm birth*. *The Journal of Maternal-Fetal & Neonatal Medicine*, 2016. **29**(17): p. 2840-2844.
179. Peixoto, A.B., et al., *Second trimester cervical length measurement for prediction spontaneous preterm birth in an unselected risk population*. *Obstet Gynecol Sci*, 2017. **60**(4): p. 329-335.
180. Owen, J., et al., *Does Mid-trimester Cervical Length \geq 25 mm Predict Preterm Birth in High-Risk Women?* *American journal of obstetrics and gynecology*, 2010. **203**(4): p. 393.e1-393.e5.
181. West, H.M., M. Jozwiak, and J.M. Dodd, *Methods of term labour induction for women with a previous caesarean section*. *Cochrane Database Syst Rev*, 2017. **6**: p. Cd009792.
182. Hezelgrave, N.L. and A.H. Shennan, *Quantitative Fetal Fibronectin to Predict Spontaneous Preterm Birth: A Review*. *Women's Health*, 2016. **12**(1): p. 121-128.
183. Abbott, D.S., et al., *Quantitative fetal fibronectin to predict preterm birth in asymptomatic women at high risk*. *Obstet Gynecol*, 2015. **125**(5): p. 1168-76.
184. Peaceman, A.M., et al., *Fetal fibronectin as a predictor of preterm birth in patients with symptoms: a multicenter trial*. *Am J Obstet Gynecol*, 1997. **177**(1): p. 13-8.
185. Deshpande, S.N., et al., *Rapid fetal fibronectin testing to predict preterm birth in women with symptoms of premature labour: a systematic review and cost analysis*. *Health Technol Assess*, 2013. **17**(40): p. 1-138.
186. Honest H, F.C., Durée KH, Norman G, Duffy SB, Tsourapas A, Roberts TE, Barton PM, Jowett SM, Hyde CJ, Khan KS., *Screening to prevent spontaneous preterm birth: systematic reviews of accuracy and effectiveness literature with economic modelling*. *Health Technol Assess*, 2009. **43**(1): p. 627.
187. Sadosky, Y., and Friedman, S. A. , *Fetal fibronectin and preterm labo*. *N. Engl. J. Med*, 1992 **326**: p. 709.
188. Joffe, G.M., et al., *Impact of the fetal fibronectin assay on admissions for preterm labor*. *Am J Obstet Gynecol*, 1999. **180**(3 Pt 1): p. 581-6.
189. Giles, W., et al., *The effect of fetal fibronectin testing on admissions to a tertiary maternal-fetal medicine unit and cost savings*. *Am J Obstet Gynecol*, 2000. **182**(2): p. 439-42.
190. Bruijn, M.M.C., et al., *Quantitative fetal fibronectin testing in combination with cervical length measurement in the prediction of spontaneous preterm delivery in symptomatic women*. *BJOG: An International Journal of Obstetrics & Gynaecology*, 2015. **123**(12): p. 1965-1971.
191. Agustin Conde-Agudelo, R.R., *Cervical phosphorylated insulin-like growth factor binding protein-1 test for the prediction of preterm birth: a systematic review and metaanalysis* *American Journal of Obstetrics and Gynecology*, 2016. **214** (1): p. 57-73.
192. Nikolova, T., et al., *Comparison of a novel test for placental alpha microglobulin-1 with fetal fibronectin and cervical length measurement for the prediction of imminent spontaneous*

- preterm delivery in patients with threatened preterm labor.* J Perinat Med, 2015. **43**(4): p. 395-402.
193. Abbott, D.S., et al., *Evaluation of a quantitative fetal fibronectin test for spontaneous preterm birth in symptomatic women.* American Journal of Obstetrics and Gynecology, 2013. **208**(2): p. 122.e1-122.e6.
 194. Cooper, S., et al., *Diagnostic accuracy of rapid pHIGFBP-I assay for predicting preterm labor in symptomatic patients.* Journal Of Perinatology, 2011. **32**: p. 460.
 195. Levine, L.D., et al., *Quantitative fetal fibronectin and cervical length in symptomatic women: results from a prospective blinded cohort study.* The Journal of Maternal-Fetal & Neonatal Medicine, 2018: p. 1-9.
 196. Hezelgrave Elliott, N., et al., *Quantitative Fetal Fibronectin at 18 Weeks of Gestation to Predict Preterm Birth in Asymptomatic High-Risk Women.* Obstetrics and Gynecology, 2016. **127**(2): p. 255-263.
 197. Faron, G., et al., *The fetal fibronectin test: 25 years after its development, what is the evidence regarding its clinical utility? A systematic review and meta-analysis.* The Journal of Maternal-Fetal & Neonatal Medicine, 2018: p. 1-31.
 198. Akercan, F., et al., *Value of cervical phosphorylated insulinlike growth factor binding protein-1 in the prediction of preterm labor.* J Reprod Med, 2004. **49**(5): p. 368-72.
 199. Hassan, S.S., et al., *Does cervical cerclage prevent preterm delivery in patients with a short cervix?* Am J Obstet Gynecol, 2001. **184**(7): p. 1325-9; discussion 1329-31.
 200. Odibo, A.O., M. Talucci, and V. Berghella, *Prediction of preterm premature rupture of membranes by transvaginal ultrasound features and risk factors in a high-risk population.* Ultrasound Obstet Gynecol, 2002. **20**(3): p. 245-51.
 201. Lee, S.M., et al., *The clinical significance of a positive Amnisure Test (™) in women with preterm labour and intact membranes.* The journal of maternal-fetal & neonatal medicine : the official journal of the European Association of Perinatal Medicine, the Federation of Asia and Oceania Perinatal Societies, the International Society of Perinatal Obstetricians, 2012. **25**(9): p. 1690-1698.
 202. Nikolova, T., et al., *Evaluation of a novel placental alpha microglobulin-1 (PAMG-1) test to predict spontaneous preterm delivery,* in *Journal of Perinatal Medicine.* 2014. p. 473.
 203. Werlen, S., et al., *[Preterm labor: Reproducibility of detection test of PAMG-1 before and after digital examination, and transvaginal ultrasound cervical length].* Gynecologie, obstetrique & fertilité, 2015. **43**(10): p. 640-645.
 204. Menon, R., et al., *Biomarkers of spontaneous preterm birth: an overview of the literature in the last four decades.* Reprod Sci, 2011. **18**(11): p. 1046-70.
 205. Anderson, L., et al., *The effect of progesterone on myometrial contractility, potassium channels, and tocolytic efficacy.* Reprod Sci, 2009. **16**.
 206. Norman, J.E. and P. Bennett, *Preterm birth prevention — Time to PROGRESS beyond progesterone.* PLOS Medicine, 2017. **14**(9): p. e1002391.
 207. Campbell, S., *Prevention of spontaneous preterm birth: universal cervical length assessment and vaginal progesterone in women with a short cervix: time for action!* American Journal of Obstetrics and Gynecology, 2018. **218**(2): p. 151-158.
 208. Romero, R., et al., *Vaginal progesterone for preventing preterm birth and adverse perinatal outcomes in singleton gestations with a short cervix: a meta-analysis of individual patient data.* American Journal of Obstetrics & Gynecology, 2018. **218**(2): p. 161-180.
 209. Conde-Agudelo, A., et al., *Vaginal Progesterone is as Effective as Cervical Cerclage to Prevent Preterm Birth in Women with a Singleton Gestation, Previous Spontaneous Preterm Birth and a Short Cervix: Updated Indirect Comparison Meta-Analysis.* American Journal of Obstetrics and Gynecology, 2018.
 210. Norman, J.E., et al., *Vaginal progesterone prophylaxis for preterm birth (the OPPTIMUM study): a multicentre, randomised, double-blind trial.* Lancet, 2016.

211. O'Brien, J.M., et al., *Effect of progesterone on cervical shortening in women at risk for preterm birth: secondary analysis from a multinational, randomized, double-blind, placebo-controlled trial*. *Ultrasound Obstet Gynecol*, 2009. **34**(6): p. 653-9.
212. Crowther, C.A., et al., *Vaginal progesterone pessaries for pregnant women with a previous preterm birth to prevent neonatal respiratory distress syndrome (the PROGRESS Study): A multicentre, randomised, placebo-controlled trial*. *PLOS Medicine*, 2017. **14**(9): p. e1002390.
213. Hein, M., et al., *Antimicrobial factors in the cervical mucus plug*. *Am J Obstet Gynecol*, 2002. **187**(1): p. 137-44.
214. Ethicon, Inc, *Ethicon Wound Closure Manual*, D.L. Dunn, Editor. 2007: www.ethicon.com. p. 1-119.
215. Berghella, V., et al., *Cerclage for short cervix on ultrasonography in women with singleton gestations and previous preterm birth: a meta-analysis*. *Obstet Gynecol*, 2011. **117**(3): p. 663-71.
216. Berghella, V., et al., *Cerclage for sonographic short cervix in singleton gestations without prior spontaneous preterm birth: systematic review and meta-analysis of randomized controlled trials using individual patient-level data*. *Ultrasound in Obstetrics & Gynecology*, 2017. **50**(5): p. 569-577.
217. Alfirevic, Z., T. Stampalija, and N. Medley, *Cervical stitch (cerclage) for preventing preterm birth in singleton pregnancy*. *Cochrane Database of Systematic Reviews*, 2017(6).
218. Israfil-Bayli, F., et al., *Cerclage outcome by the type of suture material (COTS): study protocol for a pilot and feasibility randomised controlled trial*. *Trials*, 2014. **15**: p. 415.
219. Kindinger, L.M., et al., *Relationship between vaginal microbial dysbiosis, inflammation, and pregnancy outcomes in cervical cerclage*. *Sci Transl Med*, 2016. **8**(350): p. 350ra102.
220. Hillier, S.L., *Diagnostic microbiology of bacterial vaginosis*. *Am J Obstet Gynecol*, 1993. **169**(2 Pt 2): p. 455-9.
221. Eschenbach, D.A., et al., *Prevalence of hydrogen peroxide-producing Lactobacillus species in normal women and women with bacterial vaginosis*. *J Clin Microbiol*, 1989. **27**(2): p. 251-6.
222. Haggerty, C.L., et al., *Bacterial vaginosis and anaerobic bacteria are associated with endometritis*. *Clin Infect Dis*, 2004. **39**(7): p. 990-5.
223. Brotman, R.M., *Vaginal microbiome and sexually transmitted infections: an epidemiologic perspective*. *J Clin Invest*, 2011. **121**(12): p. 4610-7.
224. Taha, T.E., et al., *Bacterial vaginosis and disturbances of vaginal flora: association with increased acquisition of HIV*. *AIDS*, 1998. **12**(13): p. 1699-706.
225. Borgdorff, H., et al., *Lactobacillus-dominated cervicovaginal microbiota associated with reduced HIV/STI prevalence and genital HIV viral load in African women*. *Isme Journal*, 2014. **8**(9): p. 1781-1793.
226. Anahtar, M.N., et al., *Cervicovaginal bacteria are a major modulator of host inflammatory responses in the female genital tract*. *Immunity*, 2015. **42**(5): p. 965-76.
227. Hay, P.E., et al., *Abnormal bacterial colonisation of the genital tract and subsequent preterm delivery and late miscarriage*. *BMJ*, 1994. **308**(6924): p. 295-8.
228. Kurki, T., et al., *Bacterial vaginosis in early pregnancy and pregnancy outcome*. *Obstet Gynecol*, 1992. **80**(2): p. 173-7.
229. Guaschino, S., et al., *Aetiology of preterm labour: bacterial vaginosis*. *BJOG*, 2006. **113 Suppl 3**: p. 46-51.
230. Hay, P.E., *Therapy of bacterial vaginosis*. *J Antimicrob Chemother*, 1998. **41**(1): p. 6-9.
231. Hay, P., *Recurrent Bacterial Vaginosis*. *Curr Infect Dis Rep*, 2000. **2**(6): p. 506-512.
232. Ravel, J., et al., *Daily temporal dynamics of vaginal microbiota before, during and after episodes of bacterial vaginosis*. *Microbiome*, 2013. **1**(1): p. 29.
233. Wang, B., et al., *Molecular analysis of the relationship between specific vaginal bacteria and bacterial vaginosis metronidazole therapy failure*. *Eur J Clin Microbiol Infect Dis*, 2014. **33**(10): p. 1749-56.

234. Patti, G.J., O. Yanes, and G. Siuzdak, *Innovation: Metabolomics: the apogee of the omics trilogy*. Nature reviews. Molecular cell biology, 2012. **13**(4): p. 263-269.
235. Leitich, H., et al., *Bacterial vaginosis as a risk factor for preterm delivery: A meta-analysis*. American Journal of Obstetrics and Gynecology, 2003. **189**(1): p. 139-147.
236. Daniel B. DiGiulio, B.J.C., Paul J. McMurdiea, Elizabeth K. Costelloa, , *Temporal and spatial variation of the human microbiota during pregnancy*. PNAS, 2015. **112**(35): p. 11060-11065.
237. Brocklehurst, P., et al., *Antibiotics for treating bacterial vaginosis in pregnancy*. Cochrane Database Syst Rev, 2013. **1**: p. CD000262.
238. Lamont, R.F., *Advances in the Prevention of Infection-Related Preterm Birth*. Front Immunol, 2015. **6**: p. 566.
239. Lamont, R.F., et al., *Treatment of abnormal vaginal flora in early pregnancy with clindamycin for the prevention of spontaneous preterm birth: a systematic review and metaanalysis*. Am J Obstet Gynecol, 2011. **205**(3): p. 177-90.
240. Rampersaud, R., T.M. Randis, and A.J. Ratner, *Microbiota of the upper and lower genital tract*. Seminars in fetal & neonatal medicine, 2012. **17**(1): p. 51-57.
241. Zhou, X., et al., *Characterization of vaginal microbial communities in adult healthy women using cultivation-independent methods*. Microbiology, 2004. **150**(Pt 8): p. 2565-73.
242. Koumans, E.H., et al., *The prevalence of bacterial vaginosis in the United States, 2001-2004; associations with symptoms, sexual behaviors, and reproductive health*. Sex Transm Dis, 2007. **34**(11): p. 864-9.
243. Haas, D.M., et al., *Tocolytic therapy for preterm delivery: systematic review and network meta-analysis*. BMJ, 2012. **345**: p. e6226.
244. Roos, C., et al., *Effect of maintenance tocolysis with nifedipine in threatened preterm labor on perinatal outcomes: A randomized controlled trial*. JAMA, 2013. **309**(1): p. 41-47.
245. van Vliet, E.O.G., et al., *Nifedipine maintenance tocolysis and perinatal outcome: an individual participant data meta-analysis*. BJOG: An International Journal of Obstetrics & Gynaecology, 2016. **123**(11): p. 1753-1760.
246. van Vliet, E.O.G., et al., *Nifedipine versus atosiban for threatened preterm birth (APOSTEL III): a multicentre, randomised controlled trial*. The Lancet, 2016. **387**(10033): p. 2117-2124.
247. Kenyon, S., et al., *Has publication of the results of the ORACLE Children Study changed practice in the UK? Bjog-an International Journal of Obstetrics and Gynaecology*, 2010. **117**(11): p. 1344-1349.
248. Excellence, N.I.f.H.a.C., *Preterm labour. (New guideline 25.) 2015*. <http://www.nice.org.uk/guidance/ng25>, 2015.
249. Organisation, W.H., *WHO recommendations on interventions to improve preterm birth outcomes*. http://www.who.int/reproductivehealth/publications/maternal_perinatal_health/preterm-birth-guideline, 2015.
250. Kenyon, S.L., et al., *Broad-spectrum antibiotics for preterm, prelabour rupture of fetal membranes: the ORACLE I randomised trial*. ORACLE Collaborative Group. Lancet, 2001. **357**(9261): p. 979-88.
251. Kenyon, S., et al., *Childhood outcomes after prescription of antibiotics to pregnant women with preterm rupture of the membranes: 7-year follow-up of the ORACLE I trial*. Lancet, 2008. **372**(9646): p. 1310-8.
252. Marlow, N., et al., *The ORACLE Children Study: educational outcomes at 11 years of age following antenatal prescription of erythromycin or co-amoxiclav*. Arch Dis Child Fetal Neonatal Ed, 2016.
253. Kenyon, S., et al., *Childhood outcomes after prescription of antibiotics to pregnant women with spontaneous preterm labour: 7-year follow-up of the ORACLE II trial*. Lancet, 2008. **372**(9646): p. 1319-27.

254. Meeraus, W.H., I. Petersen, and R. Gilbert, *Association between Antibiotic Prescribing in Pregnancy and Cerebral Palsy or Epilepsy in Children Born at Term: A Cohort Study Using The Health Improvement Network*. Plos One, 2015. **10**(3).
255. Kenyon, S.L., et al., *Broad-spectrum antibiotics for spontaneous preterm labour: the ORACLE II randomised trial*. ORACLE Collaborative Group. Lancet, 2001. **357**(9261): p. 989-94.
256. Marchesi, J.R. and J. Ravel, *The vocabulary of microbiome research: a proposal*. Microbiome, 2015. **3**(1 %@ 2049-2618): p. 1-3.
257. Llahi-Camp, J.M., et al., *Association of bacterial vaginosis with a history of second trimester miscarriage*. Hum Reprod, 1996. **11**(7): p. 1575-8.
258. Ralph, S.G., A.J. Rutherford, and J.D. Wilson, *Influence of bacterial vaginosis on conception and miscarriage in the first trimester: cohort study*. BMJ, 1999. **319**(7204): p. 220.
259. Azargoon, A. and S. Darvishzadeh, *Association of bacterial vaginosis, trichomonas vaginalis, and vaginal acidity with outcome of pregnancy*. Arch Iran Med, 2006. **9**(3): p. 213-7.
260. Gravett, M.G., et al., *Independent associations of bacterial vaginosis and Chlamydia trachomatis infection with adverse pregnancy outcome*. Jama, 1986. **256**(14): p. 1899-903.
261. DiGiulio, D.B., et al., *Temporal and spatial variation of the human microbiota during pregnancy*. Proc Natl Acad Sci U S A, 2015. **112**(35): p. 11060-5.
262. Hyman, R.W., et al., *Diversity of the vaginal microbiome correlates with preterm birth*. Reprod Sci, 2014. **21**(1): p. 32-40.
263. Kindinger, L.M., et al., *The interaction between vaginal microbiota, cervical length, and vaginal progesterone treatment for preterm birth risk*. Microbiome, 2017. **5**(1): p. 6.
264. Nelson, D.B., et al., *The Gestational Vaginal Microbiome and Spontaneous Preterm Birth among Nulliparous African American Women*. Am J Perinatol, 2016. **33**(9): p. 887-93.
265. Petricevic, L., et al., *Characterisation of the vaginal Lactobacillus microbiota associated with preterm delivery*. Sci Rep, 2014. **4**: p. 5136.
266. Amsel, R., et al., *Nonspecific vaginitis. Diagnostic criteria and microbial and epidemiologic associations*. Am J Med, 1983. **74**(1): p. 14-22.
267. Ison, C.A. and P.E. Hay, *Validation of a simplified grading of Gram stained vaginal smears for use in genitourinary medicine clinics*. Sexually Transmitted Infections, 2002. **78**(6): p. 413-415.
268. Larsen, B. and G.R. Monif, *Understanding the bacterial flora of the female genital tract*. Clin Infect Dis, 2001. **32**(4): p. e69-77.
269. Nugent, R.P., M.A. Krohn, and S.L. Hillier, *Reliability of diagnosing bacterial vaginosis is improved by a standardized method of gram stain interpretation*. J Clin Microbiol, 1991. **29**(2): p. 297-301.
270. Hyman, R.W., et al., *Microbes on the human vaginal epithelium*. Proc Natl Acad Sci U S A, 2005. **102**(22): p. 7952-7.
271. Zhou, X., et al., *Recent advances in understanding the microbiology of the female reproductive tract and the causes of premature birth*. Infect Dis Obstet Gynecol, 2010. **2010**: p. 737425.
272. Ma, J., A. Prince, and K.M. Aagaard, *Use of whole genome shotgun metagenomics: a practical guide for the microbiome-minded physician scientist*. Semin Reprod Med, 2014. **32**(1): p. 5-13.
273. Turnbaugh, P.J., et al., *The human microbiome project*. Nature, 2007. **449**(7164): p. 804-10.
274. Quince, C. and A.W. Walker, *Shotgun metagenomics, from sampling to analysis*. 2017. **35**(9): p. 833-844.
275. Chakravorty, S., et al., *A detailed analysis of 16S ribosomal RNA gene segments for the diagnosis of pathogenic bacteria*. J Microbiol Methods, 2007. **69**(2): p. 330-9.
276. Hilton, S.K., et al., *Metataxonomic and Metagenomic Approaches vs. Culture-Based Techniques for Clinical Pathology*. Frontiers in microbiology, 2016. **7**: p. 484-484.

277. P. Gajer, R.M.B., G. Bai, J. Sakamoto, U. M. E. Schütte, X. Zhong, S. S. K. Koenig, L. Fu, Z. S. Ma, X. Zhou, Z. Abdo, L. J. Forney, J. Ravel, , *Temporal dynamics of the human vaginal microbiota*. *Sci. Transl. Med.* , 2012. **4** , : p. 132ra52
278. Ravel, J., et al., *Vaginal microbiome of reproductive-age women*. *Proc Natl Acad Sci U S A*, 2011. **108 Suppl 1**: p. 4680-7.
279. Roy, E.J.a.M., R., *The concentration of oestrogens in blood during pregnancy*. *BJOG* 1962 **69**: p. 13–17.
280. Farage, M. and H. Maibach, *Lifetime changes in the vulva and vagina*. *Arch Gynecol Obstet*, 2006. **273**(4): p. 195-202.
281. Spear, G.T., et al., *Human alpha-amylase present in lower-genital-tract mucosal fluid processes glycogen to support vaginal colonization by Lactobacillus*. *J Infect Dis*, 2014. **210**(7): p. 1019-28.
282. MacIntyre, D.A., et al., *The vaginal microbiome during pregnancy and the postpartum period in a European population*. *Sci Rep*, 2015. **5**: p. 8988.
283. R. Romero, S.S.H., P. Gajer, A. L. Tarca, D. W. Fadrosh, L. Nikita, M. Galuppi, R. F. Lamont, P. Chaemsathong, J. Miranda, T. Chaiworapongsa, J. Ravel,, *The composition and stability of the vaginal microbiota of normal pregnant women is different from that of non-pregnant women*. . *Microbiome* 2014. **2**(4) .
284. MacIntyre, D.A., L. Sykes, and P.R. Bennett, *The human female urogenital microbiome: complexity in normality*. *Emerging Topics in Life Sciences*, 2017. **1**(4): p. 362-372.
285. Linhares, I.M., et al., *Contemporary perspectives on vaginal pH and lactobacilli*. *Am J Obstet Gynecol*, 2011. **204**(2): p. 120 e1-5.
286. D.E. O'Hanlon, T.R.M., R.A. Cone, *In vaginal fluid, bacteria associated with bacterial vaginosis can be suppressed with lactic acid but not hydrogen peroxide*. *BMC Infect. Dis.*,, 2001. **11** p. 200.
287. Witkin, S.S., *The vaginal microbiome, vaginal anti-microbial defence mechanisms and the clinical challenge of reducing infection-related preterm birth*. *Bjog*, 2015. **122**(2): p. 213-8.
288. Sakai, M., et al., *Relationship between cervical mucus interleukin-8 concentrations and vaginal bacteria in pregnancy*. *Am J Reprod Immunol*, 2004. **52**(2): p. 106-12.
289. Nold, C., et al., *Inflammation promotes a cytokine response and disrupts the cervical epithelial barrier: a possible mechanism of premature cervical remodeling and preterm birth*. *Am J Obstet Gynecol*, 2012. **206**(3): p. 208 e1-7.
290. Pruski, P., et al., *Assessment of microbiota:host interactions at the vaginal mucosa interface*. *Methods*, 2018.
291. Ravel, J., et al., *Vaginal microbiome of reproductive-age women*. *Proc Natl Acad Sci U S A*, 2011. **108**.
292. Luppi, P., *How immune mechanisms are affected by pregnancy*. . *Vaccine*, , 2003. **21**(24): p. 3352-7.
293. Mirmonsef, P., et al., *The effects of commensal bacteria on innate immune responses in the female genital tract*. *Am J Reprod Immunol*, 2011. **65**(3): p. 190-5.
294. Valore, E.V., et al., *Antimicrobial components of vaginal fluid*. *Am J Obstet Gynecol*, 2002. **187**(3): p. 561-8.
295. Anderson, D.J., Marathe, J., and Pudney, J. (2014). , *The structure of the human vaginal stratum corneum and its role in immune defense*. . *Am. J. Reprod. Immunol.* . **71**: p. 618-623.
296. Blaskewicz, C.D., Pudney, J., and Anderson, D. J. , *Structure and function of intercellular junctions in human cervical and vaginal mucosal epithelia*. . *Biol. Reprod.* , (2011). . **85**: p. 97-104.
297. Politch, J.A., Marathe, J., and Anderson, D. J. , *Characteristics and quantities of HIV host cells in human genital secretions*. *J. Infect Dis.* , 2014. **210**(Suppl. 3).

298. Aldunate, M., et al., *Antimicrobial and immune modulatory effects of lactic acid and short chain fatty acids produced by vaginal microbiota associated with eubiosis and bacterial vaginosis*. *Frontiers in Physiology*, 2015. **6**: p. 164.
299. Boris, S., et al., *Adherence of Human Vaginal Lactobacilli to Vaginal Epithelial Cells and Interaction with Uropathogens*. *Infection and Immunity*, 1998. **66**(5): p. 1985-1989.
300. Fichorova, R.N., and Anderson, D. J. , *Differential expression of immunobiological mediators by immortalized human cervical and vaginal epithelial cells*. . *Biol. Reprod.* , 1999. **60**: p. 508-514.
301. Herbst-Kralovetz, M.M., Quayle, A. J., Ficarra, M., Greene, S., Rose, W. A. II, Chesson, R., et al. , *Quantification and comparison of toll-like receptor expression and responsiveness in primary and immortalized human female lower genital tract epithelia*. *Am. J. Reprod. Immunol.* , (2008). . **59**: p. 212-224.
302. Rose, W.A.I., Mcgowin, C. L., Spagnuolo, R. A., Eaves-Pyles, T. D., Popov, and a.P. V. L., R. B. , *Commensal bacteria modulate innate immune responses of vaginal epithelial cell multilayer cultures*. *PLoS ONE* 2012
303. M. Hein, E.V.V., R.B. Helmig, N. Uldbjerg, T. Ganz, *Antimicrobial factors in the cervical mucus plug*. *Am J Obstet Gynecol*, 2002. **187** p. 137-144.
304. Sandler, N.G., Bosinger, S. E., Estes, J. D., Zhu, R. T., Tharp, G. K., Boritz, E., et al., *Type I interferon responses in rhesus macaques prevent SIV infection and slow disease progression*. *Nature* 2014. **511**(601-605).
305. Nazli, A., Chan, O., Dobson-Belaire, W. N., Ouellet, M., Tremblay, M. J., GrayOwen, S. D., et al., *Exposure to HIV-1 directly impairs mucosal epithelial barrier integrity allowing microbial translocation*. . *PLoS Pathog*, 2010. **6**(e1000852).
306. Li, Q., Estes, J. D., Schlievert, P. M., Duan, L., Brosnahan, A. J., Southern, P. J., et al., *Glycerol monolaurate prevents mucosal SIV transmission*. . *Nature* 2009. **458**: p. 1034-1038.
307. Witkin SS, L.I., *Why do lactobacilli dominate the human vaginal microbiota?* *BJOG* 2017; **124**: p. 606-611.
308. Witkin SS, M.-S.H., Linhares IM, Jayaram A, Ledger WJ, Forney LJ, *Influence of vaginal bacteria and D- and L-lactic acid isomers on vaginal extracellular matrix metalloproteinase inducer: implications for protection against upper genital tract infections*. . *MBio*, 2013. **4**(4): p. e00460-13.
309. Cole, A.M., *Innate host defense of human vaginal and cervical mucosae*. *Antimicrobial Peptides and Human Disease*, 2006. **306**: p. 199-230.
310. Anahtar, M.N., et al., *Cervicovaginal bacteria are a major modulator of host inflammatory responses in the female genital tract*. *Immunity*, 2015. **42**.
311. Hedge, S.R., et al., *Local and Systemic Cytokine Levels in Relation to Changes in Vaginal Flora*. *The Journal of Infectious Diseases*, 2006. **193**(4): p. 556-562.
312. Mattsby-Baltzer, I., et al., *IL-16, IL-6, TNF α , fetal fibronectin and endotoxin in the lower genital tract of pregnant women with bacterial vaginosis*. *Acta Obstetrica et Gynecologica Scandinavica*, 1998. **77**(7): p. 701-706.
313. Preti, G. and G.R. Huggins, *Cyclical changes in volatile acidic metabolites of human vaginal secretions and their relation to ovulation*. *Journal of Chemical Ecology*, 1975. **1**(3): p. 361-376.
314. Spiegel, C.A., et al., *Anaerobic-bacteria in nonspecific vaginitis*. *New England Journal of Medicine*, 1980. **303**(11): p. 601-607.
315. Piot, P., et al., *The vaginal microbial flora in non-specific vaginitis*. *European Journal of Clinical Microbiology*, 1982. **1**(5): p. 301-306.
316. Ison, C.A., et al., *Non-volatile fatty acids in the diagnosis of non-specific vaginitis*. *Journal of clinical pathology*, 1983. **36**(12): p. 1367-1370.

317. Krohn, M.A., S.L. Hillier, and D.A. Eschenbach, *Comparison of methods for diagnosing bacterial vaginosis among pregnant women*. Journal of Clinical Microbiology, 1989. **27**(6): p. 1266-1271.
318. Stanek, R., et al., *High performance ion exclusion chromatographic characterization of the vaginal organic acids in women with bacterial vaginosis*. Biomedical Chromatography, 1992. **6**(5): p. 231-235.
319. Chaudry, A.N., et al., *Analysis of vaginal acetic acid in patients undergoing treatment for bacterial vaginosis*. Journal of Clinical Microbiology, 2004. **42**(11): p. 5170-5175.
320. Wolrath, H., et al., *Analysis of bacterial vaginosis-related amines in vaginal fluid by gas chromatography and mass spectrometry*. Journal of Clinical Microbiology, 2001. **39**(11): p. 4026-4031.
321. Al-Mushrif, S., A. Eley, and B.M. Jones, *Inhibition of chemotaxis by organic acids from anaerobes may prevent a purulent response in bacterial vaginosis*. Journal of Medical Microbiology, 2000. **49**(11): p. 1023-1030.
322. Aldunate, M., et al., *Vaginal concentrations of lactic acid potentially inactivate HIV*. Journal of Antimicrobial Chemotherapy, 2013. **68**(9): p. 2015-2025.
323. Mirmonsef, P., et al., *Short-Chain Fatty Acids Induce Pro-Inflammatory Cytokine Production Alone and in Combination with Toll-Like Receptor Ligands*. American Journal of Reproductive Immunology, 2012. **67**(5): p. 391-400.
324. O'Hanlon, D.E., T.R. Moench, and R.A. Cone, *In vaginal fluid, bacteria associated with bacterial vaginosis can be suppressed with lactic acid but not hydrogen peroxide*. BMC Infectious Diseases, 2011. **11**.
325. Nazli, A., et al., *Exposure to HIV-1 Directly Impairs Mucosal Epithelial Barrier Integrity Allowing Microbial Translocation*. Plos Pathogens, 2010. **6**(4).
326. Reis Machado, J., et al., *Mucosal Immunity in the Female Genital Tract, HIV/AIDS*. BioMed Research International, 2014. **2014**: p. 20.
327. Y. Nakanishi, B.L., C. Gerard, and A. Iwasaki, *"CD8 + T lymphocyte mobilization to virus-infected tissue requires CD4 + T-cell help,"* Nature, 2009. **462**,(7272): p. 510-513.
328. A. L. Givan, H.D.W., J. E. Stern et al., *"Flow cytometric analysis of leukocytes in the human female reproductive tract: comparison of fallopian tube, uterus, cervix, and vagina,"* The American Journal of Reproductive Immunology, 1997. **38**(5): p. 350-359.
329. Hannun, Y.A. and L.M. Obeid, *Sphingolipids and their metabolism in physiology and disease*. Nature reviews. Molecular cell biology, 2018. **19**(3): p. 175-191.
330. Elovitz, M.A., et al., *Distinct cervical microRNA profiles are present in women destined to have a preterm birth*. Am J Obstet Gynecol, 2014. **210**(3): p. 221.e1-11.
331. Pereira, L., et al., *Identification of novel protein biomarkers of preterm birth in human cervical-vaginal fluid*. J Proteome Res, 2007. **6**(4): p. 1269-76.
332. Shah, S.J., et al., *Identification and quantification of preterm birth biomarkers in human cervicovaginal fluid by liquid chromatography/tandem mass spectrometry*. J Proteome Res, 2009. **8**(5): p. 2407-17.
333. Ghartey, J., et al., *Women with preterm birth have a distinct cervicovaginal metabolome*. Am J Obstet Gynecol, 2015. **212**(6): p. 776 e1-776 e12.
334. Thomas, M.M., et al., *Metabolite Profile of Cervicovaginal Fluids from Early Pregnancy Is Not Predictive of Spontaneous Preterm Birth*. International Journal of Molecular Sciences, 2015. **16**(11): p. 27741-27748.
335. Amabebe, E., et al., *Cervicovaginal Fluid Acetate: A Metabolite Marker of Preterm Birth in Symptomatic Pregnant Women*. Frontiers in Medicine, 2016. **3**: p. 48.
336. Urbanczyk-Wochniak, E., et al., *Parallel analysis of transcript and metabolic profiles: a new approach in systems biology*. EMBO Rep, 2003. **4**(10): p. 989-93.

337. Romero, R., et al., *The use of high-dimensional biology (genomics, transcriptomics, proteomics, and metabolomics) to understand the preterm parturition syndrome*. *Bjog*, 2006. **113 Suppl 3**: p. 118-35.
338. Lopes dos Santos Santiago, G., et al., *Longitudinal qPCR Study of the Dynamics of L. crispatus, L. iners, A. vaginae, (Sialidase Positive) G. vaginalis, and P. bivia in the Vagina*. *PLOS ONE*, 2012. **7(9)**: p. e45281.
339. Fanos, V., et al., *Metabolomics Application in Maternal-Fetal Medicine*. BioMed Research International, 2013. **2013**: p. 9.
340. Nicholson, J.K., et al., *Metabolic phenotyping in clinical and surgical environments*. *Nature*, 2012. **491(7424)**: p. 384-92.
341. MacIntyre, D.A., L. Sykes, and P.R. Bennett, *The human female urogenital microbiome: complexity in normality*. *Emerging Topics in Life Sciences*, 2017. **1(4)**: p. 363.
342. Zhou, X., et al., *Differences in the composition of vaginal microbial communities found in healthy Caucasian and black women*. *ISME J*, 2007. **1(2)**: p. 121-133.
343. Borgdorff, H., van der Veer, C., van Houdt, R., Alberts, C.J., de Vries, H.J., Bruisten, S.M. et al, *The association between ethnicity and vaginal microbiota composition in Amsterdam, the Netherlands*. *PLoS ONE* 2017 **12**.
344. McMillan, A., et al., *A multi-platform metabolomics approach identifies highly specific biomarkers of bacterial diversity in the vagina of pregnant and non-pregnant women*. *Scientific Reports*, 2015. **5**.
345. Srinivasan, S., et al., *Bacterial communities in women with bacterial vaginosis: high resolution phylogenetic analyses reveal relationships of microbiota to clinical criteria*. *PLoS One*, 2012. **7**.
346. !!! INVALID CITATION !!!
347. Mirmonsef, P., et al., *Short-chain fatty acids induce pro-inflammatory cytokine production alone and in combination with toll-like receptor ligands*. *Am J Reprod Immunol*, 2012. **67(5)**: p. 391-400.
348. Yeoman, C.J., et al., *A Multi-Omic Systems-Based Approach Reveals Metabolic Markers of Bacterial Vaginosis and Insight into the Disease*. *PLoS ONE*, 2013. **8(2)**.
349. Laghi, L., et al., *Rifaximin Modulates the Vaginal Microbiome and Metabolome in Women Affected by Bacterial Vaginosis*. *Antimicrobial Agents and Chemotherapy*, 2014. **58(6)**: p. 3411-3420.
350. Dudzik, D., et al., *LC-MS-based metabolomics identification of novel biomarkers of chorioamnionitis and its associated perinatal neurological damage*. *J Proteome Res*, 2015. **14(3)**: p. 1432-44.
351. Menon, R., et al., *Amniotic fluid eicosanoids in preterm and term births: effects of risk factors for spontaneous preterm labor*. *Obstetrics and gynecology*, 2011. **118(1)**: p. 121-134.
352. Maddipati, K.R., et al., *Clinical chorioamnionitis at term: the amniotic fluid fatty acyl lipidome*. *J Lipid Res*, 2016. **57(10)**: p. 1906-1916.
353. Witkin SS1, S.D., Herway C, Rudge MV, Saito F, Harris M., *Fatty acid composition of mid-trimester amniotic fluid in women of different ethnicities*. *J Matern Fetal Neonatal Med*, 2012: p. 818-21.
354. Auray-Blais, C., et al., *Metabolomics and preterm birth: What biomarkers in cervicovaginal secretions are predictive of high-risk pregnant women?* *International Journal of Mass Spectrometry*, 2011. **307(1)**: p. 33-38.
355. Amabebe, E., et al., *Identifying metabolite markers for preterm birth in cervicovaginal fluid by magnetic resonance spectroscopy*. *Metabolomics*, 2016. **12**: p. 67.
356. Narice, B.F., et al., *Spectroscopic techniques as potential screening tools for preterm birth: A review and an exploratory study*. *Applied Spectroscopy Reviews*, 2018: p. 1-20.

357. Stafford, G.P., et al., *Spontaneous Preterm Birth Is Associated with Differential Expression of Vaginal Metabolites by Lactobacilli-Dominated Microflora*. *Frontiers in Physiology*, 2017. **8**: p. 615.
358. López-Marure, R., et al., *Ceramide promotes the death of human cervical tumor cells in the absence of biochemical and morphological markers of apoptosis*. *Biochemical and Biophysical Research Communications*, 2002. **293**(3): p. 1028-1036.
359. Johnson, C.H., J. Ivanisevic, and G. Siuzdak, *Metabolomics: beyond biomarkers and towards mechanisms*. *Nature Reviews Molecular Cell Biology*, 2016. **17**: p. 451.
360. Dettmer, K., P.A. Aronov, and B.D. Hammock, *Mass spectrometry-based metabolomics*. *Mass Spectrometry Reviews*, 2007. **26**(1): p. 51-78.
361. Wang JH, B.J., Pennathur S., *Analytical Approaches to Metabolomics and Applications to Systems Biology*. . *Seminars in nephrology*. , 2010. **30**(5): p. 500-511.
362. Cooks RG, O.Z., Takats Z, Wiseman JM *Detection technologies. Ambient mass spectrometry*. *Science* 2006 **311**(5767): p. 1566-70.
363. Venter, A., M. Nefliu, and R. Graham Cooks, *Ambient desorption ionization mass spectrometry*. *TrAC Trends in Analytical Chemistry*, 2008. **27**(4): p. 284-290.
364. Huang, M., et al., *Ambient ionization mass spectrometry*. *Annual review of analytical chemistry*, 2010. **3**: p. 43-65.
365. Takats, Z., J.M. Wiseman, and R.G. Cooks, *Ambient mass spectrometry using desorption electrospray ionization (DESI): instrumentation, mechanisms and applications in forensics, chemistry, and biology*. *Journal of Mass Spectrometry*, 2005. **40**(10): p. 1261-1275.
366. Takats, Z., et al., *Mass spectrometry sampling under ambient conditions with desorption electrospray ionization*. *Science*, 2004. **306**(5695): p. 471-473.
367. Venter, A., P.E. Sojka, and R.G. Cooks, *Droplet dynamics and ionization mechanisms in desorption electrospray ionization mass spectrometry*. *Anal Chem*, 2006. **78**(24): p. 8549-55.
368. Srinivasan, S., et al., *Metabolic signatures of bacterial vaginosis*. *MBio*, 2015. **6**(2).
369. Pruski, P., et al., *Medical Swab Analysis Using Desorption Electrospray Ionization Mass Spectrometry: A Noninvasive Approach for Mucosal Diagnostics*. *Analytical Chemistry*, 2017. **89**(3): p. 1540-1550.
370. Schramm T, H.A., Klinkert I, Both JP, Heeren RM, Brunelle A, Laprévote O, De sbenoit N, Robbe MF, Stoeckli M, Spengler B, Römpf A., *imzML : a common data format for the flexible exchange and processing of mass spectrometry imaging data*. . *J Proteomics*. , 2012; . **75**(16): p. 5106-10.
371. Chambers, M.C., et al., *A cross-platform toolkit for mass spectrometry and proteomics*. *Nature Biotechnology*, 2012. **30**(10): p. 918-920.
372. Veselkov, K.A., et al., *Optimized Preprocessing of Ultra-Performance Liquid Chromatography/Mass Spectrometry Urinary Metabolic Profiles for Improved Information Recovery*. *Analytical Chemistry*, 2011. **83**(15): p. 5864-5872.
373. Jeffries, N., *Algorithms for alignment of mass spectrometry proteomic data*. *Bioinformatics*, 2005. **21**(14): p. 3066-3073.
374. Trygg, J., E. Holmes, and T. Lundstedt, *Chemometrics in metabonomics*. *J Proteome Res*, 2007. **6**(2): p. 469-79.
375. Wold, S., M. Sjostrom, and L. Eriksson, *PLS-regression: A Basic Tool of Chemometrics*. Vol. 58. 2001. 109-130.
376. Breiman, L., *Random forests*. *Machine Learning*, 2001. **45**(1): p. 5-32.
377. Chen, T., et al., *Random Forest in Clinical Metabolomics for Phenotypic Discrimination and Biomarker Selection*. *Evidence-Based Complementary and Alternative Medicine*, 2013. **2013**: p. 11.
378. Huang, Y.J., R. Powers, and G.T. Montelione, *Protein NMR recall, precision, and F-measure scores (RPF scores): Structure quality assessment measures based on information retrieval statistics*. *Journal of the American Chemical Society*, 2005. **127**(6): p. 1665-1674.

379. Smith, C.A., et al., *METLIN - A metabolite mass spectral database*. Therapeutic Drug Monitoring, 2005. **27**(6): p. 747-751.
380. Schmelzer, K., et al., *The lipid maps initiative in lipidomics*, in *Lipidomics and Bioactive Lipids: Mass-Spectrometry-Based Lipid Analysis*, H.A. Brown, Editor. 2007. p. 171-183.
381. Yeoman, C.J., et al., *A multi-omic systems-based approach reveals metabolic markers of bacterial vaginosis and insight into the disease*. PLoS One, 2013. **8**(2): p. e56111.
382. McMillan, A., et al., *A multi-platform metabolomics approach identifies highly specific biomarkers of bacterial diversity in the vagina of pregnant and non-pregnant women*. 2015. **5**: p. 14174.
383. Baraldi E, G.G., Stocchero M, et al., *Untargeted Metabolomic Analysis of Amniotic Fluid in the Prediction of Preterm Delivery and Bronchopulmonary Dysplasia*. . PLoS ONE. 2016. **11**(10).
384. Ison, C.A. and P.E. Hay, *Validation of a simplified grading of Gram stained vaginal smears for use in genitourinary medicine clinics*. Sex Transm Infect, 2002. **78**(6): p. 413-5.
385. Sundquist, A., et al., *Bacterial flora-typing with targeted, chip-based Pyrosequencing*. BMC Microbiology, 2007. **7**: p. 108-108.
386. Kozich, J.J., et al., *Development of a dual-index sequencing strategy and curation pipeline for analyzing amplicon sequence data on the MiSeq Illumina sequencing platform*. Appl Environ Microbiol, 2013. **79**(17): p. 5112-20.
387. Wang, Q., et al., *Naive Bayesian classifier for rapid assignment of rRNA sequences into the new bacterial taxonomy*. Appl Environ Microbiol, 2007. **73**(16): p. 5261-7.
388. Edgar, R.C., *Search and clustering orders of magnitude faster than BLAST*. Bioinformatics, 2010. **26**(19): p. 2460-1.
389. Parks, D.H. and R.G. Beiko, *Identifying biologically relevant differences between metagenomic communities*. Bioinformatics, 2010. **26**(6): p. 715-21.
390. Proctor, L.M., et al., *The Integrative Human Microbiome Project*. Nature, 2019. **569**(7758): p. 641-648.
391. Levine, N.S., et al., *Quantitative swab culture and smear - quick, simple method for determining number of viable aerobic bacteria on open wounds*. Journal of Trauma-Injury Infection and Critical Care, 1976. **16**(2): p. 89-94.
392. Linden, S.K., et al., *Mucins in the mucosal barrier to infection*. Mucosal Immunology, 2008. **1**(3): p. 183-197.
393. Neish, A.S., *Mucosal immunity and the microbiome*. Annals of the American Thoracic Society, 2014. **11 Suppl 1**: p. S28-32.
394. McMillan, A., et al., *A multi-platform metabolomics approach identifies highly specific biomarkers of bacterial diversity in the vagina of pregnant and non-pregnant women*. Sci Rep, 2015. **5**: p. 14174.
395. Takats, Z., N. Strittmatter, and J.S. McKenzie, *Chapter Nine - Ambient Mass Spectrometry in Cancer Research*, in *Advances in Cancer Research*, R.R. Drake and L.A. McDonnell, Editors. 2017, Academic Press. p. 231-256.
396. Cooks, R.G., et al., *Ambient mass spectrometry*. Science, 2006. **311**(5767): p. 1566-1570.
397. Strittmatter, N., et al., *Analysis of intact bacteria using rapid evaporative ionisation mass spectrometry*. Chemical Communications, 2013. **49**(55): p. 6188-6190.
398. Ferreira, C.R., et al., *Ambient Ionization Mass Spectrometry for Point-of-Care Diagnostics and Other Clinical Measurements*. Clinical chemistry, 2016. **62**(1): p. 99-110.
399. Jarmusch, A.K., et al., *Detection of strep throat causing bacterium directly from medical swabs by touch spray-mass spectrometry*. Analyst, 2014. **139**(19): p. 4785-4789.
400. Eberlin, L.S., et al., *Desorption electrospray ionization mass spectrometry for lipid characterization and biological tissue imaging*. Biochimica et Biophysica Acta (BBA) - Molecular and Cell Biology of Lipids, 2011. **1811**(11): p. 946-960.

401. Guenther, S., et al., *Spatially Resolved Metabolic Phenotyping of Breast Cancer by Desorption Electrospray Ionization Mass Spectrometry*. *Cancer Research*, 2015. **75**(9): p. 1828-1837.
402. Woolman, M., et al., *An Assessment of the Utility of Tissue Smears in Rapid Cancer Profiling with Desorption Electrospray Ionization Mass Spectrometry (DESI-MS)*. *Journal of The American Society for Mass Spectrometry*, 2017. **28**(1): p. 145-153.
403. Shariatgorji, M., et al., *Simultaneous imaging of multiple neurotransmitters and neuroactive substances in the brain by desorption electrospray ionization mass spectrometry*. *NeuroImage*, 2016. **136**: p. 129-138.
404. Abbassi-Ghadi, N., et al., *Repeatability and reproducibility of desorption electrospray ionization-mass spectrometry (DESI-MS) for the imaging analysis of human cancer tissue: a gateway for clinical applications*. *Analytical Methods*, 2015. **7**(1): p. 71-80.
405. Zhang, J.I., et al., *Rapid direct lipid profiling of bacteria using desorption electrospray ionization mass spectrometry*. *International Journal of Mass Spectrometry*, 2011. **301**(1-3): p. 37-44.
406. Song, Y., et al., *Rapid ambient mass spectrometric profiling of intact, untreated bacteria using desorption electrospray ionization*. *Chem Commun (Camb)*, 2007(1): p. 61-3.
407. Dunn, W.B., *Chapter two - Mass Spectrometry in Systems Biology: An Introduction*, in *Methods in Enzymology*, D. Jameson, M. Verma, and H.V. Westerhoff, Editors. 2011, Academic Press. p. 15-35.
408. Manicke, N.E., et al., *Desorption electrospray ionization (DESI) mass spectrometry and tandem mass spectrometry (MS/MS) of phospholipids and sphingolipids: ionization, adduct formation, and fragmentation*. *J Am Soc Mass Spectrom*, 2008. **19**(4): p. 531-43.
409. science., A.m.c.A.t.b.T.-t.k.t.u.a. *Part 1: Accuracy, precision and uncertainty*. Available from: http://www.rsc.org/lap/rsccom/amc/amc_index.htm 2003.
410. Bioanalytical Method Validation available from: <http://www.fda.gov/downloads/Drugs/GuidanceComplianceRegulatoryInformation/Guidances/UCM368107.pdf>,
411. Gerbig S, G.O., Balog J, Denes J, Baranyai Z, Zarand A, Raso E, Timar J, Takats Z. , *Analysis of colorectal adenocarcinoma tissue by desorption electrospray ionisation mass spectrometric imaging*. *Anal Bioanal Chem*, 2012; . **403**(8): p. 2315-25.
412. Terashi, H., et al., *Human stratified squamous epithelia differ in cellular fatty acid composition*. *J Dermatol Sci*, 2000. **24**(1): p. 14-24.
413. Nomura, T., et al., *Lipid analysis of normal dermis and hypertrophic scars*. *Wound Repair and Regeneration*, 2007. **15**(6): p. 833-837.
414. Anton, L., et al., *Common Cervicovaginal Microbial Supernatants Alter Cervical Epithelial Function: Mechanisms by Which Lactobacillus crispatus Contributes to Cervical Health*. *Frontiers in Microbiology*, 2018. **9**(2181).
415. van der Meer-Janssen, Y.P.M., et al., *Lipids in host-pathogen interactions: Pathogens exploit the complexity of the host cell lipidome*. *Progress in Lipid Research*, 2010. **49**(1): p. 1-26.
416. Vromman, F. and A. Subtil, *Exploitation of host lipids by bacteria*. *Current Opinion in Microbiology*, 2014. **17**: p. 38-45.
417. Sohlenkamp, C. and O. Geiger, *Bacterial membrane lipids: diversity in structures and pathways*. *FEMS Microbiol Rev*, 2016. **40**(1): p. 133-59.
418. Geiger, O., I.M. Lopez-Lara, and C. Sohlenkamp, *Phosphatidylcholine biosynthesis and function in bacteria*. *Biochim Biophys Acta*, 2013. **1831**(3): p. 503-13.
419. Badu-Tawiah, A., et al., *Non-aqueous spray solvents and solubility effects in desorption electrospray ionization*. *J Am Soc Mass Spectrom*, 2010. **21**(4): p. 572-9.
420. Green, F.M., et al., *The effect of electrospray solvent composition on desorption electrospray ionisation (DESI) efficiency and spatial resolution*. *Analyst*, 2010. **135**(4): p. 731-737.

421. Eberlin, L.S., et al., *Three-dimensional visualization of mouse brain by lipid analysis using ambient ionization mass spectrometry*. *Angewandte Chemie (International ed. in English)*, 2010. **49**(5): p. 873-876.
422. Girod, M., et al., *Desorption electrospray ionization imaging mass spectrometry of lipids in rat spinal cord*. *J Am Soc Mass Spectrom*, 2010. **21**(7): p. 1177-89.
423. Wiseman, J.M. and J.B. Li, *Elution, partial separation, and identification of lipids directly from tissue slices on planar chromatography media by desorption electrospray ionization mass spectrometry*. *Anal Chem*, 2010. **82**(21): p. 8866-74.
424. Abbassi-Ghadi, N., et al., *Repeatability and reproducibility of desorption electrospray ionization-mass spectrometry (DESI-MS) for the imaging analysis of human cancer tissue: a gateway for clinical applications*. *Analytical Methods*, 2015. **7**(1): p. 71-80.
425. Wertz, P.W., et al., *Lipids of epidermis and keratinized and non-keratinized oral epithelia*. *Comparative Biochemistry and Physiology Part B: Comparative Biochemistry*, 1986. **83**(3): p. 529-531.
426. Diaz-del Consuelo, I., et al., *Comparison of the lipid composition of porcine buccal and esophageal permeability barriers*. *Archives of Oral Biology*, 2005. **50**(12): p. 981-987.
427. Squier, C.A., et al., *The lipid composition of porcine epidermis and oral epithelium*. *Archives of Oral Biology*, 1986. **31**(11): p. 741-747.
428. Strott, C.A. and Y. Higashi, *Cholesterol sulfate in human physiology: what's it all about?* *Journal of Lipid Research*, 2003. **44**(7): p. 1268-1278.
429. Ikuta, T., et al., *Cholesterol sulfate, a novel activator for the ϵ isoform of protein kinase C*. *Cell growth & differentiation: the molecular biology journal of the American Association for Cancer Research*, 1994. **5**(9): p. 943-947.
430. Ding, N.-Z., et al., *De novo synthesis of sphingolipids is essential for decidualization in mice*. *Theriogenology*, 2018. **106**: p. 227-236.
431. Mizugishi, K., et al., *Maternal disturbance in activated sphingolipid metabolism causes pregnancy loss in mice*. *The Journal of Clinical Investigation*, 2007. **117**(10): p. 2993-3006.
432. Lindqvist, M., et al., *The Mucosal Adjuvant Effect of α -Galactosylceramide for Induction of Protective Immunity to Sexually Transmitted Viral Infection*. *The Journal of Immunology*, 2009. **182**(10): p. 6435-6443.
433. A McMillan, S.R., G Reid, *A multi-platform metabolomics approach identifies highly specific biomarkers of bacterial diversity in the vagina of pregnant and non-pregnant women*. *Scientific Reports* 2015. **5**.
434. H. Leitich, H.K., *Asymptomatic bacterial vaginosis and intermediate flora as risk factors for adverse pregnancy outcome*. *Best Pract. Res. Clin. Obstet. Gynaecol.*, 2007. **21**: p. 375-390.
435. Tabatabaei, N., et al., *Vaginal microbiome in early pregnancy and subsequent risk of spontaneous preterm birth: a case-control study*. *BJOG: An International Journal of Obstetrics & Gynaecology*, 2019. **126**(3): p. 349-358.
436. Wolrath, H., et al., *Analysis of bacterial vaginosis-related amines in vaginal fluid by gas chromatography and mass spectrometry*. *J Clin Microbiol*, 2001. **39**(11): p. 4026-31.
437. Gardner, H.L. and C.D. Duker, *Haemophilus vaginalis vaginitis: A newly defined specific infection previously classified "nonspecific" vaginitis*. *American Journal of Obstetrics and Gynecology*, 1955. **69**(5): p. 962-976.
438. Stafford, G.P., et al., *Spontaneous Preterm Birth Is Associated with Differential Expression of Vaginal Metabolites by Lactobacilli-Dominated Microflora*. *Front Physiol*, 2017. **8**: p. 615.
439. Paavonen, J., *Physiology and ecology of the vagina*. *Scandinavian Journal of Infectious Diseases*, 1983: p. 31-35.
440. Wilson, W.A., et al., *Regulation of glycogen metabolism in yeast and bacteria*. *Fems Microbiology Reviews*, 2010. **34**(6): p. 952-985.
441. Vitali, B., et al., *Vaginal microbiome and metabolome highlight specific signatures of bacterial vaginosis*. *Eur J Clin Microbiol Infect Dis*, 2015. **34**(12): p. 2367-76.

442. Watts, D.H., et al., *The association of occult amniotic fluid infection with gestational age and neonatal outcome among women in preterm labor*. *Obstet Gynecol*, 1992. **79**(3): p. 351-7.
443. Grimes-Dennis, J. and V. Berghella, *Cervical length and prediction of preterm delivery*. *Curr Opin Obstet Gynecol*, 2007. **19**(2): p. 191-5.
444. Brown, R.G., et al., *Prospective observational study of vaginal microbiota pre- and post-rescue cervical cerclage*. *BJOG: An International Journal of Obstetrics & Gynaecology*, 2019. **0**(0).
445. Balepa, L., et al., *The fetal fibronectin test: 25 years after its development, what is the evidence regarding its clinical utility? A systematic review and meta-analysis AU - Faron, Gilles*. *The Journal of Maternal-Fetal & Neonatal Medicine*, 2018: p. 1-31.
446. O'Hanlon, D.E., T.R. Moench, and R.A. Cone, *In vaginal fluid, bacteria associated with bacterial vaginosis can be suppressed with lactic acid but not hydrogen peroxide*. *BMC Infect Dis*, 2011. **11**: p. 200.
447. Vitali, B., et al., *Vaginal microbiome and metabolome highlight specific signatures of bacterial vaginosis*. *European Journal of Clinical Microbiology & Infectious Diseases*, 2015. **34**(12): p. 2367-2376.
448. Beloborodova, N., et al., *Effect of phenolic acids of microbial origin on production of reactive oxygen species in mitochondria and neutrophils*. *Journal of Biomedical Science*, 2012. **19**(1): p. 89.
449. Linhares, I.M., et al., *Contemporary perspectives on vaginal pH and lactobacilli*. *Am J Obstet Gynecol*, 2011. **204**.
450. Jackowski, S.C., jr., John E.; Rock, Charles O, *Chapter 2: Lipid metabolism in procaryotes*. *J. Biochemistry of Lipids, Lipoproteins and Membranes*. Elsevier. pp. 80–81. ISBN 0-444-89321-0., ed. D.E.V. Vance, *J. Biochemistry of Lipids, Lipoproteins and Membranes*. Elsevier. pp. 80–81. ISBN 0-444-89321-0. 1991: Elsevier.
451. Kennedy, V.D., *Phosphatidylcholine Metabolism, Discovery of the pathways for the biosynthesis of phosphatidylcholine*, ed CRC, ed. V. D. 1989, FL: Boca Raton
452. Spaapen, L.J.M., et al., *Urinary D-4-hydroxyphenyllactate, D-phenyllactate and D-2-hydroxyisocaproate, abnormalities of bacterial origin*. *Journal of Inherited Metabolic Disease*, 1987. **10**(4): p. 383-390.
453. Shen, T.T., et al., *A population-based study of race-specific risk for preterm premature rupture of membranes*. *American Journal of Obstetrics and Gynecology*, 2008. **199**(4): p. 373.e1-373.e7.
454. Modi, B.P., et al., *Mutations in fetal genes involved in innate immunity and host defense against microbes increase risk of preterm premature rupture of membranes (PPROM)*. *Molecular Genetics & Genomic Medicine*, 2017. **5**(6): p. 720-729.
455. Oh, Y.T., et al., *Oleamide suppresses lipopolysaccharide-induced expression of iNOS and COX-2 through inhibition of NF-kappaB activation in BV2 murine microglial cells*. *Neurosci Lett*, 2010. **474**(3): p. 148-153.
456. Brown, R.G., et al., *Establishment of vaginal microbiota composition in early pregnancy and its association with subsequent preterm prelabour rupture of the fetal membranes*. *Translational Research*, 2018.
457. Witkin, S.S., Mendes-Soares, H., Linhares, I. M., Jayarm, A., Ledger, W. J., & Forney, L. J., *Influence of vaginal bacteria and D- and L-lactic acid isomers on vaginal extracellular matrix metalloproteinase inducer: Implications for protection against upper genital tract infections*. *MBio*, 2013.
458. Wilson, W.A., et al., *Regulation of glycogen metabolism in yeast and bacteria*. *FEMS Microbiol Rev*, 2010. **34**(6): p. 952-85.
459. Parry, S. and J.F. Strauss, 3rd, *Premature rupture of the fetal membranes*. *N Engl J Med*, 1998. **338**(10): p. 663-70.

460. Peaceman, A.M., et al., *Length of latency with preterm premature rupture of membranes before 32 weeks' gestation*. Am J Perinatol, 2015. **32**(1): p. 57-62.
461. Rocha, G., et al., *Chorioamnionitis and brain damage in the preterm newborn*. J Matern Fetal Neonatal Med, 2007. **20**(10): p. 745-9.
462. Korpela, K., et al., *Intestinal microbiome is related to lifetime antibiotic use in Finnish pre-school children*. Nat Commun, 2016. **7**: p. 10410.
463. Vigneswaran, R., *Infection and preterm birth: evidence of a common causal relationship with bronchopulmonary dysplasia and cerebral palsy*. J Paediatr Child Health, 2000. **36**(4): p. 293-6.
464. Yoon, B.H., et al., *Fetal exposure to an intra-amniotic inflammation and the development of cerebral palsy at the age of three years*. Am J Obstet Gynecol, 2000. **182**(3): p. 675-81.
465. Drassinower, D., et al., *Prolonged latency of preterm premature rupture of membranes and risk of cerebral palsy*. J Matern Fetal Neonatal Med, 2015: p. 1-5.
466. van Dillen, J., et al., *Maternal sepsis: epidemiology, etiology and outcome*. Current Opinion in Infectious Diseases, 2010. **23**(3): p. 249-254.
467. Puri, K., et al., *Association of Chorioamnionitis with Aberrant Neonatal Gut Colonization and Adverse Clinical Outcomes*. PLoS One, 2016. **11**(9): p. e0162734.
468. Kacerovsky M, V.F., Kutova R, Pliskova L, Andrys C, Musilova I, *Cervical microbiota in women with preterm prelabor rupture of membranes*. PLoS One. , 2015. **10**.
469. McGregor, J.A., J.I. French, and K. Seo, *Premature rupture of membranes and bacterial vaginosis*. Am J Obstet Gynecol, 1993. **169**(2 Pt 2): p. 463-6.
470. Kanayama, N., T. Terao, and K. Horiuchi, *The role of human neutrophil elastase in the premature rupture of membranes*. Asia Oceania J Obstet Gynaecol, 1988. **14**(3): p. 389-97.
471. Fortunato, S.J., R. Menon, and S.J. Lombardi, *Role of tumor necrosis factor-alpha in the premature rupture of membranes and preterm labor pathways*. Am J Obstet Gynecol, 2002. **187**(5): p. 1159-62.
472. Shobokshi, A. and M. Shaarawy, *Maternal serum and amniotic fluid cytokines in patients with preterm premature rupture of membranes with and without intrauterine infection*. Int J Gynaecol Obstet, 2002. **79**(3): p. 209-15.
473. Helmig, B.R., et al., *Neutrophil elastase and secretory leukocyte protease inhibitor in prelabor rupture of membranes, parturition and intra-amniotic infection*. J Matern Fetal Neonatal Med, 2002. **12**(4): p. 237-46.
474. Lamont, R.F., et al., *Intravaginal clindamycin to reduce preterm birth in women with abnormal genital tract flora*. Obstetrics & Gynecology, 2003. **101**(3): p. 516-522.
475. Pappas, A., et al., *Chorioamnionitis and early childhood outcomes among extremely low-gestational-age neonates*. JAMA Pediatrics, 2014. **168**(2): p. 137-147.
476. Lee, M.Y., et al., *Prevalence and Antibiotic Susceptibility of Mycoplasma hominis and Ureaplasma urealyticum in Pregnant Women*. Yonsei Medical Journal, 2016. **57**(5): p. 1271-1275.
477. Palacio, M., et al., *Meta-analysis of studies on biochemical marker tests for the diagnosis of premature rupture of membranes: comparison of performance indexes*. BMC Pregnancy and Childbirth, 2014. **14**(1): p. 183.
478. Igbiosa, I., et al., *Comparison of rapid immunoassays for rupture of fetal membranes*. BMC pregnancy and childbirth, 2017. **17**(1): p. 128-128.
479. Yoon, B.H., C.-W. Park, and T. Chaiworapongsa, *Intrauterine infection and the development of cerebral palsy*. BJOG: An International Journal of Obstetrics & Gynaecology, 2003. **110**: p. 124-127.
480. Romero, R., et al., *A comparative study of the diagnostic performance of amniotic fluid glucose, white blood cell count, interleukin-6, and Gram stain in the detection of microbial invasion in patients with preterm premature rupture of membranes*. American Journal of Obstetrics and Gynecology, 1993. **169**(4): p. 839-851.

481. Marcellin, L., A Goffinet, François, *Are biological markers relevant for the diagnosis and the prognosis of preterm premature rupture of membranes (PPROM)?* Clinical chemistry and laboratory medicine, 2012: p. 1015-9.
482. Longini, M., et al., *Association between oxidative stress in pregnancy and preterm premature rupture of membranes.* Clinical Biochemistry, 2007. **40**(11): p. 793-797.
483. Biggio, J.R., et al., *Midtrimester amniotic fluid matrix metalloproteinase-8 (MMP-8) levels above the 90th percentile are a marker for subsequent preterm premature rupture of membranes.* American Journal of Obstetrics and Gynecology, 2005. **192**(1): p. 109-113.
484. Rahkonen, L., et al., *Matrix metalloproteinase-8 in cervical fluid in early and mid pregnancy: relation to spontaneous preterm delivery.* Prenatal Diagnosis, 2010. **30**(11): p. 1079-1085.
485. Liong, S., et al., *Proteomic analysis of human cervicovaginal fluid collected before preterm premature rupture of the fetal membranes.* Reproduction, 2013. **145**(2): p. 137-147.
486. Kenyon, C., Colebunders, R. and Crucitti, T., *The global epidemiology of bacterial vaginosis: a systematic review.* . Am. J. Obstet. Gynecol., 2013. **209**: p. 505-523.
487. Nohr, E.A., et al., *Obesity, gestational weight gain and preterm birth: a study within the Danish National Birth Cohort.* Paediatr Perinat Epidemiol, 2007. **21**(1): p. 5-14.
488. Tisi, D.K., J.J. Emard, and K.G. Koski, *Total Protein Concentration in Human Amniotic Fluid Is Negatively Associated with Infant Birth Weight.* The Journal of Nutrition, 2004. **134**(7): p. 1754-1758.
489. Annesley, T.M., *Ion Suppression in Mass Spectrometry.* Clinical Chemistry, 2003. **49**(7): p. 1041.
490. Ribar, S., M. Mesaric, and M. Sedic, *Sphingoid bases as possible diagnostic parameters.* Croat Med J, 2003. **44**(2): p. 165-70.
491. Kenyon, S.L., D.J. Taylor, and W. Tarnow-Mordi, *Broad-spectrum antibiotics for preterm, prelabour rupture of fetal membranes: the ORACLE I randomised trial.* The Lancet. **357**(9261): p. 979-988.
492. Kuriyama, T., et al., *Antimicrobial susceptibility of 800 anaerobic isolates from patients with dentoalveolar infection to 13 oral antibiotics.* Oral Microbiol Immunol, 2007. **22**(4): p. 285-8.
493. Harwich, M.D., et al., *Genomic sequence analysis and characterization of Sneathia amnii sp. nov.* BMC Genomics, 2012. **13**(8): p. S4.
494. Salminen, M.K., et al., *Lactobacillus bacteremia, species identification, and antimicrobial susceptibility of 85 blood isolates.* Clin Infect Dis, 2006. **42**(5): p. e35-44.
495. Menon R, T.M., Voltolini C, Torricelli M, Merialdi M, Betran AP, et al., *Biomarkers of spontaneous preterm birth: an overview of the literature in the last four decades.* . Reprod Sci 2011. **18**: p. 1046-70.
496. Chandler, J.D., et al., *Metabolic pathways of lung inflammation revealed by high-resolution metabolomics (HRM) of H1N1 influenza virus infection in mice.* American Journal of Physiology - Regulatory, Integrative and Comparative Physiology, 2016. **311**(5): p. R906-R916.
497. Cheng, Y.-F., et al., *Activation of AMP-Activated Protein Kinase by Adenine Alleviates TNF-Alpha-Induced Inflammation in Human Umbilical Vein Endothelial Cells.* PLOS ONE, 2015. **10**(11): p. e0142283.
498. Flynn, C.A., A.L. Helwig, and L.N. Meurer, *Bacterial vaginosis in pregnancy and the risk of prematurity: a meta-analysis.* J Fam Pract, 1999. **48**(11): p. 885-92.
499. Beloborodova, N.V., A.Y. Olenin, and A.K. Pautova, *Metabolomic findings in sepsis as a damage of host-microbial metabolism integration.* Journal of Critical Care, 2018. **43**: p. 246-255.
500. Fedotcheva, N.I., et al., *Toxic effects of microbial phenolic acids on the functions of mitochondria.* Toxicology Letters, 2008. **180**(3): p. 182-188.
501. Smith, S., A. Witkowski, and A.K. Joshi, *Structural and functional organization of the animal fatty acid synthase.* Progress in Lipid Research, 2003. **42**(4): p. 289-317.

502. Pschera, H., B. Larsson, and A. Kjaeldgaard, *Changes in fatty acid composition of cervical mucus lecithin during pregnancy*. Gynecol Obstet Invest, 1989. **28**(3): p. 118-22.
503. Pearson, J.R., Wiggins, H. S. and Drasar, B. S. , *Conversion of long-chain unsaturated fatty acids to hydroxy acids by human intestinal bacteria*. . J. Med. Microbiol, , 1974. . **7**: p. 265.
504. Hudson JA1, C.Y., Corner RJ, Morvan B, Joblin KN., *Identification and enumeration of oleic acid and linoleic acid hydrating bacteria in the rumen of sheep and cows*. J Appl Microbiol., 2000. **88**(2): p. 286-92.
505. Yamada, Y., et al., *Production of Hydroxy Fatty Acid (10-Hydroxy-12(Z)-octadecenoic acid) by Lactobacillus plantarum from Linoleic Acid and Its Cardiac Effects to Guinea Pig Papillary Muscles*. Biochemical and Biophysical Research Communications, 1996. **226**(2): p. 391-395.
506. Kim, K.-R. and D.-K. Oh, *Production of hydroxy fatty acids by microbial fatty acid-hydroxylation enzymes*. Vol. 31. 2013.
507. Parolin, C., et al., *Mechanism and stereoselectivity of HDAC I inhibition by (R)-9-hydroxystearic acid in colon cancer*. Biochim Biophys Acta, 2012. **1821**(10): p. 1334-40.
508. Desbois, A.P. and V.J. Smith, *Antibacterial free fatty acids: activities, mechanisms of action and biotechnological potential*. Applied Microbiology and Biotechnology, 2010. **85**(6): p. 1629-1642.
509. Donders, G.G., et al., *Pathogenesis of abnormal vaginal bacterial flora*. Am J Obstet Gynecol, 2000. **182**.
510. Vinolo, M.A., et al., *Short-chain fatty acids stimulate the migration of neutrophils to inflammatory sites*. Clin Sci (Lond), 2009. **117**(9): p. 331-8.
511. France, M.T., H. Mendes-Soares, and L.J. Forney, *Genomic Comparisons of Lactobacillus crispatus and Lactobacillus iners Reveal Potential Ecological Drivers of Community Composition in the Vagina*. Applied and Environmental Microbiology, 2016. **82**(24): p. 7063-7073.
512. Pamela Pruski, D.A.M., Holly V. Lewis, Paolo Inglese, Gonçalo DS Correia, Trevor T. Hansel, Phillip R. Bennett, Elaine Holmes and Zoltan Takats, *Medical swab analysis using desorption electrospray ionization mass spectrometry (DESI-MS) - a novel, non-invasive approach for mucosal diagnostics*. Analytical Chemistry, 2016 - Under Review.
513. Kindinger, L.M., et al., *Relationship between vaginal microbial dysbiosis, inflammation, and pregnancy outcomes in cervical cerclage*. Sci Transl Med, 2016. **8**.
514. Norman, M., et al., *Association of Short Antenatal Corticosteroid Administration-to-Birth Intervals With Survival and Morbidity Among Very Preterm Infants: Results From the EPICE Cohort* *Timing of Antenatal Corticosteroids for Preterm Birth Revisited* *Timing of Antenatal Corticosteroids for Preterm Birth Revisited*. JAMA Pediatrics, 2017. **171**(7): p. 678-686.
515. Schwebke, J.R. and R.A. Desmond, *A randomized trial of the duration of therapy with metronidazole plus or minus azithromycin for treatment of symptomatic bacterial vaginosis*. Clin Infect Dis, 2007. **44**(2): p. 213-9.
516. Petricevic, L. and A. Witt, *The role of Lactobacillus casei rhamnosus Lcr35 in restoring the normal vaginal flora after antibiotic treatment of bacterial vaginosis*. Bjog, 2008. **115**(11): p. 1369-74.
517. Anukam, K., et al., *Augmentation of antimicrobial metronidazole therapy of bacterial vaginosis with oral probiotic Lactobacillus rhamnosus GR-1 and Lactobacillus reuteri RC-14: randomized, double-blind, placebo controlled trial*. Microbes Infect, 2006. **8**(6): p. 1450-4.
518. Husain, S., et al., *Effects of oral probiotic supplements on vaginal microbiota during pregnancy: a randomised, double-blind, placebo-controlled trial with microbiome analysis*. BJOG: An International Journal of Obstetrics & Gynaecology, 2019. **0**(0).
519. Zheng, J., et al., *Diversity and dynamics of bacteriocins from human microbiome*. Environ Microbiol, 2015. **17**(6): p. 2133-43.

520. Rizzo, A., A. Losacco, and C.R. Carratelli, *Lactobacillus crispatus* modulates epithelial cell defense against *Candida albicans* through Toll-like receptors 2 and 4, interleukin 8 and human beta-defensins 2 and 3. *Immunol Lett*, 2013. **156**(1-2): p. 102-9.
521. Castro, J., et al., *Reciprocal interference between Lactobacillus spp. and Gardnerella vaginalis on initial adherence to epithelial cells*. *International journal of medical sciences*, 2013. **10**(9): p. 1193-1198.
522. Ghartey, J.P., et al., *Lactobacillus crispatus* dominant vaginal microbiome is associated with inhibitory activity of female genital tract secretions against *Escherichia coli*. *PLoS One*, 2014. **9**(5): p. e96659.
523. Kwok, L., et al., *Adherence of Lactobacillus crispatus to vaginal epithelial cells from women with or without a history of recurrent urinary tract infection*. *J Urol*, 2006. **176**(5): p. 2050-4; discussion 2054.
524. Antonio, M.A., et al., *Vaginal colonization by probiotic Lactobacillus crispatus CTV-05 is decreased by sexual activity and endogenous Lactobacilli*. *J Infect Dis*, 2009. **199**(10): p. 1506-13.
525. Goodwin, R.J., *Sample preparation for mass spectrometry imaging: small mistakes can lead to big consequences*. *J Proteomics*, 2012. **75**(16): p. 4893-911.
526. Pu, F., et al., *Direct sampling mass spectrometry for clinical analysis*. *Analyst*, 2019.
527. Bradford, L.L. and J. Ravel, *The vaginal mycobiome: A contemporary perspective on fungi in women's health and diseases*. *Virulence*, 2017. **8**(3): p. 342-351.
528. Taha TE, e.a., *Bacterial vaginosis and disturbances of vaginal flora: Association with increased acquisition of HIV*. *AIDS* 1998 **12**: p. 1699–1706.
529. Martin, J.H.L., et al., *Vaginal Lactobacilli, Microbial Flora, and Risk of Human Immunodeficiency Virus Type 1 and Sexually Transmitted Disease Acquisition*. *The Journal of Infectious Diseases*, 1999. **180**(6): p. 1863-1868.

8 APPENDICES

Table 12. Metabolites differentially expressed in bacterial vaginosis (BV) vs Healthy controls (H)

<i>m/z measured</i>	Sum formula	Compound	Adduct	Mod e	↑	FC	log2 (FC)	q-value (FDR)
311.2955	C20H40O2	Arachidic acid (C20:0)	M-H-	NEG	BV	8.3	3.0	1.50E-06
339.3270	C22H44O2	Docosanoic acid (C22:0)	M-H-	NEG	BV	18.7	4.2	9.18E-06
367.3579	C24H48O2	Lignoceric acid (C24:0)	M-H-	NEG	BV	5.9	2.6	9.18E-06
365.3419	C24H46O2	Nervonic acid (C24:1)	M-H-	NEG	BV	12.0	3.6	9.68E-06
337.3109	C22H42O2	Docosenoic acid (C22:1)	M-H-	NEG	BV	57.0	5.8	1.03E-05
297.2797	C19H38O2	Nonadecanoic acid (C19:0)	M-H-	NEG	BV	76.2	6.3	2.48E-05
309.2796	C20H38O2	Eicosenoic Acid (C20:1)	M-H-	NEG	BV	8.6	3.1	4.23E-05
353.3430	C23H46O2	Tricosanoic acid (C23:0)	M-H-	NEG	BV	22.4	4.5	8.16E-05
279.2331	C18H32O2	Linoleic acid (C18:2)	M-H-	NEG	BV	5.9	2.6	1.35E-04
269.2487	C17H34O2	Margaric acid (C17:0)	M-H-	NEG	BV	3.6	1.9	1.60E-04
307.2647	C20H36O2	Eicosadienoic acid (C20:2)	M-H-	NEG	BV	17.0	4.1	1.71E-04
283.2644	C18H36O2	Stearic acid (C18:0)	M-H-	NEG	BV	2.6	1.4	1.99E-04
281.2488	C18H34O2	Oleic acid (C18:1)	M-H-	NEG	BV	3.7	1.9	2.71E-04
131.0717	C6H12O3	Hydroxyisocaproic acid	M-H-	NEG	BV	19.4	4.3	3.35E-04
117.0562	C5H10O3	Hydroxyvaleric acid	M-H-	NEG	BV	2017.3	11.0	7.82E-04
393.3742	C26H50O2	Ximenic acid (C26:1)	M-H-	NEG	BV	12.8	3.7	7.82E-04
103.0408	C4H8O3	Hydroxybutyric acid	M-H-	NEG	BV	901.9	9.8	1.14E-03
565.5209	C36H70O4	9-SAHSa / FAHFA(18:0-9-O-18:0)	M-H-	NEG	BV	7.4	2.9	1.73E-03
267.2327	C17H32O2	Heptadecenoic acid (C17:1)	M-H-	NEG	BV	6.5	2.7	2.35E-03
259.0226	C6H13O9P	Glucose 6-phosphate	M-H-	NEG	BV	9.9	3.3	3.37E-03
567.5368	C36H72O4	Nonyl-bis(dodecyloxy)- propanoate	M-H-	NEG	BV	9.6	3.3	3.99E-03
253.2175	C16H30O2	Gaidic acid (C16:1)	M-H-	NEG	BV	3.1	1.6	5.37E-03
395.3899	C26H52O2	Cerotic acid (C26:0)	M-H-	NEG	BV	5.9	2.6	5.58E-03
563.5043	C36H68O4	9-OAHSa	M-H-	NEG	BV	9.9	3.3	7.76E-03
295.2656	C19H36O2	Nonadecenoic acid (C19:1)	M-H-	NEG	BV	40.1	5.3	7.89E-03
381.3741	C25H50O2	Pentacosanoic acid (C25:0)	M-H-	NEG	BV	6.7	2.8	7.89E-03
241.2174	C15H30O2	Pentadecylic acid	M-H-	NEG	BV	2.6	1.4	7.95E-03
227.2023	C14H28O2	Myristic acid (C14:0)	M-H-	NEG	BV	2.5	1.3	1.23E-02
353.2332	C20H34O5	PGD1	M-H-	NEG	BV	29.3	4.9	1.92E-02
399.2689	C21H40N2O3 S	N-(5-Oxo-2-sulfanyl-1,3-oxazolidin-2-yl)octadecanamide	M-H-	NEG	H	0.2	-2.4	1.99E-02
147.0667	C6H12O4	Mevalonic acid	M-H-	NEG	BV	17.9	4.2	2.00E-02
161.0458	C6H10O5	Hydroxyadipic acid	M-H-	NEG	BV	4.7	2.2	2.00E-02
537.4893	C34H66O4	Ethylene glycol dipalmitate	M-H-	NEG	BV	5.7	2.5	2.00E-02

<i>m/z</i> <i>measured</i>	Sum formula	Compound	Adduct	Mod e	↑	FC	log2 (FC)	q-value (FDR)
747.5188	C40H77O10P	PG(16:0/18:1)	M-H-	NEG	BV	5.0	2.3	2.88E-02
295.2274	C18H32O3	Hydroxy-octadecadienoic acid	M-H-	NEG	BV	72.2	6.2	2.90E-02
117.0197	C4H6O4	Succinic acid	M-H-	NEG	BV	4.2	2.1	3.23E-02
114.0247	C4H7N2S	4,5-Dihydro-1,3-thiazol- 5-ylmethanamine	M-H-	NEG	H	0.2	-2.4	3.27E-02
115.0211	C5H10O2S	Methyl 3- mercaptobutanoate	M-H, O- H-	NEG	H	0.2	-2.2	3.63E-02
307.0348	C9H13N2O8P	Deoxyuridine monophosphate	M-H-	NEG	H	0.1	-3.5	3.79E-02
103.1231	C5H14N2	Cadaverine	M+H+	POS	BV	50.4	5.7	9.06E-04
121.0651	C8H8O	Phenylacetaldehyde	M+H+	POS	BV	29.2	4.9	9.06E-04
138.0915	C8H11NO	Tyramine	M+H+	POS	BV	34.1	5.1	9.06E-04
95.0605	C5H6N2	Methylpyrazine	M+H+	POS	BV	78.0	6.3	1.22E-03
542.2659	C25H46NO7P	LysoPE(20:3)	M+K+	POS	BV	2.7	1.5	1.68E-03
409.1837	C17H21N5O6	Lys-His-OH	M+NH4 +	POS	BV	2.8	1.5	2.41E-03
585.2883	C29H44O12	Glycosides	M+H+	POS	BV	2.2	1.2	4.77E-03
112.0871	C5H9N3	Histamine	M+H+	POS	BV	29.1	4.9	5.06E-03
122.0966	C8H11N	Phenylethylamine	M+H+	POS	BV	403.6	8.7	5.49E-03
89.1074	C4H12N2	Putrescine	M+H+	POS	BV	360160.0	18.5	5.94E-03
105.0701	C8H8	Styrene	M+H+	POS	BV	419.7	8.7	8.14E-03
162.9979	C4H4Na2O4	Disodium succinate	M+H+	POS	BV	424.7	8.7	1.54E-02
145.1339	C7H16N2O	N-Acetylcadaverine	M+H+	POS	BV	4898.8	12.3	1.69E-02
200.9540	C4H4Na2O4	Disodium succinate	M+K+	POS	BV	5021.5	12.3	2.43E-02
381.0795	C12H22O11	Lactose	M+K+	POS	BV	6.3	2.7	2.64E-02
101.0600	C5H8O2	2-Ethylacrylic acid	M+H+	POS	BV	197.3	7.6	2.99E-02
103.0547	C8H6	Phenylacetylene	M+H+	POS	BV	25.9	4.7	3.50E-02
91.0544	C7H6	Cycloheptatetraene	M+H+	POS	BV	17.6	4.1	4.08E-02
93.0662	C2H8N2O2	Hydrazine, monoacetate	M+H+	POS	BV	27.7	4.8	4.08E-02
438.2398	C25H31N3O4	Dicoumaroylspermidine	M+H+	POS	BV	3.5	1.8	4.08E-02
104.1071	C5H13NO	Choline	M+H+	POS	BV	5.1	2.4	4.48E-02

Table 13. Metabolites differentially expressed in PPR0M and controls with intact membranes. Top 45 metabolites used in random forest analysis.

mz observed	m/z theoretical	MSMS	PPROM vs controls	Mode	Adduct	fold-change	p value	Formula	Compound	MSMs
522.3548	522.3548	0.00	↓ in PPR0M	(+)	[M+H] ⁺	0.05	2.33E-12	C26H52NO7P	LysoPC(18:1)	MSMS
718.5745	718.5745	0.00	↓ in PPR0M	(+)	[M+H] ⁺	0.03	7.48E-13	C40H80NO7P	PC(O-32:1)	MSMS
788.6161	788.6164	0.42	↓ in PPR0M	(+)	[M+H] ⁺	0.05	6.89E-13	C44H86NO8P	PC(36:1)	MSMS
703.5738	703.5749	1.51	↓ in PPR0M	(+)	[M+H] ⁺	0.06	6.89E-13	C39H79N2O6P	SM(d34:1)	MSMS
760.5854	760.5851	-0.35	↓ in PPR0M	(+)	[M+H] ⁺	0.08	6.89E-13	C42H82NO8P	PC(34:1)	MSMS
786.5993	786.6007	1.77	↓ in PPR0M	(+)	[M+H] ⁺	0.06	6.89E-13	C44H84NO8P	PE(39:1)	MSMS
300.2895	300.2897	0.78	↓ in PPR0M	(+)	[M+H] ⁺	0.05	6.89E-13	C18H37NO2	Sphingosine	MSMS
744.5888	744.5888	0.00	↓ in PPR0M	(+)	[M+H] ⁺	0.03	1.82E-12	C42H82NO7P	PC(O-34:2)	MSMS
302.3052	302.3053	0.46	↓ in PPR0M	(+)	[M+H] ⁺	0.04	7.48E-13	C18H39NO2	Sphinganine	MSMS
746.6042	746.6058	2.12	↓ in PPR0M	(+)	[M+H] ⁺	0.05	1.82E-12	C42H84NO7P	PC(O-34:1)	MSMS
633.4849	633.4854	0.67	↓ in PPR0M	(+)	[M+H] ⁺	0.08	2.99E-12	C35H69O7P	PA(O-32:1)	Putative
282.2790	282.2791	0.58	↓ in PPR0M	(+)	[M+H] ⁺	0.08	1.82E-12	C18H35NO	Oleamide	Putative
128.0356	128.0353	-2.57	↓ in PPR0M	(-)	[M-H] ⁻	0.10	3.30E-12	C5H7NO3	5-Oxoproline	MSMS
758.5701	758.5694	-0.84	↓ in PPR0M	(+)	[M+H] ⁺	0.09	1.41E-12	C42H80NO8P	PE(37:2)	MSMS
117.0198	117.0193	-3.89	↓ in PPR0M	(-)	[M-H] ⁻	0.02	4.31E-12	C4H6O4	Succinate	MSMS
826.5715	826.5732	2.00	↓ in PPR0M	(+)	[M+H] ⁺	0.08	2.62E-12	C47H82NO7P	PE(P-42:6)	Putative
732.5532	732.5538	0.78	↓ in PPR0M	(+)	[M+H] ⁺	0.03	5.13E-12	C40H78NO8P	PC(32:1)	MSMS
187.0422	187.0431	4.76	↓ in PPR0M	(-)	[M-H] ⁻	0.11	1.61E-10	C10H9N2P	2,2'-Phosphanediyldipyridine	Putative
824.5557	824.5552	-0.65	↓ in PPR0M	(+)	[M+H] ⁺	0.15	6.89E-12	C42H81NO12S	C18-OH Sulfatide	Putative
132.1020	132.1019	-0.62	↓ in PPR0M	(+)	[M+H] ⁺	0.05	6.54E-12	C6H13NO2	Leucine	MSMS
342.2473	342.2472	-0.24	↓ in PPR0M	(-)	[M-H] ⁻	0.08	6.51E-11	C19H37NO2S	NA	MSMS
560.3114	560.3124	1.64	↓ in PPR0M	(+)	[M+K] ⁺	0.13	1.24E-10	C26H52NO7P	LysoPC(18:1)	Putative
605.4541	605.4541	0.00	↓ in PPR0M	(+)	[M+H] ⁺	0.07	1.51E-11	C33H65O7P	PA(O-30:1)	Putative
798.5412	798.5419	0.83	↓ in PPR0M	(+)	[M+H] ⁺	0.19	1.06E-11	C45H78NO7P	PE(P-40:6)	Putative
741.5302	741.5318	2.11	↓ in PPR0M	(+)	[M+K] ⁺	0.13	6.54E-12	C39H79N2O6P	SM(d34:1)	Putative
86.0964	86.0964	0.70	↓ in PPR0M	(+)	[M+H] ⁺	0.39	5.72E-10	C5H11N	Piperidine	Putative
400.3423	400.3421	-0.32	↓ in PPR0M	(+)	[M+H] ⁺	0.06	3.81E-11	C23H45NO4	Palmitoyl-L-carnitine	MSMS
184.0733	184.0733	0.21	↓ in PPR0M	(+)	[M+H] ⁺	0.14	9.23E-10	C5H14NO4P	Phosphocholine	Putative
146.0461	146.0459	-1.37	↓ in PPR0M	(-)	[M-H] ⁻	0.10	6.89E-12	C5H9NO4	Glutamate	MSMS
428.3737	428.3734	-0.69	↓ in PPR0M	(+)	[M+H] ⁺	0.05	3.89E-11	C25H49NO4	Stearoylcarnitine	MSMS
822.5426	822.5432	0.72	↓ in PPR0M	(+)	[M+H] ⁺	0.16	7.13E-10	C42H82NO7P	PC(O-34:2)	Putative
603.5330	603.5334	0.69	↓ in PPR0M	(+)	[M+Na] ⁺	0.14	5.00E-10	C37H72O4	DG(O-34:1)	MSMS
114.0248	114.0248	0.00	↓ in PPR0M	(-)	[M-H] ⁻	0.09	4.49E-10	C5H7O3	3-keto-2-Methylbutyrate	Putative
631.4707	631.4697	-1.62	↓ in PPR0M	(+)	[M+H] ⁺	0.30	4.04E-08	C35H67O7P	PA(P-32:1)	Putative
114.0662	114.0673	9.35	↓ in PPR0M	(+)	[M+H] ⁺	0.32	7.08E-10	C4H7N3O	Creatinine	MSMS
399.2690	399.2687	-0.67	↓ in PPR0M	(-)	[M-H] ⁻	0.11	5.60E-10	C21H40N2O3S	N-(5-Oxo-2-sulfanyl-1,3-oxazolidin-2-yl)octadecanamide	MSMS
115.0212	115.0223	9.58	↓ in PPR0M	(-)	[M-H] ⁻	0.14	1.54E-09	C5H10O2S	Methyl 3-mercaptobutanoate	MSMS
426.3577	426.3578	0.09	↓ in PPR0M	(+)	[M+H] ⁺	0.05	4.49E-10	C25H47NO4	Vaccenyl carnitine	MSMS
740.5581	740.5589	1.00	↓ in PPR0M	(+)	[M+H] ⁺	0.28	4.49E-10	C42H78NO7P	PC(O-34:4)	Putative
379.2818	379.2819	0.25	↓ in PPR0M	(+)	[M+Na] ⁺	0.30	4.05E-08	C21H40O4	MG(18:1)	Putative
659.5003	659.5010	1.02	↓ in PPR0M	(+)	[M+H] ⁺	0.21	3.38E-10	C37H71O7P	PA(O-34:2)	Putative
796.5252	796.5262	1.24	↓ in PPR0M	(+)	[M+K] ⁺	0.33	6.31E-09	C42H80NO8P	PC(34:2)	MSMS
186.0452	186.0450	-1.08	↓ in PPR0M	(-)	[M-H] ⁻	0.07	7.13E-10	C8H12O3P	NA	MSMS
772.6212	772.6215	0.36	↓ in PPR0M	(+)	[M+H] ⁺	0.03	4.48E-10	C44H86NO7P	PC(P-36:1)	MSMS
544.3377	544.3384	1.30	↓ in PPR0M	(+)	[M+Na] ⁺	0.31	3.09E-08	C26H52NO7P	LysoPC(18:1)	Putative

Table 14. Metabolites differentially expressed in *Lactobacillus* spp. dominant and *Lactobacillus* spp deplete samples following PPRM. Top 50 metabolites used in random forest analysis.

m/z observed	m/z theoretical	PPM	Mode	Adduct	Formula	Dominant vs Dysbiosis	Fold-change	P value	q value	Compound	Assignment
589.4804	589.4802	-0.31	(+)	[M+Na] ⁺	C35H66O5	↑ in dominant	3.6245	0.0054	0.1514	DG(32:1)	Putative
672.4979	672.4974	-0.85	(-)	[M-H] ⁻	C37H72N07P	↑ in dominant	2.8204	0.0115	0.1514	PE(16:0/P-16:1)	MSMS
702.5459	702.5443	-2.28	(-)	[M-H] ⁻	C39H78N07P	↑ in dominant	3.3694	0.0118	0.1514	PE(O-34:1)	MSMS
617.5116	617.5115	-0.15	(+)	[M+Na] ⁺	C37H70O5	↑ in dominant	3.2720	0.0134	0.1514	DG(34:1)	Putative
465.3042	465.3044	-0.34	(-)	[M-H] ⁻	C27H46O4S	↑ in dominant	2.4372	0.0158	0.1514	cholesterol sulfate	MSMS
509.2886	509.2885	0.24	(-)	[M-H] ⁻	C24H47O9P	↑ in dominant	4.7889	0.0212	0.1514	PG(18:1)	Putative
478.2937	478.2939	-0.52	(-)	[M-H] ⁻	C23H46N07P	↑ in dominant	6.2114	0.0290	0.1514	PE(18:1)	MSMS
567.5368	567.5358	1.79	(-)	[M-H] ⁻	C36H72O4	↑ in deplete	0.3640	0.0309	0.1514	Nonyl 2,3-bis(dodecyloxy)propanoate	MSMS
643.5270	643.5296	-4.06	(+)	[M+H] ⁺	C41H70O5	↑ in dominant	3.2203	0.0344	0.1514	DG(38:5)	Putative
674.5134	674.5130	0.50	(-)	[M-H] ⁻	C37H74N07P	↑ in dominant	3.4413	0.0345	0.1514	PE(14:0/P-18:0)	Putative
700.5289	700.5287	0.35	(-)	[M-H] ⁻	C39H76N07P	↑ in dominant	1.8017	0.0384	0.1514	PE(16:0/P-18:1)	Putative
284.3305	284.3312	-2.32	(+)	[M+H] ⁺	C19H41N	↑ in deplete	0.3528	0.0393	0.1514	Cetrimonium	Putative
152.9960	152.9958	1.09	(-)	[M-H] ⁻	C3H7O5P	↑ in dominant	9.3189	0.0394	0.1514	Propanoyl phosphate	Putative
184.0732	184.0733	0.21	(+)	[M+H] ⁺	C5H14NO4P	↑ in dominant	17.1162	0.0516	0.1785	Phosphocholine	Putative
556.3176	556.3175	0.07	(-)	[M+Cl] ⁻	C26H52N07P	↑ in dominant	3.6615	0.0536	0.1785	PC(18:1)	Putative
175.0247	175.0248	-0.71	(-)	[M-H] ⁻	C6H8O6	↑ in dominant	1.7333	0.0589	0.1839	Propane-1,2,3-tricarboxylate	MSMS
360.3240	360.3237	0.91	(+)	[M+Na] ⁺	C22H43N0	↑ in dominant	7.8197	0.0664	0.1953	Docosenamide	Putative
773.5345	773.5338	0.88	(-)	[M-H] ⁻	C42H79O10P	↑ in dominant	2.2811	0.0733	0.2036	PG(40:9)	Putative
828.5511	828.5538	-3.19	(+)	[M+H] ⁺	C48H78N08P	↑ in deplete	0.5518	0.0891	0.2310	PC(40:9)	Putative
832.5859	832.5851	0.95	(+)	[M+H] ⁺	C48H82N08P	↑ in deplete	0.4927	0.0924	0.2310	PC(40:7)	Putative
282.2784	282.2791	0.58	(+)	[M+H] ⁺	C18H35N0	↑ in dominant	6.3145	0.1190	0.2833	Oleamide	Putative
740.5573	740.5589	-2.11	(+)	[M+H] ⁺	C42H78N07P	↑ in dominant	2.5131	0.1301	0.2993	PC(O-14:0/20:4)	Putative
804.5524	804.5538	-1.75	(+)	[M+H] ⁺	C46H78N08P	↑ in deplete	0.5928	0.1377	0.2958	PC(38:7)	Putative
94.9255	94.9261	-7.18	(-)	[M-H2O-H] ⁻	H2O3S2	↑ in deplete	0.6351	0.1456	0.3034	Thiosulfic acid	Putative
760.5133	760.5134	-0.12	(-)	[M-H] ⁻	C40H76N010P	↑ in dominant	2.1104	0.1584	0.3169	PS(32:1)	Putative
599.3221	599.3202	3.22	(-)	[M-H] ⁻	C27H53O12P	↑ in deplete	0.4098	0.1679	0.3230	PI(18:0)	Putative
588.4772	588.4764	1.31	(+)	[M+Cl] ⁻	C34H67N04	↑ in deplete	0.8233	0.2006	0.3657	Cer(14:1/20:0(2OH))	Putative
112.9873	112.9875	-1.23	(-)	[M-H2O-H] ⁻	C4H4O5	↑ in dominant	1.9782	0.2088	0.3657	Oxaloacetate	Putative
772.5271	772.5252	2.53	(+)	[M+Na] ⁺	C43H76N07P	↑ in deplete	0.5661	0.2175	0.3657	PE(20:4)/P-18:1	Putative
768.5323	768.5316	0.97	(-)	[M+Cl] ⁻	C40H80N08P	↑ in deplete	0.8429	0.2194	0.3657	PC(32:0)	Putative
725.5579	725.5578	-0.05	(+)	[M+Na] ⁺	C39H79N2O6P	↑ in dominant	1.5207	0.2358	0.3804	SM(34:1)	Putative
745.4210	745.4205	0.69	(+)	[M+K] ⁺	C40H67O8P	↑ in dominant	1.5173	0.2630	0.4110	PA(37:6)	Putative
377.0853	377.0856	-0.83	(-)	[M+Cl] ⁻	C12H22O11	↑ in deplete	0.8810	0.3059	0.4635	Lactose	MSMS
108.0220	108.0222	-1.60	(-)	[M+Cl] ⁻	C3H7N0	↑ in dominant	3.4977	0.3633	0.5342	Aminoacetone	Putative
780.5527	780.5538	-1.39	(+)	[M+H] ⁺	C44H78N08P	↑ in deplete	0.8163	0.3784	0.5406	PC(36:5)	Putative
756.5536	756.5538	-0.28	(+)	[M+H] ⁺	C42H78N08P	↑ in deplete	0.5138	0.4015	0.5442	PC(34:3)	Putative
792.5326	792.5316	1.28	(+)	[M+Cl] ⁻	C42H80N08P	↑ in deplete	0.6382	0.4027	0.5442	PC(34:2)	Putative
506.2886	506.2883	0.70	(-)	[M-H2O-H] ⁻	C24H48N09P	↑ in dominant	1.2808	0.4906	0.6455	PS(18:0)	Putative
124.0076	124.0074	1.41	(-)	[M-H] ⁻	C2H7N03S	↑ in deplete	0.5534	0.5577	0.7087	Taurine	Putative
810.6008	810.6007	0.05	(+)	[M+H] ⁺	C46H84N08P	↑ in dominant	1.0465	0.5669	0.7087	PC(38:4)	Putative
539.1384	539.1384	-0.05	(-)	[M+Cl] ⁻	C18H32O16	↑ in deplete	0.9781	0.6103	0.7443	Raffinose	Putative
794.5508	794.5472	4.58	(-)	[M+Cl] ⁻	C42H82N08P	↑ in deplete	0.8203	0.6596	0.7670	PC(34:1)	Putative
806.5687	806.5694	-0.92	(+)	[M+H] ⁺	C46H80N08P	↑ in deplete	0.9002	0.6596	0.7670	PC(38:6)	Putative
161.0454	161.0455	-0.71	(-)	[M-H] ⁻	C6H10O5	↑ in dominant	1.1242	0.6791	0.7717	Dimethylmalate	MSMS
794.6038	794.6058	-2.50	(+)	[M+H] ⁺	C46H84N07P	↑ in deplete	0.5413	0.7882	0.8568	PC(O-18:1/20:4)	Putative
722.5144	722.5130	1.90	(-)	[M-H] ⁻	C41H74N07P	↑ in deplete	0.8723	0.8253	0.8779	PE(18:3)/P-18:1	Putative
835.5355	835.5342	1.57	(-)	[M-H] ⁻	C43H81O13P	↑ in deplete	0.9845	0.8556	0.8913	PI(34:1)	Putative
541.1352	541.1346	1.07	(-)	[M-H2O-H] ⁻	C27H28O13	↑ in deplete	0.8399	0.8873	0.9054	Deoxydaunorubicinol aglycone 13-O-β-glucuronide	Putative
796.5252	796.5262	1.24	(+)	[M+Na] ⁺	C45H76N07P	↑ in dominant	1.0417	0.9647	0.9647	PC(34:2)	MSMS

Table 15. Metabolites differentially expressed women that subsequently PPROM compared to women that experience term deliveries. Samples for the prediction analysis were taken before PPROM at 16 weeks gestation. Samples nearer to rupture event were retrospectively assigned; 5-9 wks prior to rupture and 2 weeks prior to rupture

	m/z observed	m/z theoretical	PPM	Mode	Adduct	Formula	Before PPROM vs controls	Fold- change	P-value	Compound	Assignment
Distal	165.0560	165.0557	-1.82	(-)	[M-H]-	C9H10O3	↓ in before PPROM	0.13	3.07E-03	Phenyllactic acid	MSMS
	379.2817	379.2820	0.74	(+)	[M+Na]+	C21H40O4	↓ in before PPROM	0.43	9.71E-03	MG(18:1)	Putative
	181.0509	181.0506	-1.66	(-)	[M-H]-	C9H10O4	↓ in before PPROM	0.14	3.07E-03	Hydroxyphenyllactic acid	MSMS
	89.0248	89.0244	-4.75	(-)	[M-H]-	C3H6O3	↓ in before PPROM	0.43	1.75E-02	lactic acid	Putative
	271.2278	271.2279	0.25	(-)	[M-H]-	C16H32O3	↓ in before PPROM	0.33	1.86E-02	hydroxy palmitic acid	MSMS
	117.0197	117.0193	-3.42	(-)	[M-H]-	C4H6O4	↓ in before PPROM	0.27	5.20E-03	Succinic acid	MSMS
	489.3154	489.3141	-2.66	(-)	[M-H]-	C30H46O3	↓ in before PPROM	0.21	4.61E-03	3beta-3-Hydroxy-11-oxolanosta-8,24-dien-26-al	Putative
	758.5711	758.5694	-2.18	(+)	[M+H]+	C42H80N08P	↓ in before PPROM	0.74	3.81E-02	PE(37:2)	MSMS
	299.2593	299.2592	-0.44	(-)	[M-H]-	C18H36O3	↑ in before PPROM	2.53	2.16E-02	hydroxy stearic acid	putative
	BMI	N/A	N/A	N/A	N/A	N/A	↑ in before PPROM	47.05	3.94E-02	N/A	N/A
Mid	271.2278	271.2279	0.25	(-)	[M-H]-	C16H32O3	↓ in before PPROM	0.15	1.52E-02	4-hydroxy palmitic acid	MSMS
	134.0475	134.0472	-2.20	(-)	[M-H]-	C5H5N5	↑ in before PPROM	5.01	1.70E-02	Adenine	Putative
	87.0092	87.0088	-4.98	(-)	[M-H]-	C3H4O3	↑ in before PPROM	4.16	1.70E-02	Pyruvate	Putative
	655.5075	655.5069	-0.93	(-)	[M-H]-	C39H72O5	↑ in before PPROM	1.94	1.70E-02	DG(18:0/18:2)	Putative
	520.2690	520.2681	-1.81	(-)	[M-H]-	C24H44N09P	↑ in before PPROM	2.10	1.70E-02	PS(18:2)	MSMS
Proximal	96.9700	96.9696	-3.96	(-)	M-H-	H3O4P	↑ in before PPROM	8.17	1.98E-03	Sulfuric acid	MSMS
	Black	N/A	N/A	N/A	N/A	N/A	↑ in before PPROM	Inf	7.98E-04	N/A	N/A
	782.5688	782.5694	0.77	(+)	[M+H]+	C44H80N08P	↑ in before PPROM	1.55	2.06E-02	PC(36:4)	MSMS
	483.2734	483.2728	-1.16	(-)	M-H-	C22H45O9P	↓ in before PPROM	0.20	9.38E-03	PG(16:0)	MSMS
	134.0475	134.0472	-2.20	(-)	M-H-	C5H5N5	↑ in before PPROM	13.44	9.75E-03	Adenine	Putative
	365.2808	365.2810	0.58	(-)	M-H-	C21H38N2O3	↓ in before PPROM	0.21	9.38E-03	N-Benzyl-N,N-dimethyldodecan-1-amium nitrate	Putative
	87.0092	87.0088	-4.98	(-)	[M-H]-	C3H4O3	↑ in before PPROM	6.26	9.38E-03	Pyruvate	Putative
	175.0250	175.0248	-1.40	(-)	[M-H]-	C6H8O6	↑ in before PPROM	10.02	9.38E-03	Propane-1,2,3-tricarboxylate	MSMS
	771.5181	771.5181	0.00	(-)	[M-H]-	C42H77O10P	↓ in before PPROM	0.54	2.66E-02	PG(18:1/18:2)	MSMS
	78.9594	78.9590	-4.87	(-)	[M+Cl]-	CO2	↑ in before PPROM	5.26	2.52E-02	Carbon dioxide	Putative
	601.5165	601.5166	0.23	(+)	[M+Na]+	C37H70O4	↓ in before PPROM	0.27	9.75E-03	2-(Hexadecanoyloxy)prop-2-en-1-yl octadecanoate	Putative
	428.3737	428.3734	-0.72	(+)	[M+H]+	C25H49NO4	↓ in before PPROM	0.44	0.00E+00	Stearoylcarnitine	MSMS
	575.5016	575.5010	-1.06	(+)	[M+Na]+	C35H68O4	↓ in before PPROM	0.20	9.38E-03	dihexadecyl propanedioate	Putative
	427.2995	427.2984	-2.55	(-)	[M+Cl]-	C25H44O3	↓ in before PPROM	0.38	3.90E-02	5-Methyl-2-octadecanoylcyclohexane-1,3-dione	Putative
	413.2844	413.2828	-3.75	(-)	[M+Cl]-	C24H42O3	↓ in before PPROM	0.12	9.38E-03	5β-Cholane-3α,6α,24-triol	Putative
	702.5451	702.5443	-1.11	(-)	[M-H]-	C39H78NO7P	↓ in before PPROM	0.63	9.75E-03	PE(O-16:0/18:1)	MSMS
	399.2689	399.2687	-0.61	(-)	[M-H]-	C21H40N2O3S	↓ in before PPROM	0.48	2.60E-02	N-(5-Oxo-2-sulfanyl-1,3-oxazolidin-2-yl)octadecanamide	Putative
	89.0248	89.0244	-4.75	(-)	[M-H]-	C3H6O3	↑ in before PPROM	1.78	3.10E-02	lactic acid	Putative
	400.3423	400.3421	-0.36	(+)	[M+H]+	C23H45NO4	↓ in before PPROM	0.56	5.25E-02	Palmitoyl-L-carnitine	MSMS
	342.2473	342.2472	-0.43	(-)	M-H-	C19H37NO2S	↓ in before PPROM	0.40	3.10E-02	N/A	MSMS